

SCIENTIFIC ASPECTS OF UROLITHIASIS:  
QUANTITATIVE STONE ANALYSES AND  
CRYSTALLIZATION EXPERIMENTS

by

MICHAEL ALEXANDER ERICH WANDT

Dissertation presented to the  
University of Cape Town  
in fulfilment of the requirements  
for the degree of

DOCTOR OF PHILOSOPHY

The University of Cape Town has been given  
the right to reproduce this thesis in whole  
or in part. Copyright is held by the author.

Department of Physical Chemistry

March 1986

The copyright of this thesis vests in the author. No quotation from it or information derived from it is to be published without full acknowledgement of the source. The thesis is to be used for private study or non-commercial research purposes only.

Published by the University of Cape Town (UCT) in terms of the non-exclusive license granted to UCT by the author.

*Il faut n'appeler Science: que  
l'ensemble des recettes qui  
réussissent toujours. - Tout  
le reste est littérature.*

Paul Valéry

## ACKNOWLEDGEMENTS

I am indebted to a number of people without whose assistance this work would not have been possible. Without devaluating the help of others, I feel happy to mention at least some:

- Dr A L Rodgers who introduced me to the difficult but challenging subject of urolithiasis research. His supervision and his assistance in my ongoing struggle with the English language was greatly appreciated; most of the SEM pictures are due to his help;
- Dr C R Hubbard (NBS, Washington, USA) and Dr P Szabo (University of New South Wales, Kensington, Australia) I thank for their interest and useful comments regarding the XRD techniques investigated. Both of them, as well as Drs C R Houska (Virginia Polytechnic Institute, Blacksburg, USA) and C G Vonk (DSM, Geleen, Holland) did not hesitate in supplying me with their computer programmes;
- I owe special thanks to M A Bruno Pougnet (Analytical Chemistry department, UCT) for his always constructive criticism. Besides, I could only do my ICP-AES work because Bruno taught me how to do it and was ready to help at any time, be it day or night.
- Prof J P Willis (Geochemistry department, UCT) who let me use his facilities and helped with the  $\mu^*$  measurements;
- Prof P W Linder (Physical Chemistry department, UCT) who disclosed MINEQL results to me before publication;
- Prof L Underhill (Mathematical Statistics Dept, UCT) without whom (and SVDD) I would not have managed the statistical analyses;

- Prof P O Schwille (Universitätsklinik, Erlangen, Germany), Prof W Valhllensieck and Dr A Hesse (Universitätsklinik, Bonn, Germany), Prof W Prandl (Universität Tübingen, Germany) and the UCT Alumni Fund deserve my thanks for their joint contributions which allowed me to attend the Vth International Symposium on Urolithiasis Research. I very much appreciated the hospitality shown by Dr Hesse and Prof Prandl when visiting their institutions;
- Financial support in the form of bursaries from the Council for Scientific and Industrial Research and the University of Cape Town is gratefully acknowledged. The Medical Research Council also contributed to this study in the person of Dr Rodgers;
- Barbara Collocot provided the microwave oven for stone digestions;
- Mr S Hendricks took care of the photography;
- Christel Gevers and Ginny Blewett helped with the typing;
- Dr Pretorius (NAC, Van de Graaff Group, Faure) I am indebted for his 'understanding' during the final months this thesis took shape;
- Sevi Papanicolou - her much needed support during my first year in South Africa made this time a memorable one;
- Last but not least, my gratitude to Christel and many friends for their moral support and encouragement. They had to face some perhaps not very social behaviour lately.

## ABSTRACT

This thesis describes two aspects of the various scientific approaches to the study of urolithiasis. In the first instance, the theory, development and results of three quantitative analytical procedures are described while in the second, crystallization experiments in a rotary evaporator are presented.

Of the different methods of quantitative X-ray powder diffraction analyses, the 'internal standard method' and a microanalytical technique were identified as being potentially the two most useful procedures for the quantitative analysis of urinary calculi. 'Reference intensity ratios' for 6 major stone phases were determined and were used in the analysis of 20 calculi by the 'internal standard method'. It is concluded that the attainment of accurate results using this procedure is not easily achieved because of problems such as the unavailability of standards which realistically mimic stone composition, sample preparation, overlap of reflections from sample components and standards and the requirement of 'infinitely thick' specimens ( $> 250$  mg). For the microanalytical technique, micro-quantities of 10 calculi from the original 20 were deposited on silver filters and were quantitatively analysed using both, the attenuation of the Ag peak and the separately measured absorption coefficients  $\mu^*$ .

Inductively coupled plasma atomic emission spectroscopic (ICP-AES) methods were also investigated, developed and used in this study. Various procedures for the digestion of calculi were tested and a mixture of  $\text{HNO}_3$  and  $\text{HClO}_4$  was eventually found to be the most successful. The major elements Ca, Mg, and P in 41 calculi were determined. For the determination of trace elements, a new microwave-assisted digestion procedure was developed and used for the digestion of 100 calculi. Thereafter the major elements Ca, Mg and P together with the minor and trace elements Al, Cu, Fe, K, Li, Mn, Mo, Na, Pb, S, Sr and Zn in all 100 stones were simultaneously determined. The data so obtained were subjected to 3 types of statistical analyses involving direct correlations, scatter plots and a relatively new multivariate analysis of logarithmic data known as a 'covariance biplot'. Several interesting correlations were obtained.

Fluoride concentrations in two stone collections - 20 calculi from India and 42 from South Africa - were determined using a fluoride-ion sensitive electrode and the  $\text{HNO}_3/\text{HClO}_4$  digestion procedure used for the ICP study. Direct measurement of fluoride proved unsuccessful thereby necessitating the investigation and development of a diffusion technique. Using this method the fluoride content of both collections was determined.

A series of crystallization experiments involving a standard reference artificial urine was carried out in a rotary evaporator. The effect of pH and urine composition was studied by varying the former and by including certain components (uric acid, urea, creatinine,  $\text{MgO}$ , methylene blue, chondroitin sulphate A, fluoride) in the reference solution. Crystals formed in these experiments were subjected to qualitative and semi-quantitative X-ray powder diffraction analyses. Scanning electron microscopy of several deposits was also carried out. Similar deposits to those observed in calculi were obtained with the fast evaporator. The results presented suggest that this system provides a simple, yet very useful means for studying the crystallization characteristics of urine solutions.

The quantitative analytical procedures described in detail in this thesis can serve as model techniques for other workers involved in stone research. Together with other approaches such as the crystallization experiments discussed, these procedures can lead to a better understanding of the aetiological processes which govern stone formation.

## SAMEVATTING

Twee wetenskaplike benaderings tot die bestudering van "urolithiasis", word in hierdie tesis beskryf. Eerstens word die teorie, ontwikkeling en resultate van drie kwantitatiewe analitiese prosedures beskryf en daarna word kristallisatie eksperimente behandel wat uitgevoer is in 'n roterende verdampapparaat.

Van die verskillende X-straal poeierdiffraksietegnieke is gevind dat die "interne standaard metode" en 'n mikro-analitiese tegniek die geskikste is vir kwantitatiewe analiese van urinêre "calculi". Intensiteitsverhoudings vir 6 hoof steenfases was bepaal en gebruik vir die analiese van 20 "calculi" deur die interne standaard metode. Daar is afgelei dat die verkryging van akkurate resultate met behulp van die metode nie maklik bereikbaar is nie weens probleme soos die beskikbaarheid van standaarde vir die nabootsing van steen samestelling, monster voorbereiding, oorvleuling van refleksies van komponente in die monsters en standaarde en die vereiste vir oneindige dik monsters (>250mg). Vir die mikro-analitiese tegniek, is mikro-kwantiteite van 10 "calculi" van die oorspronklike 20 gedeponeer op silwer filters en kwantitatief ge-analiseer deur attenuasie van beide die Ag piek en die afsonderlik gemete absorpsie koëffisiënte .

Atoom-emissie spektroskopie vanaf 'n induktiefgekoppelde plasma is ook ontwikkel en gebruik in hierdie studie. Verskeie metodes om die "calculi" te verteer is getoets en daar is gevind dat 'n mengsel van  $\text{HNO}_3$  en  $\text{HClO}_4$  die geskikste is. Die hoof-elemente Ca, Mg en P is in 41 "calculi" bepaal. Vir die bepaling van spoorelemente, is 'n nuwe mikrogolf-ondersteunde prosedure gebruik vir die vertering van 100 "calculi". Daarna is die hoof-elemente Ca, Mg en P gelyktydig met die minderheid- en spoorelemente Al, Cu, Fe, K, Li, Mn, Mo, Na, Pb, S, Sr en Zn in al 100 stene bepaal. Die data so verkry was volgens 3 verskillende statistiese metodes ge-analiseer, naamlik direkte korrelasies, "scatter plots" en multi-variante analise. Verskeie interessante korrelasies is gevind.

Fluoried konsentrasies in twee steen versamelings - 20 "calculi" vanaf Indië en 42 van Suid-Afrika - was bepaal deur gebruik te maak van 'n fluoried-ioonsensitiewe elektrode en die  $\text{HNO}_3/\text{HClO}_4$  verteringsprosedure vir atoom-emissie spektroskopie. Direkte meting van fluoried was onsuksesvol en 'n diffusietegniek moes ondersoek en ontwikkel word. Deur gebruik te maak van hierdie tegniek kon die fluoried inhoud van beide versamelings bepaal word.

'n Reeks kristallisatie eksperimente met 'n kunsmatige urine standaard is uitgevoer in 'n roterende verdampapparaat. Die effek van pH en urine samestelling was bestudeer deur die pH te varieer en deur sekere komponente (Urinesuur, Urea, Kreatinine,  $\text{MgO}$ , metileen-blou, chondraitin sulfaat A, fluoried) by die standaardoplossing by te voeg. Kristalle wat sodoende gevorm is, is ge-analiseer deur kwalitatiewe en semi-kwantitatiewe X-straal poeierdiffraksieanaliese. Skandeer-elektronmikroskopie is ook uitgevoer. Soortgelyke neerslae soos die waargeneem in "calculi", is verkry in die vinnige verdampapparaat. Die resultate wat gevind is dui aan dat hierdie sisteem 'n eenvoudige, dog baie bruikbare metode bied vir die bestudering van kristallasie in urine oplossings.

Die kwantitatiewe analitiese prosedure wat ontwikkel en beskryf word in hierdie tesis, kan dien as model tegnieke vir ander werkers in steen navorsing. Saam met ander metodes soos die kristallisatie eksperimente wat bespreek is, kan hierdie prosedures lei tot 'n beter kennis en insig van aetiologiese prosesse wat steenvorming bepaal.

## Publications

A.L. Rodgers, S. Scaillet and M. Wandt

Procedure for the characterization of apatite in urinary calculi

Urinary Stone, Proc. 2nd Int. Urinary Stone Conf., Singapore, 1983; R.L. Ryall, J.G. Brockis, V.R. Marshall, B. Finlayson (Eds.), Churchill Livingstone, Melbourne, 1984, pp. 331-338

M.A.E. Wandt, M.A.B. Pougnet and A.L. Rodgers

Determination of calcium, magnesium and phosphorus in human stones by inductively coupled plasma atomic-emission spectroscopy

Analyst (London) 109(8), 1071-1074, 1984

M.A.E. Wandt, M.A.B. Pougnet and A.L. Rodgers

Analysis of urinary calculi by inductively coupled plasma-atomic emission spectroscopy: New insight into stone structure

Urolithiasis Related Clin. Res., Proc. 5th Int. Symp., Garmisch-Partenkirchen, 1984; P.O. Schwille, L.H. Smith, W.G. Robertson, W. Vahlensieck (Eds.), Plenum, New York, 1985, pp. 699-702

A.L. Rodgers and M.A.E. Wandt

Crystallization characteristics of synthetic urine in a fast evaporator

Urolithiasis Related Clin. Res., Proc. 5th Int. Symp., Garmisch-Partenkirchen, 1984; P.O. Schwille, L.H. Smith, W.G. Robertson, W. Vahlensieck (Eds.), Plenum, New York, 1985, pp. 765-768

M.A.B. Pougnet and M.A.E. Wandt

Microwave digestion procedure for ICP-AES analysis of biological samples

ChemSA 12(1), 16-18, 1986



## Contents

	page
Abstract . . . . .	(iv)
Acknowledgements . . . . .	(vi)
Publications . . . . .	(viii)
Contents . . . . .	(ix)
Abbreviations . . . . .	(xiii)
Symbols . . . . .	(xv)
 Introduction . . . . .	 1
1. Urinary stone disease . . . . .	1
2. Theories of stone formation . . . . .	4
3. Therapeutic regimens . . . . .	6
4. Stone analysis . . . . .	7
5. Objectives . . . . .	10
 Chapter I. Quantitative x-ray diffraction analysis of uroliths	 13
1. Introduction . . . . .	13
2. Qualitative x-ray powder diffraction analysis . . . . .	16
2.1 Methods of x-ray powder diffraction . . . . .	16
2.2 Theory and practical realization . . . . .	17
3. Intensity - composition . . . . .	20
4. Factors influencing intensity determination . . . . .	23
4.1 Diffraction geometry . . . . .	23
4.2 Sample dependent parameters . . . . .	24
4.2.1 Sample properties . . . . .	24
4.2.2 Sample preparation . . . . .	26
4.3 Intensity measurement . . . . .	29
5. Methods of quantitative x-ray powder diffraction analysis	30
5.1 External standard technique . . . . .	31
5.2 Diffraction-absorption technique . . . . .	32
5.3 Doping techniques . . . . .	32
5.4 Internal standard techniques . . . . .	33
5.4.1 Standard requirements . . . . .	34
5.4.2 Calibration curves . . . . .	35

5.4.3 Reference intensity ratio . . . . .	36
5.4.4 Flushing agent . . . . .	38
5.5 Microanalysis . . . . .	40
5.6 Comparison of methods . . . . .	43
6. Experimental procedures . . . . .	45
6.1 Equipment . . . . .	47
6.2 Standards and samples . . . . .	47
6.2.1 Materials . . . . .	47
6.2.2 Sample preparation . . . . .	48
6.2.3 Membrane mount . . . . .	50
6.3 Phase and intensity determination . . . . .	54
7. Results and discussion . . . . .	57
8. Conclusions . . . . .	66

## Chapter II. Application of inductively coupled plasma atomic-emission spectroscopy as an analytical tool in urolithiasis studies . . . . .

1. Introduction . . . . .	69
2. ICP-AES . . . . .	71
2.1 Introduction . . . . .	71
2.2 Instrumentation and operating principles . . . . .	74
2.2.1 ICP torch . . . . .	74
2.2.2 Sample introduction . . . . .	77
2.2.3 Optical system . . . . .	78
2.2.4 Electronics . . . . .	80
2.3 Method development . . . . .	80
2.3.1 Spectral lines . . . . .	81
2.3.2 Detection limits . . . . .	81
2.3.3 Calibration curves and dynamic range . . . . .	82
2.3.4 Interferences . . . . .	82
3. Sample preparation procedures . . . . .	85
3.1 Wet digestion techniques . . . . .	85
3.2 Microwave digestion procedure . . . . .	88
4. Determination of calcium, magnesium and phosphorus in human stones . . . . .	91
4.1 Instrumentation and apparatus . . . . .	91
4.2 Samples and standards . . . . .	92
4.3 ICP experimental conditions . . . . .	94

4.4 Results and discussion . . . . .	98
4.5 Conclusions . . . . .	102
5. Major and trace element analysis of urinary calculi . . . . .	102
5.1 Instrumentation and apparatus . . . . .	103
5.2 Samples and standards . . . . .	105
5.3 ICP experimental conditions . . . . .	107
5.4 Results and comment . . . . .	116
5.4.1 Procedural tests . . . . .	116
5.4.2 Analytical data . . . . .	119
5.5 Discussion . . . . .	124
5.5.1 Statistical analysis . . . . .	128
5.5.2 Trace elements in calculi and their significance in urolithiasis . . . . .	133
5.6 Conclusions . . . . .	139

### Chapter III. Quantitative analysis of fluoride in urinary

calculi . . . . .	143
1. Introduction: Fluorine and urolithiasis . . . . .	143
2. Analytical techniques for fluoride determination . . . . .	144
3. Direct determination of fluoride with ion selective electrode . . . . .	147
3.1 Measurement techniques . . . . .	148
3.2 Factors influencing fluoride determination . . . . .	149
3.2.1 Electrode performance . . . . .	149
3.2.2 Temperature . . . . .	150
3.2.3 Response time . . . . .	150
3.2.4 Stirring . . . . .	151
3.2.5 pH . . . . .	151
3.2.6 Interferences . . . . .	152
3.2.7 Ionic strength . . . . .	153
3.3 Equipment and procedure . . . . .	154
3.3.1 Electrode . . . . .	154
3.3.2 Standards . . . . .	154
3.3.3 Sample preparation . . . . .	154
3.4 Calibration . . . . .	155
3.5 Detection limit . . . . .	158
3.6 Total ionic strength adjustment buffers (TISABs) . . . . .	160
3.7 Conclusions . . . . .	165

4. Diffusion method . . . . .	166
4.1 Method development and procedure . . . . .	166
4.1.1 Apparatus . . . . .	166
4.1.2 Reagents . . . . .	167
4.1.3 Procedure . . . . .	168
4.2 Diffusion parameters . . . . .	169
4.3 Recovery, calibration and reproducibility . . . . .	170
5. Results and discussion . . . . .	178
 <b>Chapter IV. Crystallization characteristics of synthetic urines</b>	
in a fast evaporator . . . . .	187
1. Introduction . . . . .	187
2. Experimental conditions . . . . .	188
3. Results . . . . .	194
4. Discussion . . . . .	199
 <b>Concluding comments . . . . .</b>	<b>210</b>
 <b>References . . . . .</b>	<b>211</b>
1. Introduction . . . . .	211
2. Chapter I . . . . .	219
3. Chapter II . . . . .	238
4. Chapter III . . . . .	253
5. Chapter IV . . . . .	262

## Abbreviations

AAS	atomic absorption spectroscopy
AAU	ammonium acid urate
ac	alternating current
AES	atomic emission spectroscopy
AOAC	Association of Official Analytical Chemists
APA	calcium phosphate (apatite)
BRU	brushite
CaOx	calcium oxalate
CAP	carbonate apatite
COD	calcium oxalate dihydrate (weddellite)
COM	calcium oxalate monohydrate (whewellite)
COT	calcium oxalate trihydrate
CYS	cystine
dc	direct current
dd	deionized distilled (water)
FWHM	full width half maximum
HAP	hydroxyapatite
HMDS	hexamethyldisiloxane
IAEA	International Atomic Energy Agency
ICP	inductively coupled plasma
IR	infra-red (spectroscopy)
IUPAC	International Union of Pure and Applied Chemistry
JCPDS	Joint Committee on Powder Diffraction Standards
lld	lower limit of detection
MSMPR	mixed suspension mixed product removal (crystallizer)
NAA	nuclear activation analysis
NBS	National Bureau of Standards (U.S.)
nd	not detectable
NEW	magnesium hydrogen phosphate (newberyite)
OCP	octacalcium phosphate
OES	optical emission spectrography
PDF	powder diffraction file
PTFE	polytetrafluoro ethylene
QXRD	quantitative x-ray-diffraction analysis

rf	radiofrequency
RIR	reference intensity ratio
RSD	relative standard deviation
SAU	sodium acid urate
SEM	scanning electron microscope (microscopy)
SOEKOR	Southern Oil Exploration Corporation (Pty) Ltd.
SRAU	standard reference artificial urine
SRM	standard reference material
STR	magnesium ammonium phosphate hexahydrate (struvite)
TISAB	total ionic strength adjustment buffer
UA	uric acid
UAD	uric acid dihydrate
WHI	tri-calcium phosphate (whitlockite)
WHO	World Health Organization
XAN	xanthine
XRD	x-ray diffraction
XRF	x-ray fluorescence spectroscopy

# Symbols

$a_A$	activity of element A
$A$	absorption factor
$A$	area (over which sample is distributed)
$b$	particle size
$c$	velocity of light
$c_A$	true concentration of element A
$c_A^m$	apparent concentration of element A
$c_{lld}^l$	lower limit of detection in sample solution (liquid)
$c_{lld}^s$	lower limit of detection in sample (solid)
$d_{hkl}$	inter planar spacing
$e$	electron charge ( $1.602 \cdot 10^{-19}$ Cb)
$E$	cell potential
$E_0$	reference electrode and junction potential contributions
$f_m(\theta)$	atomic form factor (of atom m)
$F$	Faraday constant ( $96484.56$ Cb.mol $^{-1}$ )
$F_{hkl}$	structure amplitude (of reflex hkl)
$\underline{G}$	reciprocal lattice vector
$I_A$	from element A emitted intensity
$I_B$	background intensity
$I_C$	intensity of (113) corundum reflection
$I_{hkl}$	intensity of x-rays diffracted by plane (hkl)
$I^i$	integrated intensity
$I_{ij}$	diffracted intensity of reflex i of component J
$(I_{ij})_0$	intensity of reflex i of component J in pure phase J
$I^p$	peak intensity
$I^{zz}$	relative intensity zz (scaled to 100 for strongest peak)
$I_0$	incident (primary) x-ray intensity
$\underline{k}$	wave vector
$k_{ij}$	proportional constant in intensity-concentration relationship
$K_1$	diffractometer constant
$K_2$	specimen constant
$L_p$	Lorentz polarization factor
$m_e$	electron mass ( $9.1095 \cdot 10^{-31}$ kg)
$M$	sample mass

N	number of unit cells per unit volume
p	multiplicity of a reflection
p	proton
R	gas constant ( $8.3144 \text{ J mol}^{-1} \text{ K}^{-1}$ )
$RIR_{A,S}$	reference intensity ratio (analyte A, standard S)
r	sample-detector distance
$r^2$	coefficient of determination
RSD	relative standard deviation
$RSD_0$	within laboratory RSD
$RSD_x$	among laboratories RSD
S	electrode slope ( $=R \cdot T \cdot F^{-1}$ )
t	sample thickness
T	absolute temperature
T	by sample transmitted intensity
$T_{DW}$	Debye-Waller temperature factor
$T_J$	by sample of pure component J transmitted intensity
V	irradiated sample volume
$V_J$	volume fraction of compound J
w	slit width of detector
$x_m$	x-coordinate of atom m's position in the unit cell
$X_F$	mass fraction of flushing agent
$X_J$	mass fraction of component J
$y_m$	y-coordinate of atom m's position in the unit cell
$z_m$	z-coordinate of atom m's position in the unit cell
$\alpha$	alpha particle
$\gamma$	activity coefficient
$\gamma$	gamma ray
$\Delta$	difference of two quantities
$\eta$	amount of component sought, added per gram of sample
$\theta_{hkl}$	diffraction angle
$\kappa$	scaling factor
$\lambda$	wave length
$\mu$	linear absorption coefficient
$\bar{\mu}$	mean linear absorption coefficient of sample
$\mu_J$	linear absorption coefficient of phase J
$\mu^*$	mass absorption coefficient
$\bar{\mu}^*$	mass absorption coefficient of mixture
$\mu_J^*$	mass absorption coefficient of phase J



$\mu_M^*$	mass absorption coefficient of matrix M
$\rho$	mean sample density
$\rho_J$	density of component J
$\rho'$	density of mounted powder (incl. interstices)
$\sigma$	mass per unit area of sample
$\sigma$	standard deviation
$\sigma_B$	standard deviation of 10 blank signal readings
$\sigma_J$	mass per unit area of component J



## Introduction

### 1. Urinary stone disease

Stones are an age-old anguish of the human body and occur at several sites, in particular the kidney, bladder, gall-bladder, prostate gland, salivary gland and pancreas /LON68, LON68a, ROD81/. Reports from antiquity as well as from modern time clinicians reveal that, although not necessarily life-threatening, stones were - and still are - a source of considerable pain /BUT56, CLA68, MOD80/. Hence, many techniques have been developed over the years to investigate this disease and today the most sophisticated of these are utilized in concerted efforts directed at gaining insight into the mechanism of stone growth.

Various similarities and common features of the different types of stone have emerged. For example, basic physico-chemical principles dictate that the formation of a concretion is always associated with a highly concentrated fluid in a particular gland or secretory organ followed by precipitation of the stone salt. An organic matrix within the stone structure is another common feature.

Among the different stone afflictions, urinary calculus disease is one of the oldest known medical disorders of mankind. As early as the third century BC the Greek physician Ammonios used the technique of lithotritry to break up bladder stones mechanically so that they could be passed in the urine. The bladder stone was the typical urinary concrement of history. Today, a fundamental change in the pattern of calculus disease reveals renal and ureteric stones to be the characteristic clinical manifestation of the ailment. Over the past 30 years, world-wide prevalence of renal calculi in particular has multiplied, paralleled by generally increasing prosperity. It is reported that in 1979 about 5% of the entire (West) German population contracted one or more stones during their lifetime /HES81a/. In the United States, where even the occurrence of calculi in space has attracted attention /BUS68/, about 200,000 kidney stone patients are admitted to hospital

annually /ENG84/. In South Africa also, renal stones are fairly common /MOD69/. Since figures of stone frequency are usually based on hospital statistics only, many more people might be potential stone sufferers. Hence, some researchers believe that kidney stones are as common as diabetes and high blood pressure /ENG84/. This has led to the ailment of urinary stones being designated a 'public disease' /HES83/.

From the aforesaid it is not surprising that a great deal of scientific effort has been directed at investigating the prevention and dissolution of calculi /BRO81, FLE76, SCH85, SMI81/. However, the hope that such studies would reveal the cause of urinary lithiasis has not yet been realized, the main difficulty being the multiplicity of factors contributing to the formation of stones. As a result, the specific combination of these factors has to be determined separately in each individual case.

Amongst the causal factors, pathological changes of the kidney and metabolic disorders like hypercalciuria, hyperoxaluria, cystinuria, etc. /PAK76a/ in addition to geographical, environmental, ethnic and familial parameters have been shown to predispose certain people to stone disease /VAH79/.

Geographic correlations of urolithiasis show differences in incidence related to the development and economy of countries and communities. According to Gundlach /GUN68/, the prevalence of renal calculi is correlated directly with the net income of a population group, probably as a result of increased ingestion of animal protein with increasing wealth. Sutor observed changes in stone type and composition, as countries become technologically developed /SUT71/. Further evidence in support of the suggested role of diet in urolithiasis is provided by the occurrence of stone waves in times of prosperity /VAH79/.

Environmental variables include climate, occupation and personal circumstances. An increased incidence of renal stones with rise in atmospheric temperature has been observed and a higher prevalence of stones in persons with occupations which entail exposure to high environmental temperatures (e.g. cooks, ship-board engineers) is well documented /BLA82/. Another factor is the physical activity associated with

certain occupations - the more sedentary a job, the higher the frequency of stones.

Regarding other 'personal' parameters, a positive family history also seems to be correlated with multiple occurrences of calculi /KLE80/. The observation that calculi are rare amongst certain racial groups further raises the question of the importance of genetic influences and heredity. Most studies, however, point more to the involvement of nutritional and dietary factors which are nowadays considered to represent the most significant determinant in the epidemiology of stones.

It is thus understood that urinary stone formation is a complex process involving many variables, the pathogenesis of which is not completely clear. Of the multitude of factors, only a few are well known and in only 2 cases, hyperparathyroidism and uric acid stone formation, has consensus about the underlying principles been reached.

Investigation of the fundamental causes of urolithiasis involves both clinical and scientific approaches. On the one hand, the clinician is mostly concerned with in vivo characterization of the primary aetiological-biological factors of the various metabolic disorders contributing to the disease. From such studies new (empirical) measures for the treatment of the clinical picture of stones can be derived. On the other hand, scientific approaches to urolithiasis essentially embrace two areas: stone analysis and crystallization experiments.

Stone analysis enables the investigator to accurately characterize the chemical conditions prevailing at the time of nucleation and growth. A comprehensive analysis is important since identification of the stone nidus is vital in postulating aetiology and prescribing treatment. Moreover, careful analysis of the structure of a stone with respect to the sequential deposition of the various components provides data which reflect the changing chemical conditions during the stone's growth. In addition, nucleation and growth mechanisms may be deduced from ultra-structural studies. The analysis of calculi has shown that all stones formed within the urinary tract, irrespective of cause or composition, have, in addition to the crystalline inorganic substances,

a second basic component, namely an organic 'matrix' admixed with the crystal aggregates /BOY59/. This knowledge, together with data obtained from crystallization experiments, has led to the development of two well-substantiated theories of stone formation. These are discussed in section 2 below.

The crystallization approach considers stone formation to be part of the field of biomineralization, a special case of general crystallization phenomena of slightly soluble salts. Both real and artificial urines have been employed in investigating the influence of physico-chemical parameters such as concentration and pH on crystallization products. In particular stagnant systems as well as continuous crystallizers have been used extensively to simulate the crystallization properties of the urinary tract. Experiments conducted with the fast evaporator represent another recent attempt to gain insight into the more fundamental factors of stone formation (see chapter IV). Common to all these procedures is the objective of studying the basic concepts underlying the genesis of calculi in the hope of identifying inhibitors of stone formation which will eventually lead to the discovery of new therapeutic regimens.

## 2. Theories of stone formation

Definition of the initiating factor in stone formation is under much dispute. On the one hand is the hypothesis that stone matrix, which constitutes about 2-10% of the total mass, plays an extremely important and decisive role /BOY54, BOY55, BOY56/. According to this theory, the condensation of specific organic colloids is thought to be the primary process in calculogenesis /BOY63, SNA36/. The deposition of inorganic salts is then regarded as a secondary phenomenon. It is conceivable that the organic substances which have been detected in calculi act as a trigger for heterogeneous nucleation of stone salts, which are then adsorbed onto the matrix skeleton. Nevertheless, direct proof that active sites in the matrix induce formation of crystal nuclei or that matrix plays the suggested architectonic role is still to be presented.

On the other hand is another hypothesis according to which stone matrix is not considered crucial but rather as being incidentally included in the stone by protein co-precipitation /FIN61, VER65/. This (crystallization) theory, which has its origin in the work of Keyser /KEY23/ and Meyer /MEY29/, emphasizes the physico-chemical and crystallographic elements of stone nucleation and growth /PHI58, PRI55, RAA63/. According to this approach, urinary supersaturation is the driving force: when the activity product of the crystal forming ions is greater than the minimal thermodynamic solubility product, spontaneous precipitation of stone salts will occur /FIN77/. By evaluating urinary supersaturation, conclusions about possible precipitates can be drawn, and it is feasible to further investigate (experimentally) mechanisms of precipitation and stone growth.

There are 3 mechanisms which are of importance in stone formation. These are nucleation, crystal growth and aggregation /FIN78, NAN83/. Nucleation refers to the 'birth' of sub-microscopic molecular species of 'critical size' within the supersaturated solution /VER66/. This initial event can be either of the homogeneous type in which case particles of the same compound nucleate on each other or of the heterogeneous type involving nucleation of one compound on another. Once nuclei are present, the second mechanism becomes operative, i.e. growth /NAN76/. As a consequence of ongoing or recurrent supersaturation and other factors, aggregation of the formed crystals may occur, either by 'sintering' or by interparticle bridging of polymeric material /FIN77/. With the subsequent trapping of the resulting polycrystalline mass in the kidney, a stone is formed.

An additional important concept for explaining (heterogeneous) nucleation and growth of multi-component urinary calculi was introduced by Lonsdale /LON68/. Epitaxy involves the interaction of two or more different substances with matching crystalline lattices. Many such systems have been investigated over the past 10 years /KOU80, KOU81, MAN80, PAK76/. It has been confirmed that seed crystals of one substance can induce the growth of a second phase from metastable supersaturated solutions (e.g. COM on HAP /MEY75/ and COM on UA /MEY76/).

Interest in stone ultrastructure has resulted in new ideas of stone formation mechanisms /FIN72, MAL77, MEY71/. Following the promotion of the stone matrix theory by Boyce and co-workers in the 1950s, complex chemical and crystallographic theories dominated the following decade. Today it is the role of macromolecules which is receiving most attention. Recently, isolated mucoproteins have been shown to promote precipitation of all the more important stone salts /HAL79, PAT80/. The new role ascribed to matrix is now "that of a binder, serving to 'cement' an otherwise loose aggregate of crystals into a structurally cohesive unit" /OGB81/.

In contrast to the above, other human urinary macromolecules are thought to have a protective (inhibitory) effect on the crystallization or agglomeration of stone salts /GIL76, LEA77, ROB76/. Low molecular weight substances present in urine were also shown to prevent calcification /BAR74, FIN74/. Amongst these are natural inhibitors like citrate, pyrophosphate and magnesium. Synthetic inhibitors such as diphosphonates are also very powerful in suppressing precipitation and aggregation of crystals /FLE78, PAK75/. Promoters and inhibitors of stone formation are thus thought to be another important factor in modifying urine crystallization parameters. The search for more effective inhibitors has resulted in the discovery of many agents which are now used in the treatment of urolithiasis.

### 3. Therapeutic regimens

Notwithstanding the afore-said, current modes of therapy are mostly directed towards reducing urinary (super)saturation of stone forming salts. If a state of undersaturation can be reached, existing stones should dissolve. The validity of this hypothesis has been demonstrated by local irrigation of calculi and their dissolution with (calcium) chelating agents /MUL62, RUT61, ZIO77/. Shifting the pH of urine to make it less congenial for stone formation is another approach to the dissolution of calculi based on crystallization theory. In this way, struvite stones in rats were dissolved by acidification of urine /VER51/, while dissolution of uric acid calculi in man was achieved by



rigorously monitored alkalinization of urine /VER65/.

Dissolution of already existing calculi by a conservative medicinal treatment as well as prophylactic oral medication to prevent stone recurrence are the ultimate goals of all therapies. To achieve this, moderately successful therapeutic regimens have been developed for all types of stones over the past twenty years /ALK66, BAC83, NOR72, THO75/. Nevertheless, only the most recent pathophysiological findings allow the correlation of a certain stone type with distinct metabolic disorders /ALK82, MOD81, SCH67/. An exact stone analysis is, however, an essential prerequisite as a guide to selection of the appropriate therapy /SAG78, SCH71, SCH71a/. The popular belief that an incorrect analysis is better than none, cannot be accepted anymore, since an erroneous analysis might lead to a dangerous misapplication of medications /HES82a/.

#### 4. Stone analysis

As mentioned before, accurate knowledge of the chemical composition of calculi is important with regard to understanding its genesis and hence the introduction of suitable prophylactic measures. Conventional qualitative (wet chemical) analytical techniques are not adequate to meet modern requirements. At the very least, semi-quantitative determination of stone constituents is necessary for positive classification of a calculus. Prien /PRI74/ has listed the requirements of such a procedure: (i) accuracy, (ii) identification of compounds rather than radicals, (iii) sensitivity, (iv) at least semi-quantitative, (v) rapid, (vi) simple, (vii) convenient, and (viii) inexpensive. Hence many different techniques have been used in stone analysis in an attempt to fulfil these stringent demands.

Chemical analysis, while still the most extensively used technique, is unsatisfactory, since the qualitative procedures employed have only little diagnostic value and can produce erroneous results with stones of mixed composition. Confusion also exists as to the exact nature of reactions which take place in the very many procedures em-

ployed, most of which are based on schemes used in the 19th century. Most (wet) chemical analyses which have been employed in the past are limited almost entirely to qualitative or at most semi-quantitative results. Even when quantitative, the analyses have been restricted to only a few radicals or species. Truly quantitative procedures (e.g. /MAU69/) are usually unjustifiably laborious and time consuming. Hence, even in 1947 Prien and Frondel /PRI47/ found this type of analysis "unsatisfactory" and a recent round robin revealed it to be totally unacceptable /HES81/.

To improve the determination of metallic elements, atomic absorption spectroscopy (AAS) /ROB60/ has often been employed for the analysis of Ca and Mg /HOD71/. However, the determination of calcium in particular, is negatively affected by interferences from Na and K, as well as from organic matter. In addition, the action of certain anions, such as phosphate, have also been shown to affect calcium emission in a complex way. With the advent of better excitation sources (see chapter II), AAS has lost most of its appeal among the element sensitive methods available for the analysis of calculi.

Another element specific analytical technique is x-ray fluorescence /BER78, JEN70/. This method relies on determining the intensity of inner atomic transitions and not on excitation of outer-shell electrons, as is the case with AAS. The electronic state of the element has thus no influence on the concentration measurement. However, complicated absorption and enhancement effects in the sample influence the accurate determination of all elements, particularly in samples of varying composition, such as urinary stones.

The identification and quantification of elements using their characteristic x-radiation only gained significance after the advent of the scanning electron microscope (SEM) and the development of energy-dispersive x-ray analyzers. Although the (standardless) electron probe microanalysis is semiquantitative at best, it can nevertheless be very helpful in the investigation of uroliths, since the sample can be examined visually at the same time. This permits the operator to decide which phases are present on the basis of morphology, supplemented by elemental information /BAS74, BLA81, HES81b, SPE76/.

Thermogravimetric methods based on the thermal decomposition of a sample has also been used in the analysis of calculi /LIP67, STR66, STR69/. With this method, changes in the specimen's mass at particular temperatures are recorded during heating. Using thermal decomposition profiles, the presence of certain phases can be deduced /BER68, BER73, ROS76/. Because of its many sources of error, its complicated operation and the time involved for an analysis, this technique is not, however, suited for routine identification of calculi.

A shortcoming of most techniques discussed thus far, is their inability to identify the actual compounds present in a sample. Methods based on crystallographic investigations are far superior in this respect. For example, use of a polarizing microscope permits positive identification of the crystalline constituents in calculi /PRI41, RAN42/. This petrographic technique also offers the advantage that primary crystallization centres and distinct growth periods can be identified by investigation of thin sections /GEB, HES82b/. However, this method needs highly skilled personnel. On the other hand, x-ray diffraction analysis does not require trained technicians. The identification of stone constituents from powder diffraction patterns is by far the most powerful single method for distinct characterization of uroliths. Moreover, XRD has the potential of being truly quantitative, although this aspect has been largely neglected in its application to urolithiasis studies. An in-depth discussion of this technique is presented in chapter I of this thesis.

Infrared spectroscopy (IR) is another compound-selective method with superior features to conventional techniques /BEI55, OTT67, WEI59/. Many researchers believe that IR is the most appropriate and suitable method for routine qualitative and quantitative analysis of calculi /HES72, MOD81a, TSA61/. However, quantitative application of IR spectroscopy deserves special comment since it utilizes the principle of comparing the sample spectrum with spectra of known (mixtures of) compounds. Deviations in crystallinity, substitutions at the atomic level and sample preparation in general seem to hamper the proper quantitative application of this procedure /GRI73, KLI74/. Nevertheless, recent technical progress in instrument design has resulted in IR spectroscopy developing into a valuable tool for stone analysis

/HES82c, HES82d/.

During the past decade many authors have reported special analytical techniques which, although not without merit, have not enjoyed widespread application. These include activation analyses /MCC73/, mass spectrometry /HES77/, density gradient columns /ROD81a/, autoradiography /MCC80/, chromatographic contact prints /TOZ81/, etc. On the other hand, multiple technique approaches to stone analysis have also been advocated /BAK66, ROD81b, ROD82/. While a single technique might not independently provide a detailed picture of a stone's composition, the combination of two or more procedures can utilize each other's advantages and thereby acquire meaningful data.

Several workers have compared the efficiency of the various analytical methods available for characterization of calculi /BEE64, DOS74, SCH73/. Combinations of a crystallographic technique with one of the element sensitive procedures, or SEM, seem to be of great promise /HES81b, LEU81, ROD81c/. The only limitation on accurate compositional analyses, apart from the expense, thus appears to be the size of a stone, the majority of which are small (70% weigh less than 500 mg, 55% weigh less than 100 mg, 40% weigh less than 25 mg and 15% weigh less than 10 mg /GUN68, HOD69, MAU69, SCH71a/). Non-destructive analyses like XRD, which do not alter sample composition and permit specimens to be re-used, are therefore of great advantage.

## 5. Objectives

The search for more efficient therapeutic regimens has led to a demand for more accurate analyses of calculi. Qualitative techniques no longer fulfil present-day requirements and must be supplemented with more quantitative procedures. It is surprising that the unparalleled success of x-ray diffraction in the qualitative identification of stone constituents has not resulted in more quantitative applications of this technique. However, only but a few studies employing quantitative x-ray diffraction analysis (QXRDA) of uroliths have been published thus far. The first objective of the present study was therefore to review,

adapt, develop and test QXRDA procedures applicable to the powder diffractometer in the hope of establishing routine guidelines for other stone researchers interested in quantitative analyses.

In defining the above objective, it was recognized that a detailed, intimate picture of stone composition and structure is more likely to be attained by application of an element-specific analytical procedure in conjunction with QXRDA. The second objective in this study was thus to select a technique whereby major, minor and trace elements in calculi could be simultaneously determined using the same sample. Such a technique is inductively coupled plasma-atomic emission spectroscopy (ICP-AES). Investigation of its suitability in the field of stone research and definition of instrument parameters were thus undertaken as part of this objective.

Fluorine is a trace element of special interest. However, its quantitative measurement has many associated practical problems. Detailed, easy-to-follow procedures and methodologies have not been described with the result that investigators interested in this element are required to struggle with ill-defined and tedious experimental procedures. The third objective of this study was thus to determine fluoride by employing a diffusion procedure and electrochemical methods.

In an attempt to gain some insight into the physico-chemical factors which govern calcium oxalate crystallization processes, a fourth objective was defined. This was to conduct a series of crystallization experiments using a standard reference artificial urine (SRAU) in a rotary evaporator. Examination of the influence of pH and SRAU composition as well as the role of various natural and synthetic inhibitors were undertaken as part of this objective.

As suggested earlier in this section, scientific studies of urolithiasis embrace 2 main areas - that of stone analysis and that of crystallization experiments. The objectives as outlined above may thus be regarded as a double-pronged scientific study in which both approaches are utilized. In this way it is hoped that this thesis will ultimately make contributions to both the study and the understanding

of urolithiasis.

## Chapter I

### Quantitative x-ray diffraction analysis of uroliths

#### 1. Introduction

Accurate knowledge of the mineralogical composition of human stones should be helpful in understanding stone aetiology and has been proven to be fundamental to the introduction of prophylactic measures /MOD81/. Since urinary calculi are composed mainly of relatively insoluble crystalline substances, these can be easily identified by x-ray diffraction analytical techniques /LAG61/.

X-ray crystallographic methods are based on the ability of crystalline substances to diffract x-rays in a regular manner. 'Fingerprint-like' patterns, which alone depend on the symmetry class of a crystal and the position of its atoms in its unit cell, are obtained when monochromatic x-rays, diffracted from different parts of a crystal, interfere. Since urinary stones are not single-crystal in nature, but rather built from many crystallites, only powdered specimens can be examined. The powder diffraction patterns which such samples yield, are solely characteristic of the crystalline phase(s) present. They do neither indicate the elements nor the chemical radicals present in the samples. However, while the position of the peaks on the diffractogram can be utilized to identify all (crystalline) substances present, their respective intensities are a measure of the amount of each detected phase.

Historically, analytical powder x-ray diffraction started shortly after the discovery of the "x"-radiation by W.C. Röntgen in 1895 /ROE1895/ and the demonstration that x-rays can be diffracted with crystals by Friedrich et al. /FRI13/. Hull was the first to utilize powder patterns for qualitative chemical analysis and suggested intensity measurements to yield quantitative results /HUL17, HUL19/. Although as early as 1921 a compact and easy to operate commercial x-ray diffraction apparatus was marketed /DAV21/, 'useful' quantitative re-

sults were obtained only in the early 1930s, after absorption effects in the sample were taken into account. Thereafter, the development of quantitative x-ray diffraction analysis (QXRDA) took place in 3 distinct stages /ALE77/.

The early era (1935-1950) was marked by an empirical approach and by the photographic technique with all the limitations inherent in photometric measurements. Peak intensities were almost exclusively employed in the calculation of constituent concentrations, while extinction and microabsorption effects were largely neglected. In the transition period, lasting from the 50's to the 70's, the parafofocussing counter diffractometer was developed /FRI45, PAR65/ and the theoretical basis for the quantitative analysis of mixed polycrystalline phases was laid /ALE48, ALE48a, WIL50/. Later, the diffraction-absorption technique /LER53, LER57/ comprising the direct measurement of the absorption coefficient of diffracting samples, and the dilution method /COP58/ were brought into use. Also, the problem of superimposed lines was theoretically solved /COP58/. Finally, the recent era saw the development of microanalytical techniques for the determination of  $\mu\text{g}$  amounts of sample constituents /LER69, LER69a, LER70/. Most recently, computers have been applied to almost all aspects of QXRDA /SZA78a/. These applications include automated data acquisition systems /JEN71, KIN74, RIC71, SEG72, SLA72, SNY81, SNY82/, search/match identification procedures /EDM80, FRE76, MAR79, NIC80, PAR82, TIA83/ and analytical routines /GOE83, HUA82, JEN75, JOB82, PYR83/ like the NBS\*QUANT82 /HUB83/ and QXDA /HEC75/ programmes used in the present study.

Although Griffith /GRI78/ mentioned MacIntyre to have demonstrated renal calculi with x-rays as early as 1896, Saupe /SAU31/ is generally accepted to have been the first to report the application of x-radiation to the investigation of human concretions. Subsequently, Ranganathan /RAN31/ undertook XRD studies of vesical and biliary calculi, while Burgers /BUR33/ diagnosed an ureter stone by comparing its interference pattern with that of calcium oxalate. Phemister /PHE39/ employed "roentgenographic powder diagrams" to identify gall stones and already in 1940 Jensen /JEN40, JEN41/ found the x-ray powder method superior to other analytical techniques when unequivocal identification of concrement substances was desired. In the following decade many researchers



used XRD to examine human and animal calculi with the aim of identifying the crystalline phases present /BAN47, BAR44, BRA47, BRA47a, BRA48, BRA49, CAR53, EPP50, FRO42, HED53/. Soon, the similarity of the XRD patterns from calcified substances in man (e.g. bone, prostatic calculi) and the apatite series of minerals was discovered /BRA45, HUG44/. In this and other cases, XRD was a helpful instrument in exactly defining the then somewhat vague terms for different concreted substances. As a result, from then on, the XRD technique has been employed as the analytical method of choice in almost all the large stone studies for composition identification (/BAS74/ (200), /CAR69/ (800), /GIB74/ (15000), /GRU64/ (1000), /HAZ74, HAZ74a/ (200), /HER62/ (10000), /MOR67/ (460), /PAR64/ (880), /PRI49/ (1000), /SCH70/ (200), /SCH74/ (3500); figures in brackets denote the number of calculi analysed in each respective study). In addition, the extensive investigations by Sutor and Wooley deserve to be mentioned /SUT69, SUT70, SUT71, SUT72, SUT74/. However, discrepancies were noted among results from the various series of analyses /MOR67/. These differences might have originated as a result of both the difficulties experienced when attempting to identify the apatite XRD pattern, and the discovery of new stone phases with increasing sensitivity of the XRD technique. Therefore, comparison of the different stone collections must be made with caution.

Nevertheless, round robin tests have revealed x-ray crystal analysis to be the best procedure, closely followed by IR, for the characterization of urinary calculi /HES81/. The advantages of XRD identification, as summarized by Warren in 1934 /WAR34/, are still valid today:

- (i) a definite crystalline modification is identified;
- (ii) sharp differentiation between crystalline and amorphous materials is made;
- (iii) definite identification of different components in one sample is possible;
- (iv) samples can be re-used;
- (v) the production of an XRD pattern is very simple.

The only criticism to be made is probably the high cost of the instrument, calling for a centralization of analyses /SCH70a/.

Although XRD thus seems to be a favourable qualitative procedure,

the advancement of **quantitative** XRD techniques for urinary stone analysis has been impeded by the problems created through the variable degrees of crystallinity of calculi components. Since most of them are crystallographically heterogeneous and / or contain considerable amounts of inorganic matter and loosely bound water, quantitative classification of the calculi themselves is not an easy task. Hence, of the very many research projects employing XRD methods, only few have thus far utilized their quantitative potential /GEB76, LAG56, OTN80, SCH74a/. Therefore, in the present study, it was decided to first review the theories underlying QXRDA and to examine and evaluate the available analytical approaches in implementing these general principles in practice. After briefly discussing qualitative XRD (section 2), an intensity-composition relationship will be derived (section 3). In section 4 experimental parameters influencing analyses are evaluated, while in section 5 quantitative techniques are thoroughly described including microanalytical procedures. After a discussion of the experimental procedures employed in the present study, 'reference intensity ratios' /HUB76/, which were measured for 6 major stone phases, are listed. Subsequently results for 20 calculi analysed by different methods are compared with data obtained from ICP-AES analyses (chapter II).

## 2. Qualitative x-ray powder diffraction analysis

### 2.1 Methods of x-ray powder diffraction

Currently 4 techniques are available for the acquisition of powder patterns, two of which yield strip-charts, while the remaining two require photographic processing facilities:

- (i) Debye-Scherrer film method,
- (ii) Guinier-film method,
- (iii) goniometer (diffractometer) technique,
- (iv) Guinier-goniometer technique /JUM65/.

The pros and cons of these methods have been extensively discussed by other workers /GEB79, HES82, JUM65, SCH74a/ and their advantages shall be mentioned here only briefly.

While the small sample size of 0.1 - 0.3 mg for the Debye-Scherrer method is advantageous, the Guinier-film method features a much better resolution and allows simultaneous analysis of more than one sample. The goniometer, on the other hand, dispenses with recording the patterns on film, but employs a counting tube. Although at least 10 - 15 mg sample mass is needed, this method is widely applied since it is about 10 times faster than the film methods. The best results, however, are obtained with the Guinier goniometer /JUM65/. However, alignment of this apparatus is very complicated which is why it is deemed unsuitable for routine analysis of calculi /SCH74a/.

In the present study, a Debye-Scherrer camera and powder diffractometer with Bragg-Brentano geometry were extensively used. This type of goniometer is probably the most versatile and widely known instrument available. The results obtained in the present study should therefore be applicable to many stone laboratories utilizing XRD procedures. In the following section, the generation of diffraction patterns is described.

## 2.2 Theory and practical realization

Any diffraction pattern, i.e. a plot of diffraction angle vs. intensity, can be considered to consist of (i) the positions of diffraction maxima, and (ii) the intensities of these maxima. In qualitative analysis it is the peak positions and their relative intensities which are of interest. The diffraction angles are related to the size and shape of the crystal lattice (symmetry) on which the crystal structure is built. This relationship is expressed by the Bragg equation

$$n \cdot \lambda = 2 \cdot d_{hkl} \cdot \sin \theta_{hkl} \quad (I.1)$$

which relates the observed diffraction angle  $\theta_{hkl}$  with the wavelength  $\lambda$  of the used radiation and the interplanar spacing  $d_{hkl}$  of the diffracting planes. Equations relating the  $d_{hkl}$  values and the parameters which describe the direct lattice are very complex and are more simply stated in terms of the reciprocal lattice. In this model the Bragg equation is simplified to

$$\Delta \underline{k} = \underline{G}$$

(I.2)

i.e., the change in the wavevector  $\Delta \underline{k}$  of the diffracted ray equals a reciprocal lattice vector  $\underline{G}$ .

By measuring all prominent diffracted maxima and calculating the respective d-spacings, a diffractogram allows the unequivocal identification of the crystalline phase producing it. However, the vital first step in obtaining accurate d-spacings is a well aligned diffractometer. This is usually not available in a multi-user environment whereby allowance for experimental errors has to be made.

If the sample is a mixture of more than one crystalline compound, the diffraction pattern obtained will be a superposition of the individual patterns characteristic of each component. Unscrambling such a pattern then either proceeds by comparison with standard diagrams or with the help of the JCPDS powder diffraction file (PDF). The PDF currently consists of about 40000 XRD patterns /WON83/ and its use in the identification of unknown materials with the help of the Hanawalt index /HAN38/ has been demonstrated as early as 1939 /DAV39/. In the case of urinary calculi, where all important components are known, the search need only be carried out over a limited range of about 25 to 30 compounds (table I.1). It has therefore been concluded that qualitative XRD analysis with its exact reproducibility, non time-consuming procedures, minimal sample size requirements and maximum exposition is an excellent technique for the qualitative analysis of uroliths /SCH74a/.

Since the second quantity which can be derived from the diffraction pattern, viz., the intensity of the interferences, is indispensable to quantitative analysis, its theoretical derivation and measurement in practice will be discussed in the next section. However, all expressions derived will be limited to those applicable to the powder diffractometer.

Table I.1. Chemical composition and mineralogical names of components demonstrated in urinary calculi.

component	mineral name	formula
(i) major components		
calcium oxalate monohydrate	whewellite	$\text{CaC}_2\text{O}_4 \cdot \text{H}_2\text{O}$
calcium oxalate dihydrate	weddellite	$\text{CaC}_2\text{O}_4 \cdot 2\text{H}_2\text{O}$
hydroxyapatite		$\text{Ca}_{10}(\text{PO}_4)_6(\text{OH})_2$
carbonateapatite	dahllite	$\text{Ca}_{10}(\text{PO}_4, \text{CO}_3)_6(\text{CO}_3, \text{OH})_2$
calcium monohydrogen phosphate dihydrate	brushite	$\text{CaHPO}_4 \cdot 2\text{H}_2\text{O}$
$\beta$ -tricalcium phosphate	whitlockite	$\text{Ca}_3(\text{PO}_4)_2$
magnesium ammonium phosphate hexahydrate	struvite	$\text{MgNH}_4\text{PO}_4 \cdot 6\text{H}_2\text{O}$
uric acid	uricite	$\text{C}_5\text{H}_4\text{N}_4\text{O}_3$
uric acid dihydrate	-	$\text{C}_5\text{H}_4\text{N}_4\text{O}_3 \cdot 2\text{H}_2\text{O}$
(ii) minor components		
iron oxalate dihydrate	humboldtine	$\text{FeC}_2\text{O}_4 \cdot 2\text{H}_2\text{O}$
octacalcium phosphate	-	$\text{Ca}_8\text{H}_2(\text{PO}_4)_6 \cdot 5\text{H}_2\text{O}$
calcium monohydrogen phosphate	monetite	$\text{CaHPO}_4$
tri-magnesium phosphate octahydrate	bobierite	$\text{Mg}_3(\text{PO}_4)_2 \cdot 8\text{H}_2\text{O}$
magnesium monohydrogen phosphate trihydrate	newberyite	$\text{MgHPO}_4 \cdot 3\text{H}_2\text{O}$
zinc phosphate tetrahydrate	hopeite	$\text{Zn}_3(\text{PO}_4)_2 \cdot 4\text{H}_2\text{O}$
magnesium ammonium phosphate monohydrate	-	$\text{MgNH}_4\text{PO}_4 \cdot \text{H}_2\text{O}$
calcium carbonate	calcite	$\text{CaCO}_3$
silicon dioxide	$\alpha$ -quartz	$\text{SiO}_2$
mono-ammonium urate	-	$\text{C}_5\text{H}_7\text{N}_5\text{O}_3$
mono-sodium urate monohydrate	-	$\text{NaC}_5\text{H}_3\text{N}_4\text{O}_3 \cdot \text{H}_2\text{O}$
l-cystine	-	$\text{C}_6\text{H}_{12}\text{N}_2\text{O}_4\text{S}_2$
xanthine	-	$\text{C}_5\text{H}_4\text{N}_4\text{O}_2$

### 3. Intensity - composition relationship

Aside from the distinct position of diffraction maxima arising from a crystalline structure, a further distinguishing feature of powder patterns are the relative intensities of the different lines. The intensity  $I_{hkl}$  of a reflection (hkl) is a function of the type of atoms in the unit cell and the arrangement thereof. For the standard diffractometer, the expression relating the measured intensity from a single-phase sample to these variables can be derived from x-ray diffraction theory /AZA68, BUN61/ and is given below:

$$I_{hkl} = \kappa \cdot [I_0 \cdot k_1 \cdot k_2] \cdot [N^2 \cdot p \cdot |F_{hkl}|^2] \cdot L_p \cdot T_{DW} \cdot A \cdot V \quad (I.3)$$

where  $I_{hkl}$  is the intensity of x-rays diffracted by plane (hkl) and  $I_0$  denotes the intensity of the primary beam.  $\kappa$  is a scaling factor and chosen to scale the intensity set to a maximum value, usually 100. The quantity

$$k_1 = [e^2 \cdot (m_e \cdot c^2)^{-1}]^2 \quad (I.4)$$

is a product of natural constants, while

$$k_2 = w \cdot \lambda^3 \cdot (32 \cdot \pi \cdot r)^{-1} \quad (I.5)$$

is an apparatus constant, incorporating the sample-detector distance  $r$ , the detector slit width  $w$  and the x-ray wavelength  $\lambda$ . The three quantities  $I_0$ ,  $k_1$  and  $k_2$  can be combined to a single diffractometer constant  $K_1$  containing all physical constants based on the recording equipment:

$$K_1 = I_0 \cdot k_1 \cdot k_2 \quad (I.6)$$

$N$  is the number of unit cells per unit volume,  $p$  the multiplicity of the reflection and

$$F_{hkl} = \sum_{m=1}^M f_m(\theta) \cdot \exp[2\pi i \cdot (hx_m + ky_m + lz_m)] \quad (I.7)$$

is the structure amplitude - the term which expresses the effect of atomic arrangement and atom type. The vectors  $(x_m, y_m, z_m)$  denote the

positions of atoms  $1 \leq m \leq M$  in unit cell coordinates while  $f_m$  represents the atomic scattering factor of atom  $m$ . For a specific reflection  $hkl$ , i.e. a fixed diffraction angle  $\theta$ , the structure factor  $|F_{hkl}|^2$ ,  $N$  and  $p$  are again constant and a function of the sample only:

$$K_2 = N^2 \cdot p \cdot |F_{hkl}|^2 \quad (I.8)$$

The Lorentz polarization factor

$$L_p = (1 + \cos^2 2\theta) \cdot (\sin^2 \theta \cdot \cos \theta) \quad (I.9)$$

and the Debye-Waller temperature factor

$$T_{DW} = \exp(-2 \cdot B \cdot \sin^2 \theta \cdot \lambda^{-2}) \quad (I.10)$$

can be regarded as constant for a particular reflection and ambient (constant temperature and pressure), while the absorption factor

$$A = \int_0^t \exp(-\mu \cdot s) \, ds \quad (I.11)$$

is a function of the sample's linear absorption coefficient  $\mu$  and thickness  $t$ . For an 'infinitely thick' sample ( $t \rightarrow \infty$ )

$$A = \mu^{-1} \quad (I.12)$$

When combining all constants, equation (I.3) can be simplified to

$$I_{hkl} = \text{const.} \cdot V \cdot \mu^{-1} \quad (I.13)$$

where  $V$  is the irradiated sample volume. It must be emphasized that this equation holds for any one peak of any one pure phase of 'infinite thickness'.

Since the same substance always gives the same diffractogram and since each compound contributes its own pattern independently of the others, the XRD pattern of a powder mixture consists of the superimposed sum of the diffraction patterns of its constituent compounds, each contribution being proportional to the amount present in the

mixture /BRA67/. Zwetsch et al. /ZWE29/ were the first to have utilized this basic law of QXRDA in the analysis of ceramics, long before other workers only hesitantly applied this method /FAV39, GLO33, SCH38/.

Considering a mixture of  $J$  phases ( $1 \leq J \leq N$ ) and  $i$  diffraction peaks ( $1 \leq i \leq n$ ) - and substituting  $I_{hkl}$  with the intensity of reflection  $i$  of phase  $J$  ( $I_{i,J}$ ); sample volume  $V$  with the volume portion  $V_J$  of phase  $J$ ;  $\mu$  with the actual linear absorption coefficient,  $\bar{\mu}$ , of the sample

$$(\bar{\mu} = \sum_{J=1}^N \mu_J \cdot V_J) \quad (I.14)$$

- equation (I.13) can be rewritten. Unfortunately, the total diffracted intensity is not simply the direct sum of the patterns of each substance, but is rather modified by a complicated function, which depends on the absorption coefficients of the phases of the mixture /AZA58/:

$$\text{total diffracted intensity} = \sum_{i,J} I_{i,J} + \text{matrix absorption effects.} \quad (I.15)$$

However, using weight portions  $X_J$  rather than volume fractions

$$X_J = V_J \cdot \rho_J \quad (I.16)$$

( $\rho$  = density), introducing the mass absorption coefficient

$$\mu^* = \mu \cdot \rho^{-1} \quad (I.17)$$

and taking advantage of the scaling relations

$$\sum_J V_J = 1 \quad (I.18)$$

$$\sum_J X_J = 1, \quad (I.19)$$

an intensity - composition relationship can be derived from equation (I.13):

$$I_{i,J} = k_{iJ} \cdot X_J \cdot \left( \sum_J X_J \cdot \mu_J^* \right)^{-1} \quad (I.20)$$

This equation can be re-written in a very useful form when the mixture



of N compounds is regarded as if it were composed of just 2 components - the component to be analysed (component J) and the sum of the other components (matrix M):

$$I_{IJ} = k_{IJ} \cdot X_J \cdot [X_J \cdot (\mu_J^* - \mu_M^*) + \mu_M^*]^{-1} \quad (I.21)$$

or with the sample's mass absorption coefficient  $\bar{\mu}^*$ :

$$X_J = k_{IJ}^{-1} \cdot \bar{\mu}^* \cdot I_{IJ} \quad (I.22)$$

Practically all methods of QXRDA are based on this formula, which was first deduced by Klug and Alexander /ALE48, KLU74/.

The basic steps required in the setting up of a quantitative analytical procedure using the powder diffractometer thus include the selection of a suitable diffracted peak, the measurement of its net intensity (either integrated or peak) and the correlation of this net intensity with phase concentration according to equation (I.22). Many different ways exist in which this correlation can be practically implemented. Yet, before these are discussed the factors influencing the actual intensity measurement shall be examined.

#### 4. Factors influencing intensity determination

Many factors have an influence on the magnitude of the measured intensity. These can be divided into 3 major groups: (i) the diffraction geometry, (ii) sample dependent parameters, and (iii) the measurement itself /SNY83, SU077/.

##### 4.1 Diffraction geometry

Complications in the intensity measurement arising from the diffraction geometry /JEN83/ can be due to geometrical aberrations like misalignment, beam divergencies and beam penetration into the sample ('out of focus'). These factors are not necessarily negligible and can

have pronounced effects on the measured intensities. Furthermore air and slit scatter may show up as undesirable (parasitic) components in the diffracted beam. Monochromators can also affect the measured values in various ways. Errors can be introduced depending on the characteristics of the crystal, the spectral content of the beam and the geometrical arrangement (monochromator positioned before or after the sample). Usually the sum of these contributions is, however, small, although their influence on intensity measurements should not be overlooked.

## 4.2 Sample dependent parameters

Factors due to the sample can be attributed to either the particles themselves or the interaction between them. More general, a distinction between factors related to properties of the sample and factors owing to sample preparation can be made /SAA58/.

### 4.2.1 Sample properties

X-ray powder diffraction intensities are influenced dramatically by the **crystallite sizes** of the phases present /BRI45, DEW59, WIL51/. Quantitative analysis can be in error by a factor of 2 or more as a result of these effects /CLI83/. Although complete diffraction patterns can be observed from crystallites as minute as 5 nm /MOR53/, profile broadening from small ( $< 200$  nm) crystallites is well known. This is particularly significant when (colloidal) apatite is a sample constituent /CAR59/. As the diffraction peaks broaden with decreasing crystallite size, peaks grow shorter. Peak areas (integrated intensities) are then to be preferred over peak heights as they are more applicable where variable degrees of perfection or particle size of the components can be expected.

On the other hand, an upper limit to the size of crystallites is imposed by the requirement to minimize intensity fluctuations and thus to achieve reasonable sample statistics. In this connection Brindley /BRI45/ showed that powders can be classified according to their value of  $\mu \cdot b$  ( $b$  = particle size). As a rule, absorption effects in the indi-

vidual particles can be neglected, and the number of particles is high enough for good reproducibility (better than 1%), when the following relationship is satisfied /ALE48a, BRI45, TAY44/

$$\mu \cdot b < 0.01 \quad . \quad (I.23)$$

Crystallites must thus be neither too small nor too large. Particle sizes between 0.1 and 5  $\mu\text{m}$  are generally satisfactory.

Primary and secondary extinction, both of which act as an extra absorption coefficient, are two additional factors in sample characterization.

**Primary extinction** arises from multiple reflections of the incident radiation in perfect crystals, resulting in some of the primary energy being back-reflected, which in turn weakens the diffracted intensity. Sufficiently fine powders, however, hardly show this effect /BRE35/.

On the other hand, **secondary extinction** occurs in imperfect crystals. In this case, the higher absorption is due to the slight misorientation of mosaic blocks, which manifests itself in part of the intensity being diffracted at other angles. Again, powders of small particle size do not show this effect, since there are not many crystallites critically orientated to reflect the incident beam.

Undoubtedly the most common problem in powder samples is the tendency of non-spherical particles to arrange themselves in parallel orientation to the sample surface. This effect of **preferred orientation** enhances the intensity of diffraction parallel to a single cleavage, while non-basal reflections are diminished relative to the former and relative to all reflections from non-platy and non-fibrous components /BOR69, CRA66, MOS67/. In the case of compounds with more than one perfect cleavage, enhancement and diminution effects become very complex. In urinary concretions, particularly platy uric acid and trapezoidal struvite crystals will show preferred orientation if not crushed fine enough. Thus, if preferred orientation is not controlled, this effect will prevent accurate quantitative phase determinations.

Aside from reduction in particle size, various different methods have been suggested to obtain randomly orientated preparations. These include mixing the sample with cork /ENG55/ or powdered glass /POS73/, the use of a thermoplastic cement /BRI61/ and special sample preparation procedures /BLO67, FLO55, SMI79/. Mixing the sample with an internal standard that will orient to the same degree as the sample components themselves ('orientation indicator') has also been proposed /MOS67, QUA67/. However, most of these methods dilute the sample which might result in obscuring low concentration sample constituents.

Crystallographic data of the 7 compounds investigated in detail in the present study are given in table I.2. There, symmetry class and space group, number of formula weights in the unit cell ( $Z$ ), unit cell parameters, published density  $\rho_x$  (calculated from unit cell data), mass attenuation coefficient  $\mu^*$  (calculated from /IBE74/), upper limit for crystallite size  $b$  (calculated from equation (I.23)), and optimum thickness  $t$  (calculated according to equation (I.24), assuming a maximum diffraction angle of  $50^\circ 2\theta$ ) are listed. Crystallographic data for apatites vary considerably, depending on the type and number of substitutions in the lattice (cf. chapters II and III). For more in depth discussion of apatite structural properties see for example /CAR55, MCC65, MCC73/. For powder patterns consult PDF cards 9-432 (hydroxyapatite), 19-272 (carbonate apatite), 21-145 (dahllite), 24-33 (hydroxyapatite), 25-166 (chloride, fluoride, hydroxy apatite).

#### 4.2.2 Sample preparation

The preparation of satisfactory specimens is of fundamental importance for the quality of the diffraction data /SMI79a/. As was shown in 4.2.1, the absorption and / or diffraction properties are mainly determined by the particles' size and shape. Grinding of samples is commonly accepted to effectively reduce the crystallite sizes to the necessary extent. However, various adverse effects of prolonged grinding have been observed /LEG61/, all affecting the magnitude of the measured intensities. On the one hand, a decrease in diffracted intensities was demonstrated and attributed to the existence of an 'amorphous layer', i.e. a gradual decrease of crystallinity from the interior of a par-

Table I.2. Crystallographic data of 6 major constituents of urinary calculi and reference material alpha-alumina.

constituent	symmetry	space group	Z	a [Å]	b [Å]	c [Å]	$\xi$ [deg.]	$\rho_x$ [g cm <sup>-3</sup> ]	$\mu^*$ [cm <sup>2</sup> g <sup>-1</sup> ]	b [μm]	t [mm]	references
$\alpha$ -Al <sub>2</sub> O <sub>3</sub>	hexagonal	R $\bar{3}$ c	6	4.758	-	12.991	-	3.987	31.777	0.8	0.2	/NBSd/, PDF card 10-173 /JOI/
OOM	monoclinic	P2 <sub>1</sub> /c	8	6.24	14.58	9.89	107.0	2.25	53.754	0.8	0.2	/OOC61, OOC62/
	monoclinic	P2 <sub>1</sub> /c	8	6.28	14.46	11.10	109.4	2.254	"	"	"	/ARN65/
	monoclinic	P2 <sub>1</sub> /n	8	9.976	14.588	6.291	107.03	-	"	"	"	/DEG80/
	monoclinic	P2 <sub>1</sub> /c	8	6.290	14.583	10.116	109.46	-	"	"	"	/TAZ80/
	monoclinic	P2 <sub>1</sub> /n	4	9.976	7.294	6.291	107.03	2.216	"	"	"	PDF card 20-231 /JOI/
OOD	tetragonal	I4/m	8	12.40	-	7.37	-	1.91	48.934	1.1	0.3	/BAN36/
	tetragonal	I4/m	8	12.30	-	7.34	-	1.962	"	"	"	/STE65/
	tetragonal	I4/m	8	12.371	-	7.357	-	-	"	"	"	/TAZ80/
	tetragonal	I4/m	8	12.35	-	7.363	-	1.940	"	"	"	PDF card 17-541 /JOI/
HAP	hexagonal	P6 <sub>3</sub> /m	2	9.432	-	6.881	-	3.156	87.243	0.4	0.1	/KAY64, POS58/
CAP	monoclinic	P2 <sub>1</sub> /b	2	9.421	~ 2a	6.881	120.0	-	"	"	"	/ELL73/
	monoclinic	Pb	2	9.557	~ 2a	6.872	120.36	-	-	"	"	/ELL80/
BRU	monoclinic	Ia	4	5.812	15.180	6.239	116.25	2.318	59.993	0.7	0.2	/BEE54, BEE58, JON62/
	monoclinic	(I2/a)	4	6.363	15.19	5.815	118.48	2.32	"	"	"	PDF card 9-77 /JOI/
STR	orthorhombic	Pm2 <sub>1</sub> /n	2	6.945	11.208	6.136	-	1.706	21.427	2.7	0.7	/NBSc/, PDF card 15-762 /JOI/
	orthorhombic	Pm2 <sub>1</sub> /n	2	6.13	11.19	6.92	-	-	"	"	"	/BLA59/
UA	monoclinic	P2 <sub>1</sub> /a	4	14.464	7.403	6.208	65.1	1.851	7.046	7.7	1.9	/RIN65, RIN66, NBSa/
	monoclinic	P2 <sub>1</sub> /a	4	13.12	7.40	6.21	90.5	1.844	"	"	"	/SHI66, SHI68/, PDF card 21-1959 /JOI/
	monoclinic	P2 <sub>1</sub> /a	4	13.102	7.416	6.225	90.37	1.846	"	"	"	/NBSb/

ticle towards its surface /ALT81, ENG55, GOR55, MAT68/. The amorphous portion contributes to the mass of a constituent but not to its diffracted intensity, resulting in erroneous concentration determinations.

Similar changes of crystallinity have been reported for apatite crystals, where broadening of reflections was found to occur instantaneously when the grinding process is started /DAH72, FRA69, FRA70/. In this case, crystallite damage was thought to be due to strain or distortion of the crystal lattice. In addition, grinding can completely alter the composition of certain constituents. For example, hydrated species can dehydrate, e.g. COD can be changed to COM, UAD to UA, and struvite can be transformed to newberyite by loss of ammonia and water /SUT68/. These results clearly show that the selected grinding procedure is of great significance in preparing powders for QXRDA.

Additional factors controlling sample absorption properties are the degree of surface roughness and porosity of the specimen. These qualities are mainly determined by the application of one of the many preparative procedures, i.e. preparation of powders by spray drying or liquid phase spherical agglomeration /CAL80, CAL83/, pressing or sieving these powders into the sample holder cavity, use of 'side drifting' or 'back loading' techniques or fabrication of pellets /KLU74a/. The aim is always to obtain a sufficient number of randomly oriented particles in a homogeneous sample.

Perhaps one of the most important considerations when mounting a sample is the thickness of the powder layer. As the specimen thickness increases, absorption cuts down the amount of radiation transmitted through the sample. At the same time, the total diffracted intensity of a peak increases with the volume of a sample, i.e. its thickness  $t$ . Thus there exists an optimum thickness which should be of such a magnitude as to give maximum intensity ('effectively infinitely thick'). A satisfactory criterion for this condition is

$$t \geq 3.2 \cdot \rho \cdot \sin \theta \cdot (\bar{\mu} \cdot \rho')^{-1} \quad (I.24)$$

where  $\rho$  is the average density of the sample material and  $\rho'$  the density of the mounted powder (inclusive interstices) /ALE48, TAY44/. A

thickness of 2 mm (standard sample holder) usually satisfies this requirement.

#### 4.3 Intensity measurement

In the measurement and comparison of intensities, peak heights have been routinely used. This is only valid when the full width at half maximum (FWHM) is identical for the diffracted profiles of all sample constituents, or when peak intensities  $I^P$  are proportional to the corresponding integrated intensities  $I^I$ . Variations in crystallite size, lattice perfection, diffraction geometry, etc., affect the reflection breadths (FWHM), which in turn affect the peak heights. Furthermore, for sharp peaks, the ratio  $I^I/I^P$  increases with increasing diffraction angle, due to separation of the  $\alpha_1$  and  $\alpha_2$  component peaks, the spectral distribution of the incident radiation and other instrument factors. It is thus concluded that integrated intensities are the only reliable quantities to be used in concentration measurements.

In addition, measured intensity values are influenced by the choice of instrumental conditions /VAS67/. The ultimate upper limit for the precision of a measured value is set by the stability of the x-ray apparatus itself. Restriction to reasonable counting times and average counting rates further limit the attainable precision due to counting statistics. Application of continuous or step scanning modes is another decision to be made. The output count data of a continuous scan are falsified by the pulse-averaging circuit, and the choice of the time constant is crucial for the correct interpretation of strip chart records. On the other hand, the step scan mode, either fixed time or fixed count /SZA78/, allows digital registration and statistical evaluation of the precision of the results but is much more time consuming.

In many instances overlap of peaks is observed, especially in the case of the low-symmetry constituent phases of urinary calculi. Although graphical methods of resolving ( $\alpha_1$ - $\alpha_2$ ) doublets exist /PEA48, RAC48/, with more severe overlap it becomes increasingly difficult to arrive at a meaningful figure for the integrated intensity from proces-

sing of either strip chart records or step scan data. When one or more reflections overlap the reflection(s) of interest, profile fitting techniques have thus to be employed in order to eliminate interferences /LIN79, MOR77, NAI82, PAR80, SCH83/. However, the nature of the analytical expression which best describes the shape of a diffraction peak has been found to vary with the chosen experimental conditions /ALB82/. Although many different profile shape functions have been employed in fitting diffraction peaks or whole powder patterns /HEC81, HEU76, HOW83, HUA75, PAR76, PYR83a, YOU77/, the incapability of profile shape functions to exactly model reality still affects the calculation of observed intensities /YOU82/.

In special circumstances the utilization of a different x-ray tube (e.g. chromium /HON52/) might decrease the adverse effect of overlapping peaks. The longer wavelength radiation is, however, less penetrating and detrimental absorption effects are enhanced.

Therefore, considering all factors impeding accurate intensity measurements (as listed in this section), it is not surprising that the results of a powder intensity round robin revealed that even integrated intensities may not be relied upon to better than 5% /JEN69/. This error will, of course, directly influence the analytical results.

In the next section, the influence of the second parameter determining the constituent weight portion in equation (I.22), the sample's absorption coefficient, will be discussed.

## 5. Methods of quantitative x-ray powder diffraction analysis

In addition to the intensity  $I_{ij}$  there are two more variables in the intensity-composition relationship (I.22) which determine the weight portion  $X_j$  of compound J. These are  $k_{ij}$  and  $\mu^*$ . The coefficient  $k_{ij}$  depends on the nature of component J and the diffraction geometry. Assuming the powder mixture under study to consist of phase J only ( $X_j=1$ ), equation (I.22) can be re-written



$$k_{IJ} = (I_{IJ})_0 \cdot \mu_J^* \quad . \quad (I.25)$$

The coefficient(s)  $k_{IJ}$  can thus be calculated from the absorption coefficient  $\mu_J^*$  and the intensity  $(I_{IJ})_0$  of (pure) phase J. The necessity for obtaining pure samples of the components present poses, however, a problem that can hardly be overcome in the analysis of urinary stones. Small variations in the composition of uroliths due to the presence of impurities and the formation of solid solutions (structural mixtures) are very often encountered and change sample characteristics (cf. chapter II, section 5.5.2). Since these difficulties arise in applications other than stone analyses, methods of overcoming these were investigated. This has led to the development of essentially 5 different experimental techniques which are used today in the reduction of data in QXRDA /GOE82, ROE68/. These can be divided into 2 groups - (i) the absolute (direct) techniques, comprising external standard and diffraction-absorption method, and (ii) the relative (indirect) techniques, like dilution, addition and internal standard methods. Of these, the direct techniques, which require the determination of the sample's mass absorption coefficient by experiment or calculation in addition to diffraction measurements on the analyte, shall be discussed first.

### 5.1 External standard technique

In this approach, first attempted by Bale et al. /BAL35/, the ratio of diffracted intensities from the phases found in the sample are compared to previously mixed standards of the same substances. In this case equation (I.22) assumes the simplified form /COP58/

$$I_{IJ} = X_J \cdot (I_{IJ})_0 \cdot [X_J \cdot (1-\alpha) + \alpha]^{-1} \quad (I.26)$$

where  $\alpha = (\mu_m^* / \mu_J^*)$ . Depending on the ratio  $\alpha$  of the mass absorption coefficients, the intensity ratio  $I_{IJ} / (I_{IJ})_0$  is more or less linearly dependent on  $X_J$ . This method is therefore suitable for binary mixtures of COM and COD, where  $(\mu_{COM}^* / \mu_{COD}^*) = 1.1$ , but inappropriate for APA/STR mixtures where this ratio equals 4.1 /HES82/. Since the number of artificial mixtures necessary for calibration graphs includes all possible combinations of the components and thus increases dramatically

with increasing number of phases present, this procedure becomes impractical for more than 2 compounds in a mixture.

## 5.2 Diffraction-absorption technique

In the method of analysis by the diffraction-absorption technique /LEN57, LER53/, the intensity diffracted by a sample component is always compared with the intensity diffracted by the pure compound. The new intensity-concentration relationship can be deduced by substituting equation (I.25) in (I.22):

$$X_J = \frac{I_{IJ}}{(I_{IJ})_0} \cdot \frac{\bar{\mu}^*}{\mu_J^*} \quad (I.27)$$

In order to apply this equation in analysis, diffraction techniques are used to find the intensity ratio, while the mass absorption coefficient ratio is determined with the help of x-ray transmission measurements /LER53, LER57, LER60/:

$$\frac{\bar{\mu}^*}{\mu_J^*} = \frac{\sigma_J}{\sigma} \cdot \frac{\lg \left( \frac{T}{I_0} \right)}{\lg \left( \frac{T_J}{I_0} \right)}, \quad (I.28)$$

where  $\sigma$  is the surface density and  $T$  is the transmitted intensity. It was however found that in practice the introduction of an empirical exponent applying to the absorption coefficient ratio in equation (I.27) was necessary /LER53/. Often absorption coefficients are not determined for the actual diffractometer samples but for a different preparation of the same specimen. This might introduce errors due to the varying porosity of the different mounts. Additional errors are introduced by sample inhomogeneities. Furthermore, considerable time is needed to perform all necessary measurements. Direct analysis by the diffraction-absorption technique cannot, therefore, be generally recommended.

## 5.3 Doping techniques

In most cases, direct analytical techniques are impossible to accomplish. Because of the numerous effects of absorption on the inten-

sities, it is necessary to employ a standard. The selection of this standard can, however, strongly influence the accuracy of analytical results /MCC81/. Problems are also encountered in achieving a homogeneous mixture of sample and standard.

In the known addition method of QXRDA, the standard is the pure phase of interest itself, of which fixed known amounts are added to the sample /ALE65, BEZ71, GER70/. If the system is doped with only a small fraction  $\eta$  (added mass per gram sample) of the analyte, the absorption coefficient of the sample can be considered not to change and thus eliminated from the intensity-concentration relationship. Equation (I.22) then takes the form

$$X_J = \eta \cdot \frac{I_{iJ}}{I'_{iJ}} \cdot \left[1 + \eta - \frac{I_{iJ}}{I'_{iJ}}\right]^{-1}, \quad (\text{I.28})$$

where the primed quantities denote those measured after spiking. Any component can thus be determined from a single doping and from only two diffraction patterns. The simultaneous determination of the weight fractions of several components is also possible /POP79, POP83/. Precision can be increased by multiple additions and calculation of the original amount of the unknown through extrapolation from these data. Utilization of several diffraction lines further raises the precision of the measurement.

The dilution method /COP58, ZAV70/ is exactly the same as the one based on addition, except that an amorphous diluent or a phase not present is mixed with the sample. In this case, the intensities of the diffraction lines decrease, which makes this technique especially useful for samples containing relatively high concentrations of the analyte /CLA74/.

#### 5.4 Internal standard techniques

The internal standard technique, previously developed for optical spectroscopy, consists of adding a known amount of a crystalline standard material not found in the sample mixture and determining the mass fraction of any component in terms of the portion of the added sub-

stance. This principle was first applied by Glocker /GL033/, Clark et al. /CLA36/ and Agafonova /AGA37/ to the quantitative XRD analysis of metallurgical and mineralogical samples. The method has the principle advantage that it is independent of the absorption coefficient. It is the most used and most reliable procedure when the compositions of the sample vary greatly and are unknown beforehand /ZEV79/. Unfortunately, the internal standard introduces experimental complications such as a decrease in diffracted intensity owing to sample dilution and uncertainties with regard to the homogeneity of the mixture created. Above all, the successful application of the internal standard technique is determined by the proper selection of the relevant standard employed.

#### 5.4.1 Standard requirements

The most important qualities sought from a good standard have been listed by Jenkins /JEN74/ and Nenadic et al. /NEN73/. According to these workers, basic attributes are stability, purity and non-toxicity; furthermore the standard material should be easily available in small particle size and besides from being absent from the matrix show no reaction with the latter after mixing. Nevertheless, particle size, absorption coefficient, hardness, brittleness and the degree of orientation ought to match those of the matrix. Only few diffraction maxima of about the same intensity should be observed in the  $2\theta$  region of interest. Standard diffraction peaks should, however, not overlap with prominent analyte lines. In addition, strong reflections of the standard should be found next to strong reflections of the substance sought, so that the two undergo the same absorption effects. As can be easily envisaged, in general, the compliance with all these requirements can scarcely be expected and a compromise in the realization of some of the desirable attributes has to be accepted.

Many different chemical compounds have therefore been utilized as internal standards in the past. In recent years, however, the application of NBS-SRMs seems to have become generally adopted /HUB80/. These materials include (i) certified silicon powder (intensity and  $2\theta$  calibrant) SRM 640a /HUB75, HUB83a/ and (ii) intensity SRM 674 /HUB83b/. Alpha-alumina (synthetic corundum), included in the latter, is now the

most often used standard material, mainly because of its purity and chemical stability, its freedom from orientation due to shape in sample preparation, and because it is available commercially in below 1  $\mu\text{m}$  particle size /BER70/. Notwithstanding the above, tri-calcium aluminate hexahydrate has been reportedly utilized as internal standard with success in the analysis of urinary calculi /DOS74/.

#### 5.4.2 Calibration curves

In this version of the internal standard technique different mixtures of the pure compound sought and the selected standard are used to construct a linear calibration curve. In this graph the analyte to standard intensity ratio ( $I_{iJ}/I_{iS}$ ) is plotted as a function of the analyte concentration  $X_J$  for fixed amount  $X_S$  of standard added. Considering the N-component mixture to consist of N-1 unknown constituents plus the standard, i.e.

$$\sum_{J=1}^{N-1} X_J + X_S = 1 \quad (\text{I.29})$$

$$\sum_{J=1}^{N-1} X_J \mu_J^* + X_S \mu_S^* = \bar{\mu}^* \quad , \quad (\text{I.30})$$

the following equation holds

$$\frac{I_{iJ}}{I_{iS}} = \frac{k_{iJ} X_J}{k_{iS} X_S} \quad . \quad (\text{I.31})$$

When introducing a new constant  $k^\#$

$$k^\# = k_{iS} \cdot k_{iJ}^{-1} \cdot X_S \quad , \quad (\text{I.32})$$

the mass fraction of compound J is found to be a linear function of ( $I_{iJ}/I_{iS}$ ) only

$$X_J = k^\# \cdot \frac{I_{iJ}}{I_{iS}} \quad . \quad (\text{I.33})$$

Since  $k^\#$  is independent of absorption effects, once determined, the amount of analyte present in any matrix can be established from the intensities of analyte line i and standard line 1 alone.

### 5.4.3 Reference intensity ratio

From the general equation (I.33) for QXRDA based on an internal standard, an "external standard equation" /HUB76/ can be derived. To simplify matters, only the (relatively) strongest (100%) line  $I_J$  of each compound shall be considered in the following.

When all  $N$  sample components are crystalline and known, the  $N$  equations applicable to each component (cf. equation (I.22))

$$I_J = k_J \cdot X_J \quad (1 \leq J \leq N) \quad (I.34)$$

and the constraint (I.19) form a system of  $N+1$  inhomogeneous equations which, expressed in matrix notation, read

$$\underline{I} = \underline{k} \cdot \underline{X} \quad (I.35)$$

The intensity vector  $\underline{I}$  contains all intensities  $I_J$  of the single phases, whereas the mass fractions  $X_J$  of each component make up vector  $\underline{X}$ . A unique solution to (I.35) exists, when the rank  $\text{rg}(\underline{k})$  of matrix  $\underline{k}$  in which all constants  $k_J$  are embedded is equal to the rank of  $\underline{k} \cdot \underline{I}$  /CHU74/:

$$X_J = \left( \frac{k_J}{I_J} \cdot \sum_{l=1}^N \frac{I_L}{k_L} \right)^{-1} \quad (I.36)$$

In this equation, the portion  $X_J$  of any component of a multicomponent mixture is expressed in terms of ratios like  $(I_J/I_L)$  and  $(k_J/k_L)$ . Thus no standard needs to be added for the determination of  $X_J$ , but all the coefficients  $k_L$  must be known. To avoid the necessity of determining the values of all  $k_L$ 's for each analysis, the introduction of a reference constant was proposed in the mid 1960's /HUB77/. This idea related reference intensity ratio analysis with the internal standard technique.

Since equation (I.34) is valid for each of any 2 components, viz., standard  $S$  and analyte  $A$ , the quotient of 2 such equations yields an expression for the sought ratios  $(k_A/k_S)$ :

$$\frac{k_A}{k_S} = \frac{I_A}{I_S} \cdot \frac{X_S}{X_A} \quad (I.37)$$

For mixtures equal in weight  $X_S = X_A$  and

$$\frac{k_A}{k_S} = \left( \frac{I_A}{I_S} \right)_{50:50} \quad (I.38)$$

If the standard is again chosen to be corundum, then  $I_S (=I_C)$  is the intensity of the hexagonal 113  $\alpha$ - $Al_2O_3$  reflection and the quotient of  $I_A$  and  $I_C$  is known as the reference intensity ratio:

$$RIR_{A,C} = \left( \frac{I_A}{I_C} \right)_{50:50} = k_A \quad (I.39)$$

(since  $k_C = 1$ ).

The reference intensity ratio is a universal constant, applicable to any matrix and about 500 RIR values have been listed in the PDF and the JCPDS search manuals /BER70/. Generally, ratios of peak heights are reported which under favourable circumstances can be used as an approximation to the ratios of integrated intensities without introducing an error greater than 5% in  $I_A/I_C$ . A prerequisite is, however, that the FWHM is approximately equal for all materials in the mixture and that the two measured lines are within  $10^\circ$  in  $2\theta$  /HUB80/.

To fulfil these requirements, or to eliminate problems due to overlap of the strongest reflection  $I_J$ , the latter can be simply replaced by a secondary reflection  $I_J^{ZZ}$ , multiplied by a correction factor  $\frac{100}{ZZ}$ . In addition, higher precision in the determination of RIR can be achieved by measuring the intensity of several lines from both phases and to use all of these values instead of the single  $I_J$  values. Using this option  $I_J$  has to be replaced by

$$\left( \sum_{m=1}^M \frac{100}{ZZ_m} \cdot I_J^{ZZ_m} \right) \cdot M^{-1} \quad (I.40)$$

The necessary relative intensities  $I_J^{ZZ}$  can also be found in the PDF.

Peak overlap can also be circumvented by using a different standard, notwithstanding that corundum has been chosen to be the reference standard. The new quantitative constant for analyte A to standard S is

then given by (cf. equation (I.39))

$$\text{RIR}_{A,S} = \left( \frac{I_A}{I_S} \right)_{50:50} = k_A \cdot k_S^{-1} \quad . \quad (\text{I.41})$$

Due to the fact that the accuracy of RIR is best when both measured intensities are nearly the same, a change in the used mass portions of standard and analyte might become necessary. Incorporating this and all previously mentioned variations into equation (I.39), a more general definition of the reference intensity ratio emerged from Hubbard /HUB83/:

$$\text{RIR}_{A,S} = \frac{I_{iA}}{I_{iS}} \cdot \frac{I_{iS}^{ZZ}}{I_{iA}^{YY}} \cdot \frac{X_S}{X_A} \quad . \quad (\text{I.42})$$

Thus, after determining all RIR constants only once, an unlimited number of samples can be processed by simply measuring the intensity of one or more reflections of the analyte(s). The reference intensity ratio technique therefore provides a fast and easy means to analyse many samples with reasonable accuracy. Likely sources of error are the difference between ratios of peak and integrated intensities, differences in preferred orientation of analytical and standard samples, micro-absorption, primary extinction, and varying amorphous surface content. A fundamental shortcoming of this technique is, however, the need to identify and quantify all phases present, which is an impossible task in the presence of amorphous material. Since all urinary calculi are thought to contain between 3 and 6% (w/w) non-crystalline organic matter /WAR81/, this technique is only of limited value in the analysis of uroliths.

#### 5.4.4 Flushing agent

To overcome problems encountered with the RIR method of analysis, Chung proposed an extension of the internal standard method /CHU74, CHU74a, CHU74b/, which also permits quantitative estimation of the non-crystalline fraction of the samples.



If there are amorphous or unidentified components in the sample, equation (I.36) is no longer applicable. In order to obtain a new relation between concentrations and x-ray intensities, a "flushing agent" is added to the N-component sample /CHU74/. This material may be any pure compound which is not present in the sample and which fulfils the requirements of a 'good' standard (cf. 5.4.1). The equation which is equivalent to (I.19) then reads

$$X_F + X_0 = X_F + \sum_{J=1}^N X_J = 1 \quad . \quad (I.43)$$

The so-called adiabatic principle can be derived (cf. equation (I.37)) by applying Chung's matrix flushing theory to any one sample constituent and the flushing agent

$$\frac{k_J}{k_F} = \frac{I_J}{I_F} \cdot \frac{X_F}{X_J} \quad . \quad (I.44)$$

In choosing corundum as the flushing agent, i.e.  $k_F = k_C = 1$ , a new equation for quantitative multicomponent analysis is found:

$$X_J = \frac{X_C}{k_J} \cdot \frac{I_J}{I_C} \quad . \quad (I.45)$$

The amount of amorphous / non-crystalline material present in the sample can be estimated with the help of equations (I.43) and (I.46), which also provide a means of experimentally checking the correctness of the matrix flushing theory /CHU74/:

$$\sum_{J=1}^N \frac{I_{IJ}}{k_J} \begin{matrix} > \\ < \end{matrix} \frac{X_0}{X_C} \cdot I_C \quad . \quad (I.46)$$

The validity of the '>' sign would indicate faulty data, whereas '<' indicates the presence of amorphous material or an unidentified phase. In cases where both sides of equation (I.46) are equal, all constituents are identified and are crystalline.

From the adiabatic principle (I.44) it can be seen that the linear intensity-concentration relationship is independent of the presence or absence of other components. Therefore, it is theoretically possible to determine all necessary reference intensities from a single mixture /CHU75/. However, the error in such a determination will be high when

the individual constituent concentrations are low. This effectively places an upper limit on the number of phases which can be determined simultaneously with sufficient accuracy. The exceptionally good agreement between known and determined concentrations (1-2% variation) usually reported with the internal standard technique and its modifications might be biased by systematic errors /HUB76/. In general, mixtures for the measurement of RIR values and test mixtures are prepared simultaneously from the same starting materials. Errors due to factors discussed in sections 4 and 5.4 would then (approximately) cancel, leading to a level of accuracy which cannot be expected with 'real' samples. In most cases it is difficult to obtain 5% accuracy /HUB77/ and values between 5 and 10% can be regarded as being the rule rather than the exception.

### 5.5 Microanalysis

All techniques applicable to QXRDA described thus far require the sample to be of 'infinite' thickness (cf. equations (I.11) and (I.12)). Assuming a mean irradiated area of  $1.0 \times 0.5 \text{ cm}^2$  and a 'practically infinitely thick' specimen of 2mm depth (cf. table I.2), the sample volume required to fulfil these conditions is  $0.1 \text{ cm}^3$ . Thus, with an assumed mean density of approximately  $2.5 \text{ g cm}^{-3}$ , a minimum amount of 250 mg stone powder is imperative. Only few calculi will, however, be of a size large enough to meet this demand, which resulted in Iball's statement /IBA71/ that "much more use could be made of the diffractometer if experiments were undertaken to discover the optimum conditions for very small samples".

In this context it is interesting to note, that already in 1950 Wilson published the theoretical equation permitting analyses from less than 'infinitely thick' samples /WIL50/. In this case the intensity-concentration relationship (I.22) is complemented by an exponential factor which takes into account the, with the diffraction angle, changing absorption and reflection properties of the specimen:

$$I_{1j} = k_{1j} \cdot X_j \cdot (\bar{\mu}^*)^{-1} \cdot [1 - \exp(-2\bar{\mu}^* \sigma \cdot \sin^{-1} \theta_{1j})] \quad . \quad (\text{I.47})$$

The appearance of the mass absorption coefficient and the sample's mass per unit area in the exponential expression complicates the application of any previously discussed technique, most of which require the 'flushing out' of absorption related phenomena from the concentration determining equations.

One way to overcome these problems was suggested by Talvitie /TAL62/ and Bradley /BRA67a/. These researchers limited the surface density  $\sigma$  of their samples, which they deposited on membrane filters, to below  $0.5 \text{ mg cm}^{-2}$ . Then, because  $\sigma = \frac{M}{A} \ll 1$ , the exponential function can be developed into a series and  $X_J$  becomes independent of  $\bar{\mu}^*$  and linear in  $I_{iJ}$ :

$$X_J = (0.5 \cdot k_{iJ}^{-1} \cdot M^{-1} \cdot A \cdot \sin \theta_{iJ}) \cdot I_{iJ} \quad (\text{I.48})$$

where  $M$  is the total sample mass and  $A$  the area over which it is distributed. One obstacle impeding the implementation of this procedure in stone analysis is the difficulty of obtaining uniform powder layers of a suitable thickness.

An alternative approach is to either determine the attenuation coefficient directly by transmittance measurements /HAN74, LER69, LER73, SCH62/ or to use the internal standard method /BUM73, DON73, OBE68/.

A second alternative is to mount the sample on a metal specimen holder and to compensate for absorption effects using the intensity of a reflection from the holder /WIL59/. An advantage of this technique over the previously described diffraction-absorption method is that both the absorption and diffraction measurements are made in the same way and on the same sample.

Because of their extremely low diffracted background intensities, silver filters have found wide application as sample mounts /ALT77, CAR85/. The mass absorption coefficient can then be expressed using any measured silver peak reflection before ( $I_{Ag}^0$ ) and after ( $I_{Ag}$ ) deposition of the sample:

$$I_{Ag} = I_{Ag}^0 \cdot \exp(-2\bar{\mu}^* \sigma \cdot \sin^{-1} \theta_{iJ}) \quad . \quad (I.49)$$

Solving equation (I.49) for  $\bar{\mu}^* \sigma$  and substituting the result in equation (I.47) allows the calculation of  $X_J$  from measured quantities only:

$$X_J = 0.5 \cdot k_{iJ}^{-1} \cdot M^{-1} \cdot A \cdot L \cdot \sin \theta_{Ag} \cdot I_{iJ} \cdot [1 - \exp(-L \cdot \sin \theta_{Ag} \cdot \sin^{-1} \theta_{iJ})]^{-1} \quad . \quad (I.50)$$

where use of the following relation is made:

$$L = \ln \left( \frac{I_{Ag}^0}{I_{Ag}} \right) \quad . \quad (I.51)$$

When the filter load is so small that no significant difference occurs between  $I_{Ag}^0$  and  $I_{Ag}$ , equation (I.50) can be reduced to the form of equation (I.48). This relation can be used whenever the deviation from linearity is less than  $y\%$ , e.g. /ALT77/

$$L < \frac{y \cdot \sin \theta_{iJ}}{50 \cdot \sin \theta_{Ag}} \quad . \quad (I.52)$$

When using  $Cu K_{\alpha}$  radiation, the linear region can be extended by switching to a more energetic radiation like  $Mo K_{\alpha}$  /HEI74, LER69/. Employing a shorter wavelength is also beneficial with regard to estimation of the lower limit of concentration, since this radiation is more penetrating and the analysis will not be restricted to materials of fairly low absorption.

A practical drawback of the described microanalytical technique is the need to measure the intensity of each silver filter before use. As a result, one approach has been to employ a second filter type of negligible absorption, e.g. Nuclepore polycarbonate membranes on which the samples are precipitated and then always placed upon the same silver membrane /ALT77a, BYE83/.

Predicted and experienced inaccuracies of the described procedure are due mainly to a non-uniform surface density of the sample on the filter. This could represent a systematic error in the analysis. Furthermore, when handling very small samples, the reproducibility in weighing is a major factor in the overall error incurred. Thus varying figures of merit have been published for this technique, generally

ranging from 10-30% reproducibility.

## 5.6 Comparison of methods

Besides the common difficulty of obtaining a representative homogeneous sample with randomly oriented particles, the various individual approaches to QXRDA have their particular advantages and shortcomings. For example, the external standard technique necessitates great expenditure in time and labour in setting up the essential calibration graphs. Furthermore, since the matrix's absorption coefficient is an integral part of the intensity-concentration relationship (I.26), different calibrations are necessary for the wide variety of matrices encountered in calculi. Multicomponent mixtures also require preparation of an immense number of calibration samples. The external standard technique is thus clearly solely applicable to two-component mixtures such as CaOx stones consisting of COM and COD only. However, these 'pure' oxalate calculi have been shown (see chapter II) to contain varying amounts of phosphate, thought to arise from admixtures with apatite. Hence it is doubtful whether the external standard method can be successfully applied to QXRDA when high accuracy is demanded.

The diffraction-absorption technique is usually hampered by the necessity to determine the sample's mass absorption coefficient directly. In general, this measurement is not taken from the diffractometer specimen, but from a pellet, specially compressed to fit into the sample holder of the transmission apparatus. The absorption coefficient derived from this procedure is, as a rule, larger than the attenuation coefficient of the diffractometer mount. This effect is largely due to interstices created by the unavoidable loose packing of the powder. One important exception is the Guinier-diffractometer /JUM65/, which is not discussed here. With this instrument the absorption and diffraction properties of a sample are measured using the same specimen. Additional benefits include its applicability to very small samples and a better intensity yield. Unfortunately, this instrument is not widely accepted, although several reports have emphasized the high quality of data obtained with it /JUM65, GEB79, ROE68, SEI79/. It can thus be concluded that the diffraction-absorption technique, with the exception of the

Guinier-diffractometer, is not suitable for the routine application of QXRDA to calculi.

Of the more general methods, the different doping techniques have to be assessed separately. Except for the determination of major (i.e. >80% (w/w)) constituents, the use of a diluent should be discouraged. The thinning of samples with amorphous material invariably leads to a loss in intensity. Hence, small constituent concentrations cannot be quantified. Moreover, for all concentrations of the analyte, precision has been found to be low when using the dilution technique /HUB80, ZEV79/. Doping with the analyte on the other hand, is most sensitive when the weight fraction of the unknown phase is small. In this case, the method of addition gives comparatively small errors /HUB80, ROE68, ZEV79/. However, this technique becomes increasingly time consuming, when high precision is to be achieved by means of multiple additions. In addition, the method irrevocably consumes precious pure analyte. Difficulties are also encountered for constituents with similar attenuation coefficients, where even more stringent conditions are imposed on the accuracy of the intensity measurement. Although this technique might yield good results in selected applications, it was thought to be too tedious and troublesome to be implemented as a routine procedure for QXRDA of urinary stones. For this application a lack of pure stone phases also impedes the utilization of the standard addition technique.

The internal standard technique is the only method which is largely independent of the sample under investigation. It has also been found to yield greatest precision in most cases /HUB80/. Although this technique is not totally free from inadequacies - as can be seen from the discussion in section 5.4 - it is clearly superior when compared with the other approaches to QXRDA /ZEV79/. Since it takes full account of any variation in the sample's absorption coefficient, this method is the most suitable of all procedures discussed in section 5. An attempt was therefore made to apply this technique in the quantitative analysis of calculi.

Since the advantages of the microanalytical method described in section 5.5 are rather obvious, it was also included in this investigation. Experimental parameters employed in both approaches are specified

in the next section.

## 6. Experimental procedures

After it became clear that only methods employing a standard would yield analytical results of satisfactory accuracy, these techniques were further investigated. In the case of urinary stones the preparation of calibration graphs is ruled out by the great number of different compounds and the various combinations in which they occur in calculi. It was therefore decided to apply the internal standard method and to measure the  $k_{ij}$  constants from synthetic mixtures of six major stone phases, viz., COM, COD, APA, BRU, STR, UA, and the corundum standard. Constituent concentrations were then obtained by employing reference intensity ratios and application of the matrix flushing theory. For micro-samples the use of membrane filters and an internal standard was attempted. After investigating several filter types it was decided to use silver membranes only, because of their low background diffraction pattern.

### 6.1 Equipment

For most of the qualitative and all of the quantitative measurements in this study, a Philips automatic x-ray powder diffractometer equipped with PW 1050/70 vertical goniometer, PW 1390 channel control, PW 1394 motor control, PW 8203 pen recorder and PW 1395 programmer was used /PHI74, PHI76/. For the identification of exceptionally small samples, a Debye-Scherrer camera of 57.3 mm diameter was employed. In both cases, radiation was produced by a PW 2233/20 Cu normal focus tube set at 50kV and 30 mA. Take-off angle was  $6^\circ$ . After passing through Soller slits, the primary beam was limited by a  $0.5^\circ$  divergence slit, which allowed the entire specimen length to be irradiated at the lowest scanned diffraction angle ( $10^\circ 2\theta$ ). The angular resolution of the instrument was defined by inserting a 0.2 mm receiving slit into the diffracted beam path. An anti-scatter slit of  $0.5^\circ$  angular aperture prevented stray radiation from entering the detector. A focussing

graphite crystal (model E3-202 GVW 200-800, Advanced Metals Research, Burlington, Mass.) monochromatized the diffracted beam to the  $\text{Cu K}_\alpha$  wave-length. The detection system consisted of a NaI scintillation detector PW 1964/60 mounted onto the face of a photomultiplier tube. The bias voltage applied to the tube was 960 V. Driving the diffractometer to the (113) corundum reflection, detector resolution was established to be 51.9%. The RC constant for the pulse-averaging circuit was set at 1 sec. Ambient temperature was maintained at 19°C and supply voltage was allowed to stabilize for 30 min before measurements started.

Before commencement of the present study, the entire goniometer was realigned. A stable reference sample was produced by preparing a polished section of 0.3  $\mu\text{m}$  corundum embedded in an epoxy resin. This (instrument) standard permitted monitoring of long term changes as well as the performance of the diffractometer at any time by determining the peak position and intensity of the (113) alpha-alumina reflection.

For the internal standard method, the standard Philips aluminium sample holder was used, whereas for the silver filter technique a rotating sample holder Philips PW 1064/20 was employed.

Various grinding and mixing equipment which was to be used to reduce the mean particle size of standard and stone samples was first tested. The equipment included a grinder/shaker ('Grindex', Research and Industrial Instruments, London), automatic agate mortar grinders, 'Micro-Dismembrator II' (B. Braun, West Germany) and a 'Turbular' mixer (type T2C, W.A. Bachofen, Basle, Switzerland).

Attenuation coefficient measurements were carried out on a Philips PW 1220 spectrometer, equipped with a molybdenum x-ray tube, which was operated at 45 kV and 28 mA. A strontium specimen (2 g  $\text{SrCO}_3$  + 3 g  $\text{Al}_2\text{O}_3$  + 1 g wax C micropowder (Hoechst)) was used as standard target. Generated  $\text{Sr K}_\alpha$  radiation was diffracted by a  $\text{LiF}(220)$  crystal and measured with a scintillation detector at an angle of  $36.865^\circ 2\theta$ .



## 6.2 Standards and samples

### 6.2.1 Materials

Pure preparations of whewellite and struvite were obtained commercially (both BDH Chemicals), while the other two hydrates of  $\text{CaOx}$  were prepared in the laboratory. COT was found to be the major precipitate in low pH artificial urine evaporation experiments (chapter IV) and was therefore included in this investigation. Specifications published by Hammarsten /HAM29/ and Walter-Levy et al. /WAL62/ were followed in order that only one hydrate at a time was precipitated. Pure COD was synthesized by pouring 1 litre of 0.2 M sodium oxalate into an equal volume of 0.4 M calcium chloride. Both solutions were adjusted to pH 9 and cooled in an ice bath prior to mixing. By replacing sodium oxalate with oxalic acid, and using 1 litre 0.5 M solutions (pH 0.5) in each case, COT was obtained. Both reaction products were filtered through 0.45  $\mu\text{m}$  PTFE filters and subsequently washed with ice-cold dilute HCl and methanol. XRD confirmed the presence of only one hydrate in each case. These samples were refrigerated at sub-zero [ $^{\circ}\text{C}$ ] temperatures for extended periods of time (>1 year) without any change in phase.

Initially, an attempt was made to synthesize hydroxyapatite according to a procedure described by Hayek et al. /HAY63/. However, x-ray scans of samples prepared in this manner invariably revealed a mixture of  $\beta\text{-Ca}_3(\text{PO}_4)_2$  (whitlockite, PDF 9-169) and  $\text{Ca}_5(\text{PO}_4)_3\text{OH}$  (apatite, PDF 9-432). Thereafter, commercially available HAP preparations were tested. These included a suspension in water (Sigma) and finely powdered HAP (Sigma). Although the latter was found to be better crystallized than the colloidal HAP present in calculi, it was nevertheless used for standardization purposes.

A sample of brushite from Merck (extra fine powder) was found to have undergone partial dehydration as it displayed the prominent diffraction peaks of  $\text{CaHPO}_4$  (PDF 9-80). A new sample was obtained from SARCHEM which yielded satisfactory diffraction patterns. However, extensive preferred orientation of the crystallites was observed.

Uric acid preparations from Hopkin and Williams and Sigma did not yield good powder patterns, while those recorded for Merck's uric acid ('for biochemical purposes') exhibited d-values and relative intensities closely corresponding to those of PDF card 31-1982 and NBS Monograph 25 /NBSa, NBSb/.

The internal standard used was  $\alpha$ - $\text{Al}_2\text{O}_3$  (BDH, 'highly pure for polishing') with a declared mean particle size of  $0.3 \mu\text{m}$ . For the determination of the diffraction constants  $k_{ij}$ , 1:1 (w/w) mixtures of the internal standard and each of the previously listed substances were obtained by mixing precisely weighed amounts of each compound with the equivalent standard portion for 30 minutes in a mixer.

Samples of 20 urinary calculi which had been previously analysed by ICP-AES, were chosen to test internal standard and membrane XRD procedures, as described earlier in this chapter.

### 6.2.2 Sample preparation

The most difficult problem in QXRDA is that of specimen preparation. Urinary calculi for XRD analysis must be air-dried and not subjected to heat. Sawing of a stone can alter its composition /ROS82/. Selection of a particular aliquot has a decisive influence on the results of the analysis. Samples from different regions of a stone are likely to yield different concentration values. In the present study whole stones were therefore pulverized with an agate mortar and pestle. At first, the crushed segments were processed further with the 'Grindex' apparatus. However, samples tended to cake, impairing the complete pulverization of the calculi. Accordingly, a motor driven mortar and pestle were used to diminish particle size. Generally, 1-2 hours were required to grind the samples, so that the obtained powders could be easily screened through 400-mesh. Analysis of samples treated in this way revealed that the friction of the grinding process had generated sufficient heat to cause the dehydration of COD, COT, BRU and STR. The di- and tri-hydrates of  $\text{CaOx}$  were found to be partially transformed to the monohydrate while brushite lost all and struvite part of its water of crystallization, yielding anhydrous calcium monohydrogen phosphate

and magnesium ammonium phosphate monohydrate, respectively. The conversion of STR to newberyite due to loss of water and ammonia, which has been reported by other researchers /LON69/, was not observed in the present study.

The application of dispersing liquids like water, methanol and acetone /BAL43/ did prevent the above effect in the case of the phosphates, but not for the oxalates. For these, a cryogenic grinding procedure was developed. Approximately 1-1.5 g of powdered sample were enclosed in a specially machined PTFE cup together with a ceramic ball of 1 cm diameter. A tight fitting lid was held in position with a stainless-steel clamp and the cup and contents were immersed in liquid nitrogen for ca. 20 to 30 minutes. Thereafter the cup was mounted onto the 'Mikro Dismembrator II' and the grinding action was commenced. The low temperature permitted crushing to be continued for long periods without the sample temperature ever rising above 0°C. The low temperature also had the additional advantage of rendering the sample very brittle and thus easier to be ground. It also prevents any heat-induced changes from occurring /NEN73/. This technique proved to be extremely useful and all further preparations were carried out in this way.

Having crushed the (stone) sample in the manner described, the resultant powders were mixed with ca. 30-40% (w/w) alpha-alumina standard to yield aliquots of about 1 g. The described cryogenic grinding and mixing procedure was then repeated. Standards were prepared in the same way. To break up flakes that may be oriented by the grinding, samples were re-screened through 400-mesh (38  $\mu$ m). Particles passing through this screen, however, were still too coarse to attain high precision. No final conclusion could be made prior to mounting as to whether these powders would fulfil the stringent size requirements of QXRDA, viz., < 5  $\mu$ m.

Various different mounting techniques exist for the preparation of flat specimens for powder diffractometry. Amongst these, techniques involving particle settlement in aqueous solutions have been found to yield great variations in accuracy /GIB65/. The more acceptable methods of preparing a powder sample include powder press and smear techniques. However, thin binders such as acetone allow particles to settle and

shaped particles to align. Therefore, the most common method for preparing a sample of loose powder is to pack it into a flat cavity mount. (For a discussion of the various methods see for example /AZA58, NBSa/). In the present study front loading gave dissatisfactory results due to excessive orientation of the crystallites. Side drifting was only successful, when the powder was diluted with a suitable binder so that it could be fluently poured into the cavity. Dilution, however, has to be avoided when low concentration constituents are to be determined. Rear packing or back loading of the powder which has been reported to reduce preferred orientation /NIS64/, was thus the method of choice in this study. In a round robin, this procedure has been established as the "best specimen preparation technique" yielding "by far the best d and I data" /JEN79/. The procedure finally adopted consisted of a series of steps in which the powder was packed in a standard Philips sample holder against a glass plate as described in great detail by McCreery /MCC49/. The use of fritted glass as the face plate greatly helped in reducing effects due to preferred orientation. Nevertheless preferred orientation still occurred, especially in STR and BRU containing samples. However samples yielding reproducible intensities were nevertheless successfully prepared.

### 6.2.3 Membrane mount

Samples, previously prepared as described in section 6.2.2, were used for this part of the study. To implement the microanalytical techniques discussed in section 5.5, a variety of membrane filters were obtained from different manufacturers to establish the filters' diffraction properties. Membrane filters are produced from a diversity of materials, most of which cause substantial scatter of x-rays. The high background radiation commonly observed in the diffractograms of these filters generally makes them unsuitable as sample mounts for QXRDA. Table I.3 lists the observed diffraction patterns recorded for the filters investigated.

Table I.3. Diffraction patterns of membrane filters (10-50°2θ scanning range, Cu K<sub>α</sub> radiation, diffractometer settings as described in section 6.1).

make	type	pore size [μm]	filter material	diffraction pattern characteristics
Sartorius	SM 11607	0.2	regenerated cellulose	low background (<50 cps) at large diffraction angles (>30°2θ); two distinct broad (FWHM ca. 3°2θ) maxima at 12.0 and 20.5°2θ (ca. 250, 400 cps, respectively).
Gelman	Metricel GA-6	0.45	mixed cellulose ester	slightly structured background of relatively low intensity, decreasing from ca. 300 cps at 10°2θ to <50 cps for angles larger than 30°2θ.
Schleicher & Schüll	ME 24	0.2	mixed cellulose ester	background intensity decreasing from ca. 300 cps at 10°2θ to <150 cps for angles larger than 30°2θ with broad hump (ca. 400 cps) at ca. 20°2θ.
Gelman	TOM-200	0.2	cellulose triacetate	slightly structured background, decreasing from ca. 400 cps at 10°2θ to <50 cps for angles >30°2θ, with small humps at ca. 17°2θ.
Sartorius	SM 11306	0.45	cellulose nitrate	background intensity increasing from ca. 250 cps at small angles to 400 cps at ca. 20°2θ, but steadily decreasing to <100 cps for angles >34°2θ.
Sartorius	SM 11906	0.45	polyamide	low background intensity (<50 cps) except for broad hump between 16-26°2θ with superimposed peaks (ca. 400 cps) at 20.3 and 23.7°2θ.
Nuclepore	-	0.4	polyester	low angle background of ca. 500 cps up to 18°2θ; broad peak (2800 cps) at 26°2θ; very low background (ca. 20 cps) on high angle side of this peak (>32°2θ).
Nuclepore	-	0.2 0.4	poly-carbonate	low background intensity (ca. 50 cps) up to 14°2θ; broad peak (650-1100 cps) around 17.6°2θ; extremely low background (ca. 10 cps) for angles >30°2θ.
Millipore	EDWP Polyvic	0.65	PVC	very low background with average intensity of 50 cps over entire diffraction angle range; very broad hump of low intensity (<150 cps) between 14-28°2θ.

Table I.3 continued overleaf

Table I.3 continued

make	type	pore size [ $\mu\text{m}$ ]	filter	diffraction pattern characteristics
Sartorius	SM 12807	0.2	PVC	very low background (25-50 cps) over entire diffraction angle range, except for somewhat elevated (<100 cps) region between $16-26^\circ 2\theta$ .
Millipore	GWP Durapore	0.2	poly-vinylidene difluoride	broad maximum between $15-22^\circ 2\theta$ with superimposed sharp peaks (>1000 cps) at 17.8, 18.4 and $20.0^\circ 2\theta$ ; smaller peaks at 25.5, 36.0 and $38.8^\circ 2\theta$ .
Millipore	LOW Mitex	10.0	PIFE	broad maximum between $10-20^\circ 2\theta$ with superimposed sharp peak of high intensity (ca. 8000 cps) at $18.0^\circ 2\theta$ ; broad hump in background from $30-50^\circ 2\theta$ with superimposed minor sharp peaks at 31.6, 37.0 and $41.4^\circ 2\theta$ .
Millipore	FGLP Fluoropore	0.2	PIFE	low background with sharp peaks at 18.0, 21.9, 24.1, 31.8, 36.7 and $49.3^\circ 2\theta$ , the intensity of which decreases by a factor of 20 with increasing diffraction angle (from ca. 7000 cps for the first peak).
Nuclepore	Filinert	0.2	PIFE	same as Millipore FGLP (Fluoropore).
Sartorius	SM 11807	0.2	PIFE	high background on low angle side of sharp peak (ca. 22000 cps) at $18.0^\circ 2\theta$ ; otherwise low background with sharp peaks at 31.8, 36.7 and $49.3^\circ 2\theta$ .
Gelman	Teflon	0.2	PIFE	low background with high intensity maxima at 14.0 (6000 cps), 17.0 (4000 cps) and $18.0^\circ 2\theta$ (40000 cps); peaks of lower intensity at 25.7, 27.2, 28.6, 31.8, 36.7 and $49.3^\circ 2\theta$ .
Millipore	-	0.8	silver	extremely low background (<10 cps) over entire diffraction angle range; two strong sharp silver peaks (1000-5000 cps) and 3 further peaks (100-150 cps) at 27.8, 30.3 and $46.3^\circ 2\theta$ .
Selas Flo-tronics	FM-25	0.2	silver	extremely low background over entire diffraction angle range; displays only silver pattern (PDF 4-0783)
SOEKOR	-	-	ceramic tile	very rich pattern; superposition of $\alpha$ -quartz, calcium aluminium silicate and other patterns.

It can be seen that the common cellulose filters display a rather rich spectrum, in particular in the range of lower diffraction angles. Since this range ( $< 25^{\circ}2\theta$ ) is generally used to unequivocally identify urinary stone constituents, these filters cannot be utilized in such investigations. On the other hand, filters made from PVC show a very low and almost flat background over the entire diffraction angle range, which would make them ideal substrates for stone powder suspensions. However, the PVC Millipore filter is not produced with a pore size small enough to prevent passage of the small corundum particles while the Sartorius variety is no longer manufactured due to difficulties in production (Sartorius, private communication). It was therefore decided to use pure silver filters which offer the advantage of only 2 sharp diffraction maxima against an otherwise extremely low background. For this purpose silver membranes ( $\varnothing$  25 mm,  $0.2 \mu\text{m}$  pore size) from Selas-Flotronics (Flotronics Division of Selas Corp., Huntingdon Valley, Pa. 19006) were employed.

One of the practical problems encountered in the use of membranes as substrate materials is the need to prepare a thin, homogeneous powder layer on the filter. Since the procedure described in the literature has its origin in the field of occupational health in mines /CRO71/, dust chambers of varying technical complexity have been used for the purpose of sample collection /DON73, LER69b, LER70a/. For the preparation of stone samples, a filtering technique /BUM73, CRA66, QUA70, TAL62/ was more applicable. With this method aliquots of the powdered stone - with or without internal standard - are dispersed and filtered under suction. Water and acetone were used as the liquid medium in the present study. The suspension was applied to the filter by means of a syringe connected to a Millipore micro-syringe filter holder. This in turn was fitted to a filter flask under vacuum. Proper distribution of the material was ensured by the use of a wetting agent (Triton X-100, BDH). Sample masses ranging from 2 to 100 mg were tested, but were found to have only little effect on the mass distribution on the filter.

When using sample masses below 10 mg, the uncertainty in the latter becomes one of the major errors of the entire analysis. Generally, the best reproducibility of weighing with a 4 digit balance

is  $\pm 0.1$  mg. This results in an error of  $\pm 10\%$  in the mass of a 1 mg sample but larger errors in the mass of individual constituents.

Small non-uniformities in the deposition of the samples on the silver filters can be compensated for by rotating the sample about the diffraction vector. Besides smoothing intensity fluctuations due to varying particle size, specimen rotation averages preferred orientation other than that parallel to the sample's surface. In many instances the use of a rotating specimen holder has been shown to be of a beneficial effect /DEW59, PAR83/. Such a device was therefore also used in this part of the present investigation.

### 6.3 Phase and intensity determination

Peak position and intensity data were obtained by step scanning specimens for predetermined  $2\theta$  ranges (stepsize  $0.01^\circ 2\theta$ , 10 seconds fixed time). Measured values (angle, count, time) were recorded with a teletype (hard copy) and were simultaneously punched on paper-tape. These were read into a Hewlett-Packard 1000 Series Minicomputer and transferred onto magnetic tape. Data were then copied from the magnetic medium onto hard disc, where further processing took place with a Univac 1100/80 Series mainframe computer.

Single phase standard samples were first continuously scanned from  $10-50^\circ 2\theta$  at  $2^\circ 2\theta \text{ min}^{-1}$  and a chart recorder speed of  $2 \text{ cm min}^{-1}$ . These traces were used for identification purposes only and to ensure that the specimens were still in their original form. Five intensity values were determined for each  $I_{hkl}$ , either by preparing new specimens or by scanning the same sample a second time. To check reproducibility of the sample preparation procedure, each sample was mounted at least 3 times.

A stepscan ( $0.02^\circ 2\theta$ , 10 sec) of the entire diffraction angle range ( $10-50^\circ 2\theta$ ) was recorded twice in order to determine the relative intensities of all identifiable maxima. Peak positions and integrated intensities were established with the help of programme XPOWD /HEC75a, VON77/. In this routine, separation of overlapping peaks is achieved by simply drawing a vertical line through the position of minimum intensi-



ty intermediate between the two maxima. However, this may lead to errors in the peak positions and (integrated) intensities. Therefore peak intensities were determined from the chart recorder trace ( $0.5 \text{ cm min}^{-1}$ ) and teletype printout as well.

For the other preparations, i.e. mixtures of stone powders and corundum, only about 5 predetermined maxima per phase were scanned. These reflections were later employed in the quantitative analysis of calculi (table I.4).

The intensities of the listed diffraction peaks (table I.4) were determined for all 50:50 (w/w) mixtures of the 6 stone components and alpha-alumina. Data from these samples were then processed with the NBS\*QUANT82 programme package /HUB83/ in order to obtain the required reference intensity ratios.

Stone samples were first scanned continuously ( $2^\circ 2\theta \text{ min}^{-1}$ ,  $2 \text{ cm min}^{-1}$ ) and the phases present were identified from the strip chart. Thereafter, those portions of the x-ray pattern which included the stronger reflections of each component were step scanned (step size  $0.01^\circ 2\theta$ , 10 seconds fixed time). Patterns were again processed using the NBS\*QUANT82 system, where routine COBRAG handled overlapping peaks /SNY82/. On a few occasions, programme QXDA /HEC75/ was used.

Before a sample was measured, the instrument standard (cf. section 6.1) was scanned in order to establish possible drift of instrument parameters. Prior to the investigation of samples mounted on membrane filters, a rotating sample holder was fitted. Intensities were measured in the same way as for the ordinary samples, with the exception that the (111) and (200) silver peaks were also determined.

Mass absorption coefficients were determined in transmission for the same samples using a Philips PW 1220 spectrometer (cf. section 6.1). For this purpose powders were pressed into pellets. A 'blank reading' was first recorded at the strontium  $K_\alpha$  wavelength followed by three readings with sample inserted. A further 'blank reading' was recorded for each sample. Photons were counted for 40 s or until  $10^6$  counts were registered. Counts were dead-time corrected and the

Table I.4. Diffraction maxima used in the analysis of uroliths.

compound	hkl	d [Å]	scanning range [°2θ]
Al <sub>2</sub> O <sub>3</sub>	012	3.479	25.00-26.00
	104	2.552	34.50-35.65
	110	2.379	37.20-38.10
	113	2.085	42.70-43.85
	024	1.740	51.90-53.00
	116	1.601	56.80-58.10
COM	10 $\bar{1}$ ,110	5.93,5.79	14.30-15.60
	020	3.65	23.90-24.80
	202	2.966	29.90-30.45
	112	2.494	35.75-36.35
	130,41 $\bar{1}$	2.347	37.90-38.70
COD	200	6.18	13.55-14.85
	211	4.42	19.55-20.45
	400	3.09	28.45-29.15
	222,411	2.815,2.775	31.20-32.75
	510,103	2.422,2.408	36.50-37.70
	213	2.243	39.75-40.50
APA	100	8.17	10.40-11.10
	111	3.88	22.60-23.20
	002	3.44	25.50-26.35
	211,122,300	2.814,2.778,2.720	30.80-33.50
	202	2.631	33.65-34.50
	222	1.943	46.05-47.25
	213	1.841	49.00-50.00
BRU	020	7.57	10.75-12.00
	021	4.24	20.35-21.35
	111,041	3.05	28.75-29.70
	22 $\bar{1}$	2.928	30.05-30.90
	131,220&15 $\bar{1}$ ,20 $\bar{2}$	2.648,2.623,2.603	33.70-34.70
	24 $\bar{1}$ ,022	2.434,2.421	36.55-37.40
	151,242	2.172,2.148	41.20-42.35
	241	1.819	49.75-50.50
STR	110	5.905	14.55-15.20
	011	5.378	16.00-16.75
	111,021	4.257,4.139	20.20-21.80
	130	3.289	26.55-27.40
	012,211	2.958,2.919	29.80-31.05
	040	2.802	31.40-32.25
	112,022,211	2.722,2.690,2.660	32.50-34.05
UA	200	6.56	12.80-13.90
	210	4.91	17.40-18.30
	211	3.85	22.25-23.45
	400,021,121	3.28,3.18,3.09	26.60-29.30

mass absorption coefficients were calculated with the help of sample masses and absorption area ( $1.267 \text{ cm}^2$ ). To attain higher accuracy, this procedure (including preparation of a new pellet) was repeated.

The ratios of the two absorption coefficients measured at two different wavelengths are the same for all compounds (provided there is no absorption edge between). It is therefore possible to convert the mass attenuation coefficients measured at the strontium wavelength to those at the  $\text{Cu K}_\alpha$  wavelength. To achieve this, pure alpha-alumina and uric acid samples were subjected to the described procedure. A conversion factor was then calculated from the mass attenuation coefficients measured at the  $\text{Sr K}_\alpha$  wavelength and the  $\mu^*$  values derived from the International Tables /IBE74/ for the  $\text{Cu K}_\alpha$  wavelength. This factor was used to convert all measured absorption coefficients to the  $\text{Cu K}_\alpha$  wavelength for calculating constituent concentrations according to equation (I.47).

## 7. Results and discussion

Structural identification with the powder diffractometer has been found to be very well suited for the qualitative analysis of uroliths. In this study, the entire procedure, i.e. specimen preparation, scanning the range  $10-50^\circ 2\theta$  as well as calculation and interpretation of d values, was accomplished within 30 minutes. The goniometer technique was also found to be superior to the Debye-Scherrer film method. Not only is it possible for a greater number of samples to be analysed in a given time, but also accuracy is greatly improved. For example, in calculi having COD as major constituent, uric acid dihydrate was often mistakenly identified as being present from Debye-Scherrer photographs, although it could not be demonstrated on chart recorder traces. The opposite is also true, viz., the presence of UAD was commonly missed with the film procedure, but was identified from goniometer traces. With the Debye-Scherrer camera, the difficulty of deciding whether UAD is a stone constituent or not was especially pronounced when COM or UA occurred as a third phase in the multicomponent calculus. This arises because of the fact that in the COM/COD, COM/UA and UA/UAD system the

interacting crystalline lattices are totally supportive of each other at the atomic level /MAN80/, resulting in a great number of common interplanar spacings. Thus partial obscuring of UAD due to lattice match with other components, results in difficulties in its detection and is indirectly a support for the theory of an epitaxial mechanism in stone formation /LON72, SUT68a/.

A well known limitation of qualitative XRD is its failure to detect apatite at low concentrations, particularly in infection stones. Strong struvite reflections overlap almost all the identifiable apatite peaks. When using corundum as internal standard, the problem is aggravated by overlap of the  $\text{Al}_2\text{O}_3$  012 peak with the APA 002 reflection. Only the very weak 100 and 111 APA peaks are then available for positive identification of this component. In this case, the presence of APA can often only be guessed from a somewhat elevated background in the  $30-34^\circ 2\theta$  region. This 'amorphous halo' will almost always be missed on powder photographs, resulting in the failure to detect apatite. The same difficulties exist in APA/COD mixtures. The tempering of apatitic calculi at  $900^\circ\text{C}$  has therefore been suggested to improve the crystallinity of this compound and thereby augment its diffracted intensity /DOS74/. However, the complex reactions and transformations taking place at this temperature preclude any other stone constituent from being simultaneously identified. Another problem is that of identifying different kinds of apatites. Since APA always occurs in a poorly crystallized state in biological concretions, the position of its diffraction maxima cannot be determined with any accuracy. The differentiation between carbonate and hydroxyapatite is thought to be of clinical significance as the latter only forms in slightly acidic urine, while the former precipitates in more alkaline medium. The discrimination between the two APA forms is thus important in the ascertainment of an infected urine.

The quantitative analysis of apatite, already hampered by the inadequacies of its qualitative identification by XRD, is even more difficult. Homomorphous substitutions in the lattice of biological apatites (cf. chapter II, section 5.5.2) consisting of the replacement of some atoms with similar but differently-sized others, make a meaningful concentration determination almost impossible. Apart from

resulting changes in lattice parameters which cause some reflections to disappear and new ones to appear, the absorption properties of the sample are changed. Artificial apatite standards therefore seldom mimic the crystallographic properties of 'real' biological apatites. Next to overlap problems in STR and COD samples this was probably the main cause of the failure of the applied XRD techniques to give accurate apatite concentration values.

In order to utilize the internal standard technique in routine analysis, reference intensity ratios were measured for 6 substances, viz., COM, COD, HAP, BRU, STR and UA. The values listed in table I.5 represent RIR constants derived from peak height measurements, scaled to the strongest peak. These values are thus directly comparable with listed JCPDS values. The values measured in this study for STR and UA agree well with published values (1.0 /BER70/ for STR and 0.94 /NBSb/, 0.9 (PDF card 31-1982 /JOI/), and 1.0 (PDF card 21-1959 /JOI/) for UA).

Table I.5. Reference Intensity Ratios.

compound	RIR
COM	1.25
COD	0.81
HAP	0.45
BRU	1.56
STR	0.90
UA	1.03

Although RIR values were also calculated from integrated intensities, these varied from case to case. This is due to the fact that the RUNFIL routine of the NBS\*QUANT82 package does not take peak overlap into account. Thus in those cases where overlap of several peaks occurred, the intensity of the entire group of peaks was used in calculating the RIR constants. This of course entailed rescaling of all relative intensities depending on which maxima were included (cf. table I.6), which in turn affected the value of the RIR constant. Analytical results are, however, not affected by this approach as long as intensity measure-

Table I.6. Selected intensity values from standard samples.

compound	hkl	published <sup>1</sup>	teletype <sup>2</sup>	stripchart <sup>3</sup>	XPOWD <sup>4</sup>	QUANT82 <sup>5</sup>	FWHM
$\alpha$ -Al <sub>2</sub> O <sub>3</sub>	012	74	65	62	54	54	0.21
	104	92	92	94	87	89	0.22
	110	42	37	39	37	35	0.23
	113	100	100	100	100	100	0.24
	024	43	43	43	-	46	0.26
	116	81	81	86	-	98	0.28
COM	10 $\bar{1}$	100	100	100	100	75	0.12
	110	30/25	28	29	28	15	0.13
	020	70/100	91	92	93	100 <sup>6</sup>	0.14
	20 $\bar{2}$	45	51	53	55	47	0.14
	112	18/30	25	26	33	28	0.18
	130	30/90	36	38	} 68	} 64	-
	41 $\bar{1}$	12	32	35			-
HAP	100	12/29	7	8	13	4	-
	111	10	5	5	5	2	-
	002	40/45	49	48	38	35	0.29
	211	100	100	100	100	} 100 <sup>7</sup>	-
	112	60/62	79	79	60		-
	300	60/58	55	55	54	22	-
	202	25/31	23	24	21	13	0.44
	222	30	24	24	26	26	0.45
	213	40	27	26	23	21	0.39
STR	110	41/38	31	32	34	29	0.19
	011	27/22	26	26	26	24	0.18
	111	100	100	100	100	100	0.22
	021	40/34	39	40	38	32	0.21
	130	27/24	25	26	27	31	0.23
	012	23/16	17	17	22	} 75	-
	211	54/46	43	44	50		-
	040	34/26	37	36	38	42	0.21
	112	15/8	11	11	10	-	-
	022	50/37	48	48	59	-	-
	221	43/37	32	32	36	-	-

<sup>1</sup> Al<sub>2</sub>O<sub>3</sub>: /NBSd/; COM: PDF card 20-231 /JOI/ & /SUT68/; HAP: PDF card 9-432 /JOI/ & /SUT68/; STR: /NBSd/ & /SUT68/;

<sup>2</sup> calculated from teletype printout (cps);

<sup>3</sup> measured from chart recorder trace with ruler;

<sup>4</sup> as calculated by programme XPOWD /HEC75a, VON77/;

<sup>5</sup> as calculated by programme QUANT82 /HUB83/;

<sup>6</sup> rescaling due to separation of overlapping 101 and 110 peaks and resulting error in background determination;

<sup>7</sup> as a (211 and 112 peaks).

ments are consistent within any one analytical series. Nevertheless, reference intensity ratios derived in this way are of no use to other workers, since their values depend on arbitrary selection of a number of peaks as the 'scaling cluster'. Notwithstanding the discussion in section 4.3, the rather close relationship between the integrated and peak intensities observed in this study (cf. table I.6, e.g. 'teletype' and 'XPOWD' intensities) should allow the listed RIR constants to be used with confidence by other workers in QXRDA. Peak intensities were also used by Otnes and co-workers /OTN80/ when they applied the internal standard technique to the determination of stone components other than apatite. These workers did not, however, publish their RIR values thus making a comparison with the constants obtained in the present study impossible. Nevertheless, comparison of data is essential in this field, since the RIR constants, initially derived from pure phases, have to be adjusted as a result of the information gained from the analysis of many calculi. This procedure would take into account the peculiar morphology of uroliths. Another way of arriving at better RIRs would require the isolation of single constituents from stones and their use in the determination of the reference intensity ratio.

Another reason for using peak intensities in preference to integrated intensities lies in the enormous time saving enjoyed with the former. This can be illustrated by considering a 3-component sample with internal standard. The measurement of 3 peaks per component with each peak requiring a step-scan ( $0.01^\circ 2\theta$ , 10 sec) over a range of about  $0.8^\circ 2\theta$  followed by evaluation thereof would need a total measuring time of ca. 3 hours. Even when applying optimization procedures /SZA78, SZA80, SZA82/, the length of time cannot be considerably reduced. In addition, if determinations are done in duplicate for increased precision, only a few samples can be processed per day. On the other hand, determination of peak intensities requires the measurement of only a few  $\Delta 2\theta$  steps on both sides of the peak and the peak intensity itself. However, when peak intensities are utilized, the limitations of this approach and their influence on the accuracy of the method must be borne in mind as discussed in section 4.3.

The reference intensity ratio for COT could not be determined in this study, although an attempt was made. Severe preferred orientation

of the crystallites did not permit the measurement of reproducible intensities. Handling of this substance was difficult due to dehydration and phase transformation which commenced as soon as the specimen was exposed to ambient temperature. It was obvious that particle size was too large, despite the extensive grinding procedure employed. Thus a more efficient sample preparation procedure and the use of a cold finger in the diffractometer would seem to be a requirement for accurate analyses of COT.

Table I.7 displays the results for the 11 stones investigated with the internal standard (RIR) and microanalytical (filter) methods. In the latter case  $\bar{\mu}^*$  was determined directly as well as by measurement of silver peak attenuation. Generally, concentrations values agree satisfactorily between the 3 different techniques employed. However, a systematic error in the microanalytical method, especially when employing absorption correction by means of silver peak attenuation is evident. It appears that internal standard values are often larger than the true concentrations added to the sample. These discrepancies could not be explained. When correcting analyte concentrations for this error, close agreement for the different methods was found (table I.7). The results of 21 stones analysed with the internal standard method are also generally in good agreement with results obtained from ICP-AES elemental analyses (table I.8). ICP-AES phase concentrations were calculated from Ca, Mg and P concentrations with additional constituent information from XRD powder photographs. Colloidal apatite was assumed to be present in those samples where no phosphate constituent was detected by XRD but where elemental phosphorus was determined with ICP-AES. The advantage of QXRDA is clearly its ability to differentiate between the different hydrates of  $\text{CaOx}$ . In addition, XRD can detect and discriminate between anhydrous UA and UAD. Figures for these two compounds are given in the ICP-AES column and were obtained from microchemical analysis for C, H and N. Table I.8 also shows that APA is definitely missed by XRD at low concentrations. Indeed, values could not be calculated from XRD for even 50% APA concentrations as found by ICP-AES.

It can thus be concluded that for the application of the membrane mount microanalytical technique, the use of an internal standard for



Table I.7. Comparison of constituent concentrations<sup>1</sup> [wt-%] derived from different QXRDA techniques.

stone	phase	$\mu^*2$ [cm <sup>2</sup> g <sup>-1</sup> ]	internal <sup>3</sup> standard	microanalysis		mass on filter [mg]
				' $\mu^*$ ' <sup>4</sup>	'Ag' <sup>5</sup>	
137	Al <sub>2</sub> O <sub>3</sub>	20.8	44.4	40.7	54.3	8.1
	COM		8.1	6.7	7.9	
	UA		79.1	63.1	74.3	
198	Al <sub>2</sub> O <sub>3</sub>	48.7	38.5	38.6	36.9	23.4
	COM		24.9	27.1	26.2	
	UA		75.1	72.9	73.8	
237	Al <sub>2</sub> O <sub>3</sub>	54.7	34.6	40.0	45.3	11.6
	COM		13.3	11.6	14.4	
	APA		47.1	32.4	47.9	
	STR		8.2	8.4	12.7	
265	Al <sub>2</sub> O <sub>3</sub>	33.9	39.8	42.6	46.0	31.6
	STR		41.9	46.0	52.0	
322	Al <sub>2</sub> O <sub>3</sub>	49.5	44.0	70.3	64.4	8.8
	APA		53.3	36.5	42.6	
	STR		20.1	16.6	21.0	
352	Al <sub>2</sub> O <sub>3</sub>	28.0	36.2	37.6	48.1	22.3
	COM		7.7	5.8	8.5	
	COD		47.6	44.3	30.8	
	APA		42.0	31.1	42.0	
358	Al <sub>2</sub> O <sub>3</sub>	56.9	36.3	40.6	48.4	11.1
	COM		26.4	23.9	20.4	
	APA		46.2	49.7	41.2	
	STR		11.1	13.8	12.1	
458	Al <sub>2</sub> O <sub>3</sub>	47.3	34.8	48.4	46.0	22.6
	COM		41.0	35.0	43.3	
	COD		42.2	43.8	39.5	
461	Al <sub>2</sub> O <sub>3</sub>	48.8	39.9	49.9	52.3	14.1
	COM		29.9	28.4	33.7	
	COD		61.9	55.7	50.5	
477	Al <sub>2</sub> O <sub>3</sub>	52.5	40.8	46.4	48.2	25.6
	COM		30.4	23.8	35.7	
	COD		10.5	6.6	10.5	
	APA		31.2	29.3	24.4	
505	Al <sub>2</sub> O <sub>3</sub>	29.0	40.2	45.5	43.9	25.4
	COM <sup>3</sup>		21.9	15.3	24.0	
	COD		28.3	18.9	22.7	
	UA		42.3	38.6	40.3	

<sup>1</sup> concentrations of Al<sub>2</sub>O<sub>3</sub> expressed as wt-% of measured specimen, i.e. percentage of (X<sub>C</sub> + X<sub>0</sub>), whereas concentrations of stone components are expressed as wt-% of stone, i.e. percentage of X<sub>0</sub>, (cf. equation (I.43));

<sup>2</sup> as determined by transmission measurements from separate specimens;

<sup>3</sup> concentrations calculated according to equation (I.45) with k = RIR<sub>A,C</sub> from table I.6, except for Al<sub>2</sub>O<sub>3</sub> figures which give the actual concentrations added to the sample ('true concentration');

<sup>4</sup> concentrations calculated according to equation (I.47) using  $\mu^*$  values from column 2, mass values from column 7, and filter area of 4.52 cm<sup>2</sup>; corrected with ('true') internal standard concentration;

<sup>5</sup> concentrations calculated according to equation (I.50); else as above.

Table I.8. Comparison of constituent concentrations [wt-%] derived from quantitative x-ray diffraction (RIR-internal standard technique) and ICP-AES analyses (cf. table II.13).

stone sample	QXRDA	ICP-AES	stone sample	QXRDA	ICP-AES
97	49.3% COD APA	50.7% COD 39.1% APA	389	24.7% COM 13.8% COD APA 23.7% UA	8.2% COM - 45.5% APA -
137	8.1% COM 79.1% UA	9.6% COM 86.1% UA			
189	24.9% COM 75.1% COD -	COM COD 12.8%UA			
207	47.4% COM 52.6% COD	24.6% COM 67.4% COD	400	39.4% APA 22.9% STR	50.0% APA 24.8% STR
237	13.3% COM 47.1% APA 8.2% STR	22.4% COM 48.8% APA 25.0% STR	402	92.1% COD -	85.1% COD 9.5% APA
264	41.9% APA 40.7% STR	43.4% APA 47.0% STR	405	43.2% COM 51.9% UA	44.9% COM UA
265	- 41.9% STR	11.1% APA 79.6% STR	415	6.5% COM 62.9% COD - -	COM COD 8.5% APA UA
268	APA 59.8% STR	46.2% APA 44.3% STR	426	4.6% COM 95.4% COD -	COM COD 7.8% APA
322	53.3% APA 20.1% STR	54.3% APA 31.7% STR	458	41.0% COM 42.2% COD -	COM COD 10.3% APA
352	7.7% COM 47.6% COD 42.0% UA	36.0% COM - -	461	29.9% COM 61.9% COD -	COM COD 17.1% APA
358	26.4% COM 46.2% APA 11.1% STR	32.6% COM 47.5% APA 14.3% STR	477	30.4% COM 10.5% COD 31.2% APA	COM COD 47.9% APA
			505	21.9% COM 28.3% COD 42.3% UA	37.3% COM - UA

correction purposes is indispensable especially when studying small (< 10 mg) samples. In addition the use of the silver maxima suffices for the correction of changing absorption effects in the samples and a separate determination of the attenuation coefficient is unnecessary. However, each filter has to be scanned before and after the deposition of the sample, since great variations in the intensity (3400-4700 cps) were found from one filter to another.

Using the internal standard method concentration values between the two preparations of each specimen agreed within 10.6% (mean; range 1-21%). The mean agreement obtained when averaging concentrations using one analyte reflection and all standard reflections was 8.5% (mean; range 0.7-17.1%). On the other hand concentration agreement varied between 1.8 and 6.5% (mean 4.2%) when using all analyte and standard reflections. This clearly illustrates the benefit of using multiple reflections and the resulting reduction in the overall error. For the microanalytical methods, the same trend was observed, although deviations were somewhat larger. At very low filter loads (i.e. < 2 mg) quantitative measurements cannot be made. Even the positive identification of all materials in a sample is hampered when peak maxima are within the  $3\sigma$  limit of background radiation.

Detection limits were not established in the present study due to their extreme dependence on the matrix constituents. Generally it is thought that for a well crystallized phase, concentrations as low as 1% may be determined, but that for poorly crystalline phases concentrations as high as 25% (w/w) and even higher, may be completely undetected /NIC75/. Lagergren has reported that this rule applies to calcium oxalates where as little as 1% of COM and COD can be distinguished clearly /LAG56/. Schroeder et al. have reported detection limits of the same order of magnitude (2-5%) for BRU, OCP and WHI in the presence of other phosphates /SCH66/. Under unfavourable conditions, such as line broadening, these workers however report a limit for HAP detection of 30-50% (w/w). These results are in agreement with the present study, where often no apatite could be demonstrated using XRD, but a second technique revealed its presence (cf. chapter II). Although the presence of apatite could, in very many cases, be deduced from elevated background readings, no quantitative analyses were possible. Sutor /SUT68/

has published percentage detection limits for stone constituents in many 2-component mixtures. Her results have shown that minor constituents with concentrations in the range 5-20% can remain undetected. It can therefore be deduced that when 3-component mixtures are considered even higher percentages are missed.

## 8. Conclusions

**Qualitative** x-ray diffraction has in all but few cases been found to be superior to other analytical techniques, when unequivocal phase identification was required. Das et al. /DAS75/ and Sutor et al. /SUT71a/ compared chemical and x-ray crystallographic methods. Both reported only in 30-40% agreement between the two methods. Sutor et al. drew special attention to the fact that magnesium often exchanges for calcium in phosphates (and oxalates) and that this might lead to wrong interpretations when only chemical methods are used. Pollack et al. /POL69/ compared infra-red and XRD techniques for mixtures of phosphates, whereas Hesse et al. /HES72/ conducted the same kind of study for  $\text{CaOx}$  calculi. While both techniques were found to be equally well suited for the analysis of uroliths, the roentgenographic technique was shown to be more sensitive in 8 out of 10 cases /POL69/. Prien et al., who popularized the optical crystallographic technique /PRI47/, compared the use of the polarization microscope with XRD /PRI47, PRI63, PRI74/. They found the petrographic analysis superior to XRD, not so much on analytical but more on economic grounds. They rate XRD as being slow, time consuming and too expensive, a view which is shared by Korn et al. /KOR81/. This is certainly true if total quantitative analysis is attempted with XRD. However, the polarization microscope requires an experienced operator, whereas XRD can be applied after brief training. Leusmann /LEU81/ shows the benefit of employing both, XRD and SEM techniques in the analysis of urinary stones. A scanning electron microscope with an attached energy dispersive x-ray analyzer can identify stone constituents according to morphology and thus supplement phase information obtained by XRD. This should be particularly useful for small concentrations of the analyte. Beeler et al. /BEE64/, Dosch et al. /DOS74/ and Rodgers et al. /ROD82/ undertook a comparison of

multiple technique approaches to stone analysis. All three groups rated XRD as being the most informative phase analytical procedure investigated.

Although the concept and underlying theory of quantitative QXRDA are simple, practical details are more complex. Factors limiting the accuracy of the analyses are a result of several systematic errors (e.g. preferred orientation, microabsorption), random errors (particle statistics, generator instabilities, counting statistics) and calibration errors (improper matching of standard and analyte in RIR determinations with respect to impurities and crystallinity).

Several difficulties were shown to impede the proper implementation of the RIR-internal standard technique. Quantifying constants have to be determined by diffraction measurements of pure phases. In many cases these are not, however, readily available, nor do they provide a close enough match to the analytes. This was found to be one of the major shortcomings of the technique as far as quantitative apatite determinations are concerned. A possible solution to overcome this problem is the use of calculated XRD data, where the necessary constants  $k_{ij}$  can be derived from structural parameters only /ALT78/. This would enable the effect of substitutions to be calculated, while all intensities would be placed on an absolute scale /CLA73, HUB77/. However, a more accurate knowledge of the true spectral profile will be required; a goal that is still to be achieved. Furthermore, while accurate integrated intensities are easily obtainable from well-determined structures, the most readily available data from the diffractometer, the peak intensities, are the most difficult to synthesize /CLA73, SMI68/. However, only peak intensities can be used in practice, if analyses are to be completed in a short time.

Overlap of diffraction maxima, a common problem of all techniques discussed in this chapter, is another factor which greatly reduces the possible applications of QXRDA. As with the calculation of theoretical powder patterns, the use of whole pattern profile fitting methods might be able to alleviate this problem /HUA78, WEI83/. When applying peak separation /HAY81/ and profile fitting /HOU81, NAI82/ procedures in the present study, it was, however, noticed, that very stringent conditions

have to be posed on the acquisition of experimental data. Particularly when employing least-squares procedures, a small step size, e.g.  $0.01^{\circ}2\theta$ , is necessary to obtain convergence of the computed constants. This again would necessitate longer measuring times but position-sensitive detectors, presently under development might prove helpful in this respect /GOE81/.

Thus, although promising developments such as reliable computer phase identification have been forecast for the near future, the results of the present study show that QXRDA cannot be considered to be an excellent technique for the analysis of calculi. This is in agreement with the findings of other researchers, who have expressed the belief that a "conclusion concerning the exact stone composition can only be reached after XRD has been completed in conjunction with a second procedure" /JO083/. Indeed, when accurate elemental data obtained from techniques such as ICP-AES (cf. chapter II) are used to facilitate the quantitative assessment of phases identified by XRD, meaningful results can be obtained in conjunction with quantitative XRD analysis. The many advantages of such an approach have been discussed in detail by Garbaskas et al. /GAR82/. It is thus obvious "that the analyst's time would be better spent on obtaining chemical information than on making improvements in diffraction data" /MCC79/. The good results obtained in the round robin tests (see chapter II, table II.19) with such an approach, entirely support this view. It is therefore concluded that semiquantitative XRD analysis supplemented by accurate quantitative elemental data and a simple chemical (acid) test to distinguish hydroxy- and carbonate-apatite /FR042/, allows precise determination of the true stone composition. For this purpose, easily available peak intensities or even diffraction data recorded on a strip-chart recorder would suffice. Mixture series such as those reported by Schneider et al. /SCH74a/ would also be helpful in this respect.

## Chapter II

### Application of inductively coupled plasma atomic-emission spectroscopy as an analytical tool in urolithiasis studies

#### 1. Introduction

There are over 40 elements thought to be present in the human body, many of them having biological functions that are essential to optimum health. Occuring at highly variable concentrations, several of these metals and metalloids are present at such low levels that the concentration values reported vary over a wide range, often depending on the analytical method employed /FEL84, YAN85/. Therefore there exists a tremendous demand for simultaneous multielement analytical methods, a problem gaining more and more importance with growing pollution threats over the past 15 years.

In principal there are several techniques suitable for this purpose, namely optical emission spectrography (OES), mass spectroscopy, x-ray fluorescence spectroscopy (XRF) and neutron activation analysis (NAA). From its early stages of development in the 1930's until about twenty years ago, OES was often the only method available for the determination of major, minor and trace constituents in virtually all sample types. During the past 15 years, the wide acceptance of atomic absorption spectroscopy (AAS) as an analytical tool for the determination of the concentrations of metallic elements has resulted in a decline in the use of OES. However, with the advent of new excitation sources, arguments in favour of atomic emission spectroscopy (AES) as the most adequate procedure for simultaneous multielement analysis abound /BOU76/.

In contrast to AAS or atomic fluorescence spectroscopy, the observation of free atoms and ions in emission does not require an auxiliary primary source. Analyte atoms are energized directly by the combustion flame, either air / acetylene (2600 K) or nitrous oxide / acetylene (3300 K). The main limitations of a flame source, however, are (i)

spectral lines with wavelengths below 350 nm are insufficiently excited, and (ii) stable compound molecules are only partially, or sometimes not at all, broken up. This leads to unfavourable effects on the detection power and the sensitivity and also causes interferences from band spectra /BOU75a/.

The belief that excitation capability, sensitivity and freedom from chemical interference increase with higher temperatures has led to the development of electrical and plasma discharge sources /GRE75a/. Early dc and ac arc and spark sources, although very useful, were found to be "notoriously demanding of the analyst" /DAH78/, and these techniques have been sacrificed almost completely in favour of plasma sources. As plasma methods appeared to have all of the advantages of the classical emission methods and of flame excitation, with few if any of their disadvantages /SK080/, various different approaches have been followed in the investigation of possible utilizable plasma sources. Among the proposed technologies were direct current (dc) plasmas, capacitively coupled plasmas, microwave plasmas, and radiofrequency inductively coupled plasmas (ICPs) /BOU76, BOU78, GRE75a, GRE75b, GRE76/. Comparison of detection limits and precision revealed ICPs to be superior to the other plasma systems, and further evolution of these techniques has been deferred in favour of ICP-AES. Today, less than ten years after its first commercial introduction /BAR81/, ICP-AES is one of the most used new analytical tools of the decade.

The University of Cape Town was the first university in the Republic of South Africa to purchase a commercial ICP-AES system /MO082/, thereby starting a new era in spectroscopy in this country /DEV83/. When compared with flame AAS, the absence of the classical Ca and  $\text{PO}_4$  solute vaporization interference combined with the fact that sufficiently high excitation of phosphorus atoms can be achieved, suggested the ICP as an ideal analytical source for the simultaneous determination of the three most abundant elements (apart from oxygen) in human calculi, viz., calcium, magnesium, and phosphorus. The present study was thus undertaken to investigate the feasibility of determining these elements in human pathological concretions /ROD84, WAN84, WAN85, WAN86/. In addition, studies involving trace element determinations were also undertaken. Several workers /AND84, DON77, HES78, LEV78,



MEY77/ believe that such elements may play a key role in urolithiasis. Furthermore it was also decided to attempt the analysis of crystallization products obtained from evaporation experiments with artificial urines (chapter 4) using this method in order to try to correlate the quantitative measurement of crystalline phases with other techniques, such as x-ray powder diffraction.

In the following paragraphs the technique of ICP-AES is described together with the parameters which determine its analytical utility. As currently only solution samples can be conveniently analysed by ICP-AES a discussion of sample preparation procedures then follows. Thereafter, results for more than 100 South African human calculi analysed for Al, Ca, Cu, Fe, K, Li, Mg, Mn, Mo, Na, P, Pb, S, Sr, and Zn are presented.

## 2. ICP-AES

### 2.1 Introduction

By definition, a plasma is a radiation emitting gaseous mixture, in which a significant fraction of the atomic and / or molecular species is ionized. The ICP torch plasma consists of a very hot ball of argon and analyte atoms, ions and electrons generated by inductively coupling of a small volume of preionized atoms to the work coil of a radiofrequency (rf) generator.

Based on the early work of Babat on electrodeless discharges in high-frequency electromagnetic fields /BAB47/, Reed first developed such a plasma torch grounded on inductive coupling to an ionized gas /REE61/. He already mentioned argon as being the simplest gas in which to start and operate the plasma, and described his approach to the (vortex) stabilization and thermal isolation of these Ar plasmas. At first the ICP was employed for the growth of refractory crystals /REE61a/, but soon afterwards the flexibility of the ICP torch as a spectral source was intimated and its application in analytical spectroscopy was suggested /REE62/. Independently of each other, Greenfield et al. /GRE64/ and Wendt et al. /WEN65, WEN66/ realized the potential

of the much higher temperature of the argon 'flame' to overcome elemental interferences experienced until then in flame photometry and AAS. Later, a succession of workers in various countries also explored the practicability of ICP-AES /FAS74, KNI73, WIN77/. Yet, this technique was only slowly accepted as a viable analytical tool. With the greater availability of commercial instruments, the ICP was finally recognized as an excellent vaporization - atomization - excitation - ionization source for analytical AES. Advantages of ICP-AES systems include /FAS78/:

- (i) all elements can be determined. Exceptions are argon (plasma) and hydrogen in aqueous sample solutions. Nitrogen and oxygen analyte signals can be measured when atmospheric contamination is excluded by viewing low in the plasma or employing special torch designs /NOR80, NOR80a/. The determination of halides is possible, but currently not practical for fluorine in routine work /NYG85/;
- (ii) true simultaneous multielement determinations from major to ultratrace levels with a single set of excitation parameters are common;
- (iii) almost complete absence of interelement effects (except spectral interferences) as well as minimal background is observed;
- (iv) linear calibrations over a large (4 to 6 orders of magnitude) concentration range are obtained;
- (v) capability of providing rapid, automatic analysis;
- (vi) acceptable precision and accuracy, and good detection limits, comparable to those of other techniques, owing to remarkable stability;
- (vii) applicability to microlitre and microgram samples;
- (viii) direct analysis of gases, liquids, and (after dissolution) solids.

The practicability of determining phosphorus simultaneously with calcium and magnesium makes ICP-AES an especially favourable technique for the analysis of calculi. Phosphorus, one of the four most abundant elements in stones, can in these circumstances usually be determined only with great time consuming and often inaccurate colorimetric methods /FIS25, FOG58, GOM42/. In addition, the  $\text{Ca} - \text{PO}_4$  solute vaporization

zation interference which has been attributed to the formation of thermally stable  $\text{Ca}_2\text{P}_2\text{O}_7$  or  $\text{Ca}_3(\text{PO}_4)_2$  compounds is of no importance. As a result of the high plasma temperature, the sharp depression of the calcium emission (absorption) in the presence of phosphorus observed in flame photometry (AAS) is markedly reduced or non-existent /LAR75, WEN66/.

This high degree of compliance of ICP-AES with the requirements of an ideal element-specific analytical system, shows that ICP-AES, under properly chosen experimental conditions, can either compete with other methods, including AAS, or possesses greater capabilities than these /KAH82, KAH82a/. To understand the influence of instrumental parameters on the listed advantages and on the overall performance of an ICP-AES system, a brief description of such an instrument and its underlying principles is given below.

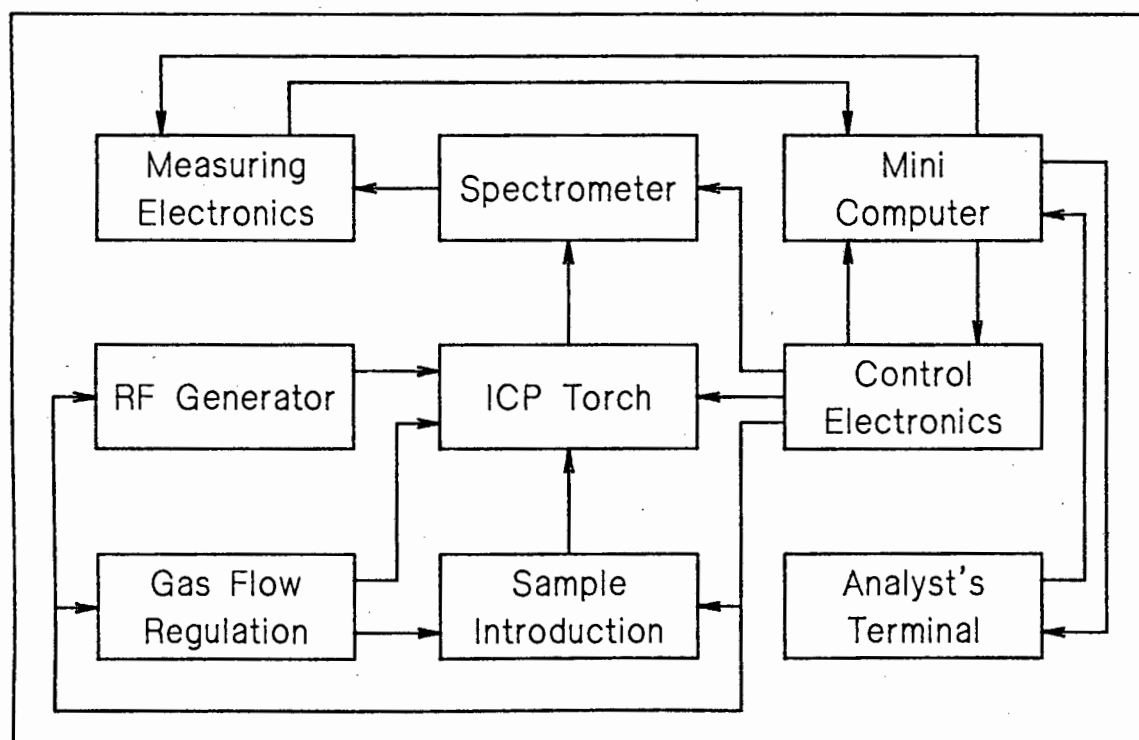


Figure II.1. Typical ICP-AES instrument layout.

## 2.2 Instrumentation and operating principles

Generally, an ICP instrument consists of a torch with matching rf power supply, a sample introduction device, an optical system, and a microprocessor which controls and drives the different parts of the apparatus /GRE75/. A schematic representation of the computer interaction is given in figure II.1.

### 2.2.1 ICP torch

Most of today's instruments use a design in which the ICP load is directly coupled to a rf power amplifier. Generators usually work in the 4 - 80 MHz range with output levels from 0.5 to 15 kW /OLS84/. However, the present tendency is to favour ICPs operated in a more limited frequency range of 27 - 50 MHz, and low power (1 - 2 kW), which yield the best analytical performance /BOU78/.

The work coil of the generator surrounds an assembly of three concentric tubes, usually made of silica (figure II.2). The plasma gas is injected tangentially between the outer two tubes, so that a toroidal (or annular) plasma is easily produced. This results in a vortex stabilization of the plasma discharge. Sample introduction through the centre tube allows efficient and reproducible injection of solution aerosols into the 'doughnut' hole of the plasma, where the analyte particles experience temperatures of between 6000 and 10000 K /GRE75a/. An auxiliary gas flow between the sample introduction jet and the next quartz tube anchors the discharge slightly above the inner tube assembly, so as to prevent them from melting. After ignition, the power dissipated in the plasma results in Joule heating of the flowing argon. The aerosol is principally heated by conduction and radiation from the surrounding Ar /SC074/, resulting in an exceptionally high degree of atomization for all elements. Argon gas flows are typically in the 15 l min<sup>-1</sup> range with an additional flow of about 1 l min<sup>-1</sup> that transports the sample to the plasma /FAS74a/. The plasma has the general appearance of a bright flame with three distinguishable zones. The first region, the plasma core, extends from inside the induction coil to a few millimeters above it. An intense continuum stemming from

recombination processes as well as a fully developed Ar spectrum is emitted at this position. The second zone is also bright, but slightly transparent and occupies the region from ca. 10 to 30 mm above the current carrying coil. Here the continuum emission is sharply reduced by several orders of magnitude, providing an almost ideal emission source, as this part of the flame is optically thin and gives rise to

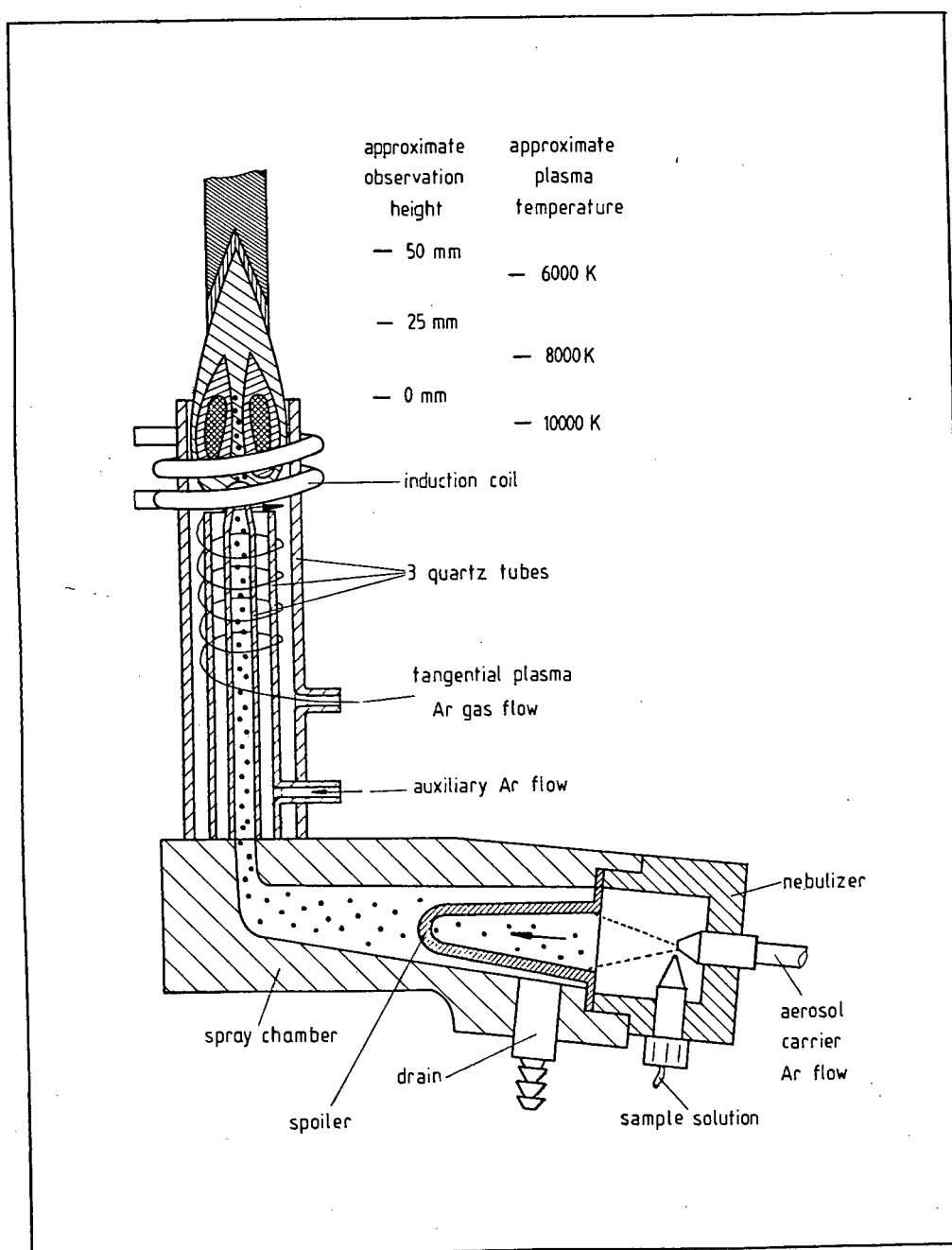


Figure II.2. ICP torch.

very little self-absorption. The tail flame or third zone is distinctly separated from the second region and assumes typical flame colours when analytes are aspirated. In general, the highest signal to noise ratios for analyte species are observed in the middle and upper part of the second zone.

Usually three parameters - the torch power, the plasma gas flow, and the torch observation height - enable the analyst to tune the ICP instrument to optimum conditions for the relevant sample solutions.

High analyte signal to background intensity ratios can be derived from low powered plasmas /BOU77/. However, atomization and excitation of complex matrices might be inefficient at lower torch powers, and enhancement effects from easily ionizable concomitants can occur, due to a change in the ionization equilibrium. Organic compounds or solvents also require more power than aqueous solutions.

Higher power necessitates increased plasma gas flow to contain the plasma discharge above the sample introduction tube. Owing to reduced intensity of OH, CN and SiO emission bands, increased argon flow also diminishes detrimental effects of the air atmosphere mixing with the plasma jet.

For stone samples medium powers were generally found to be adequate in this study to break up possible Ca -  $\text{PO}_4$  compounds and to prevent adverse effects from matrices with high organic and alkali metal (Na, K) levels.

Keeping the other parameters constant, the optimal signal to background ratio is obtained at a different torch observation height for each element, mostly depending on its excitation potential. Because the region of highest background intensity coincides with the region of the highest temperatures, different analyte elements should be observed at the highest positions in the flame which their excitation energies allow. To decrease the sensitivity of calcium emission lines (to avoid saturation of the photomultiplier - section 5.3), the viewing height can be increased for stones rich in Ca. On the other hand, sodium and potassium should be observed lower in the flame, because they are

easily ionizable and the ion emission lines are more intense at this position, thus making possible trace determinations of these elements.

### 2.2.2 Sample introduction

Requirements of a good sample introduction system are high reproducibility and low retention of sample, as well as inertness and versatility, to enable the system to cope with high dissolved solid levels and organic solvents. At present there is still a need to take samples into solution prior to injecting them into the ICP.

Thus, sample introduction is mostly in the form of aerosols produced either by ultrasonic breakdown of the liquid surface or employing pneumatic nebulizers of the conventional concentric or more advanced cross-flow type. To ensure constant sample flow a peristaltic pump is employed in most cases. By increasing the sample delivery speed, the intensity equilibration time can be shortened when a new sample is aspirated. However, an increased sample aspiration rate also reduces the temperature of the plasma. This again might be beneficial for elements with low excitation energies, like the alkali metals.

While the sample feed is determined by the volume flow rate of the peristaltic pump, sample residence time in the plasma is controlled by the nebulizer driving pressure. The setting of this parameter defines the velocity of sample flow through the discharge. Elements with high excitation energies and complex compound samples require long residence times and thus low pressures, to ensure complete excitation and total atomization, respectively.

To overcome the low efficiency of only 0.5 - 2% associated with conventional nebulization, direct insertion of sample solutions into the plasma, using a graphite rod, has been successfully applied /KIR82/. However, the inevitable necessity to convert solid materials into solution form is most often the time-limiting factor in the entire analytical procedure. Another serious limitation of the nebulization of dissolved samples is the problem of devising a multi-element dissolution method. This situation has led to calls for the development of new

procedures for the sample introduction step. Various improvements have been suggested recently /BRO83/. Among them is the Babington nebulizer system, an effective means of introducing samples as slurries, or samples containing very high levels of suspended particles /FRY77/. Flow injection, a wide-ranging approach to chemical analysis /BET78, TYS81/, has attracted much attention, as it allows single-shot calibrations /GRE81/ and therefore permits the use of micro-samples. Direct vaporization of samples using tantalum filaments /NIX74/ or graphite furnaces /AZI82/ is another technique permitting trace determinations on a multielement basis in microlitre- or microgram-sized samples. Sparks have been used for sampling and nebulizing material from solid conducting samples /HUM76/, while laser ablation has been employed for the unselective volatilization of nonconducting solids /THO81/.

Despite the fact that Salin /SAL79/ has described a sample introduction system that allows the direct insertion of small amounts of solids into the plasma, a practical solution to the several problems of injecting powdered samples into a continuous discharge and performing quantitative analysis, has yet to be found. Dissolution of solid samples prior to analysis by ICP-AES is thus still required for most applications.

### 2.2.3 Optical system

Since an ICP discharge has a temperature of between 6000 and 10000 K it emits complex line spectra. Therefore an optical system of medium to high resolving power is required. A resolution of 0.01 to 0.02 nm and a stray light exclusion ratio of  $1:10^6$  will usually be adequate. Three different signal recording systems are, in the main, available. These are (i) a spectrograph which records a photographic image of the emission lines, (ii) a polychromator providing a separate detector for each element of interest and (iii) a scanning monochromator, utilizing a movable grating to bring the light from the wavelength of interest to a single detector. While the polychromator is well adapted for the simultaneous analysis of many elements in routine samples, the monochromator is a highly flexible system for single-element determinations /BOU78a/. Nowadays computer-controlled programm-



able monochromators with automatic wavelength calibration and background correction facilities can solve problems far beyond the capabilities of the inflexible polychromator, the only disadvantage being that a little more analytical time is required /BOU76b, SPI76/. The design of the optical systems used in this study is shown in figure II.3.

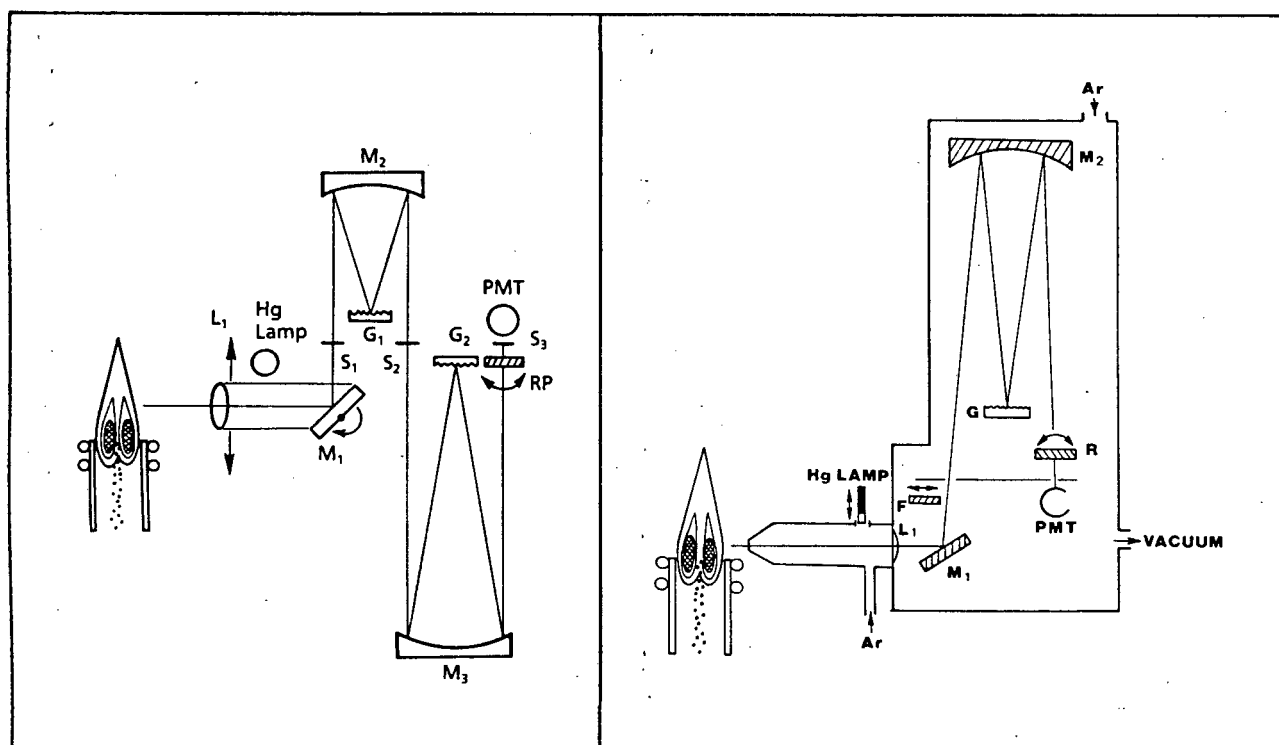


Figure II.3. Optical system designs.

a) Air path double monochromator diagram (Plasma-100: channels A and B; Plasma-200: channel A).

b) Vacuum monochromator diagram (Plasma-200: channel B).

F=filter, G=grating, L=lens, M=mirror, PMT=photomultiplier, RP=refractory plate, S=slit.

With the free choice of the wavelength, the analyst has the primary means to overcome spectral interferences, and to optimize the

analytical procedure with regard to linearity of calibration curves and good detection limits.

#### 2.2.4 Electronics

Most of present day ICP instruments are microcomputer controlled. The computer monitors interrupts and initiates and controls functions like plasma torch ignition, gas flows, monochromator drives, etc. Automatic sample change facilities and on-line analytical programmes allow the automatic processing of huge amounts of samples with determinations of more than 20 elements per sample /GRE75b, FLO85/.

#### 2.3 Method development

As discussed before, the analytical performance of an ICP may be greatly affected by the choice of operating parameters. Essentially four parameters are of importance: (i) the torch power input, (ii) the plasma argon flow rate, (iii) the observation height above the torch coil, and (iv) the carrier gas flow rate and nebulizer driving pressure. The tedious approach of optimizing all parameters for each element separately is usually not justified and one set of experimental parameters provides virtually optimal conditions for all the elements in question /BOU75/. Only in extreme cases, like the simultaneous determination of alkalis and precious metals, or when the signal intensity exceeds the dynamic range of the instrument, might a single optimization be necessary and justifiable. Details of such an approach are described, for example, by Nygaard /NYG84/ and Leighty /LEI81/. After identification of these compromise conditions only the choice of a spectral line for each of the relevant elements is left to the analyst. Then a systematic approach is essential in studying the capabilities of the instrument to analyse the particular elements at a desired level, i.e. to obtain estimates of detection and upper concentration limits, the linearity of calibration graphs, and spectral and background interference data.

### 2.3.1 Spectral lines

The choice of spectral lines is usually based on information from the literature and by using line coincidence tables, e.g. those of Boumans /BOU80/, considering possible interferences by other elements present in the samples. Data on anticipated concentration levels also influence the selection of emission lines owing to the different sensitivity of atom and ion lines /BOU75/. The parameters described below are used to compare the usefulness of spectral lines.

### 2.3.2 Detection limits

The detection limit is usually defined as the analyte concentration which will produce a net line intensity that is twice or three (IUPAC recommendation) times greater than the standard deviation of the background signal for a blank solution not containing the analyte, with a minimum of 10 successive measurements. The least quantitatively determinable amounts, i.e. values with a precision of 10% or better, are generally concentrations five times greater than the reported detection limits. These are listed for most of the elements in almost all of the earlier publications on ICP-AES although considerable improvements were observed over the years. Commonly they are found to be in the 0.7 to 10 ng ml<sup>-1</sup> range for most of the elements. Differences of up to a factor of three are not significant, as variations and day to day changes in any instrument as well as operator skills can easily alter the values by such an amount. Often, however, unrealistically low detection limits are reported. These invariably are obtained by using an excessively large number of readings and long integration times. Proper lower limits of detection thus have to be established for each study anew.

The upper concentration limit is the maximum concentration that can be aspirated without the signal intensity saturating the photomultiplier tube of the detection system. Choice of a less sensitive line or use of a less efficient observation height, as well as sample dilution can help to alleviate this problem.

### 2.3.3 Calibration curves and dynamic range

The linearity of calibration plots from blank to upper limit concentration levels must be verified in each case. Due to the high temperature of the plasma and confinement of the analyte atoms and ions into a narrow channel, self-absorption and recombination processes are usually not detected. The absence of these effects, which often cause nonlinearity of the response when 'ordinary' flames are employed, renders possible linear calibration graphs from the detection limit to concentrations four to five orders of magnitude higher. The wide linear range has particular advantages as it conveniently limits the number of reference samples required and allows high level and trace concentrations to be determined in samples with the same dilution factor. Sample preparation and calibration procedures are therefore drastically simplified.

It is good experimental practice to check instrumental drift by frequent recalibration using the highest concentration standard and the blank. To eliminate adverse effects on precision and accuracy of the measurement, the blank, reference and analysis samples should be roughly matched in acid content and salt matrix. Failure to do so may lead to inaccurate concentration determinations, as will be shown later.

### 2.3.4 Interferences

Two types, additive and multiplicative interferences are commonly observed. The first type gives rise to a change in the intercept of the calibration curve when a sample constituent generates a signal that adds to the analyte intensity. The second type changes the slope of the calibration graph when a sample constituent enhances or suppresses the analyte signal without generating a signal of its own. Furthermore, interferences are divided in three categories, namely spectral, chemical, and physical /BOU75/.

Spectral interferences are generally additive and occur due to either overlap of two emission lines or background phenomena like

emission from OH bands or stray light. These interferences can frequently be entirely eliminated by judicious selection of the lines to be used. If spectral line interferences cannot be avoided altogether, correction schemes based on the measurement of the concentration of interfering elements must be used /BOU76a/. True background shifts can be allowed for with background correction facilities, now available in most ICP-AES systems: after measurement of the background intensity on one or both sides of the analyte peak, this 'base line' is automatically subtracted from the emission line. Spectral interferences thus play only a minor role in ICP-AES.

Chemical interferences are comprised of the classical 'stable-compound-formation' interference and ionization interferences. These are generally multiplicative and are caused by chemical interaction of the sample constituents. Due to the high temperature of the plasma and the long residence time of the injected aerosol particles, complete atomization is obtained and 'stable-compound-formation' interferences are therefore virtually negligible. The magnitude of ionization interferences depends largely on the ionization potentials of both the analyte and concomitant and on the type of spectral line which is either atomic or ionic. These interelement interferences are sometimes reported as the effects of alkali metals (present as 'matrix' in the solution) on spectral line intensities. In most cases ICP operation conditions can be chosen so that these effects do not influence the accurate quantitative assessment of the analyte.

Physical interferences can originate in direct environmental effects (e.g. temperature and pressure variations) on instrumental performance which then become apparent as drift and increased noise levels during the analysis. More conspicuous are physical interferences caused by changes in the bulk properties of the samples, like alterations in viscosity, surface tension, and volatility. These 'nebulizer interferences' affect sample transport into the plasma and are generally multiplicative. They can be minimized by avoiding large variations in dissolved solid levels and solvent type.

Physical interferences in the nebulization and aerosol transport system can of course pose as apparent excitation interferences in the

plasma source when large solvent variations are encountered. For example, the rather sensitive dependence of the elemental emission on the concentration of mineral acids is sometimes attributed to a change in the width of the sample channel through the plasma and other excitation conditions. Others relate the probable cause to factors such as variations in sample uptake as a result of different viscosities, different droplet size and aerosol generation efficiencies. Although their origin is not well understood these acid effects have to be taken into account as they not only change the absolute intensities measured in the ICP, but also cause considerable background shifts. Unusually long memory effects in the nebulizers have also been observed /POU86a/ which might in some cases require longer washout times.

Many workers have discussed the influence of varying acid concentrations on line intensities in atomic spectroscopy /BOT85, CHU80, DAH78, KOI75, KOI81, WAN84/. Three techniques are currently in use for compensating for acid / salt matrix interferences in ICP-AES: (i) standard addition method, (ii) internal reference standard method, and (iii) the usual practice of matching the matrix of calibration reference and sample solutions. As all these procedures require additional steps in the sample preparation or analysis, Botto proposed a new method based on the measurement of the intensity of the H<sub>g</sub> line /BOT85/. Rough matching of the acid content of the analysis and standard samples is, however, still the most common approach to overcome systematic errors due to variable acid strength in the analysis samples. The effect of variations in the sample matrix is also minor when the acid employed for digestion is made the predominant component in the analytical sample.

Therefore, although physical 'matrix' interferences do occur in the nebulization, aerosol transport and excitation system of ICPs, they are easily dealt with by appropriate control of reference standards.

### 3. Sample preparation procedures

A stable solution of the elements to be measured is still a prerequisite in ICP-AES. The complete transformation of biological samples into solution, however, remains in many cases a major problem where it requires total destruction of the samples. Generally, wet digestion provides better recovery for elements while dry-ashing requires fewer preparative steps and less attention. Dissolution methods must be appropriate for simultaneous multielement analysis and compatible with the plasma nebulization system. As most ICP torches are assembled from quartz tubes, the use of hydrofluoric acid is precluded from most decomposition procedures, due to the possibility of erosion of the sample introduction system /FRY80/. An account of the variable success of different acids and acid mixtures in the decomposition of urinary concrements is given below.

#### 3.1 Wet digestion techniques

Acids employed to destroy the organic and inorganic constituents of human stones include HCl /LE056/,  $\text{HNO}_3$  /HOL53/,  $\text{HClO}_4$  /WES70/, and  $\text{H}_2\text{SO}_4$  /BR039/. Preliminary dissolution experiments regarding these acids were conducted in the present study and the results are presented in table II.1. The aim was to find an acid or acid mixture which would attack all major stone components indiscriminately.

Hydrochloric acid dissolves calcium phosphates and oxalates, but not uric acid /PHI53/. Although the acid was apparently successfully employed in hour long, hot digestions of uricites /LEV78/, it remains unsatisfactory as most samples leave a flocculent residue after the solution has cooled /LE056/.

Destruction by hot oxidation with concentrated sulphuric acid, though a prevalent practice for the digestion of organic matter, has a tendency to form indestructible charred residues /ADR73, BOC79a/. Even in combination with nitric acid, sulphuric acid is not suitable when calcium is a major constituent, because of the precipitation of calcium sulphate, thus precluding stones high in calcium from analysis.

Furthermore, these precipitates can retain small amounts of other elements, making quantitative recovery of trace constituents difficult. Moreover, the determination of sulphur in calculi thus becomes an impossibility.

Table II.1. Effectiveness of various acids in the digestion of stone constituents.

acid	HCl	HNO <sub>3</sub>	HClO <sub>4</sub>	H <sub>2</sub> SO <sub>4</sub>
component				
COM	+#	+	t	-
APA	+	+	t	v,t
STR	+	+	t	v
UA	t	t	+	v,t
AAU	-	v	-	-
SAU	-	v	+	v

# + = effective dissolution

- = no visible reaction

v = vigorous reaction - losses due to spattering possible

t = turbid solution after reaction

Nitric acid is used very widely in analytical chemistry as primary oxidant for both inorganic and organic substances. Simple decomposition with nitric acid alone, however, proceeds with difficulty in most cases /BOC79/ and often leads to an insoluble yellow cake owing to high organic contents. If the acid is heated to fumes, mechanical loss of elements, in particular of sulphur, has been reported /BOC79, SHE02/.

The most efficient and routinely employed wet oxidation methods involve the use of perchloric acid as oxidant /SMI65/. No hazard is attached to perchloric acid digestion if simple precautions are observed /ANA59, MUS72/. Difficulties encountered with perchloric acid solutions are mostly due to the formation of the anhydrous acid or its derivatives. Conversion of the aqueous acid to the dehydrated form or



formation of unstable perchlorates has led to fires and explosions of quite stunning violence /BUR55, HAR49, SCH60/. Because of these dangers,  $\text{HClO}_4$  is rarely used on its own. Also the low solubility of the perchlorates of ammonium and the alkali metals /DEB83/ limits the scope of this acid. A very common approach is, therefore, to treat the samples with both nitric and perchloric acids, thus retaining the advantages of the oxidizing power of  $\text{HClO}_4$  while moderating the reaction by (prior) decomposition of the more reactive compounds with  $\text{HNO}_3$  at lower temperatures /BOC79b/. This combination of acids, applied either in succession or as a mixture, was found to be the most effective of all procedures tested in the present study. This is substantiated by a comparative study of the effects of wet ashing techniques on the determination of trace element concentrations in biological samples /LON80/ which reported the use of  $\text{HNO}_3$  /  $\text{HClO}_4$  mixtures to be among the two best digestion procedures. Outstanding accuracy, high precision, and excellent sample recoveries make this approach superior to other acids, acid combinations or base digestions.

A great advantage provided by perchloric acid during the decomposition of kidney stones is that elements such as calcium and phosphorus remain in solution throughout the digestion. Total recovery of almost all elements to be determined in the ashed samples is achieved /GOR70/. Even volatile elements are retained through the positive influence of the refluxing acid medium /SMI57/. Furthermore, organic stone components like oxalates, which react by liberating large amounts of  $\text{CO}_2$ , are rapidly and completely oxidized without uncontrolled reaction.

Although Gourley /GOU52/ obtained poor recoveries when digesting stable phosphorus compounds with concentrated nitric and fuming perchloric acids, Kirsten et al. /KIR60/ found the open tube wet combustion method employing these acids to be the "fastest, simplest, and most convenient" procedure for samples containing only a few micrograms of phosphorus. Low phosphorus values could, however, arise from the reported strong adsorption of phosphate onto polyethylene and PVC /MUR56/. Sample storage bottles constructed from these materials will influence measured P levels. Yet Harwood et al. /HAR73/ have shown that acidification of the samples helps to prevent phosphate adsorption. Likewise, no adverse effect of long-period sample storage in poly-

ethylene bottles was observed in the present study. Washing and pre-conditioning of the storage vessels' inner surface as suggested by Knapp /KNA84/ also helped to further minimize adsorption and / or desorption.

Foaming of samples, sometimes a problem during wet digestion of urines /DEL74, DUN73/, was seldom observed during the course of this study. However, the considerable volumes of gaseous oxidation products resulting from perchloric acid oxidations, can cause sufficient effervescence leading to mechanical loss of compounds in the form of spray. This in turn results in losses of all elements to the extent of 0.1 - 1% /BOC79b/. The rate of reaction and / or effervescence thus has to be kept at a moderate level to avoid the elimination of compounds /FEL74/.

Due to the extreme sensitivity of ICP-AES, contamination of the samples during their collection and preparation for analysis has to be controlled. As the main source of this contamination is constituted by reagent impurities, acids of analytical reagent grade (or superior) have to be employed in the digestion procedure. Therefore, high purity reagents were used throughout in this study when trace constituents were determined.

It was thus concluded that combined  $\text{HNO}_3$  /  $\text{HClO}_4$  attack, whether in a successive manner or as a mixture, is the most efficient method for decomposing urinary stones. However, when employing these acids in the conventional wet ashing method with a hot plate, the time required for the whole analytical procedure (i.e. sample preparation plus analysis by ICP-AES) was found to be limited by the time needed for sample preparation (about 3 - 4 hours in the most stubborn cases (see section 4.2)). As a result it was decided to investigate a microwave assisted digestion procedure which offers the advantage of substantially shorter sample preparation times /POU86/.

### 3.2 Microwave digestion procedure

Microwaves are part of the electromagnetic spectrum with a frequency range of 100 MHz - 100 GHz. Commercial microwave ovens operate

mostly at 2450 MHz. Heat is generated rapidly when microwaves interact with dipolar (water) molecules owing to coupling of the respective electric field vectors and attenuation of the induced oscillations. Therefore microwaves have found increasing applications in domestic cooking and have been receiving more and more attention in industrial and laboratory drying applications /AND84a, HES74, KOH80, STR78, STU85/.

The use of a microwave oven for wet ashing and dissolution of samples was first reported by Abu-Samra et al. /ABU75/. However, a literature survey covering the past ten years revealed that with few exceptions (table II.2), this publication seems to have gone largely unnoticed. Conventional heating with a hot plate still prevails despite the fact that microwave assisted decomposition incorporates the following advantages:

- (i) ashing time is diminished by a factor of 2 - 10 or even greater and operator attention is greatly reduced, thereby allowing more samples to be prepared in the available time /ABU75, BOY78/;
- (ii) due to the shorter digestion time, samples are exposed to air for shorter periods which decreases possible atmospheric contamination /BAR78/.

In the present study, for example, digestion of human concretions by microwave irradiation for 1 - 3 minutes was found to yield good results (see section 5.2) compared to the 2 - 4 hours of heating required with a hot plate. This agrees well with reported /BAR78/ microwave sample preparation times of 3 min as compared to 30 min and 4 hours for two different AOAC methods. The increased speed and efficacy of the dissolution process is thought to arise from internal as well as external heating of the solution by microwave energy as opposed to traditional heating which is only external. Better mixing of sample and acids and faster reaction rates are thus achieved.

Certain precautions have to be taken, however, when employing microwave ovens for wet ashing of samples. Acid fumes generated during the dissolution must not make contact with the interior of the oven and thereby damage the magnetron and exposed electronic parts. Only 4 workers have so far described their experimental set-up and the first

Table II.2. Microwave assisted digestion procedures.

sample	digestion medium	analytical technique	elements	reference
NBS SRMs 1571 and 1577	HNO <sub>3</sub> + HClO <sub>4</sub>	AAS NAA	Cu,Pb,Zn As,Co,Cr,Ni,Se	/ABU75/
aquatic plants	HClO <sub>4</sub> + HNO <sub>3</sub>	AAS	trace metals	/OOO77/
teeth	HNO <sub>3</sub> + HClO <sub>4</sub> + H <sub>2</sub> SO <sub>4</sub>	AAS	Hg,Pb	/BAR78/
NBS SRM 1571	HNO <sub>3</sub> + HClO <sub>4</sub>	AAS	Cu,Pb,Zn	/KRA79/
plants	HNO <sub>3</sub> + H <sub>2</sub> SO <sub>4</sub>	AAS	Cd,Pb	/WAL79/
blood	HNO <sub>3</sub> + HClO <sub>4</sub>	radioactive tracer	Fe	/CAR80/
bone, food	HNO <sub>3</sub>	AAS	Pb	/DEN80/
NBS SRMs	HNO <sub>3</sub> + HClO <sub>4</sub>	NAA	Se	/MOR80/
biological materials	HNO <sub>3</sub>	AAS	—	/NIC80/
blood and red blood cells	HNO <sub>3</sub> + H <sub>2</sub> O <sub>2</sub>	radioactive tracer	Zn	/JAN81/
human kidney & liver autopsy samples	HNO <sub>3</sub> + HClO <sub>4</sub>	ICP-AES	Ag,Ba,Be,Ca,Cd,Co,Cr, Cu,K,Fe,Mg,Mo,Mn,Na, Ni,P,Sr,Th,Ti,Zn	/SUB82/
NBS SRM 1577	HNO <sub>3</sub> + HClO <sub>4</sub>	ICP-AES	Cd,Cu,Fe,Mn,Pb,Zn	/DEB83/
NBS SRMs	aqua regia + HF	ICP-AES	Al,As,Ba,Be,Ca,Co,Cr, Cu,Fe,K,Li,Mg,Mn,Na, Ni,P,Pb,Si,Sr,Ti,V,Zn	/NAD84/

commercial microwave digestion system (CEM Corp., Indian Trail, NC, USA) has become available only in recent months. These researchers used vented Pyrex and Perspex boxes inside the oven and removed corrosive reaction products with bubblers and scrubbers outside the oven /ABU75, BAR78, CO077/ or they employed partially evacuated desiccators to contain acid fumes /NAD84/. The assembly used in the present study incorporated both designs and is described in section 5.1. Acid fumes produced were first trapped in a flask containing KOH solution. Excess gas was bubbled through a beaker filled with water which also acted as a power absorber to protect the magnetron. This is important as the oven loses its load when dryness of a sample is approached. Although energy is still supplied to the cavity, in the absence of an absorber damage of the magnetron can occur as a result of arcing /AND84a, HES74/. No such problems were observed in this study and excellent agreement between the two digestion procedures (i.e. hot plate and microwave assisted) was obtained in determining Ca, Mg, and P.

#### 4. Determination of calcium, magnesium and phosphorus in human stones /WAN84, WAN85/

ICP-AES has not yet been used routinely in stone analysis, although one study employing a plasma emission torch coupled with a spectrograph yielded promising results in determining trace elements in urinary stones /LEV78/. In the present study a suitable method for the preparation of a wide variety of calculi for ICP-AES analysis was developed. Forty-one South African human stones were subsequently analysed for calcium, magnesium, and phosphorus.

##### 4.1 Instrumentation and apparatus

The measurements were carried out using an IL Plasma-100 ICP spectrometer (Instrumentation Laboratory Inc.) coupled to a line and video printer. The instrument has been described by Smith et al. /SMI83/. It features a 27.12 MHz crystal-locked rf generator with adjustable output power at 6 levels from 950 - 1750 W. In the three-

tube torch the plasma gas flow is divided between vortex stabilized primary flow and concentric secondary flow by a fixed orifice system. Total gas flow is set at 15 or 20 l min<sup>-1</sup> respectively, depending on the power level selected. The sample introduction system consists of a peristaltic pump allowing aspiration rates of 0.1 - 2.5 ml min<sup>-1</sup>, and an acid inert pressure driven nebulizer and a premix assembly to break up larger droplets. The optical system is built around a 1/3 m Ebert-Fastie primary monochromator with a 1/6 m premonochromator. A mercury vapour lamp serves for wavelength calibration. All components of the IL-100 are controlled by an Intel 8080A microprocessor programmed in FORTH /DES80/ allowing built-in graphics. The selected compromise conditions for the determination of calcium, magnesium, and phosphorus are summarized in table II.3.

#### 4.2 Samples and standards

Thirty-seven kidney stones and four gall stones were obtained from different hospitals in the Cape Town area. Representative aliquots or whole calculi were ground to fine powders using an agate mortar and pestle. Thereafter the samples were subjected to x-ray powder diffraction analysis using both film and goniometer procedures so as to identify qualitatively the crystalline phases present. Microchemical analysis for carbon, hydrogen, and nitrogen in each stone was also performed using a method based on the Haraeus universal combustion analyzer as described by Monar /MON72/.

About 100 mg aliquots of the powders were transferred to digestion vessels which were assembled from 50 ml Erlenmeyer flasks fitted with Quick-Fit extension tubes (110 mm long, 15 mm i.d.). These act as air condensers and prevent sample losses due to vigorous boiling and spattering. Samples were digested to low bulk with 5 ml of nitric acid (BDH Chemicals, 69-71%, AR grade) on a hot plate after refluxing at low temperature. Stones of essentially inorganic content gave clear solutions after a few minutes, whereas those with high organic contents required longer oxidation periods and in some instances yellow 'oily like' substances could not be destroyed further. After cooling, 5 ml of a 1:1 (v/v) mixture of nitric and perchloric (BDH Chemicals, 60-62%, AR

grade) acids were added and the vessels were heated slowly. The rate of boiling and / or effervescence was kept at a moderate level to avoid sample losses (cf. 3.1). After the evolution of nitrous oxides, the remaining nitric acid was driven off by gradually increasing the temperature until the perchloric acid started to react and fuming occurred. After cooling, the clear solutions were transferred to 100 ml calibrated flasks containing 5 ml concentrated nitric acid and 1 ml of 1% (m/v) Triton X-100 solution (surfactant, BDH Chemicals). These were diluted to volume with deionized distilled (dd) water which was used

Table II.3. ICP operating conditions.

rf power supply	27.12 MHz, 950 - 1750 W, selectable in seven steps (0 to 6), (3)*;
optical system primary monochromator premonochromator resolution 1st order 2nd order peak search window size	2 double monochromators, channels A and B; 1/3 m Ebert-Fastie configuration; 1/6 m Ebert-Fastie configuration; 0.02 nm; 190 -365 nm; 365 -900 nm; 0.033, 0.067*, 0.1 nm (user selectable);
computer system	Intel 8080A microprocessor, FORTH language;
sample introduction  nebulizer driving pressure sample feed	polypropylene spray chamber and cross-system flow nebulizer with synthetic sapphire capillaries and concentric quartz tube torch; 137.9 to 344.7 kPa (20 to 50 psi), (30 psi)*; peristaltic pump, 0.1 to 2.5 ml min <sup>-1</sup> ;
plasma coolant gas flow torch observation height	15 to 20 l min <sup>-1</sup> ; 0 to 48 mm above rf coil (2 mm increments), (16mm)*.
* settings used	

throughout for all preparations and for washing of the equipment. For stones with high organic contents, the time required for preparing samples was as long as 3 - 4 hours in some cases.

Calcium and magnesium standards were prepared from 1 g l<sup>-1</sup> aqueous standards for AAS (BDH Chemicals, Spectrosol) while a phosphorus 1 g l<sup>-1</sup> standard was prepared by dissolving 3.7136 g of (NH<sub>4</sub>)H<sub>2</sub>PO<sub>4</sub> (Merck, AR grade) in 1 litre of 1 N nitric acid. Standards of lower concentrations were obtained by serial dilution of these.

To investigate the precision and accuracy of the method, artificial stone mixtures were prepared from the following: calcium oxalate monohydrate (BDH Chemicals); ammonium magnesium orthophosphate [NH<sub>4</sub>MgPO<sub>4</sub>·6H<sub>2</sub>O, struvite] (BDH Chemicals); calcium phosphate, tribasic, type IV [approximately Ca<sub>10</sub>(OH)<sub>2</sub>(PO<sub>4</sub>)<sub>6</sub>, hydroxyapatite] (Sigma); magnesium hydrogen phosphate trihydrate [newberyite] (Riedel-de Haën).

All standards and a blank were subjected to the entire preparative procedure as described earlier. All solutions were stored in polyethylene bottles.

The surface-active agent Triton X-100 was added to all solutions used for ICP-AES analysis. The presence of this surfactant is thought to facilitate nebulization and transport to the ICP torch, thus improving precision, especially with solutions containing high concentrations (>3%) of dissolved salts. Furthermore it helps to reduce the 'memory effects' observed with certain elements, presumably by more efficient 'cleaning' of the system.

#### 4.3 ICP experimental conditions

After the preparation of some typical (stone) samples, standard solutions and the blank were used to optimize the instrumental conditions. Different spectral lines were investigated for each element as described in section 2.3. The graphics facilities on the video display were used to check for background and spectral interferences by the addition of various amounts of high-purity concomitants to standard



solutions of the analyte. In this way the effect of calcium, magnesium, and phosphorus on each other were studied. The sensitivities, detection limits and linearity of the calibration graphs over the required range were calculated for each spectral line. This procedure revealed the transitions at 315.89, 383.83, and 213.62 nm to yield the best results for Ca, Mg, and P, respectively. Wavelength scans (x-axis: wavelength, y-axis: relative intensity) in the vicinity of these lines while aspirating a single-element standard and a 'typical' sample containing all three elements, respectively, are shown in figure II.4.

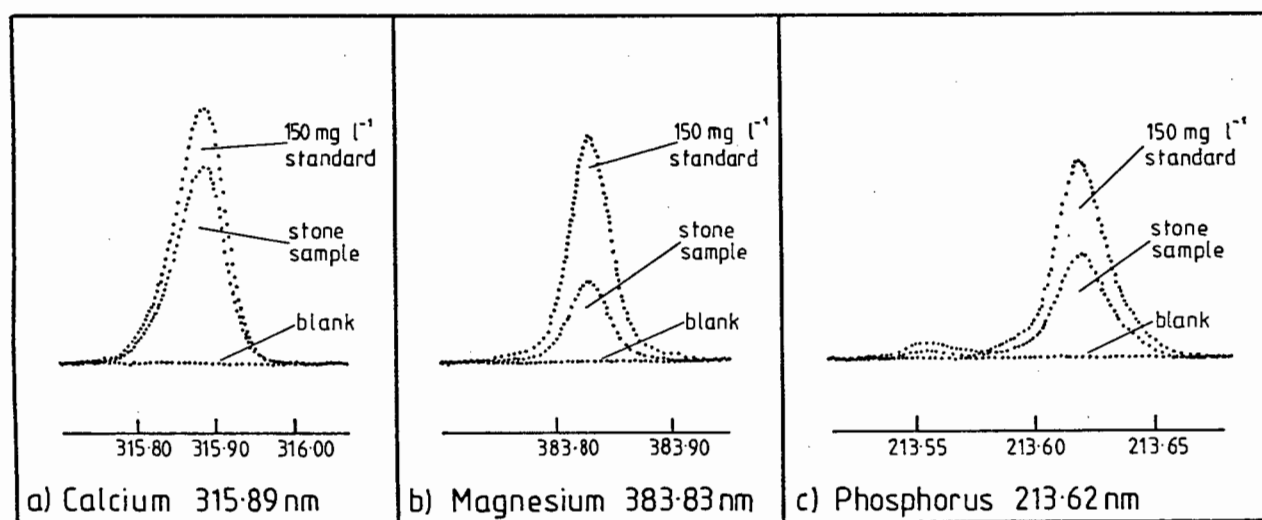


Figure II.4. Wavelength scan of spectral lines used for the determination of calcium, magnesium and phosphorus; comparison between 150 mg l<sup>-1</sup> standard solutions and typical stone sample (APA/STR).

After choosing these 'best' spectral lines, the instrumental conditions were varied for both the samples and standards to obtain optimum values for parameters such as the torch power, the nebulizer driving pressure, the observation height above the torch coil and the sample aspiration flow rate (cf. 2.2.1 and 2.2.2). For certain elements these parameters are very critical if maximum sensitivity and good precision are to be attained. For multielement analysis, a compromise between the optimum conditions for different elements is required. No

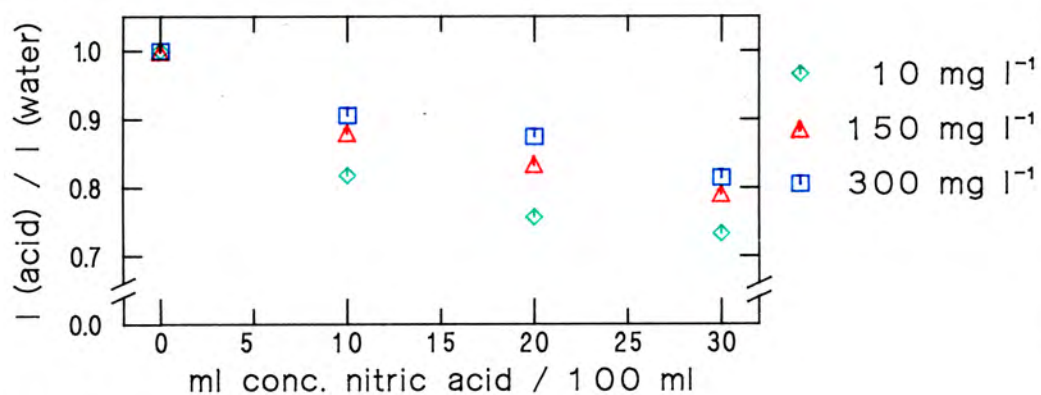
difficulties were encountered when choosing these for the three elements concerned.

No inter-element corrections were required and no background shift between the samples and standards was observed (figure II.4). The effect of using background correction on one side of the peak was investigated for several samples and confirmed the freedom from interferences. The phosphorus line used is part of a doublet with a much less sensitive peak on the low wavelength side (figure II.4c). However, the doublet is well resolved and causes no interference or non-linearity of the calibration graph. A series of standards was used to check linearity of the three lines up to levels of 300, 200, and 200 mg l<sup>-1</sup> for Ca, Mg, and P, respectively.

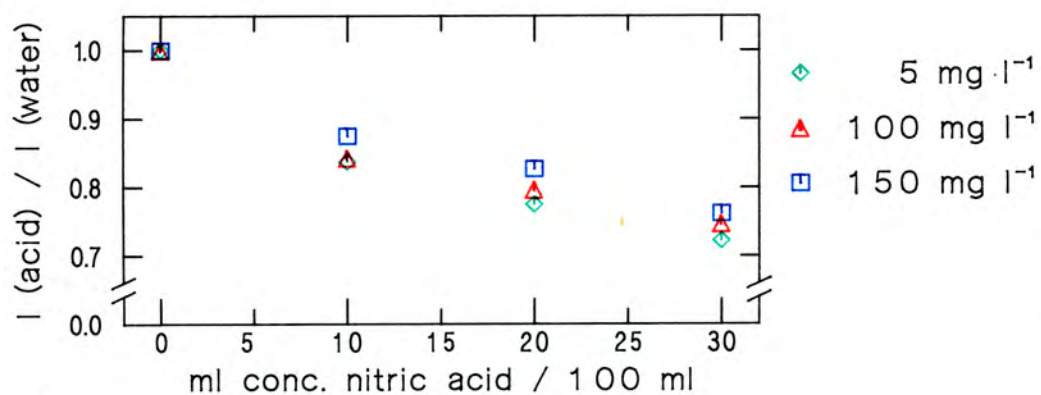
The effect of nitric acid on the three emission lines was investigated by preparing and aspirating standards of varying concentrations with different acid matrices. In figure II.5 the ratios of the ICP signals obtained from samples without ('water') and with nitric acid are plotted against sample acid concentration. It is thought that the cause of the observed intensity depression is the lower nebulization efficiency in the presence of acids and is related to the transport of the aerosol into the plasma (cf. 2.3.4). To overcome systematic errors due to interference by high acid contents in the analysis samples, approximate matching of the acid content of the analysis and standard samples was employed. By adding 5 ml of conc. nitric acid to each sample, the former was made the predominant component in the analytical sample, thus further minimizing variations in the sample matrix.

Each determination is a mean of three readings (3 s integration time for each reading). Samples and standards were aspirated for 40 s at 2.5 ml min<sup>-1</sup> before readings were recorded at the analytical programme's sample flow rate of 1 ml min<sup>-1</sup>. Between analyses water was aspirated at 2.5 ml min<sup>-1</sup> for about 30 s for adequate washout. The observation height in the plasma was 16 mm from the torch coil for all three elements. A power level of 3 (1.2 kW) and a nebulizer pressure of 206.8 kPa (30 psi) were used. The peak search window size used was 0.067 nm. The instrument was calibrated with a set of four mixed standards and a blank. The stability of the analytical system was monitored

## a) Calcium



## b) Magnesium



## c) Phosphorus

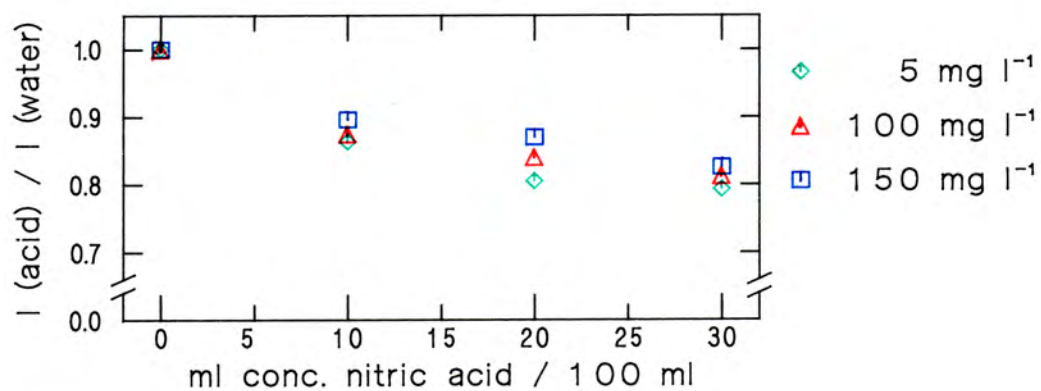


Figure II.5. Dependence of ICP signal on sample acid concentration.

by analysis of a reference solution at regular intervals (i.e. every fifth or tenth sample) and by regular blank determinations. Instrumental drift of the IL Plasma-100 was experienced in the present study and has been reported by other workers /HAR85/. As a result, recalibration using the highest standard and the blank was necessary after the analysis of about ten samples.

#### 4.4 Results and discussion

Since well characterized (i.e. elemental composition) stone standards were not available, the precision and accuracy of the method were investigated by analysing (i) solutions prepared by subjecting aqueous standards to the entire preparative procedure and (ii) by repeating (i) with artificial mixtures of the stone salts hydroxyapatite (HAP),

Table II.4. Analysis of 10 mg l <sup>-1</sup> digested standards and artificial stone mixtures.						
mixture (by weight)	element	concentration [mg l <sup>-1</sup> ]		standard deviation	RSD [%]	Error [%]
		expected	measured			
10 mg l <sup>-1</sup> digested standards	Ca	10.00	9.92	0.17	1.7	- 0.8
	Mg	10.00	9.80	0.12	1.2	- 2.0
	P	10.00	9.86	0.14	1.4	- 1.4
COM + HAP + NEW (1:1:1)	Ca	224.24	227.50	3.62	1.6	+ 1.4
	Mg	46.48	46.94	0.86	1.8	+ 1.0
	P	120.90	117.44	1.84	1.6	- 2.9
COM + NEW (1:1)	Ca	137.15	134.67	2.69	2.0	- 1.8
	Mg	69.71	69.12	0.35	0.5	- 0.9
	P	88.84	86.82	2.13	2.5	- 2.3
HAP + STR (1:1)	Ca	132.98	134.19	2.57	1.9	+ 0.9
	Mg	66.03	65.19	1.17	1.8	- 1.3
	P	145.80	146.72	1.75	1.2	+ 0.6

calcium oxalate monohydrate (COM), struvite (STR), and newberyite (NEW). Ten replicate preparations were made for (i) and five for each mixture in (ii). Results are presented in table II.4. As can be seen, the agreement between replicate preparations is good. Although these artificial stone powders do not contain any organic material they represent the closest match to 'real' powdered stones, especially with regard to the common inorganic stones. A problem that may be encountered in this approach is that the stoichiometry of these compounds is not always exactly known, which therefore prevents their use for calibration purposes.

Usually the small size of calculi does not permit replicate preparations as all the powder has to be shared to characterize the whole stone by various methods in a multiple-technique approach /ROD82/. However, three large stones were used to test the reproducibility of the entire technique for 'real' samples (table II.5). It can be seen that the precision ranged from 0.5 to 2.0% (relative standard deviation, RSD) for the three elements (five preparations).

Table II.5. Replicate analysis of stone samples (mean of five preparations).

stone	constituents	element	concentration [wt-%]	standard deviation	RSD [%]
97	COD + APA	Ca	25.64	0.28	1.1
		Mg	0.19	0.003	1.5
		P	7.49	0.09	1.2
211	STR + APA	Ca	8.87	0.18	2.0
		Mg	6.34	0.06	0.9
		P	12.72	0.24	1.9
265	STR + APA	Ca	3.95	0.05	1.2
		Mg	9.32	0.07	0.7
		P	10.53	0.05	0.5

Results obtained for the 41 stones analysed by the method described in section 4 are presented in figure II.6. These represent levels typical of those to be expected in the analysis of a wide variety of calculi. With the help of other compound-selective analytical techniques, these data were used to calculate the amounts of each phase present. Thus, of the 37 urinary calculi, 21 belonged to the struvite/apatite (STR/APA) group, 11 to the uric acid/calcium oxalate monohydrate (UA/COM) group, 4 to the calcium oxalate (COM/COD) group, and 1 to the cystine group. Calcium was thus present in all stones except the cystine calculus.

In the STR/APA group the amount of APA ranged between 2 and 56% (w/w). A third component, calcium oxalate was identified in 5 stones from this group. The relative amounts of each phase in the remaining 16 two-component stones were independently calculated from the Ca and Mg figures which each yielded a separate HAP and STR concentration value (by balancing the amount of phosphorus present). Both values generally agreed within 2 to 3%. It was also possible /HOD69/ to calculate the amount of organic matrix present by assuming that excess nitrogen (i.e. N unaccounted for after stoichiometric calculations involving its presence in STR) was associated with such deposits. This varied but never exceeded 6% in 13 of the calculi. In the remaining stones of this group, the excess N was exceptionally high indicating either an abnormally high matrix content, or, more likely, the presence of an additional, undetected organic phase (e.g. ammonium acid urate).

In the UA/COM group, UA always occurred as the major component. Uric acid dihydrate (UAD) was also detected in 3 stones from this group. With regard to the 4 COM/COD stones, small amounts of phosphorus, corresponding to APA concentrations between 1 and 12%, were detected.

The four gall stones in the series consisted of cholesterol monohydrate. Small amounts of calcium were detected in these samples (<3.3%) and magnesium and phosphorus were present only at trace levels.

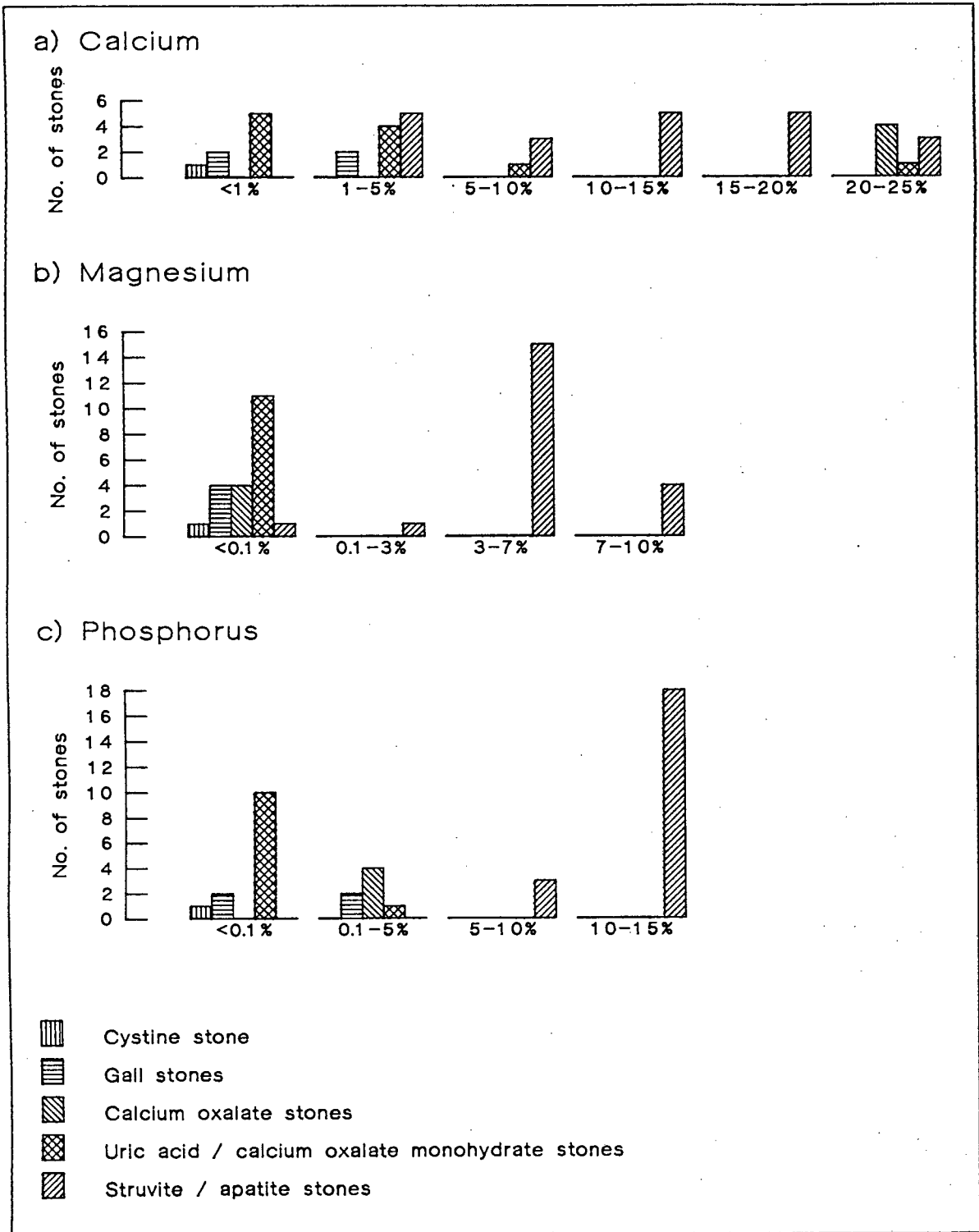


Figure II.6. Calcium, magnesium, and phosphorus concentrations in 41 human stones (wt-% of total stone mass).

#### 4.5 Conclusions

The application of ICP-AES in the analysis of human stones using the method of sample preparation described in section 4.2 has been shown to be extremely useful. The results of this study illustrate the value of using highly sensitive instrumentation for the detection of very small constituent concentrations that would otherwise remain undetected by common routine analytical procedures. Accurate elemental information revealed by ICP-AES can conveniently be utilized, together with data obtained from other techniques, as a constraint in calculating the amount of each crystalline phase in a stone. This can be of vital importance in determining the so-called nucleus of a calculus. Often this may be undetected because of its low concentration whereas another component, deposited in secondary processes, might mislead investigators into interpreting its presence as having occurred in a primary event. Knowledge of the relative concentrations of the different components present in a stone can provide some insight into understanding the mechanisms of stone nucleation and growth.

The several advantages of the ICP-AES analysis outlined will, without doubt, render it attractive to (clinical) biochemistry laboratories, as is already evident by the growing number of applications in this field /DAH78, KLU81, LEE83a, SCH83/.

The positive results obtained in this study prompted additional investigations involving trace element determinations. The aim was to develop a method whereby both major and trace elements could be quantified simultaneously. The procedure developed for this purpose is described in the next section.

#### 5. Major and trace element analysis of urinary calculi /WAN86/

In recent years, the functions of trace elements in the human body and environment and their importance for medical practice has been increasingly recognized in the biomedical field /FEI80, SCH82/. Although most mechanisms concerning the behaviour of trace elements in



biological systems are far from being understood, many researchers are convinced that trace elements play a major role in causing disease such as urolithiasis by either influencing cell biology or other regulatory functions /GUN68, HES78, LEV78, MEY77, THO82/. This challenging area in stone research led to the investigation of the possibility of including trace element determinations in the previously reported procedure concerning the ICP-AES analysis of the three major elements in calculi. Preliminary studies showed that trace element concentrations in the sample solutions already prepared were too low to allow accurate determination thereof. More concentrated samples had to be used. When the stone mass was increased, the already time consuming dissolution step was, however, further lengthened, thereby limiting the speed of the entire analysis. A microwave digestion procedure was therefore developed. This shortened sample preparation times considerably owing to more rapid and efficient digestion. Subsequently more than 100 urinary calculi obtained from Cape Town hospitals were analysed for Al, Ca, Cu, Fe, K, Li, Mg, Mn, Mo, Na, P, Pb, S, Sr, and Zn.

### 5.1 Instrumentation and apparatus

All experimental work was performed on a two-channel Plasma-200 ICP spectrometer (Allied Analytical Systems). This instrument is an updated model of the IL Plasma-100 which has been described in section 4.1. The model employed in this study is fitted with two monochromators - the standard air path and a vacuum monochromator, which allows the observation of emission lines in vacuum below 300 nm. Further instrumentation details are given in table II.6.

An unmodified, commercially available microwave oven (Sharp model R 6950 E) was borrowed for the duration of this study. This particular model has a stainless steel cavity and operates at 2450 MHz. The maximum output power is rated at 650 W (with a 2 l water load). A "variable cooking control" allows cycling on and off of the microwave energy at various intervals.

Table II.6. ICP instrumentation (Plasma-200).

rf generator	27.12 MHz, 5 power levels (1.0, 1.1, 1.2, 1.4, and 1.6 kW);
plasma torch	3 concentric quartz tubes; vortex stabilized primary flow; fixed orifice system for secondary flow; total plasma gas flow 15 or 20 l min <sup>-1</sup> depending on rf power;
sample introduction	polypropylene spray chamber and cross-flow nebulizer with synthetic sapphire capillaries; peristaltic pump;
optical system	two scanning monochromators; channels A (air path) and B (vacuum);
channel A	1/3 m Ebert-Fastie primary monochromator and 1/6 m Ebert-Fastie secondary monochromator; 1st order 190 - 365 nm, 2nd order 365 - 900 nm; Hamamatsu R 106 UH or R 955 photomultipliers;
channel B	1/3 m F/8 monochromator; 160 - 300 nm; Hamamatsu R 166 UH photomultiplier;
computer system	Intel 8080A microprocessor.

The digestion vessel assembly is illustrated in figure II.7. An acid fume scrubber was constructed from a flask containing an approximately 2 M KOH solution and a beaker filled with water. These were connected to a desiccator which could accommodate up to 5 digestion vessels. These consisted of 50 ml Erlenmeyer flasks covered with small beakers to prevent spattering and possible sample losses. In this way cross-contamination was also minimized. The whole assembly was stationary on a thick glass plate which could be easily placed in the oven cavity.

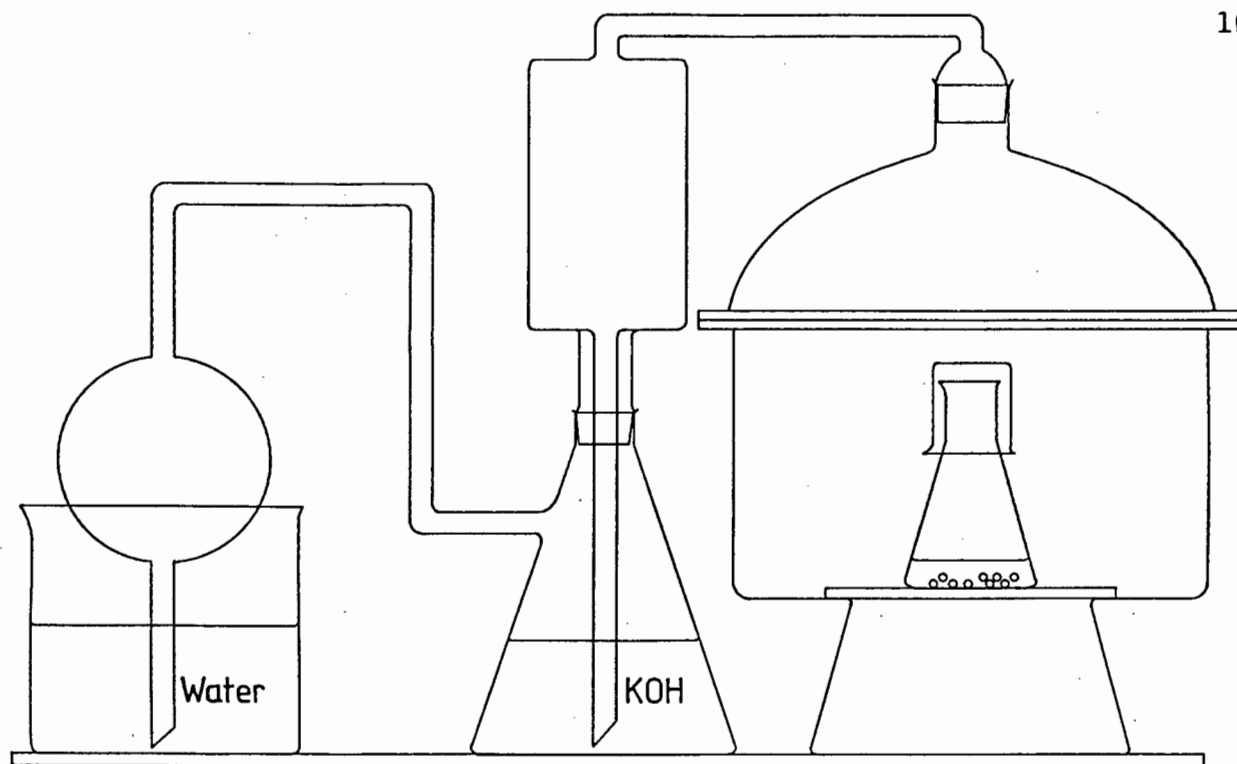


Figure II.7. Microwave digestion assembly with KOH acid fume scrubber.

## 5.2 Samples and standards

Over 100 urinary calculi were selected from a collection of about 550 human stones from 2 Cape Town hospitals. Criteria for including a stone in the selection were mainly based on the available mass (more than 250 mg required) as well as on its composition as determined by x-ray powder diffraction. The aim was to obtain significant numbers of calculi in each of the major three stone groupings, viz. calcium oxalate, phosphate and uric acid stones.

Chips from the larger specimens or whole stones were ground to fine powders. Care was, however, taken not to include the outermost parts of the calculi. These surface layers were rejected because of possible contamination of the latter prior to reaching the laboratory. Traces of tissue or blood clots embedded in the surface of a stone might falsify elemental results; e.g. high iron concentrations could originate in haemoglobin molecules attached to the stone and not come from the stone building mineral phases.

Approximately 260 mg aliquots of these powders were transferred to the Erlenmeyer flasks and 2 ml of conc. nitric (65%) and 1 ml conc.

perchloric (70%) acids (both Riedel-de Haën, AR grade) were added. The flasks were then covered with small beakers and placed in the desiccator which was sealed with high vacuum silicone grease. After coupling with the acid fume scrubber, the entire assembly was placed in the microwave oven. Three minutes of uninterrupted irradiation at the highest power level was usually sufficient to obtain clear solutions. Although some samples required only ca. 1 minute for the reaction to be completed, all samples were exposed to the microwaves for the same length of time. The few cases which did not yield clear solutions were, after adding some drops of nitric acid, put back in the oven for another few minutes. To avoid possible precipitates, solutions were diluted with a few ml of dd water immediately after removal from the oven. After cooling, the solutions were transferred quantitatively to 50 ml calibrated flasks containing 1 ml conc. nitric acid and 1 ml of 1% (m/v) Triton X-100 surfactant. These were diluted to volume with dd water. All solutions were stored in polyethylene bottles which were leached with nitric acid beforehand. No precipitation was observed after more than 3 months of storage.

Acid fumes produced by the digested samples could escape from the vessels through small lips in the rims of the Erlenmeyer flasks. The resulting slight over-pressure in the desiccator then forced the evolving acidic fumes through the KOH solution where they were neutralized. No acid fumes could be detected (by smell) in the oven cavity after removing the sample container, and no signs of corrosion were found after completing this study. The alkaline solution and the water were routinely changed after three successive digestions in the oven. This was found to be necessary to avoid boiling of the liquids caused by the fast microwave heating.

$10\text{ g l}^{-1}$  stock standard solutions for calcium and magnesium were prepared by dissolving calcium carbonate and magnesium metal flakes (both Johnson Matthey, Specpure), respectively, with some drops of nitric acid.  $(\text{NH}_4)_2\text{H}_2\text{PO}_4$  (Merck, AR grade) was used for a phosphorus standard of the same concentration.  $1\text{ g l}^{-1}$  primary trace element standards used were Spectrosol solutions (BDH Chemicals), except for sulphur and lithium, for which standards were prepared from  $(\text{NH}_4)_2\text{SO}_4$  (BDH Chemicals, AR grade) and LiCl (Merck, Titrisol), respectively. Stan-

dards of lower concentrations were obtained by serial dilution of these stock solutions with a blank which was prepared by subjecting only acids to the whole preparative procedure. Low concentration Ca, Mg, and P standards prepared in the same way were cross-checked against standards of the same concentration obtained by dilution of Spectrosol solutions of these elements. Mixed element standards for ICP calibration purposes were prepared in the same way.

### 5.3 ICP experimental conditions

Optimization of the instrumental parameters followed the procedures already described in sections 2.3 and 4.3. Firstly, the most sensitive prominent spectral lines were investigated for each (trace) element of interest for potential interferences, i.e. spectral overlap and background shifts. In the analysis of urinary calculi, in particular, matrix interferences are encountered owing to the combined effects of high calcium and sometimes magnesium concentrations, as well as high sodium levels. These may result in plasma fluctuations and suppression or enhancement of analyte signals /LEE83/. On the other hand, high phosphate concentrations do not cause any severe effects owing to the weak emission of phosphorus in the plasma.

To avoid systematic errors in the determination of trace element concentrations, the effect of the major elements Ca, Mg, and P and other elements, such as Al, Fe, K, Na, and S on the analyte emission were evaluated by observing the recorded intensity profiles on a video display. These were obtained by pre-nebulization mixing of various concentrations of analyte and concomitants, e.g.  $1000 \text{ mg l}^{-1}$  Ca and  $10 \text{ mg l}^{-1}$  Fe. This was carried out by using a mixing device as described by Pougnet et al. /POU85/. The advantage of this method is that it does not require the very tedious procedure of preparing two-element mixtures of the analyte together with all potential interferants. The problematic spectral lines investigated with this device are listed in table II.7 together with detection limits as given by the manufacturer /NYG84, NYG84a/ and the type of interference encountered. Where interferences for the other trace elements determined in this study were reported in the literature, their emission lines were also included in

this investigation.

Table II.7. Analytical lines investigated.

element	wavelength [nm]	sensitivity [ng ml <sup>-1</sup> ]	interferences
Al	226.92 237.32 308.22 309.27 396.15	40 24 30 18 10	Fe wing, Mg continuum Fe wing OH band, structured background OH band, Mg wing Ca continuum
Cu	224.70 324.75	4 1	Fe line, Pb interference, structured background background shift
Fe	238.20 239.56 259.94	2 2 2	structured background structured background Mn wing
K	766.49 769.90	50 150	Mg line none
Li	610.36 670.78	20 2	Ca wing none
Mg	279.81 383.83	10 -	background shift too insensitive
Mn	257.61 259.37	1 1	Fe wing Fe line
Mo	203.84	10	background shift
Na	589.59	7	none
Pb	220.35	25	Al wing
S	180.73 182.04 182.63	15 45 75	Ca line, Fe wing none none
Sr	346.45 407.77	7 0.2	none too sensitive
Zn	202.55 213.86	3 2	Mg wing Cu line

Some typical interferences encountered during this investigation are illustrated in figures II.8 to II.10. For example, the calcium 180.74 nm emission line directly overlaps with the 180.73 nm sulphur line (figure II.8). Owing to the high Ca to S ratio usually found in calculi, this overlap effectively prevents the use of this most sensitive sulphur line. As can be further seen from figure II.8, background

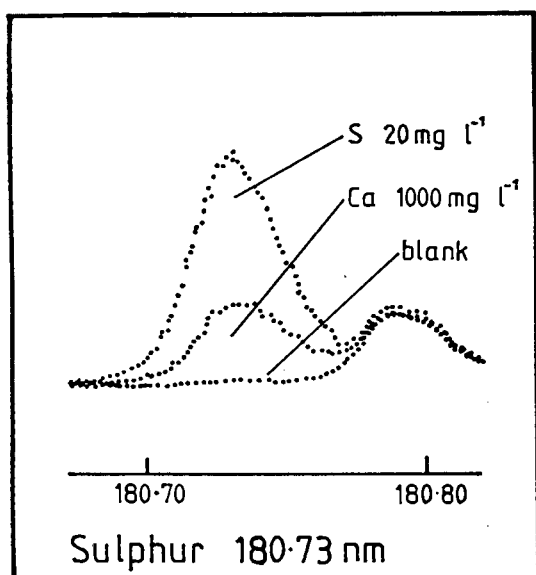


Figure II.8. Calcium and background spectral interference on S 180.73 nm line.

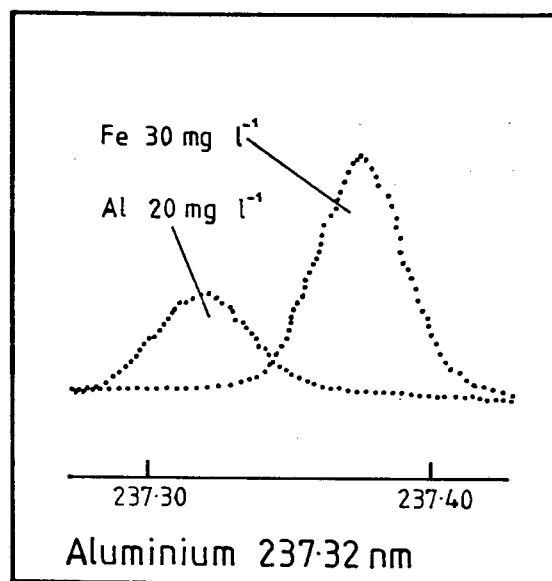


Figure II.9. Iron spectral interference on aluminium (partial overlap).

emission at the high wavelength side of the analyte peak partially obscures this emission line. A further example of spectral interference is shown in figure II.9, where the low wavelength wing of the 237.37 nm iron line contributes to the signal from the 237.32 nm aluminium line. Because other Al emission lines suffered even more severe interferences, particularly from calcium and magnesium (table II.7), special overlap corrections had to be applied. A correction factor  $K$  was calculated as the ratio of the measured, apparent aluminium concentration at the Al analytical wavelength ( $c_{Al}^m$ ) to the iron concentration  $c_{Fe}$ . The

latter was first determined from the iron 259.94 nm emission and the correction then applied to the measured Al concentration  $c_{Al}^m$ :

$$\text{corrected } c_{Al} = c_{Al}^m - K \cdot c_{Fe} \quad (\text{II.1})$$

In some cases, background shift between standards and samples was observed. This shift is caused either by a continuum emission, wing broadening, or stray light from strong emission lines in the vicinity of the analyte wavelength, or it arises from variations in the sample matrix. One such example is illustrated in figure II.10, where the

shift in the background intensity between a standard and a typical sample near the magnesium 279.80 nm line is shown. This type of interference was automatically corrected for during analysis by measuring the background intensity on one side of the analytical line. The background correction position must be carefully chosen in an unstructured region of the spectrum, which is free from matrix spectral lines and which accurately reflects the background under the analyte peak. Shifts were observed for Cu, Mg, Mo, Pb and S for which the correction positions (left or right) are given in table II.8. The

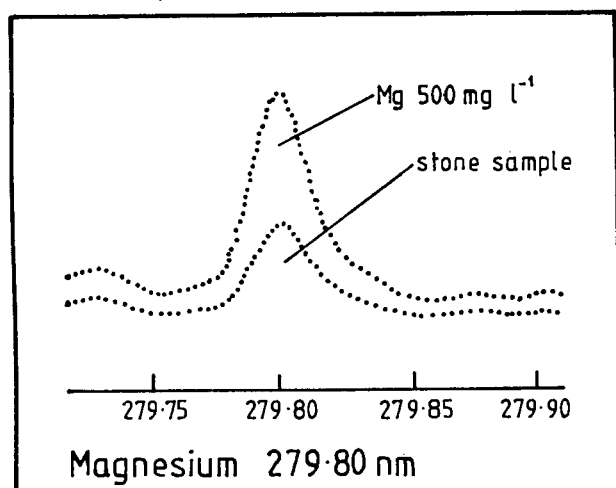


Figure II.10. Background shift at the magnesium 279.80 nm line.

positions were usually 0.05 to 0.08 nm off the peak centre. It was not considered necessary to perform background correction at both sides of the analyte line for the above elements, nor was a correction for the other elements found to be essential, since this procedure lengthens analytical time considerably, thereby increasing analysis costs.



Table II.8. Wavelength data.

element	wavelength [nm]	background correction	mono- chromator	viewing height [mm]	detection limits	
					solution [mg l <sup>-1</sup> ]	calculus [ng mg <sup>-1</sup> ]
Ca	315.89	-	air path	25	30	6
Mg	279.81	rhs	air path	14	40	8
P	213.62	-	air path	14	90	17
Al	237.32	-	vacuum	-	54	10
Cu	324.75	rhs	air path	14	5	1
Fe	259.94	-	vacuum	-	4	1
K	769.90	-	air path	5	940	180
Li	670.78	-	air path	14	7	1.5
Mn	257.61	-	air path	14	5	1
Mo	203.84	rhs	vacuum	-	8	1.5
Na	589.59	-	air path	2	30	6
Pb	220.35	lhs	vacuum	-	70	14
S	182.04	lhs	vacuum	-	110	21
Sr	346.45	-	air path	14	30	6
Zn	213.86	-	vacuum	-	5	1

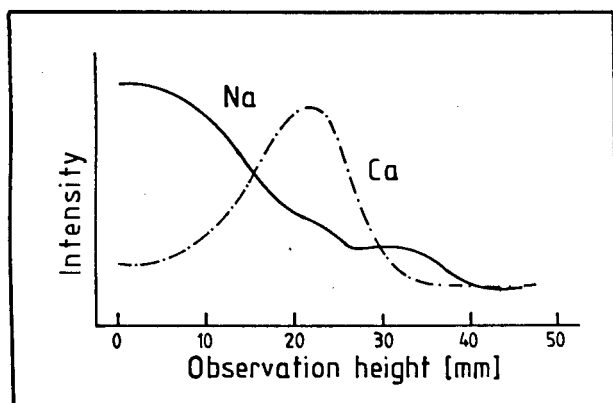


Figure II.11. Torch profile at the calcium 315.89 nm and sodium 589.59 nm lines.

All analytical wavelengths used in this study are summarized in table II.8 together with other important line parameters. The intensity measurements were divided between the two monochromator systems (channels A and B) for time saving reasons. One constraint was, however, that only emission lines at wavelengths shorter than 300 nm could be measured with B (vacuum monochromator). A further drawback of this channel is that the viewing height cannot be individually adjusted for different elements for any one analytical programme. This parameter is usually optimized and set manually for the least sensitive element in the programme. On the other hand,

not be individually adjusted for different elements for any one analytical programme. This parameter is usually optimized and set manually for the least sensitive element in the programme. On the other hand,

observation heights, used in connection with channel A could be optimized for each element separately and the heights utilized are also listed in table II.8. These values are derived by studying the emission profile of the plasma while aspirating the analyte. Typical profiles (for Ca and Na) are depicted in figure II.11. It can be seen that sodium (as well as potassium) emit more strongly at lower observation heights. In the case of calcium, a high viewing height is noted to reduce sensitivity considerably (cf. 2.2.1).

Detection limits achieved for the analytical lines using the given settings and instrumental conditions (tables II.8 and II.9) are also included in table II.8. These lower limits of detection in the sample solution  $c_{11d}^1$  were established as three times the standard deviation of the background signal from 10 successive readings in accordance with IUPAC recommendations (cf. 2.3.2):

$$c_{11d}^1 = \frac{3 \cdot \sigma_B}{I_A - I_B} \cdot c_A \quad (\text{II.2})$$

where  $\sigma_B$  = standard deviation of 10 blank signal readings (3 seconds each)

$c_A$  = concentration giving signal  $I_A$  (mean)

$I_B$  = mean blank signal

An estimate of the detection limits for each element in the calculi  $c_{11d}^s$  (expressed as ng mg<sup>-1</sup> stone mass) was calculated from  $c_{11d}^1$  by taking into account the dilution factor (50ml) and an average mass of 265 mg (mean of all weigh-ins) (cf. 5.2).

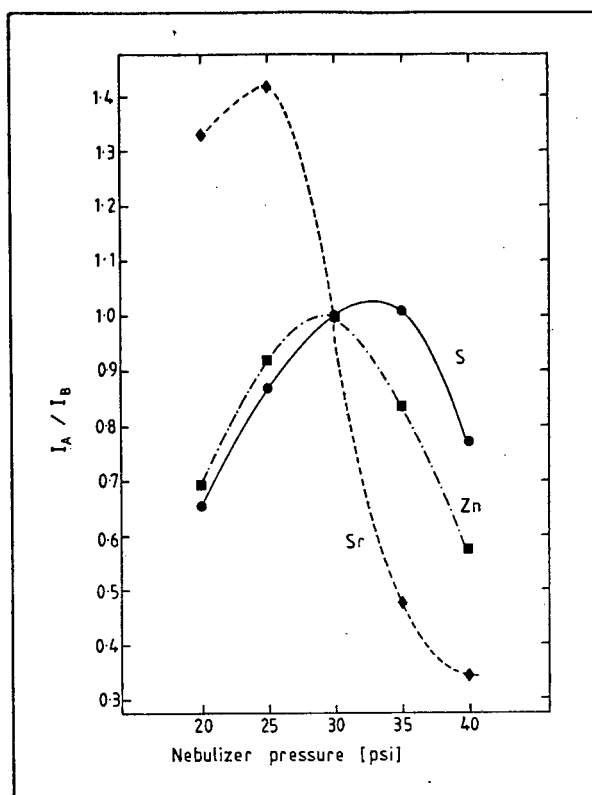
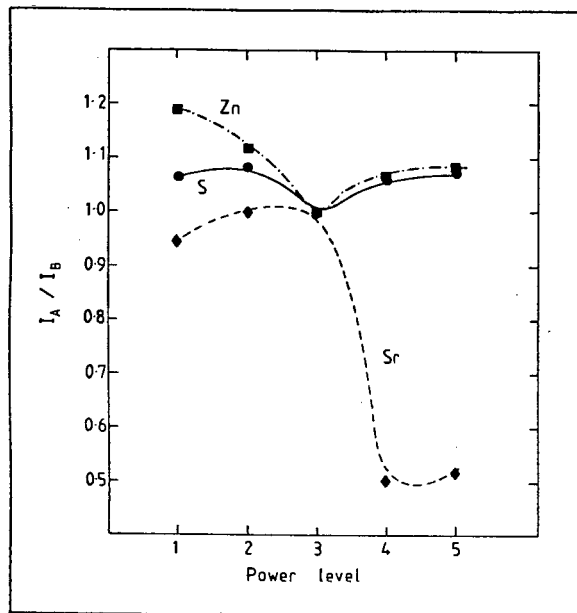
For magnesium, an emission line (279.81 nm) different to that used in the first part of this study (383.83 nm) was employed. The former is approximately 200 times more sensitive and is thus more suited for the determination of Mg at trace levels. No problems were encountered with this line when analysing struvite samples, that is, no deviation from linearity of the calibration curve were observed for high magnesium concentrations.

Potassium could not be determined at the same time as the other elements because of the low sensitivity of the 769.90 nm line. In order to measure low concentrations of this element, the standard photomultiplier tube in channel A (Hamamatsu R 106 UH) was replaced by a more red-sensitive photomultiplier (Hamamatsu T 955). This model is sensitive up to 930 nm compared to 650 nm for the standard tube, thus giving better results at longer wavelengths.

Multielement standard solutions were used to optimize instrumental conditions. The effects of varying rf power, nebulizer driving pressure (carrier gas flow rate) and sample feed rate were studied. Typical response of the analyte to background signal ratio ( $I_A/I_B$ ) for some of the elements investigated (S, Sr, Zn) to changes in the above parameters is illustrated in figures II.12 to II.14. Samples of 10 mg l<sup>-1</sup> analyte concentration were used and all other instrument parameters were kept at the settings listed in tables II.8 and II.9. Typical error bars were  $0.1 \cdot (I_A/I_B)$ .

Five rf output powers, which are divided into two groups, could be selected. For levels 1 to 3 (1.0, 1.1, 1.2 kW) constant gas flow was set to approximately 13 l min<sup>-1</sup>, whereas for levels 4 to 6 (1.2, 1.4, 1.6 kW) a coolant gas flow of 18 l min<sup>-1</sup> was maintained. Both parameters interact to determine the temperature of the discharge. Figure II.12 shows plots of  $I_A/I_B$  for sulphur, strontium, and zinc, when the rf power was changed, while the other parameters were kept constant. Power level 6 could not be used, as this is reserved for organic solvents. It is clearly seen that S and Zn ratios of analyte emission to noise in the background is hardly affected by the power level chosen, whereas for Sr this ratio drops dramatically for higher coolant gas flow rates and powers.

Figure II.13. shows the effect of changes in the nebulizer driving pressure on the signal to background ratio for the same three elements. Depending on this pressure, an argon stream of between 0.3 - 0.5 l min<sup>-1</sup> carries the sample aerosol into the plasma. Again, Sr exhibits the strongest dependence on this variable. The chosen compromise pressure of 206.8 kPa (30 psi) gives best results for S and Zn while still being acceptable for Sr. Higher pressures would lower Sr



Figures II.12 and II.13. Effects of changes in rf power (figure II.12) and nebulizer driving pressure (figure II.13) on signal to background ratio of S 182.04 nm, Sr 346.45 nm, and Zn 213.86 nm (normalized to power level 3 (figure II.12) and pressure of 30 psi (figure II.13), respectively); (1 psi = 6.895 kPa).

response extremely. All subsequent measurements were therefore carried out at a power level of 3 (1.2 kW, 15 l min<sup>-1</sup> total Ar flow) and a nebulizer driving pressure of 206.8 kPa (30 psi) with an argon aerosol carrier flow rate of 0.4 l min<sup>-1</sup>.

In figure II.14 the dependence of the analyte signal to background noise ratio on the sample flow rate can be seen for S, Sr, and Zn. These ratios show maxima with pump rates between 1.0 and 1.5 ml min<sup>-1</sup>, extending to 2.0 ml min<sup>-1</sup> for S and Zn. For limited sample volumes, however, it is necessary to use a lower pump rate and 1 ml min<sup>-1</sup> was chosen for all elements.

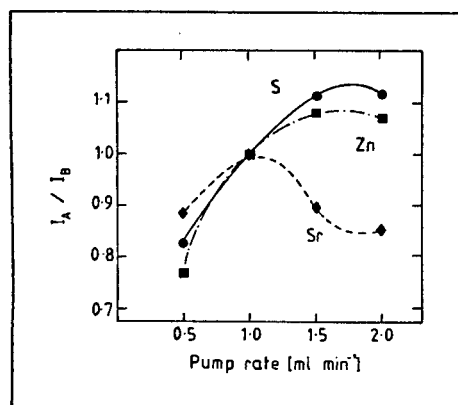


Figure II.14. Effect of changes in sample flow rate on signal to background ratio of S 182.04 nm, Sr 346.45 nm, and Zn 213.86 nm (normalized to pump rate of 1.0 l min<sup>-1</sup>).

All these analytical variables are, however, interdependent and changing one might affect the optimal conditions for the others. Furthermore, some system variables, like the nebulizer driving pressure, cannot be optimized for each element separately. Therefore compromise settings, which would give 'best' performance for all analytes, had to be chosen. These conditions are listed in table II.9.

Table II.9. Operating conditions (Plasma-200).	
power	1.2 kW;
plasma coolant gas flow	13 l min <sup>-1</sup> ;
sample feed rate	1 ml min <sup>-1</sup> ;
nebulizer driving pressure	206.8 kPa (30 psi);
aerosol carrier flow rate	0.4 l min <sup>-1</sup> ;
pump delay	30 s;
peak window	0.067 nm;
integration time	3 s;
observation height	5 - 25 mm, varied;
number of readings	3.

After setting the spectrometer to the 'optimized' parameters, it was first calibrated for each element using the standards listed in table II.10 and the blank. This calibration was carried out mainly to confirm linearity of the calibration graph over the entire expected concentration range, as well as to ascertain accuracy of the prepared standards. Recalibration of the instrument during analysis was performed with the highest concentration standard and the blank only, except

for Ca, Mg and P. It was only necessary to recalibrate the instrument after every 10 to 15 samples. However, blank readings were taken after every fifth sample to monitor drift of the instrumental parameters.

Table II.10. Calibration standards.	
elements	standards [mg l <sup>-1</sup> ]
Ca	2000, 1000, 500, 100;
Mg, P	1000, 500, 200, 100;
Na, K	100, 50, 10;
S	20, 10, 5, 2, 1, 0.5;
Al, Cu, Fe, Li, Mn, Mo, Pb, Sr, Zn	10, 5, 2, 1, 0.5.

#### 5.4 Results and comment

##### 5.4.1 Procedural tests

In order to monitor possible loss of elements during the microwave digestion procedure, a series of recovery tests using aqueous 10 mg l<sup>-1</sup> standards were undertaken. As part of a general investigation of microwave assisted dissolution, many elements in addition to those occurring in calculi were included in this part of the study: Al, Cd, Co, Cr, Cu, Fe, K, Mn, Mo, Na, Ni, Pb, S, Se, Si, Sr, Ti, V, and Zn. Multielement solutions were subjected to the same preparative steps as the samples, in duplicate. No loss of any of the elements was observed. These favourable results do not, however, exclude the possibility of elemental loss if the particular element is incorporated in a more complex matrix, e.g. if the element concerned occurs in the form of a potentially volatile chloride compound.

A major shortcoming in the verification of the method was the lack of a suitable reference material. Since no certified (urinary) stone standards are available, the accuracy of the method was evaluated using NBS SRMs which were subjected to the sample preparation procedure

Table II.11. NBS SRMs analytical results.

element	trace elements in NBS SRM									
	spinach		orchard		tomato		pine		bovine	
	1570	1570	1571	1571	1573	1573	1575	1575	1577	1577
	found	reported	found	reported	found	reported	found	reported	found	reported
Ca	1.20%	1.35% ± 0.03%	2.05%	2.09% ± 0.03%	3.00%	3.00% ± 0.03%	0.40%	0.41% ± 0.02%	108	124 ± 6
Mg	0.75%	8600 ± 1200*	0.55%	0.62% ± 0.02%	0.56%	(0.7%)	0.09%	1400*	512	604 ± 9
P	0.53%	0.55% ± 0.02%	0.20%	0.21% ± 0.01%	0.37%	0.34% ± 0.02%	0.13%	0.12% ± 0.02%	1.08%	(1.1%)
Al	895	870 ± 50	327	310 ± 100*	0.14%	(0.12%)	523	545 ± 30	nd <sup>#</sup>	30 ± 20*
Cu	10	12 ± 2	11	12 ± 1	10	11 ± 1	3	3.0 ± 0.3	207	193 ± 10
Fe	500	550 ± 20	234	300 ± 20	573	690 ± 25	176	200 ± 10	263	263 ± 8
K	3.62%	3.56% ± 0.03%	1.33%	1.47% ± 0.03%	4.50%	4.46% ± 0.03%	0.35%	0.37% ± 0.02%	0.93%	0.97% ± 0.06%
Mn	155	165 ± 6	84	91 ± 4	215	238 ± 7	648	675 ± 15	10	10.3 ± 1.0
Na	1.5%	14400 ± 1200	79	82 ± 6	661	534 ± 64*	30	40*	0.23%	0.234% ± 0.013%
Sr	79	87 ± 2	34	37 ± 1	42	44.9 ± 0.3	4.5%	4.8% ± 0.2%	nd <sup>#</sup>	(0.14)
Zn	45	50 ± 2	25	25 ± 3	58	62 ± 6	63	61* ± 10	124	130 ± 13

concentrations in ng mg<sup>-1</sup> or otherwise as stated;

\* most reported values are from NBS certificates of analyses, values in parentheses are informational; other data (\*) are from Gladney et al. /GLA80/;

# not detectable.

described before for stones /POU86/. The trace element NBS SRMs spinach 1570, orchard leaves 1571, tomato leaves 1573, pine needles 1575 and bovine liver 1577 were dried in an oven at a temperature of approximately 85°C for two hours before preparation. These purely organic samples required up to 15 minutes in the microwave oven for complete destruction. However, it was not possible to maintain power supply for longer than 3 minutes at any one time since the sealing grease started to lose its viscosity thereby allowing acid fumes to escape from the desiccator. Therefore, remaining residues had to be reduced by the addition of small amounts of nitric acid and further microwave irradiation which was possible only after a short cooling period. This cycle was repeated as often as necessary. Results obtained for the NBS samples are given in table II.11 as mean values for duplicate preparations. As these determinations were part of the routine procedure for the analysis of calculi, the precision and accuracy of the listed values are representative of a true multielement analysis. In general, good agreement with certified or reported values was obtained. In a few instances, e.g. Fe in NBS SRMs 1571 and 1573, the measured concentrations were lower than expected. Losses owing to the formation of volatile reaction products were first suspected in these cases. However, other workers found that similar low Fe recoveries from tissue samples

Table II.12. Replicate analysis of 3 stone samples (mean of 5 preparations).

stone	concentration	Ca	Mg	P	Al	Cu	Fe	K	Mo	Na	Pb	S	Sr	Zn
		[% (w/w)]			[ng $\mu\text{g}^{-1}$ ]									
S1 APA/STR	mean	4.21	7.80	12.11	36.8	n.d.	n.d.	3280	4.2	3431	n.d.	134	68.0	206
	std. dev.	0.12	0.14	0.23	2.7	-	-	172	1.0	83	-	4.8	9.0	5.9
	% RSD	2.9	1.8	1.9	7.5	-	-	5.3	24.5	2.4	-	3.6	13.2	2.8
S2 APA/COM	mean	29.19	0.25	9.46	71.9	3.9	23.0	1003	2.2	5913	114	1851	141	1381
	std. dev.	0.45	0.004	0.17	3.6	0.7	1.6	104	0.5	120	12.7	39.0	4.9	13.5
	% RSD	1.5	1.8	1.8	5.0	19.1	7.0	10.4	22.4	2.0	11.2	2.1	3.5	1.0
S3 UA/UAD	mean	0.40	n.d.	0.04	n.d.	2.4	3.7	649	n.d.	459	n.d.	463	n.d.	4.5
	std. dev.	0.01	-	0.001	-	1.8	1.9	80	-	21.7	-	7.7	-	0.9
	% RSD	2.9	-	2.5	-	74.4	51.4	12.3	-	4.7	-	1.7	-	20.1



were not due to digest matrix effects but rather to extraction inefficiencies associated with digestion in open beakers as opposed to pressure vessels /MCQ79/.

Three comparatively large calculi were chosen to test the precision of the method described. Five separate aliquots were prepared from each of these and mean concentrations found are listed in table II.12 together with the standard deviations and % RSD. For the three major elements (Ca, Mg, P) reproducibility was found to be comparable to the previous study (section 4) and ranged from 1.5 to 2.9% RSD (relative standard deviation). Precision for the trace elements varied from 1.0 to 74.4% RSD. However, when concentration values below five times the detection limit ( $c_{11d}^s$ ) are excluded, a mean RSD of 5.1% is obtained. This is expected, since for any analytical technique percentage RSD increases dramatically when approaching the detection limit.

#### 5.4.2 Analytical data

All data determined in this study are listed in table II.13. Concentrations are given as percent (w/w) of total stone mass for Ca, Mg, and P, and as  $\text{ng mg}^{-1}$  for all other elements. Concentrations which were too low to be determined are denoted 'N.D.' (not detectable). Stone constituent values were calculated from elemental ICP-AES results with the help of (film) x-ray diffraction data. In cases where this was not possible, e.g. COM/COD stones, estimates established from diffracted x-ray intensities were used. These figures were rounded to the nearest five percent and do not necessarily sum to 100% owing to the possible presence of undetected mineral phases and / or organic matter ('matrix') in the calculi.

Of the 102 calculi analysed in this study, 14 belong to the calcium oxalate (COM/COD) group, 18 to the CaOx/APA group, 45 to the STR/APA group, and 19 to the uric acid (UA/UAD)/CaOx group. Two calculi containing urates, one STR/COM and 3 cystine stones were also found. In the CaOx group, COM was the major component (i.e. >50%) in 12 cases and COD in 2, whereas in the CaOx/APA group COM was predominant in 3 calculi, COD in 11 and APA in 3. In the STR/APA group, struvite occurred

Table II.13. Element and compound data for 102 South African urinary calculi as determined by ICP-AES and (film) x-ray diffraction analyses.

Stone	Ca	Mg	P	Al	Cu	Fe	K	Mo	Na	Pb	S	Sr	Zn	ICOM	ICOD	APA	STR	UA	IUAD	IAAU	ISAU	ICYS
17	26.35	0.11	0.58	88.66	N.D.	17.46	3514.00	4.13	10636.00	131.47	459.12	621.50	1315.57	95	0	0	0	0	0	0	0	0
27	2.39	<0.01	<0.01	N.D.	5.91	21.18	N.D.	N.D.	434.95	N.D.	572.11	9.35	14.12	10	0	0	0	90	0	0	0	0
34	20.06	3.75	13.49	27.37	N.D.	11.48	3868.00	N.D.	9209.00	N.D.	199.86	292.25	802.12	0	0	50	35	0	0	0	0	0
46	12.32	5.20	12.41	40.33	5.12	11.57	3326.00	N.D.	7385.00	N.D.	388.51	144.29	240.42	0	0	30	55	0	0	0	0	0
56	5.13	7.90	12.67	50.99	N.D.	18.58	1854.00	N.D.	1628.00	N.D.	334.60	78.51	57.73	0	0	15	80	0	0	0	0	0
97	27.99	0.18	7.24	20.92	N.D.	87.58	1824.00	N.D.	3492.00	44.84	822.73	172.10	416.06	0	50	40	0	0	0	0	0	0
98	13.82	5.41	12.95	50.03	N.D.	17.20	2653.00	N.D.	5043.00	N.D.	389.94	180.16	113.62	0	0	35	50	0	0	0	0	0
99	12.01	6.18	13.32	61.45	N.D.	20.53	3807.00	3.01	5402.00	N.D.	367.88	185.49	768.32	0	0	30	60	0	0	0	0	0
101	12.92	5.62	13.04	55.19	2.04	23.17	2728.00	N.D.	4970.00	N.D.	453.02	132.13	151.41	0	0	30	55	0	0	0	0	0
115	<0.01	<0.01	<0.01	19.24	N.D.	3.86	N.D.	N.D.	147.22	N.D.	271000.	N.D.	2.39	0	0	0	0	0	0	0	0	100
118	22.09	3.00	14.23	38.38	N.D.	13.98	5071.00	3.54	11506.00	N.D.	249.73	232.84	300.60	0	0	55	30	0	0	0	0	0
123	25.89	0.17	2.44	19.79	N.D.	34.27	739.89	2.28	1928.00	N.D.	477.24	88.75	199.12	0	85	15	0	0	0	0	0	0
135	7.64	5.60	10.56	51.04	2.68	57.55	3836.00	5.09	4537.00	N.D.	1428.40	110.81	110.01	0	0	20	55	0	0	0	0	0
142	1.22	0.01	0.03	N.D.	1.27	11.29	1163.00	2.37	873.68	N.D.	442.21	12.01	11.29	5	0	0	0	95	0	0	0	0
168	4.19	<0.01	0.05	N.D.	N.D.	N.D.	N.D.	N.D.	431.18	N.D.	594.29	N.D.	6.97	15	0	0	0	80	0	0	0	0
172	4.40	6.30	10.13	48.27	N.D.	20.68	6756.00	4.98	1884.00	N.D.	284.37	92.68	181.73	0	0	10	65	0	0	15	0	0
173	<0.01	<0.01	<0.01	N.D.	1.20	11.36	N.D.	1.59	211.32	N.D.	270200.	N.D.	2.99	0	0	0	0	0	0	0	0	100
178	20.70	3.94	13.48	70.46	1.30	13.73	3155.00	5.94	9310.00	138.53	534.06	458.98	993.50	0	0	50	35	0	0	0	0	0
193	1.30	9.50	12.63	64.01	N.D.	25.52	3507.00	8.33	1171.00	N.D.	159.30	12.13	67.52	0	0	5	95	0	0	0	0	0
195	15.35	5.51	13.43	63.59	2.42	21.58	1968.00	7.60	5494.00	N.D.	990.85	345.99	176.80	0	0	35	55	0	0	0	0	0
198	25.99	0.08	2.37	36.22	N.D.	46.70	653.82	2.78	1860.00	39.90	848.37	72.73	420.71	15	65	10	0	0	0	0	0	0
207	6.76	0.01	0.07	12.32	N.D.	9.08	N.D.	3.03	647.96	N.D.	769.48	8.48	10.09	25	0	0	0	75	0	0	0	0
211	9.81	7.21	13.41	72.30	N.D.	21.63	3358.00	4.61	4710.00	N.D.	439.93	131.96	316.78	0	0	25	70	0	0	0	0	0
214	21.74	0.01	0.30	26.65	1.69	17.87	387.51	2.45	1059.07	N.D.	1632.81	68.10	20.69	80	0	0	0	0	0	0	0	0
223	0.78	0.01	0.04	N.D.	1.84	22.15	278.29	1.84	486.55	N.D.	599.24	N.D.	2.58	5	0	0	0	85	0	0	0	0
234	<0.01	<0.01	0.03	N.D.	1.00	9.02	303.03	2.50	166.50	N.D.	406.84	N.D.	8.33	0	0	0	0	100	0	0	0	0
236	27.39	0.07	1.76	14.68	7.51	124.04	389.32	3.14	1477.00	51.82	1275.93	44.17	257.86	85	0	10	0	0	0	0	0	0
237	25.61	2.48	12.18	34.34	3.71	8.73	1350.00	6.67	7091.00	N.D.	915.00	252.78	622.17	25	0	50	25	0	0	0	0	0
239	16.55	5.53	13.63	46.14	N.D.	14.23	2092.00	3.04	6144.00	N.D.	241.93	204.98	471.50	0	0	40	50	0	0	0	0	0
254	2.54	6.84	9.44	42.40	1.13	34.90	2702.00	7.13	1002.00	N.D.	247.00	77.67	171.86	0	0	5	65	0	0	0	0	0
258	24.93	0.04	0.30	14.03	N.D.	51.04	591.42	N.D.	1455.00	16.52	1389.23	65.16	28.76	90	0	0	0	0	0	0	0	0
262	22.62	3.76	13.84	54.39	N.D.	13.88	2385.00	5.72	8204.00	16.91	299.10	403.65	695.64	0	0	55	30	0	0	0	0	0
264	18.17	4.97	13.96	70.20	N.D.	23.80	2487.00	4.73	6815.00	28.70	463.86	215.40	201.02	0	0	45	45	0	0	0	0	0
265	4.21	7.80	12.11	36.75	N.D.	N.D.	3280.00	4.21	3431.00	N.D.	134.42	68.02	206.26	0	0	10	80	0	0	0	0	0
268	19.38	4.73	14.15	63.90	N.D.	11.10	2504.00	5.43	9998.00	26.47	231.51	159.48	353.75	0	0	45	45	0	0	0	0	0
279	<0.01	<0.01	0.01	N.D.	1.95	13.28	N.D.	2.15	128.86	N.D.	494.83	N.D.	4.49	0	0	0	0	100	0	0	0	0
281	24.81	0.10	3.79	48.59	N.D.	128.56	847.19	N.D.	2530.00	43.86	1273.65	83.53	529.10	0	70	20	0	0	0	0	0	0

Table II.13. continued (1)

Stone	Ca	Mg	P	Al	Cu	Fe	K	Mo	Na	Pb	S	Sr	Zn	COM	COD	APA	STR	UA	UAD	AAU	SAU	CYS
282	23.17	0.02	0.34	10.84	N.D.	42.27	783.13	1.55	1115.00	N.D.	1410.32	27.01	36.34	85	0	0	0	0	0	0	0	0
288	0.01	<0.01	0.01	N.D.	N.D.	22.06	277.01	N.D.	396.35	N.D.	447.84	7.27	2.16	0	0	0	0	100	0	0	0	0
293	25.75	0.25	1.90	12.04	6.16	17.17	1112.00	N.D.	2469.00	75.55	1582.77	103.02	302.56	0	90	10	0	0	0	0	0	0
294	21.11	3.59	13.64	47.13	1.29	20.54	2173.00	N.D.	10557.00	19.76	440.58	158.89	355.99	0	0	50	35	0	0	0	0	0
296	5.72	7.98	12.77	29.15	N.D.	19.81	3395.00	1.58	3917.00	N.D.	424.38	46.86	331.55	0	0	15	80	0	0	0	0	0
297	13.43	6.28	13.29	31.96	N.D.	17.96	2094.00	2.45	5257.00	N.D.	269.54	135.57	307.02	0	0	30	55	0	0	0	0	0
300	3.13	0.01	0.63	N.D.	N.D.	24.56	320.17	N.D.	354.68	N.D.	695.80	N.D.	7.48	0	0	0	0	100	0	0	0	0
301	29.22	0.19	7.48	30.73	N.D.	57.08	876.45	N.D.	3817.00	115.68	784.06	164.06	840.15	35	25	40	0	0	0	0	0	0
303	17.35	5.58	14.04	53.92	N.D.	11.71	2035.00	3.94	6983.00	N.D.	847.69	120.66	303.23	0	0	40	50	0	0	0	0	0
311	0.12	0.01	0.02	N.D.	5.67	6.68	484.99	N.D.	226.94	N.D.	340.65	7.87	3.66	0	0	0	0	100	0	0	0	0
314	20.50	1.28	5.80	30.55	N.D.	22.71	5811.00	2.58	6278.00	68.14	520.89	142.70	231.01	40	0	25	15	0	0	0	0	0
315	25.97	0.03	0.65	N.D.	N.D.	12.36	367.29	N.D.	927.68	43.54	503.84	49.60	129.69	95	0	0	0	0	0	0	0	0
319	27.56	0.18	4.26	15.31	N.D.	54.99	1056.00	2.25	2702.00	48.24	755.58	103.32	418.97	0	60	35	0	0	0	0	0	0
320	14.98	5.61	13.10	40.93	N.D.	51.11	2968.00	3.46	6437.00	N.D.	446.47	147.91	403.00	0	0	35	55	0	0	0	0	0
321	4.96	8.32	12.55	53.98	N.D.	25.78	1964.00	5.20	1928.00	N.D.	368.90	63.55	130.30	0	0	10	85	0	0	0	0	0
322	23.37	3.18	13.31	38.24	N.D.	17.51	3435.00	3.32	8769.00	N.D.	281.42	189.92	329.43	0	0	55	30	0	0	0	0	0
338	15.74	5.50	13.43	50.73	1.71	16.50	2870.00	3.81	9078.00	N.D.	244.44	233.90	361.33	0	0	35	50	0	0	0	0	0
339	9.67	6.86	11.54	41.66	N.D.	68.69	2985.00	2.73	2304.00	N.D.	538.29	99.88	238.20	0	0	20	60	0	0	0	0	0
345	23.43	0.12	0.38	13.66	N.D.	38.09	1265.00	1.57	1579.00	N.D.	1096.76	125.74	36.48	85	0	0	0	10	5	0	0	0
349	25.30	0.03	1.44	14.55	1.99	30.32	710.31	N.D.	2353.00	N.D.	2080.78	48.15	112.51	80	0	10	0	0	0	0	0	0
351	16.66	0.15	0.35	16.20	1.42	17.29	2702.00	N.D.	3432.00	14.50	755.16	73.31	57.61	60	0	0	0	0	0	35	0	0
352	9.88	0.01	0.05	N.D.	2.57	7.06	276.86	N.D.	1169.00	N.D.	620.83	21.09	8.16	30	0	0	0	65	0	0	0	0
354	11.06	5.03	11.19	28.07	1.97	155.94	3581.00	4.33	6481.00	N.D.	698.54	164.50	290.14	0	0	25	50	0	0	0	0	0
358	27.90	1.42	10.60	32.64	N.D.	6.34	1965.00	4.27	11103.00	N.D.	457.72	128.66	359.45	0	0	60	15	0	0	0	0	0
361	1.04	9.75	12.52	49.60	N.D.	23.94	1631.00	4.76	662.90	N.D.	282.80	N.D.	22.89	5	0	0	95	0	0	0	0	0
362	<0.01	<0.01	0.01	N.D.	8.24	13.79	N.D.	N.D.	50042.00	N.D.	267100.	N.D.	3.43	0	0	0	0	2	0	0	2	95
370	21.98	3.39	14.31	37.13	N.D.	48.86	3653.00	2.16	12319.00	17.87	1302.55	259.39	528.38	0	0	55	35	0	0	0	0	0
376	24.95	0.03	0.16	N.D.	N.D.	11.76	417.76	N.D.	1554.00	N.D.	1204.20	12.18	62.66	90	0	0	0	0	0	0	0	0
379	12.92	5.98	12.71	31.75	N.D.	14.52	2034.00	4.46	7605.00	42.52	551.93	134.89	394.83	0	0	30	55	0	0	0	0	0
386	0.69	<0.01	0.02	N.D.	3.15	10.76	340.61	N.D.	343.39	N.D.	600.33	N.D.	N.D.	5	0	0	0	0	0	85	0	0
388	3.55	8.60	12.41	50.94	1.33	47.78	1734.00	4.18	3360.00	14.26	407.41	26.62	25.95	0	0	10	85	0	0	0	0	0
389	20.42	0.87	8.42	37.37	N.D.	21.27	4059.00	2.22	9877.00	29.70	372.12	286.67	858.79	55	35	0	0	0	0	0	0	0
400	22.19	3.28	12.38	54.10	N.D.	16.35	2371.00	3.36	8321.00	28.07	649.47	282.52	566.03	0	0	50	25	0	0	0	0	0
401	29.71	1.10	13.18	42.24	7.08	18.22	1831.00	3.64	10721.00	18.37	638.54	402.60	677.96	0	0	70	10	0	0	0	0	0
402	24.58	0.07	1.76	12.85	N.D.	31.16	350.35	N.D.	1428.00	14.16	418.19	73.43	159.90	0	85	10	0	0	0	0	0	0
405	12.31	0.01	0.14	N.D.	N.D.	14.19	347.00	N.D.	713.77	N.D.	1010.07	N.D.	9.35	50	0	0	0	45	0	0	0	0
406	0.09	<0.01	<0.01	20.44	N.D.	10.50	232.47	N.D.	234.29	N.D.	454.05	N.D.	5.00	0	0	0	0	100	0	0	0	0

Table II.13. continued (2)

Stone	Ca	Mg	P	Al	Cu	Fe	K	Mo	Na	Pb	S	Sr	Zn	ICOM	ICOD	IPA	ISTR	UA	UAD	AAU	SAU	CYS
408	26.04	2.57	14.23	46.16	N.D.	8.83	1601.00	N.D.	12392.00	29.24	559.85	419.74	828.89	01	01	601	201	01	01	01	01	0
415	23.68	0.12	1.58	21.26	N.D.	30.07	810.23	1.56	1738.00	14.06	637.84	109.72	131.00	401	301	01	01	201	01	01	01	0
420	16.46	3.77	10.99	49.80	N.D.	14.38	2465.00	N.D.	5440.00	39.78	376.29	194.34	428.77	01	01	401	301	01	01	01	01	0
425	25.83	0.07	0.37	21.68	N.D.	43.94	504.75	N.D.	1730.00	N.D.	829.80	93.40	67.52	951	01	01	01	01	01	01	01	0
426	20.75	0.04	1.44	19.76	N.D.	50.37	485.98	N.D.	1095.00	N.D.	436.07	48.88	109.91	251	751	01	01	01	01	01	01	0
445	0.41	0.01	0.02	18.59	N.D.	78.65	352.85	N.D.	381.93	N.D.	503.30	N.D.	13.96	01	01	01	01	701	301	01	01	0
449	31.43	0.56	16.79	30.17	N.D.	7.53	3490.00	1.68	11603.00	N.D.	449.55	78.57	240.28	01	01	851	101	01	01	01	01	0
458	25.17	0.09	1.91	27.30	N.D.	63.04	772.43	N.D.	1958.00	54.15	799.70	66.55	363.50	01	851	101	01	01	01	01	01	0
460	27.65	0.35	6.09	34.69	N.D.	19.84	1104.00	N.D.	3399.00	24.50	549.56	105.47	891.86	01	601	351	01	01	01	01	01	0
461	27.07	0.12	3.17	34.72	N.D.	30.77	556.62	N.D.	3173.00	N.D.	545.11	92.03	376.58	01	851	151	01	01	01	01	01	0
467	25.33	0.02	0.23	10.91	N.D.	21.27	475.53	N.D.	1828.00	90.17	1535.32	40.15	52.09	901	01	01	01	01	01	01	01	0
471	6.47	7.81	12.50	41.79	N.D.	16.35	1505.00	N.D.	2687.00	N.D.	352.00	77.27	51.77	01	01	151	751	01	01	01	01	0
472	7.93	4.80	9.39	33.26	N.D.	15.26	4049.00	N.D.	5594.00	23.64	371.74	118.30	89.17	01	01	201	451	01	01	01	01	0
477	27.50	1.15	8.87	46.15	N.D.	60.93	2218.00	N.D.	10955.00	118.55	396.94	294.89	864.12	01	351	501	01	01	01	01	01	0
478	25.36	1.85	11.11	46.99	N.D.	9.02	3720.00	N.D.	15212.00	N.D.	344.94	461.79	458.38	01	251	501	01	01	01	01	01	0
480	23.34	0.04	1.22	12.29	10.26	24.54	518.46	N.D.	1798.00	41.22	906.19	50.82	156.47	01	951	51	01	01	01	01	01	0
481	29.19	0.25	9.46	71.89	3.87	22.97	1003.00	2.16	5913.00	113.75	1851.00	141.13	1381.15	301	01	501	01	01	01	01	01	0
485	29.56	0.24	4.92	37.74	2.01	27.56	678.99	N.D.	3490.00	37.34	597.18	96.36	549.96	701	01	251	01	01	01	01	01	0
488	25.15	0.02	0.42	23.29	N.D.	50.27	1300.75	N.D.	2232.00	N.D.	1520.59	54.99	119.33	901	01	01	01	01	01	01	01	0
497	29.37	1.79	14.88	68.54	1.28	20.10	1042.00	N.D.	11959.00	106.60	660.17	295.46	44.46	101	01	701	201	01	01	01	01	0
499	17.50	4.78	13.69	72.96	N.D.	22.23	2397.00	N.D.	8050.00	14.37	600.99	321.94	856.12	01	01	401	451	01	01	01	01	0
500	21.93	0.02	0.22	N.D.	N.D.	27.95	556.46	N.D.	1740.00	N.D.	1074.63	40.34	84.29	801	01	01	01	01	01	01	01	0
505	10.22	0.01	0.07	72.69	N.D.	46.36	426.44	N.D.	1572.00	N.D.	1179.82	93.55	23.81	401	601	01	01	01	01	01	01	0
515	0.88	0.01	0.01	10.84	N.D.	8.41	N.D.	N.D.	137.89	N.D.	514.54	N.D.	4.16	01	01	01	01	801	201	01	01	0
518	0.40	0.01	0.04	N.D.	2.36	3.66	648.92	N.D.	459.31	N.D.	463.10	N.D.	4.52	01	01	01	01	701	301	01	01	0
519	28.11	0.03	0.31	10.20	N.D.	5.85	591.05	N.D.	1855.00	N.D.	763.39	76.22	34.81	1001	01	01	01	01	01	01	01	0
540	14.96	0.02	0.19	N.D.	2.02	6.27	289.36	N.D.	1018.00	N.D.	832.46	N.D.	27.32	551	01	01	01	401	01	01	01	0
542	7.89	5.64	11.50	29.75	N.D.	15.29	5016.00	N.D.	6140.00	N.D.	306.78	81.42	139.90	01	01	201	601	01	01	01	01	0

in 25 calculi at concentrations greater than 50% and apatite in 14. In the UA/CaOx group, UAD was detected in 4 stones, while COM was the prevailing phase in 3 of them, compared with UA in 14.

Lithium and manganese could not be determined in any of the calculi (table II.13) because of their very low concentrations. It can therefore be concluded that if these elements occur in stones they do so at concentrations below  $1 \text{ ng mg}^{-1}$ . Copper, molybdenum and lead concentrations were found to be below detection limit levels (1, 1.5 and  $14 \text{ ng mg}^{-1}$ ) in 68, 51, and 64% of all cases, respectively (table II.13).

The determination of silicon was at first attempted. However, as a result of the poor precision achieved during trial analyses the attempt was abandoned. One reason for the difficulties generally experienced when determining this element lies in the necessity of stabilizing the silicon ion in solution. In acidic media this is usually achieved by including HF (fluoride ion) in the digest, which is precluded in this case as a result of incompatibility with the torch's quartz tubes. Furthermore, erosion of the silica ICP torch and subsequent introduction of spurious Si into the plasma are additional unwanted possibilities. Lichte et al. /LIC80/ reported that trace level determinations of silicon were only possible when the torch position was adjusted to minimum Si background signal with the help of an xyz stage.

In digests of cystine calculi, sulphur concentrations exceeded the dynamic range of the calibration (each molecule of the amino acid cystine is composed of two molecules of cysteine, linked by a disulphide bond yielding 26.684% (w/w) stoichiometric sulphur). These samples were therefore diluted 5-fold and then analyzed again. On the assumption that these stones were 100% cystine, good agreement with the expected stoichiometric sulphur value was obtained (table II.13). However, possible losses of sulphur from organic samples by oxidation cannot be completely ruled out.

Aliquots of 16 stones, which had been analysed for Ca, Mg, and P in the first part of this study (section 4), were prepared and re-analysed. Mean deviations of 6.85, 5.56, and 4.24% for calcium, magne-

sium, and phosphorus, respectively, were obtained when comparing the two analyses. These figures show excellent agreement between the two digestion procedures.

It is interesting to note that for the calculi of the present study the sequence of the average trace metal concentration values is the same as the sequence of the mean concentrations of these elements in urine (as given by Lentner /LEN81/; table II.14): Na > K > Zn > Sr > Al > Fe > Pb > Mo > Cu > Mn > Li.

Table II.14. Trace element concentrations in urine (/LEN81/)  
(assuming 1245 ml mean daily urinary flowrate).

	element	concentration [ng ml <sup>-1</sup> ]	
		mean	range
	Cu	26.0	3.2-92
	Fe	69.1	0-281
	K	2169	1285-3133
	Li	0.64	-
	Mn	16.2	13-19
	Mo	65.1	18-145
	Na	4137	1446-10361
	Pb	35.0	<65
	total S	1060	996-1197
	Sr	161	-
	Zn	336	112-1009

## 5.5 Discussion

In recent years the interest in the role of trace elements in almost all fields of biomedical and environmental research has been increasing dramatically. Trace elements are currently considered to be either harmless impurities or essential, depending on their concentration and the influence they have on physiological phenomena. The extent to which the elements of the periodic table have to be included in the group of essential trace elements is, however, disputed /CHR69, FEI80/. In the field of urolithiasis Hammarsten /HAM29/ discovered, as early as 1929, the "antagonistic influence" which Co, Mg, and Ni have upon

calcium by increasing the solubility of calcium oxalate. Many more elements have been added over the years to the list, all of which are considered to be either inhibitors or promoters of stone formation /BIR63, BUS68, ELL67, EUS67, MIL79, MIN82, NAN74/. In addition to the metabolic role more and more attention has been focused on the trace element content of human concretions.

Gerlach /GER34/ is thought to have been the first to employ spark spectrography in elemental kidney stone analysis. Using this technique Mathe /MAT40, MAT40a/ and Kovalev /KOV55/ found a combined total of 27 elements to be present in urinary calculi. Ohta's extensive investigations of the inorganic constituents of biological material were the first to allow quantitative comparison of the trace element concentrations in different concretions, e.g. biliary, pancreatic and urinary stones /OHT53, OHT55, OHT55a, OHT57, OHT57a, OHT57b/. Nagy et al. /NAG63/ found K and Zn to be present at the 100 to 1000 ng mg<sup>-1</sup> ash level when analysing 85 kidney stones for 25 elements, whereas Al, Ba, Bi, Cd, Fe, Mn, Na, Ni, Pb, Si, Sn, and Sr were present at 10 - 100 ng mg<sup>-1</sup> ash, and Ag, Cu, Cr, and Mo at only 1 - 10 ng mg<sup>-1</sup> ash. Results of most of these and other studies /ABD85, BAK66, DON77, DRA80, HOO64, SCH70/ are, however, difficult to compare, because of the different approaches in publishing concentration values. Often these are reported as 'as received', 'dry weight', or '% ash'. In cases where no mean ash portions or component information are given to supplement the data, calculation of meaningful concentration values becomes an impossible task. Nevertheless, there were some reported concentrations that could be compared with values obtained in the present study. These are given in table II.15. Copper and sodium values show reasonable agreement within all 4 studies, while mean iron concentrations show excellent agreement between the two ICP-AES studies, but differ by a factor 10 from the values determined by NAA and wet chemical methods. Potassium, strontium, and zinc values, however, show a wide spread among the different investigations.

One possible reason for the inconsistent concentration values observed could be the degree to which different stone groups (e.g. calcium oxalates, APA/STR, UA, etc.) are present in the total number of calculi sampled in each case. That this parameter influences reported

Table II.15. Comparison of trace element concentrations in urinary calculi from different studies.

element	concentration [ng mg <sup>-1</sup> ]			
	present study <sup>1,2</sup> n=102	/DON77/ <sup>1,3</sup> n=8	/LEV78/ <sup>1,4</sup> n=69	/OHT57b/ <sup>5</sup> n=10
Al mean range	32 <10-89	- -	180 -	- -
Cu mean range	1.4 <1.0-10	8.0 2.0-22	2.5 -	14 4.8-27
Fe mean range	27 <1.0-156	341 116-551	33 -	215 118-340
K mean range	1737 <180-6756	433 77-945	15265 -	2890 520-8140
Mn mean range	<1.0 -	- -	0.7 -	2.3 0.7-4.5
Mo mean range	2.2 <1.5-8.3	- -	27 -	- -
Na mean range	4670 129-50042	1429 262-6139	3574 -	4570 1690-7650
Pb mean range	22 <14-139	- -	65 -	34 19-58
Sr mean range	121 <6.0-622	7 1.0-48	81 -	- -
Zn mean range	270 <1.0-1381	78 4.0-453	420 -	555 239-913

<sup>1</sup> mean and range of all calculi analysed ('as received');

<sup>2</sup> concentrations lower than detection limit (l.l.d.) are set to 0.5·(l.l.d.);

<sup>3</sup> neutron activation analysis;

<sup>4</sup> concentrations lower than l.l.d. set to zero; ICP-AES analysis (spectrograph);

<sup>5</sup> on mass/dry mass basis; wet chemical and spectrographic technique.



concentration values to a great extent can be seen from table II.16. Range, mean, and median values, as calculated with function P2D of the BMDP statistics package /DIX85/, are listed for the four major stone

Table II.16. Elemental concentrations in 4 major stone groups (Ca, Mg and P expressed as wt-%, other elements as ng mg<sup>-1</sup>).

element	CaOx	CaOx/APA	APA/STR	UA/CaOx
Ca range mean median	10.22-28.11 23.18 24.94	23.34-29.56 26.63 26.53	1.30-31.43 15.25 15.35	<0.01-23.68 5.81 1.22
Mg range mean median	<0.01-0.87 0.09 0.03	0.03-1.85 0.30 0.18	0.56-9.50 5.02 5.41	<0.01-0.15 0.03 0.01
P range mean median	0.07-1.44 0.99 0.33	1.22-11.11 4.51 3.48	5.80-16.79 12.65 13.04	<0.01-1.58 0.18 0.04
Al range mean median	<5.0-89 25.1 16.9	12-72 29.9 29.0	27-73 46.9 46.2	<5.0-21 8.7 5.0(d)
Cu range mean median	<0.50-1.7 0.59 0.50(d)	<0.50-10 2.1 0.50(d)	<0.50-7.1 1.1 0.50(d)	<0.50-5.9 1.6 0.50(d)
Fe range mean median	6.0-51 30.0 24.6	9.0-129 48.4 32.7	<0.50-156 24.1 18.0	<0.50-79 17.7 11.3
K range mean median	367-4059 1031 531	350-3270 1063 810	1042-6756 2914 2702	<90-1265 393 289
Mo range mean median	<0.75-4.1 1.3 0.75(d)	<0.75-3.1 1.2 0.75(d)	<0.75-8.3 3.3 3.4	<0.75-3.0 1.3 0.75(d)
Na range mean median	928-10636 2763 1651	1428-15212 3884 2616	1002-12392 6671 6437	129-1738 662 459
Pb range mean median	<7.0-131 27 7.0(d)	<7.0-119 47 43	<7.0-139 19 7.0(d)	<7.0-14.1 7.4 7.0(d)
S range mean median	372-1633 1022 1127	345-2081 906 792	134-1428 478 424	341-1097 605 572
Sr range mean median	12-622 113 60	44-462 126 94	12-459 180 148	<3.0-126 17.6 3.0(d)
Zn range mean median	21-1316 210 65	113-1381 483 418	26-994 345 303	2.1-131 16 8.2

groups, as presented in section 5.4 (Ca, Mg, P expressed as % (w/w); trace elements as  $\text{ng mg}^{-1}$ ). It can be clearly seen, for example, that trace elements are far less concentrated in uric acid stones than in apatite stones. Strontium and zinc especially are exceptionally low in the former group. However, even when results of similar investigations /HES77, HES78, LEV78/ including those of the present study are compared on a group basis mean concentration values do not agree.

An additional reason for the disagreement in results might be the way in which mean concentrations are evaluated. Levinson et al. /LEV78/, for example, set all concentration values which are too low for determination at zero. In the present study, these values were set at one half the detection limit value. In other studies, these figures are not considered at all when calculating the mean. To further illustrate this, table II.16 shows the mean (median) Pb concentration in CaOx calculi as 27 (7.0)  $\text{ng mg}^{-1}$ ; when discarding all values below the lower limit of detection, the mean (median) lead concentration becomes 62 (44)  $\text{ng mg}^{-1}$ ! In none of the other studies, however, are detection limits or figures for accuracy and precision stated. Meyer et al. /MEY77/ consider their data to be "accurate to about 25%", yet they fail to detect potassium in any of their stones. Levinson et al. /LEV78/ believe their results to be accurate "within 15%" of the amount present, and Hesse et al. /HES77/ report a reproducibility of "10 to 30%".

Differences between the above studies might, nevertheless, be 'real', i.e. stem from regional differences of the collection sites, giving rise to factors such as dissimilar drinking waters /KOV55/ or diets /LEV78/. The limited number of such studies, however, does not yet permit any conclusions to be drawn in this direction from the available data. In the following section the results of this study are therefore further scrutinized.

#### 5.5.1 Statistical analysis

The data presented in table II.13 were subjected to 3 types of analyses: (i) correlations between the crystalline compounds present

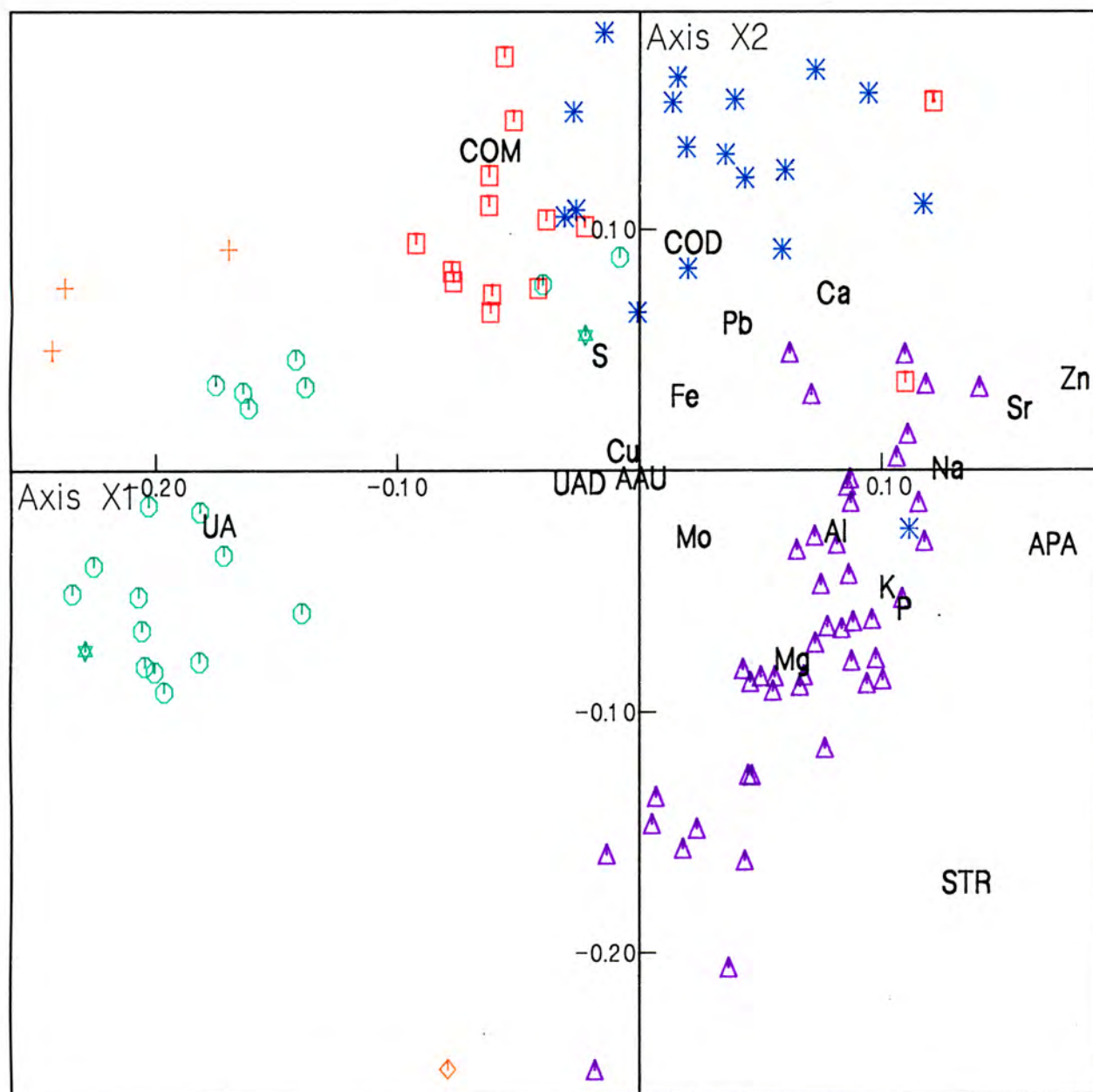
and the trace element content of each stone were sought by investigating two-dimensional scatter plots of all the 23 variables /DIX85a/; (ii) scatter plots of 2 elements at a time were examined for all 4 major stone groups separately /DIX85a/; (iii) logarithmic data were simultaneously subjected to a multivariate analysis (covariance biplot) /GAB71, GRE82, PEI82, UND85/.

The first two methods were used only in a supplementary capacity to the more powerful covariance biplot. This treats the rows and columns of the data matrix (in this case calculi and elements) as two clouds of points in high dimensional space, and projects them onto a lower (usually two-) dimensional space in such a way that as much of the versatility in the data matrix is explained, and certain properties in terms of standard deviations and correlations are displayed. The covariance biplot was performed on the elements only, and the compounds plotted in afterwards as 'supplementary points' /GRE84/. Thus the compounds have no influence on the position of elements or stones in the plot. The 3 cystine calculi were also treated as 'supplementary points' as otherwise their extremely high sulphur content (compared with other concrements) would have dominated the value decomposition.

These plots can be interpreted by drawing a line from the origin to the relevant variable symbol, which then becomes an axis of increasing concentration for the particular element or compound. A line drawn through the origin at  $90^\circ$  to the first line represents the mean concentration value for the element concerned. Data points in the half plane towards the element symbol have above average concentrations of this element, whereas points in the opposite half plane show concentrations below average. The cosine of the angle between the lines of two element symbols is approximately equal to the correlation coefficient between these two variables. However, since the biplot is a low dimensional representation of multidimensional data, there is inevitably some distortion, and there are cases where two variables seem to be correlated in the  $X_1, X_2$  plane, but where in a third or higher dimensional picture their rays enclose a large angle. Exact information about existing correlations can therefore be obtained only from the correlation matrix (table II.17). This matrix contains the standard deviations of the variables in the diagonal elements and the correlation coefficients in

Table II.17. Correlation matrix (covariance biplot).

	Ca	Mg	P	Al	Cu	Fe	K	Mo	Na	Pb	S	Sr	Zn	COM	COD	APA	STR	UA	UAD	AAU
Ca	0.9877	-0.0420	0.3058	0.3509	-0.0643	0.2397	0.3174	-0.0565	0.6734	0.4474	0.3548	0.7327	0.7212	0.3101	0.3254	0.4535	-0.3224	-0.7079	-0.3454	-0.0275
Mg	-0.0420	0.8782	0.8548	0.6937	-0.1498	-0.0470	0.7504	0.5413	0.5290	-0.1565	-0.5570	0.4383	0.4044	-0.5818	-0.3513	0.6144	0.9739	-0.4729	-0.1941	0.0124
P	0.3058	0.8548	1.1050	0.8161	-0.1152	0.0616	0.8219	0.4677	0.7859	0.1347	-0.4388	0.6965	0.7196	-0.5672	-0.0810	0.8874	0.8405	-0.6584	-0.2801	-0.0498
Al	0.3509	0.6937	0.8161	0.8168	-0.1913	0.2173	0.7321	0.4483	0.7206	0.2348	-0.2710	0.7410	0.7000	-0.3644	0.0307	0.7084	0.6634	-0.6993	-0.1989	0.0082
Cu	-0.0643	-0.1498	-0.1152	-0.1913	0.4838	-0.0234	-0.1770	0.0128	-0.0962	0.0840	0.2621	-0.0784	-0.0858	0.0296	-0.0451	-0.0043	-0.1204	0.1398	-0.0135	0.0002
Fe	0.2397	-0.0470	0.0616	0.2173	-0.0234	0.7853	0.1031	0.0065	0.0624	0.2452	0.3590	0.2031	0.2413	0.0652	0.3583	0.1010	-0.0860	-0.3185	-0.0502	-0.0174
K	0.3174	0.7504	0.8219	0.7321	-0.1770	0.1031	1.0600	0.4327	0.7977	0.1118	-0.3861	0.7219	0.6816	-0.3966	-0.1153	0.6756	0.7298	-0.6787	-0.2281	0.1680
Mo	-0.0565	0.5413	0.4677	0.4483	0.0128	0.0065	0.4327	0.5225	0.2843	-0.0554	-0.2738	0.2512	0.2809	-0.2536	-0.2691	0.3105	0.5525	-0.2359	-0.1558	0.0203
Na	0.6734	0.5290	0.7859	0.7206	-0.0962	0.0624	0.7977	0.2843	1.1267	0.3335	-0.1457	0.8901	0.8375	-0.2251	0.0157	0.8022	0.5323	-0.7377	-0.3460	-0.0009
Pb	0.4474	-0.1565	0.1347	0.2348	0.0840	0.2452	0.1118	-0.0554	0.3335	0.8794	0.2388	0.3901	0.4645	0.1292	0.3273	0.2774	-0.1725	-0.3173	-0.1370	-0.0366
S	0.3548	-0.5570	-0.4388	-0.2710	0.2621	0.3590	-0.3861	-0.2738	-0.1457	0.2388	0.5635	-0.0687	-0.0894	0.5450	0.1526	-0.2460	-0.5258	-0.0015	-0.0035	-0.0333
Sr	0.7327	0.4383	0.6965	0.7410	-0.0784	0.2031	0.7219	0.2512	0.8901	0.3901	-0.0687	1.3885	0.8625	-0.1458	0.1604	0.7331	0.4252	-0.7887	-0.3333	0.0208
Zn	0.7212	0.4044	0.7196	0.7000	-0.0858	0.2413	0.6816	0.2809	0.8375	0.4645	-0.0894	0.8625	1.5923	-0.1909	0.2692	0.7671	0.3738	-0.7903	-0.3205	-0.0215
COM	0.3101	-0.5818	-0.5672	-0.3644	0.0296	0.0652	-0.3966	-0.2536	-0.2251	0.1292	0.5450	-0.1458	-0.1909	1.8684	-0.0251	-0.5671	-0.5711	0.0356	-0.0731	0.0739
COD	0.3254	-0.3513	-0.0810	0.0307	-0.0451	0.3583	-0.1153	-0.2691	0.0157	0.3273	0.1526	0.1604	0.2692	-0.0251	1.5877	0.0589	-0.4350	-0.1883	-0.0946	-0.0674
APA	0.4535	0.6144	0.8874	0.7084	-0.0043	0.1010	0.6756	0.3105	0.8022	0.2774	-0.2460	0.7331	0.7671	-0.5671	0.0589	1.6883	0.6291	-0.6154	-0.2549	-0.0926
STR	-0.0324	0.9739	0.8405	0.6634	-0.1204	-0.0860	0.7298	0.5525	0.5323	-0.1725	-0.5258	0.4252	0.3738	-0.5711	-0.4350	0.6291	1.9387	-0.4476	-0.1854	0.0035
UA	-0.7079	-0.4729	-0.6584	-0.6993	0.1398	-0.3185	-0.6787	-0.2359	-0.7377	-0.3173	-0.0015	-0.7887	-0.7903	0.0356	-0.1883	-0.6154	-0.4476	1.6935	0.3808	-0.0694
UAD	-0.3454	-0.1941	-0.2801	-0.1989	-0.0135	-0.0502	-0.2281	-0.1558	-0.3460	-0.1370	-0.0035	-0.3333	-0.3205	-0.0731	-0.0946	-0.2549	-0.1854	0.3808	0.5978	-0.0287
AAU	-0.0275	0.0124	-0.0498	0.0082	0.0002	-0.0174	0.1680	0.0203	-0.0009	-0.0366	-0.0333	0.0208	-0.0215	0.0739	-0.0674	-0.0926	0.0035	-0.0694	-0.0287	0.4554



- ☐ Calcium Oxalate (COM/COD) Group
- ⊙ Uric Acid (UA/UAD) / CaOx Group
- ✱ Urates (AAU/SAU)
- △ Struvite / Apatite (STR/APA) Group
- \* CaOx (COM/COD) / Apatite Group
- + Cystine group
- ◇ CaOx / STR stone

Figure II.15. Covariance biplot.

all other positions.

The first ( $X_1$ ) and second ( $X_2$ ) axes account for 63.6% and 15.1% of the variance, respectively; thus the plane of the first two axes accounts for 78.7% of the variance (figure II.15). It can be clearly seen that stones of different groups cluster in different regions of the  $X_1$ ,  $X_2$  plane, which are mainly determined by their Ca, Mg, and P concentrations. Thus, the COM/COD calculi are all placed in the average to high calcium and below average magnesium and phosphorus region. This group overlaps with the CaOx/APA group towards increasing Ca values. The latter borders on the APA/STR group and is spread around the magnesium variable above and below the average calcium line, depending on the apatite content of the calculi. Uric acid and urate stones as well as cystine stones are positioned at below average concentration positions of most elements, confirming the extremely low trace element content found in these stones.

An example which illustrates the value of these biplots is the trace element distribution in the APA and COD stones. It can be seen that trace elements are enriched in these calculi, as many element vectors are enclosed in the sector formed by the relevant connecting lines to the origin of APA and COD. It is known that the formation of COD is promoted by Cu, Mg, Mn and the conversion of COD into COM depends mainly on the concentrations of these and other cations /HES76, HES76a/. It can thus be predicted that if COD is part of a calculus, it will invariably display a higher trace element content than, for example, a pure COM stone. This is clearly reflected in figure II.15.

Another benefit derived from applying multivariate statistical methods to stone analysis is accentuated by considering those concretions which do not conform to the general pattern (figure II.15). Examples are stones 17 ( $X_1=0.1210$ ,  $X_2=0.1531$ ), 389 ( $X_1=0.1097$ ,  $X_2=0.0369$ ) and 478 ( $X_1=0.1112$ ,  $X_2=-0.0241$ ), previously analysed only by the film XRD method, and which were re-analysed with the diffractometer technique. Stones 17 and 389 which were earlier placed in the COM/COD group were both found to contain additional crystalline phases not detected by the film method. These could not be identified in the case of stone 17, but the very high sodium and zinc concentrations deter-

mined in this calculus point to the possible existence in this concrement of sodium and / or zinc oxalate or a sodium urate and zinc phosphate. In stone 389 uric acid and small amounts of APA were identified in addition to COM and COD. However, no STR, which would account for the high magnesium concentration in this stone, was identified. A highly substituted (Mg for Ca) microcrystalline apatite is therefore thought to be present as well as some sodium urate (high sodium content) associated with the detected UA. In stone 478 additional STR and COM was demonstrated, which explains the position of this 'COM/COD' concrement in the STR/APA cluster.

It can thus be seen that it is possible to expose erroneous or incomplete analytical results with the outlined statistical treatment, the value of which can therefore not be overestimated.

#### 5.5.2 Trace elements in calculi and their significance in urolithiasis

Figure II.15. shows that magnesium can be considered to be a trace impurity in CaOx and CaOx/APA concrements. This element was detected in all calculi of these two groups, although in some of the COM/COD calculi it occurred at very low concentrations ( $<100 \text{ ng mg}^{-1}$ ). It is interesting to note that oral Mg in the form of MgO has been suggested /KIN68, MOO64/ and successfully employed /MEL71/ as prophylactic therapy in the treatment of this type of stone. Hammarsten /HAM37/ was the first to recognize magnesium as having an inhibitory effect on stone formation. Several studies subsequently confirmed this. For example, animals on Mg deficient diets alone produced intratubular deposits of HAP /RUS80/, and Mg deficiency markedly accelerated COM deposition within the lumina of proximal tubules /RUS81/. On the other hand, magnesium rich diets decreased the incidence of urinary tract stones when administered to rats with experimentally induced CaOx calculi /BOR69/. The present study confirms these results insofar, as no CaOx or CaOx/APA stones with high Mg concentrations were found. It might thus be concluded that high Mg concentrations prevent the formation of this type of calculus. It is thought that  $\text{Mg}^{2+}$  ions on the one hand may induce an increase in the solubility of CaOx and thus a decrease in the crystal growth rate, but on the other hand they may be

conducive to the enlargement of the  $\text{CaOx}$  crystals and aggregates by the retardation of crystallization /BER76, DES73, WUN81/. High Mg concentrations have been shown to prevent the conversion of COD to COM /BER76, ZAP73/. This is also reflected in figure II.15 where COD is at higher Mg values than COM. Even the precipitation of the unstable COT has been demonstrated in the presence of Mg and citrate /LY065/.

Interconversion of phosphate calculi from one form to another due to action of Mg ions has also been reported. Thus, the presence of Mg causes brushite to be transformed into whitlockite (WHI) instead of the expected octacalcium phosphate (OCP) /SCH66/. Magnesium also suppresses the crystallization of OCP and favours the formation of WHI at the expense of apatite /TRA64/. On the other hand, Mg can be incorporated into the apatitic lattice and replace calcium completely. This might explain the presence of one  $\text{CaOx}$ /APA concretion in the APA/STR group shown in figure II.15. Magnesium can also induce the formation of Mg-Ca apatite solid solutions /PAT80/ and in this way affect the crystallinity of the apatite phase.

It is therefore clear that magnesium, apart from its contribution to the formation product of STR, plays a vital role in  $\text{CaOx}$  and APA stone formation, not only affecting the physical properties (crystallinity, hardness, etc.) of calculi, but also modifying their crystal habits and structures. Further experimental results are, however, needed to clarify the exact mechanism(s) by which Mg interacts with other stone forming compounds. One such approach could be the fast evaporator technique described in chapter IV.

Aside from magnesium which has been shown to be a trace element in the non-struvite calculi all other trace elements investigated in this study have been reported to inhibit stone formation and / or to have a catalytic function in the crystallization process. Thus, Zn was found to be predominantly associated with apatite, which is substantiated by the mean Zn values determined in the different stone groups (table II.16) and correlations established between the Zn and apatite ( $r = 0.77$ ) and Zn and P ( $r = 0.72$ ) content of the calculi. This supports the previously reported findings that Zn substitutes for Ca in the calcium phosphate molecule /SCH68/ or that a certain percentage of



phosphates can be present as  $\text{Zn}_3(\text{PO}_4)_2 \cdot 4\text{H}_2\text{O}$  (Hopeit) /NAG63, SCH69/.

Notwithstanding these results, zinc has been found to play a role in the crystallization of urate and oxalate stones /NAG63/ and inhibits mineralization in vitro at concentrations approaching those found in normal urine /KIN71/. Zinc increases the solubility of  $\text{CaOx}$  /ELL67/, is an effective inhibitor of  $\text{CaOx}$  crystallization /SUT70/, and decreases the growth rate of this compound /EUS67/. It also decreases the solubility product of calcium phosphate /KIN67/. An association between Zn and Cd and their effect on stone prevalence in coppersmiths has also been pointed out /SC082/. Besides its role in urolithiasis, zinc is involved in glucose metabolism /AND84/ and is one of the most important trace elements /SCH83/.

As can be seen from figure II.15, Zn is positively correlated with Sr ( $r = 0.86$ ). Strontium also competes with Ca for the apatite lattice /SOB49/. It is so similar to Ca in its metabolism that it is generally known to be a companion to the latter in salts, where Sr can exchange isomorphically with Ca in the lattice /HES78, NEU53/. A linear correlation between the amount of apatite and Sr ( $r = 0.80$ ) and P and Sr ( $r = 0.84$ ) in  $\text{CaOx}$ /APA stones supported this. Besides other than these findings, Sr does not appear to play a significant role in urolithiasis. However, it is interesting to note that when radioactive  $^{90}\text{Sr}$  was released to the atmosphere during the 1950's atomic bomb tests, some concern was expressed about the possible accumulation of dangerously high levels of radiation in calcified body tissue /PHI58/.

Both Sr and Zn were found to be correlated with sodium concentrations ( $r = 0.89$  and  $r = 0.84$ , respectively), especially in the  $\text{CaOx}$  (Sr:  $r = 0.92$ , Zn:  $r = 0.96$ ) and  $\text{CaOx}$ /APA (Sr:  $r = 0.96$ ) calculi. In the  $\text{CaOx}$  group, these elements are also correlated with potassium (Sr:  $r = 0.84$ , Zn:  $r = 0.93$ ), which in turn is related to the high correlation between Na and K in this group ( $r = 0.98$ ).

As with Sr and Zn, K and Na substitute for Ca in apatites /SCH68, SIM68/. However, these elements are mainly limited to the crystal surface /NEU53, NEU62, PAK67/. In  $\text{CaOx}$  calculi the co-precipitation of small amounts of structurally related K-, Sr- and Zn-oxalates seems to

be a plausible explanation for the observed relationships.

Apart from substituting for Ca in the crystal lattice of calcium salts, urinary sodium also influences the initial crystal formation, owing to the fact that it is the major determinant of urinary ionic strength; increasing ionic strength increases solubility of the poorly soluble urinary precipitations /MOD69/.

Another element exchanging for calcium in apatite is Pb /NEU53/. It is known to decrease the solubility product of calcium phosphate /KIN67/ to the extent that extremely low concentrations ( $<10^{-5}$  M) of this element can activate calcium phosphate precipitation in vitro /FLE65/. Lead is also adsorbed to the phosphate surface /MEY77/ and thus concentrates in bone and apatitic stones with the possible formation of lead apatites /NAG63/. From the present study it can be concluded (figure II.15) that Pb concentrates in APA calculi as its position is wedged between the CaOx/APA and APA/STR groups.

The apparent correlation from figure II.15 between Fe and Pb is not reflected in the correlation matrix ( $r = 0.25$ ), and is thus an example of the distortion brought about by compression of the data matrix into 2 dimensions. The quality of the representation of Fe in 2 dimensions is only 14.8% and of Pb 48.5% (table II.18). Iron is the dominant element on the third ( $X_3$ ) axis which accounts for 5.0% of the total variation (not shown) and has a large coordinate value which takes it out of the  $X_1, X_2$  plane. Thus the true angle (correlation) between Fe and Pb is not well represented in figure II.15. In fact, the 4th axis ( $X_4$ , accounting for 4.0% of the variance) represents a weak negative correlation between Pb and Fe in a small group of stones.

Urinary iron is thought to arise, in the main, from microhematuria and epithelial cells in the renal tubules /LEN81/, where it produces a definite increase in the solubility of CaOx, owing to the formation of complexes between ferric and oxalate ions /ELL67/. Its presence in calculi is further explained by the adsorption of  $Fe^{2+}$  and  $Fe^{3+}$  ions on CaOx and Ca-phosphate /MEY77/. Indeed, the growth of strengite ( $FePO_4 \cdot 2H_2O$ ) calculi has been observed in animals /GRU64/.

Table II.18. Quality of 2-dimensional representation (covariance biplot, figure II.15).

	element	var	$X_1 + X_2$	$X_1$	$X_2$	$X_3$	$X_4$
	Ca	7.7	83.6	45.1	38.5	4.3	4.7
	Mg	6.1	90.7	35.8	54.9	1.1	0.0
	P	9.6	91.4	72.7	18.7	0.5	0.6
	Al	5.3	74.5	68.0	6.5	5.0	0.0
	Cu	1.8	3.5	1.5	2.0	0.0	2.1
	Fe	4.9	14.8	4.0	10.8	69.1	13.2
	K	8.8	84.2	69.7	14.5	0.1	0.4
	Mo	2.1	32.0	13.0	19.0	3.3	0.6
	Na	10.0	88.3	88.3	0.0	3.7	0.1
	Pb	6.1	48.5	14.8	33.7	5.6	39.0
	S	2.5	53.1	3.4	49.7	2.2	7.3
	Sr	15.2	90.6	88.2	2.4	0.7	1.2
	Zn	20.0	91.8	87.9	3.9	0.1	0.6

Explanation: 'var' is the percentage of the total variance due to each element (summing to 100 for all elements). The values in the  $X_1$  columns represent the percentage of the variance contributed by the element explained by axis  $X_1$ , where the sum over all axes again sums to 100 for each element (total representation of the element in n-dimensional space). The values in the  $X_1 + X_2$  column then display the extent to which (expressed as a percentage) the 'information' (variance) due to the element concerned is contained in figure II.15. For example, iron contributes with only 4.9% to the overall representation and only 14.8% of this is accounted for in figure II.15, whereas the bulk of information due to iron (69.1%) dominates axis  $X_3$ .

With citric acid at high ratios of citrate to metal ion,  $\text{Fe}^{3+}$  forms low molecular weight complexes which inhibit APA growth completely /MEY82/. High molecular weight  $\text{Fe}^{3+}$  citrate complexes formed at low citrate to iron ratios, on the other hand, inhibit calcium oxalate crystal growth /MEY82a/. It was therefore suggested that the  $\text{Fe}^{3+}$  - citrate system, which under different conditions suppresses the growth of the major crystalline materials of kidney stones, might play a unique role in preventing the precipitation of these compounds /MEY82,

MEY82a/. It is thus conceivable that during the course of this process Fe becomes entrapped preferentially in CaOx and APA agglomerates. This hypothesis is supported by the position of Fe relative to CaOx and APA in figure II.15.

Synergism with citric acid has also been observed with aluminium in the inhibition of APA crystal growth /MEY77, MEY82, MEY82a/. Large excess of citrate, however, reversed this effect /MEY82/. Calcium oxalate crystal growth was not affected by Al alone or in combination with citric acid /MEY77, MEY82a/. Sutor, however, found that very small concentrations of  $\text{Al}^{3+}$  removed oxalate ions and thus prevented the crystallization of CaOx /SUT69, SUT70/. In the present study, aluminium was found to be correlated with phosphorus ( $r = 0.82$ ) and was positioned in the apatite-rich part of the APA/STR group (figure II.15). This association might result from its incorporation into the apatite lattice where it probably substitutes for P /LEV78/.

Copper and molybdenum played only a minor role in the statistical analysis of this study due to the very low concentrations at which these elements were present. Copper is an essential trace element /SCH83/ and, like iron, originates from blood.  $\text{Cu}^{2+}$  ion may compete with  $\text{Ca}^{2+}$  in calcification /SOB49/; it produces a definite increase in CaOx solubility /ELL67/ and inhibits HAP crystal growth /MEY77/. The apparent correlation between molybdenum and magnesium (figure II.15) is again an effect of the low dimensional representation of the high dimensional data matrix as discussed for Fe and Pb.

Manganese and lithium, both of which could not be determined in this study, have been shown to be of some effect in urolithiasis by other workers. Manganese has been observed to reduce calcium uptake and to inhibit mineralization of cartilage matrix /BIR63, THO82/. Lithium, on the other hand, appears to be helpful in the treatment of uricites /BAD63/. Thus is the solubility product of AAU raised in the presence of lithium ions /HAM31/. Oral doses of Li might therefore be able to transform only slightly soluble urates into easily soluble Li-UA compounds. Effective concentrations, however, are extremely high and reach toxic levels /SCH71/.

Sulphur concentrations in all stones of the present study had a mean value of  $8564 \text{ ng mg}^{-1}$  (median 542, range  $134\text{--}271000 \text{ ng mg}^{-1}$ ). This is somewhat elevated due to the large contribution of the 3 cystine stones. Concentrations in the CaOx (mean 1022, range  $372\text{--}1633 \text{ ng mg}^{-1}$ ) and CaOx/APA (mean 906, range  $345\text{--}2081 \text{ ng mg}^{-1}$ ) groups compare with the (total) sulphur concentration in urine of  $1060 \text{ ng ml}^{-1}$  (range  $996\text{--}1197 \text{ ng ml}^{-1}$ ) (table II.14). In APA/STR and UA stones concentrations are only about half these values. As inorganic sulphur (as sulphate) is thought to compete with oxalate for complexing  $\text{Ca}^{2+}$  /SCH85/ it may be postulated that during the formation of a CaOx stone, small quantities of calcium sulphate may be coprecipitated. This would give rise to a relatively high S concentration in such stones. However, no further data on sulphur and its role in urolithiasis are available.

## 5.6 Conclusions

ICP-AES has been successfully applied in the simultaneous determination of major, minor and trace elements of urinary stones. This technique was found to be an extremely useful tool in the analysis of calculi and, together with other compound-selective methods, allowed the quantitative determination of the crystalline content of urinary concrements. Although it is recognized that the financial outlay for an ICP spectrometer is high, once routinely operational long-term costs compare favourably with those of other procedures such as AAS /KAH82/. The several advantages of ICP-AES analysis outlined in this chapter already make it a principal tool in the analytical laboratory /MOO85/, as is evident by the growing number of applications in the biological, biomedical, nutritional, and environmental fields /MER82, OLS85, SCH83/.

Rapidity, costeffectiveness and ease of operation have been achieved (i) by using a microwave assisted wet digestion procedure, (ii) by employing a single set of operation conditions and calibration curves, and (iii) by determining all elements directly without preconcentration. The microwave decomposition procedure employed in this study undoubtedly had a positive influence on the analytical accuracy and precision of the results. It is, however, acknowledged, that the

rather large sample mass required for precise concentration measurements precludes some of the smaller calculi from analysis by ICP-AES. Furthermore, accuracy is limited by inhomogeneities which are invariably found in the sampled aliquots. The lack of stone standards constitutes another limitation in the attempt to improve analytical reliability. Most recently an "animal bone" standard (IAEA H-5) was introduced /LEE83a, MAH83/, which currently provides the closest match between a standard and stone matrix. Unfortunately this standard was not available for the present investigation.

An independent check of the accuracy of ICP-AES and x-ray diffraction analyses was obtained by participations in three round robin tests (urinary calculus analyses) organized by the German Society for Clinical Chemistry (table II.19).

Some of the trace elements explored were found to be at concentrations too low to be measured with ICP-AES. However, the detection limits achieved under the compromise settings selected for analytical parameters in this study could possibly be improved upon by optimizing conditions specifically for the low concentration elements occurring in calculi. Further improvement may be achieved by employing more sensitive or preconcentration techniques. An effective approach, for example, is the complexation of elements with a poly(dithiocarbamate) resin to separate trace elements quantitatively from complex alkali or alkaline earth metal matrices and to concentrate them to measurable values for ICP-AES /BAR83, MAH83/. Future technical developments of the sample introduction system of ICPs and new sample preparation techniques (e.g. preconcentration) will without doubt overcome these present shortcomings.

The quantitative determination of trace elements in calculi is essential for understanding their aetiology. It is now accepted that the crystallization processes occurring during the formation of stones are influenced by these metals, even if these are present in minute concentrations only. Although their functional role in urinary calculi is still unknown, most of the elements studied in this investigation were shown to promote or inhibit the precipitation of calculi (section 5.5). In addition, other elements such as Ag /MIL79/, Si /MIN82/ and Sn

Table II.19. Surveys of urinary calculus analyses.

survey	sample	expected	found	evaluation <sup>#</sup>
S2 1984	A	80% COM 20% UA	COM UA	++ ++
	B	100% STR	STR	++
	C	60% STR 40% APA	STR APA	+ +
	D	80% CYS 20% COM	SAU COM	- ? +
S1 1985	A	90% STR 10% APA	80% STR 20% APA	++ ++
	B	100% UA	100% UA	++
	C	100% XAN	100% XAN	++
	D	40% COM 40% STR 20% AAU	40% COM 40% STR 20% AAU	++ ++ ++
S2 1985	A	90% STR 10% APA	80% STR 20% APA	++ ++
	B	60% COM 20% STR 20% APA	60% COM 20% STR 20% APA	++ ++ ++
	C	50% COM 50% UA	45% COM 55% UA	++ ++
	D	100% XAN	100% XAN	++
<sup>#</sup> ++ expected substance(s) found in right order + expected substance(s) found - expected substance(s) not found ? other than expected substance(s) found				

/MEY72, MEY77, NAN74/ have also been reported to be of importance. Investigating a causative connection between trace element content and stone formation was, however, beyond the scope of this study.

The detection of small amounts of Ca and P in almost all the stones of the present study may indicate the presence of APA in all such samples /TOZ81/. It has been shown /BLA81/ that STR stones generally contain varying amounts of APA, with the large crystals of the former often being interspersed with small spherular deposits of the latter. APA has also been reported as constituting the most prevalent second phase in all polymineral calcium oxalate stones /KOL68/. These results, together with the observation of the present study that Ca and P occur in most calculi, even in minute concentrations, suggest that APA may play the role of a "cementing" agent in stone formation. Substitutions of trace elements in the Ca positions of APA are also very common. The fact that APA is always present in microcrystalline form in body fluids, that it has the highest trace element content and that it precipitates over a wide range lends support to this theory /LAG56/.

Organic matrix is also thought to act as a binder, thus playing an architectonic role in calculus formation, serving to cement an otherwise loose aggregation of crystals into a structurally cohesive unit /OGB81/. Whether this "cementing" mechanism is analogous to that of APA as suggested above remains to be seen. What does emerge, however, is support for an aggregation mechanism as a regular process in urinary calculi formation.

On the other hand, the detection of calcium (oxalate) in almost all uric acid stones again suggests an epitaxial relationship between these two components. Furthermore the repeated association of at least 2 components in almost all stones indicates that the existence of the so called "pure" stone might be a myth and that a heterogeneous nucleation mechanism might be operative as the primary event in stone formation. By applying ICP-AES to these and other stone problems, it is believed that new insight into understanding and controlling the disease can be obtained.

The application of multivariate statistical methods was shown to be most helpful in the interpretation of the acquired data and it is hoped that this new technique will find widespread application in other studies of similar nature.



## CHAPTER III

## Quantitative analysis of fluoride in urinary calculi

## 1. Introduction: Fluorine and urolithiasis

The inclusion of fluorine among the 15 elements which are acknowledged to be essential for mammalian organisms /FEI80/ is not universally accepted /MER80/. Since first mentioned at the end of the 15th century (attributed to Blasius Valentius and Georgius Agricola /WEA82/), the element has been found to be ubiquitous, amounting to approximately 0.075% of the earth's crust and a constituent of normal body tissue. Because of its size compared with other organs, the skeleton contains 99% of all physiological fluorine /VOL36/ where it is thought to be involved in maintaining the structural integrity of the hard tissue. Like lead, fluorine is present in minute traces only and may be present as a contaminant rather than a physiological necessity. More than 90% of fluoride intake is disposed of via the kidneys. The urinary excretion of fluoride is therefore closely connected with the fluoride concentration of drinking water and other food supplies /AUE62/. The natural daily amount of fluoride ingested lies in the mg range and is strongly affected by environmental factors, like geographical region, working environment, etc.

There is a vast literature, starting in 1874 (Erhard, cited by /MUE77/) describing all aspects - including political - of the use of fluorides for protection against dental caries. In recent years drinking water fluoridation for reduction of caries susceptibility has enjoyed growing popularity and a fluoride concentration of 1 to 2 mg l<sup>-1</sup> is now recommended by the World Health Organisation /WHO58, WHO65, WHO69/. However, dispute still rages as to the efficacy and safety of this practice /EDI85/.

Teeth and bones are not, however, the only repositories of fluorides. As fluorine is only slowly excreted, significant and dangerous levels of fluorides can be accumulated in soft tissue, ranging from the

liver, kidneys, heart and arteries to the glandular and central nervous system /JUE80/. Particularly liver and kidney may show extensive and severe parenchymatous changes at doses above 50 mg F<sup>-</sup> per kg body-weight. Furthermore, an excessive intake of fluorine and fluoride compounds leads to pathological changes, known as fluorosis. Aside from death due to the corrosive action of crystalline deposits of CaF<sub>2</sub> and other fluorides in the tissue, death may result very rapidly from interference with calcium metabolism, due to the reduction of the blood calcium content /RAB45/. The apparently rather narrow range of safe intake for fluorine has given rise to much concern in some countries /NEW85/ and fluorine is now even linked with the process of aging /JUE84/.

Thus, the advent of drinking water fluoridation in the 1950s led to interest in assessing the relation of water-borne fluoride to the fluoride content of urinary and biliary tract calculi. Reports on the role of fluoride ingestion in the genesis of urolithiasis are, however, contradictory. Areas with high distribution of fluoride-bearing minerals in Finland seem to match areas with the highest incidence of urolithiasis leading to hospitalization /JUJ79/. On the other hand, in India, endemic fluorosis and bladder stone disease failed to show an interrelationship /TE083, TE084/ while studies on the effect of fluoride on rats' kidneys /HER60/ also do not support the suggestion that excess fluoride causes a higher incidence of stones.

In order to possibly contribute to the clarification of the above issue, we were approached by a research group from India to analyse a number of kidney stones for fluoride. A thorough investigation into applicable analytical techniques for fluoride determination was however necessary before this could be attempted.

## 2. Analytical techniques for fluoride determination

The solution of very many unresolved problems concerning fluoride metabolism and fluoride retention in body tissue requires accurate analytical techniques to determine this element quantitatively.

The analysis of fluorine-containing materials has generated an enormous amount of literature - probably the largest for any element. Cited stumbling-blocks in the procedure of fluoride determination are

- (i) difficulties in dissolving fluoride-bearing compounds,
- (ii) insolubility of most fluorides to varying degrees,
- (iii) high reactivity of fluorine due to it being the most electronegative element,
- (iv) considerable interferences by the presence of other ions which precipitate as fluorides or form metal-fluoride complexes, and
- (v) interaction of the fluoride ion with glassware.

Fluoride analysis consists of three individual steps each of which has its own peculiar difficulties /STE59/:

- (i) ashing of organic / inorganic materials and conversion into fluoride ion,
- (ii) separation of fluoride ion from interfering ions, and
- (iii) determination of the isolated fluoride.

When determining fluoride in kidney stones, step (i) above involves (wet) digestion of crystalline deposits intermingled with organic matter (see chapter II). In those cases where direct analysis of the ashed samples prove to be unfeasible, five separation techniques (step (ii) above) are essentially available /WIL79/: distillation of fluoro-silicic acid, microdiffusion (important for biological materials), pyrohydrolysis (requires absence of organic matter), chromatographic methods including ion-exchange, and co-precipitation. The final determination (step (iii) above) may employ gravimetric methods (precipitation as fluoride salt, e.g.  $\text{CaF}_2$  /STA12/), titrimetry /HAL60, LIG69/, spectrophotometry /WIL79/, electroanalytical methods /FRA66, BEY63/, radiochemistry (e.g. neutron activation /BRA80/ and gamma ray spectroscopy after  $^{19}\text{F}(p, \alpha\gamma) ^{16}\text{O}$  /DIE80/ or  $^{19}\text{F}(p, p'\gamma) ^{19}\text{F}$  /SHR78, HAN84/ reactions), and catalytic methods. Most recent studies /WIN79, FRY80/ employed ICP-AES (see chapter II) in connection with element selective gas chromatography.

Prior to the introduction in 1933 of steam distillation of fluoro-

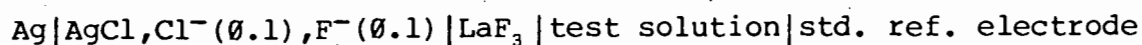
silicic acid (followed by titration of fluoride with thorium nitrate, using zirconium-alizarin /WIL33/ or sodium-alizarin-sulfonate /ARM33/ as indicator) no reliable method of fluoride determination was available. Fluoride concentration values reported in earlier studies must thus be regarded with caution /MCC62/. Pure chemical methods for the analysis of fluorine frequently were affected by its chemical form and the chemical or physical nature of the sample. Sample preparation and separation techniques were subjected to random and systematic errors either due to loss of fluorine or contamination with extraneous fluoride /JON76/.

Another means for separation of fluoride involves its conversion to HF by treatment of the sample with a strong acid, followed by the collection of the HF by either distillation /SIN54/ or trapping in a microdiffusion dish. However, the small sample size (ca. 10 mg) of most kidney stones involves only microgram amounts of fluoride which are too small to be handled with any degree of accuracy by distillation procedures /LEA63/. Hence, microdiffusion, previously employed in the separation of fluoride from materials as diverse as water, salt, milk, toothpaste, teeth and bones /BAE64a/, appeared to be the most versatile procedure and was therefore selected as one of the methods for this study. A further potential advantage of this technique lies in the possible combination of sample digestion and fluoride separation into one step, thereby shortening sample preparation times.

As far as the determination of fluoride is concerned, several older methods became obsolete with the introduction of the reagent alizarin fluorine blue for spectrophotometric determination of fluoride in 1958 /BEL58/ and the fluoride specific electrode in 1966 /FRA66/. The fluoride electrode, unsurpassed in terms of its overall utility and interference rejection and probably the fastest and easiest technique for determining fluoride in solutions /CZA85/, was employed in this study.

### 3. Direct determination of fluoride with ion selective electrode

Construction of the fluoride ion selective electrode /FRA66/ is similar in principle to that of a conventional glass pH electrode, except that the fluoride sensitive membrane is a single crystal of  $\text{LaF}_3$  doped with  $\text{Eu}^{2+}$ . The disk-shaped crystal, typically about 1 cm in diameter and a few millimeters thick, is cemented into the end of a rigid PVC tube, thus forming a water-tight seal between the fluoride ion containing test solution and the inner electrode assembly. The internal solution is typically a mixture of 0.1 M NaF and 0.1 M NaCl, with which electrical contact is made via a silver / silver chloride wire. In order to determine the potential difference between the fluoride electrode and a solution, another electrode and solution of accurately known potential difference is necessary. For this purpose a Ag / AgCl sleeve type or saturated calomel electrode is usually employed as standard reference /VOG78/. The two electrodes can then be combined to form a voltaic cell which may be represented by /LIN67/



Since the rare-earth fluoride membrane is permeable to only  $\text{F}^-$  ions, the cell potential  $E$  obeys a Nernst type equation, i.e. the sensing surface acts as a battery, generating a potential proportional to the logarithm of analyte concentration (activity)

$$E = E_0 + (R \cdot T \cdot F^{-1}) \cdot \ln(a_F) \quad (\text{III.1})$$

where  $a_F$  activity of fluoride ions in the solution

$E_0$  sum of the contributions from internal and external reference electrodes and from liquid junction potentials.

$R$  gas constant ( $8.31441 \text{ J mol}^{-1} \text{ kg}^{-1}$ )

$F$  Faraday constant ( $96484.56 \text{ Cb mol}^{-1}$ )

$T$  absolute temperature

Introducing the factor for converting natural logarithms to base 10, the expression  $(R \cdot T \cdot F^{-1})$  has a value of 59.16 mV at a temperature of 25°C. As it is sufficiently accurate for most purposes in quantitative analysis to replace fluoride ion activity by the ion concentration  $c_F$ ,

the Nernst equation assumes the well-known form

$$E \text{ [mV]} = E_0 \text{ [mV]} + 59.16 \text{ [mV]} \cdot \lg(c_F) \quad (\text{III.2})$$

In practical use, the electrode is calibrated, i.e.  $E_0$  and the actual electrode slope  $S=(R \cdot T \cdot F^{-1})$  are evaluated, with standards of known concentration of fluoride.

### 3.1 Measurement techniques

Different measurement techniques for the determination of fluoride concentration  $c_F$  are available /BAI76/:

- direct method
- standard addition / subtraction methods
- Gran's plot
- potentiometric titrimetry.

The direct calibration method is the simplest measurement technique for most routine samples. Here the sample concentration is determined in a one-step procedure from the difference,  $\Delta E$ , between the electrode's potential in the sample solution and the standardizing solution. This can be achieved by either direct comparison with a calibration curve (potential readings versus log concentration) or calculation

$$c_{\text{unknown}} = c_{\text{standard}} \cdot 10^{\Delta E \cdot S^{-1}} \quad (\text{III.3})$$

Calibration is therefore essential when direct methods of analysis are used. Calibration is also strongly advised for all incremental procedures (i.e. standard addition or subtraction) since the actual slope of the calibration graph is required in the calculation of unknown sample concentration /ORI78/

$$c_{\text{unknown}} = (p \cdot c_{\text{standard}}) \cdot \{ [1 - (1+p) \cdot 10^{\Delta E \cdot S^{-1}}] \} \quad (\text{III.4})$$

where  $p$  is the ratio of standard volume to sample volume.

The amount of standard added should be sufficient to produce a high value of  $\Delta E$ , typically in the 10 to 30 mV range, so that the error in the potential measurement is kept small. However, a basic assumption in the known addition method is that the activity coefficient is independent of sample dilution and / or salt concentration. This necessitates small additions of high concentration aqueous standards. Since the initial electrode potential in a known volume of sample solution is measured prior to the addition of a known volume of standard solution, the standard addition method effectively incorporates the standard calibration method. Drawbacks of the various spiking methods are that the concentration of the sample solution must be known in advance to within an order of magnitude, and the amount of sample and standard used in the analysis must be volumetrically determined.

Only very accurate fluoride measurements require more elaborate procedures like a lanthanum nitrate titration in which the fluoride electrode is used as an end point detector. Gran's plot and titrimetric techniques are seldom used in routine analytical applications because they are very time-consuming procedures.

### 3.2 Factors influencing fluoride ion determination

As with all electronic sensors, measurements with the fluoride sensitive electrode are affected by parameters such as temperature fluctuations, drift, variations in illumination and noise. The most important factors limiting reproducibility are briefly discussed below.

#### 3.2.1 Electrode performance

Most of the electrodes based on inorganic salts will perform reliably for two to three years if used carefully. Principally there should be no difficulty in achieving stability and reproducibility to within  $\pm 0.1$  to  $\pm 0.2$  mV. While the slope usually remains constant and close to Nernstian response, slight day to day variations of the calibration curve intercepts make it impossible to use one reference curve over an extended period of time. Interfacial changes give rise to a

drift in standard potential of several millivolts per month and dissolution of part of the membrane surface eventually produces pitting. Often, partially destroyed electrodes can be restored by regenerating the  $\text{LaF}_3$  crystal surface with fine polishing powder (e.g. diamond paste). The most frequent cause of electrode failure is the loss of internal contact due to evaporation or leakage of the internal solution /BIX84/. In normal operation, daily standardization of the equipment at one concentration permits the investigator to monitor electrode performance. With calibration every hour, highly reproducible direct concentration measurements can be achieved.

### 3.2.2 Temperature

For maximum precision, samples and standards must be at the same temperature. Fluctuations in ambient temperature should be kept at a minimum, as a one degree difference at the  $20 \text{ mg l}^{-1}$  level will give rise to about 2% measurement error /ORI77/.

### 3.2.3 Response time

In general, electrode response to a change in fluoride ion activity is rapid. Whereas almost instantaneous equilibrium is achieved in  $20 \text{ mg l}^{-1}$  ( $10^{-3} \text{ M}$ ) fluoride solutions, in more dilute solutions stable

Table III.1. Electrode response as function of fluoride concentration.

	fluoride concentration		response time	reference	
	[M]	[ $\text{mg l}^{-1}$ ]			
	$10^{-3}$	20	instantaneous	/WIL79/	
	$10^{-4}$	2	< 10 min	/RAB67/	
	$10^{-5}$	0.2	~ 3 min	/WIL79/	
	$10^{-5}$	0.2	< 15 min	/WAR69/	
	$10^{-5}$	0.2	~ 20 min	/BOC68/	
	$10^{-6}$	0.02	~ 60 min	/BOC68/	
	$10^{-7}$	0.002	several hours	/WAR69/	



potential readings are obtained somewhat more slowly (table III.1). Deviations from the actual concentrations are, therefore, largely due to slow electrode response /ERD75/.

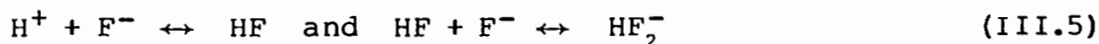
### 3.2.4 Stirring

Stirring of samples and standards during measurement is another important factor influencing potential readings. At high concentrations, stirring has been found to have little or no effect /SRI68/. At lower concentrations, potential readings are noticeably affected. On the one hand, stirring can extend the lower limit of theoretical response by minimizing the accumulation of fluoride ions at the surface of the  $\text{LaF}_3$  crystal /LIN68/. These ions arise from the finite solubility of the fluoride sensing membrane in solutions of low fluoride concentration. On the other hand, stirring causes heating of the sample solution giving rise to different E values as can be seen from equation III.1 /RAB67/.

### 3.2.5 pH

In aqueous solutions the response of the fluoride sensitive electrode is a function of  $\text{H}^+$  concentration.

At low pH values, fluoride activity is affected by the formation of hydrogen-fluoride complexes (equation III.5). According to Srinivasan et al. /SRI68/ only the following equilibria exist in acidic solutions of fluoride



The species HF and  $\text{HF}_2^-$  diminish the activity of free fluoride ion with decreasing pH. At pH 5, the dominant species are  $\text{H}^+$  and  $\text{F}^-$  /SRI68/ thus requiring pH adjustment to above this value for true fluoride concentration measurements.

On the other hand, at high pH values there is direct interference

of the  $\text{OH}^-$  ion because it is isoelectronic with  $\text{F}^-$ . Hence although the pH must be greater than 5 to avoid the effect shown in equation III.5, it must be remembered that interference of  $\text{OH}^-$  ion imposes an upper limit on pH which in turn is dependent on the fluoride concentration. (This effect is discussed in detail in 3.2.6).

For very dilute solutions pH 5 to 6 is therefore the optimal working range for the electrode, although this can be extended to higher and lower pH values with higher concentration samples.

### 3.2.6 Interferences

Some care must be exercised in using an ion-selective electrode to ensure that interferences do not arise from other ions. In the case of the fluoride sensitive electrode, the only significant interference comes from the hydroxide ion due to  $\text{OH}^-$  being isoelectronic with fluoride. Significant hydroxide interference occurs even when  $c_{\text{OH}^-}$  is approximately equal to the concentration of fluoride. When there is a ten-fold excess of hydroxide the apparent fluoride content will be double the true value /FRA66/. With  $10^{-6}$  M ( $0.02 \text{ mg l}^{-1}$ ) fluoride the pH must therefore not be higher than 8. At too high a pH, a layer of  $\text{La}(\text{OH})_3$ , which has approximately the same solubility as  $\text{LaF}_3$ , can be formed and completely passivate the sensing membrane /MUE77/.

Other common anions such as  $\text{Cl}^-$ ,  $\text{Br}^-$ ,  $\text{I}^-$ ,  $\text{SO}_4^{2-}$ ,  $\text{HCO}_3^-$ ,  $\text{NO}_3^-$ , phosphate and acetate are said not to interfere or to have only little effect on the mV output of the electrode /ORI77, LIN67, HAR69/ and can be virtually ignored. However, excess of extraneous compounds capable of binding lanthanum ions - like citrate, phosphate and hydrogencarbonate - have been found to extend response time considerably /MUE77/ while the use of an acid pH has been reported as being necessary to prevent phosphate interference at fluoride levels below  $10^{-5}$  M /MCC68/.

Most cations do not interfere, unless they form unionized or insoluble fluorides /NEE70/. Aluminium presents a significant interference due to complexation of fluoride to  $\text{AlF}_6^{3-}$  /HAR69/. Other polyvalent cations (e.g.  $\text{Fe}^{3+}$ ,  $\text{Th}^{4+}$ ,  $\text{Si}^{4+}$ ) also complex fluoride and it

becomes necessary to precomplex these ions with a chelating agent (e.g. EDTA, CDTA, citrate) or phosphoric acid /BAU68/. Moreover, presence of the silicate ion can lead to irreversible fluoride adsorption when dealing with low concentration fluoride solutions /MUE77/.

### 3.2.7 Ionic strength

While it is the fluoride concentration that is of interest, the electrode responds to the fluoride activity. Activity  $a_F$  and concentration  $c_F$  are related by the equation

$$a_F = \gamma \cdot c_F \quad (\text{III.6})$$

where  $\gamma$  is the activity coefficient.

The activity coefficient is not constant, but varies with the total ionic strength of the sample. The difference in emf between aqueous standards and standards prepared in high salt concentration solutions yields an activity correction factor, which represents the sum of contributions due to change of both activity coefficient and liquid junction potentials with the total ionic strength. If, for example, a salt in high concentration is added to a NaF solution, the potential is shifted by a large margin, but a further increase in salt concentration does not shift the potential appreciably. Hence, once determined, the activity correction factor does not change considerably when transferring to solutions of very different composition /WAR69/. The displacement of the calibration curve is dependent on the magnitude of change in ionic strength. Whereas the addition of citrate, acetate, glucose, urea, and  $H_2O_2$  shift the graph only slightly, the addition of salts like NaCl or  $MgSO_4$  naturally produces a bigger change. In all cases, however, the slope remains constant and only changes in the intercept values occur /BOC68/. The effect of ionic strength in unknown samples can therefore be compensated for by matching ionic concentration of test samples and standards /BAR68/, e.g. by diluting both with isotonic saline /SIN69/.

### 3.3 Equipment and procedure

#### 3.3.1 Electrode

An Orion 94 series single electrode together with a 90 series sleeve type Ag / AgCl reference electrode were employed in this study. Cell potential was measured with a microprocessor-controlled model 901 ionalyzer (Orion), which incorporates programmes for calculating sample concentration from a set of input data such as electrode potentials, slope, standard concentration and blank correction (where applicable) /ORI79/. Zero point drift of the 901 ionalyzer was established to be 0.8 mV during warming up procedures.

#### 3.3.2 Standards

Standard solutions in the range 0.01 to 1000 mg l<sup>-1</sup> were prepared by serial dilution from sodium fluoride (Merck, AR grade) dissolved in dd water. The powdered NaF was preheated at 130°C for 24 hours so as to remove any traces of water vapour and thus render a more precise mass determination in the preparation of the most concentrated standard. Comparison of a 100 mg l<sup>-1</sup> sodium fluoride standard with a 100 mg l<sup>-1</sup> standard supplied by Orion yielded cell potentials of -182.1 and -181.4 mV for the first reference electrode employed and -104.9 and -103.3 mV for the second, respectively.

#### 3.3.3 Sample preparation

From dissolution experiments for ICP-AES analysis (see chapter II) it was established that a mixture of nitric and perchloric acids is the only solution able to break down the complex structure of various mineral compounds intermingled with organic matter, as exists in urinary calculi. Accordingly, 10 to 200 mg aliquots of powdered stone fragments and artificial stone salt mixtures were weighed to 0.1 mg, transferred to small teflon beakers, and concentrated nitric acid (Merck, 70%, AR grade) followed by perchloric acid (Merck, 60-62%, AR grade) were added dropwise to the beakers which were heated on a hot-plate. Dissolved solids were diluted with water, pH adjusted to between

5 and 6 with drops of 10 M and 1 M NaOH prepared from caustic soda pellets (Merck, AR grade) and then quantitatively transferred to a 5 ml volumetric flask. After diluting to volume with dd water the solutions were immediately transferred to a polypropylene beaker and allowed to come to ambient temperature ( $27^{\circ}\text{C} \pm 1^{\circ}\text{C}$ ). In this way, contact time with the glassware was kept at a minimum. During measurement, samples were stirred and fluoride concentration was determined by either the direct technique or the standard addition procedure. An aliquot of "total ionic strength adjustment buffer" (TISAB) was added to some of the samples prior to fluoride determination. To prevent solution carry-over, electrodes were rinsed and blotted dry with clean, dry tissues between measurements.

### 3.4 Calibration

In a study involving the quantitative analysis of calcium-containing urinary calculi /HOD69/ a mean fluoride concentration of 0.14% (w/w) with a range from 0 [sic!] to 0.3% (w/w) was reported. Assuming an available stone mass of 20 mg and a final volume of 5 ml, a mean fluoride concentration of ca. 2 to 3  $\text{mg l}^{-1}$  could thus be expected in the present study. To allow for widely differing sample masses and fluoride concentrations, the electrodes were consequently calibrated from 0.01 to 100  $\text{mg l}^{-1}$  fluoride concentration. Figure III.1 shows the calibration curves obtained for aqueous sodium fluoride standards using two different reference electrodes at two different temperatures, while table III.2 lists the calibration line parameters for each curve as obtained from linear regression analysis. Each data point is the mean of three determinations. No stable readings could be obtained with the first reference electrode (curve 1) which was found to be leaking at an unacceptable rate, thereby diluting samples with 3 M KCl internal electrolyte and effecting an appreciable change in ionic strength. Attempts to restore the electrode were to no avail and a new reference electrode was employed (curve 2). This first showed a wide spread of mV readings around the mean calibration line, but after conditioning the assembly in a standard NaF solution and changing the internal electrolyte, overall electrode performance was vastly improved (curve 3).

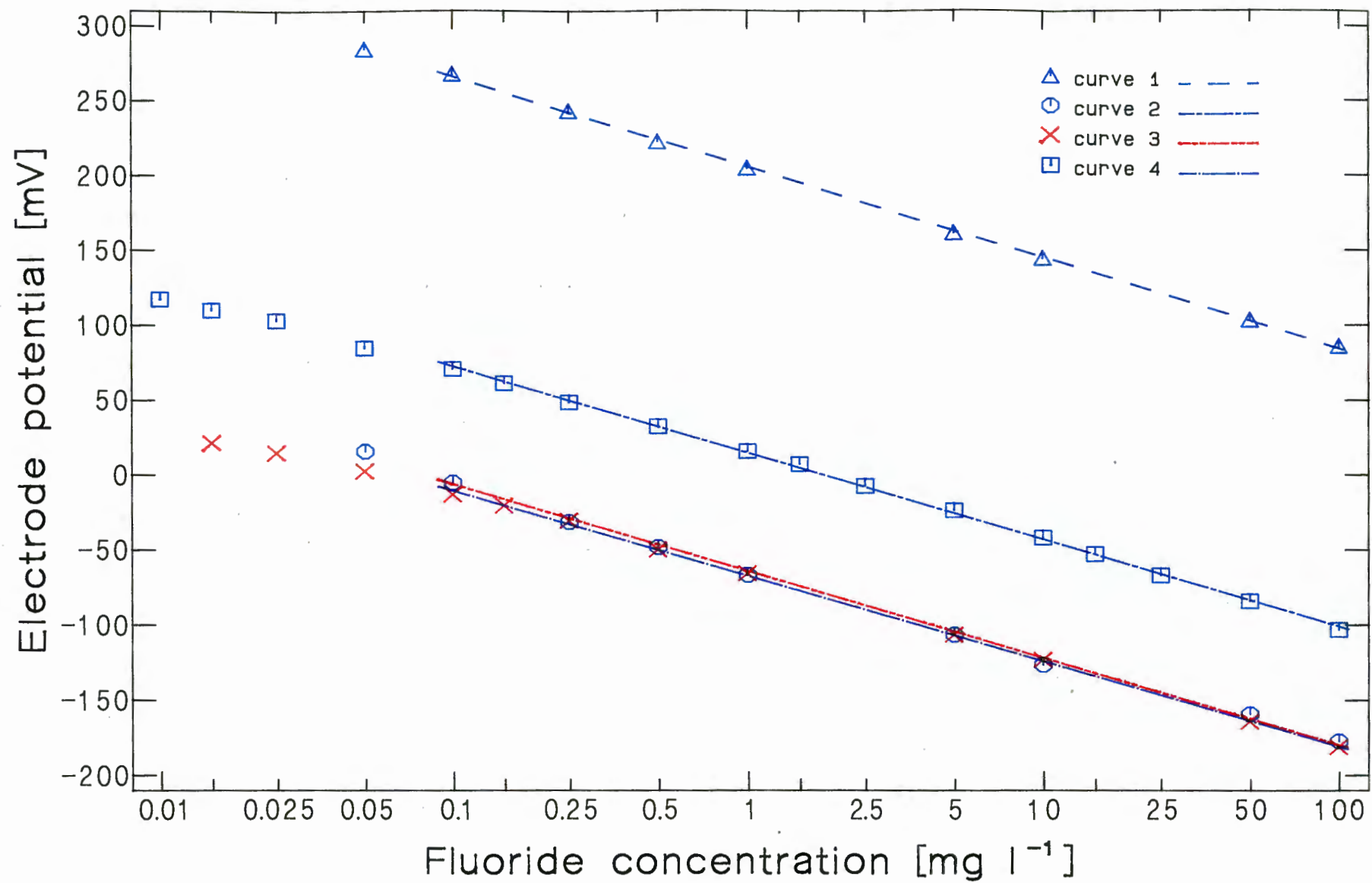


Figure III.1. Calibration of electrode assembly in aqueous (dd water) sodium fluoride standards (cf. table III.2).

Table III.2. Calibration line parameters from linear regression analysis:  $E = E_0 + S \cdot \lg(c_F)$  #.

figure III.1*	$E_0$	$S$ &	$r^2$	data points used for fit
curve 1	205.50	-60.42	0.9997	all points $\geq 0.1 \text{ mg l}^{-1}$
curve 2	-64.34	-57.85	0.9980	all points $\geq 0.1 \text{ mg l}^{-1}$
curve 3	-67.42	-56.74	0.9995	all points $\geq 0.1 \text{ mg l}^{-1}$
curve 4	12.82	-55.52	0.9980	all points $\geq 0.01 \text{ mg l}^{-1}$
curve 4	14.72	-57.82	0.9993	all points $\geq 0.1 \text{ mg l}^{-1}$
curve 4	16.86	-59.64	0.9996	all points $\geq 1.0 \text{ mg l}^{-1}$

#  $E$  relative potential reading [mV]  
 $E_0$  relative potential reading [mV] at  $c_F = 1.0 \text{ [mg l}^{-1}]$   
 $S$  electrode slope [mV]  
 $c_F$  fluoride concentration (activity) [ $\text{mg l}^{-1}$ ]  
 $r^2$  coefficient of determination

\* curve 1 reference electrode 1,  $T = 27^\circ\text{C}$   
 curve 2 reference electrode 2,  $T = 27^\circ\text{C}$ , after unpacking  
 curve 3 reference electrode 2,  $T = 20^\circ\text{C}$ , preconditioned  
 curve 4 reference electrode 2,  $T = 27^\circ\text{C}$ , after 11 months in use  
 ( $T = \pm 1^\circ$ , each point mean of 3 determinations)

& theoretical slope for  $T = 20^\circ\text{C}$  is  $-58.17 \text{ mV}$  ( $-59.56 \text{ mV}$  for  $T = 27^\circ\text{C}$ );  
 $1^\circ \approx 0.2 \text{ mV}$ .

Performance of the electrode was at first sluggish but was improved by periodic polishing of the sensing crystal with fine ( $0.3 \mu\text{m}$ ) corundum powder (BDH).

From table III.2 it can be seen that despite slight deviations a coefficient of determination ( $r^2$ ) very close to 1.0 is obtained from linear regression analysis for all curves, thus confirming the straight line behaviour of the fluoride sensing crystal. It can be further seen that when all data points for fluoride standards of concentration  $1 \text{ mg l}^{-1}$  are taken into account, the measured slope for the electrode assembly employing reference electrode 2 (curve 4) shows excellent agreement with the theoretically expected value of  $59.56 \text{ mV}$ .

The drift in  $E_0$  from -67.42 to 14.72 mV (table III.2), i.e. approximately 80 mV over a period of 11 months is equivalent to a daily change of ca. 0.24 mV. This variation, probably due to interfacial changes, again emphasizes the necessity of at least weekly calibration of the measuring equipment and a daily check of the electrode slope. This rule was observed in the present study by standardizing with 1 mg l<sup>-1</sup> and 100 mg l<sup>-1</sup> calibration samples each day before commencing measurements of unknown samples. Besides fluctuations in  $E_0$  no changes in other parameters were observed.

### 3.5 Detection limit

The expected mean fluoride concentration of 2 to 3 mg l<sup>-1</sup> (in the samples of the present study) is well above the lower limit of electrode response, posed by the solubility of the LaF<sub>3</sub> membrane. This lower limit is generally accepted to be ca. 10<sup>-6</sup> M (0.02 mg l<sup>-1</sup>) /BAU71/. In aqueous acidic medium, however, it can be extended to 2·10<sup>-7</sup> M /LIN68/. It has also been found that the presence of fluoride ion buffers extends Nernstian response right down to 10<sup>-9.5</sup> M /BAU71, BAI76/. Although these low limits are possible, straight line behaviour of pure aqueous NaF solutions has been found to be confined to the concentration range from above 10<sup>-5</sup> M to below 10<sup>-2</sup> M /BOC68/. Care must therefore be taken in making determinations below about 1 mg l<sup>-1</sup> fluoride to avoid sample contamination. This is illustrated in table III.2 where the inclusion of more and more points at lower concentrations in the linear regression calculation reveals a slight 'bending' of the calibration line at fluoride activities equal to or less than 1 mg l<sup>-1</sup>. Slope values (curve 4, table III.2) decrease from 59.64 (close to the theoretical value of 59.56) to 57.82 and further to 55.52 mV, when all data points equal to and greater than 1.0, 0.1, and 0.01 mg l<sup>-1</sup> are respectively accepted. When only those data points in the range 0.01 to 1 mg l<sup>-1</sup> are considered, a slope of merely 51.18 mV is obtained. This represents a deviation of 15% from Nernstian response. Besides contamination, this effect might have also originated as a result of incomplete equilibration as readings in the lowest concentration range were taken after only 45 min although it has been shown that much longer periods might be needed to totally equilibrate the



electrodes (cf. table III.1).

In 'real' samples (as opposed to pure NaF standards) contributions from acids, neutralizing solutions and trace impurities of fluoride in ionic strength buffers interfere and cause deviation from Nernstian behaviour at higher concentration values than those described above for standards. In these cases considerable 'bending' of the calibration line is noted already in the 0.5 to 1.0 mg l<sup>-1</sup> range, and the slope approaches zero at lower concentrations. These factors form a constant background for each measurement and account for the finite lower limit of detection of the fluoride electrode. Thus, when low concentrations approaching the detection limit are to be measured, a blank correction must be applied.

Although a lower limit of detection of 10<sup>-6</sup> M is widely accepted, a most recent report on interlaboratory variability in trace element analysis /BOY85/ showed that almost all of the scrutinized studies, representing a wide variety of analytes, matrices and measurement techniques, were distributed about a curve defined by the equation

$$\%RSD_x = 2^{1-0.5 \cdot \lg C} \quad (\text{III.7})$$

%RSD	relative standard deviation among laboratories
RSD <sub>x</sub>	ca. 3 times RSD <sub>0</sub> (within laboratory RSD)
C	concentration (from 100 mg g <sup>-1</sup> to 10 ng g <sup>-1</sup> ).

Fluoride determination by the ion-selective electrode method, however, behaved differently /BOY85/. The values for RSD<sub>x</sub> are distributed about the curve down to a particular point but then depart radically therefrom with a further decrease in concentration. It appears that there is thus a fundamental limit associated with this measurement technique which is found to be in the 30 mg l<sup>-1</sup> region. A second study /SHR82/ found this method "imprecise" with food samples containing less than 10 mg l<sup>-1</sup> fluoride. Comparison of results from a nuclear technique /HAN84/ with values obtained by use of chemical methods showed good agreement down to the 30 mg l<sup>-1</sup> region, but showed deviations below that level. These concentrations are about 30 times above the commonly accepted limit of 10<sup>-6</sup> M, a result, that still awaits further explana-

tion. To clarify this situation it will be necessary to develop suitable, accurate and reliable standard samples in the  $\text{mg l}^{-1}$  region and to conduct an extensive set of interlaboratory round-robin tests.

### 3.6 Total ionic strength adjustment buffers (TISABs)

The difficulty in applying the fluoride electrode approach to different samples is that the electrode responds to fluoride ion activity, not concentration. Thus, after digestion, the resulting acidic solutions require further treatment to minimize ionic strength differences between separate samples and to prevent other ions from interfering with fluoride determination. Fixed activity values, constant ionic strength and the presence of substances which decompose stable fluorocomplexes are required to obtain reproducible potential measurements /TUS70/. These effects are virtually eliminated by dilution of both standards and samples with an ionic strength and / or pH adjustor. This solution simultaneously performs three functions /FRA68/: (i) it swamps out differences in and fixes sample ionic strength by adding a much larger level of ions than normally found; (ii) the solution is buffered in the optimum pH range for measurement, i.e. avoiding hydroxide interference; (iii) it provides a chelating agent which preferentially complexes  $\text{Fe}^{3+}$  and  $\text{Al}^{3+}$  ions, thereby breaking up those complexes that fluoride forms with such ions by displacing bound fluoride. The TISAB approach makes possible direct concentration readings for low levels of fluoride in a wide range of aqueous systems. Table III.3 details the composition of a variety of TISABs used by different investigators, covering very different sample systems.

In the case of urinary calculi, strong acids are needed to decompose the complex mixture of inorganic and organic compounds present in the sample. The obtained acidic solution again is in need of pH adjustment with an alkaline additive. Different ionic composition as found in uric acid and apatite stones, for example, invariably requires dilution with one of the many ionic strength buffers. Accordingly, various buffers and ionic strength adjusters were investigated. Figure III.2 and table III.4 show the effect of these factors on the calibration curve. Note that nominal values of standards are used in calibrating

Table III.3. Total ionic strength adjustment buffers (TISABs) employed in fluoride determination in different materials.

sample(s)	decomposition procedure(s)	TISAB	references
mineralized tissue dental plaque, teeth, enamel, bones	HClO <sub>4</sub> fusion (Li hydroxide & Mg succinate) ashing, HCl	sodium citrate  sodium acetate NaOH	/BAR68/ /BRU68/ /GRO69/ /MCC68/ /SIN68/
phosphate rock, phosphate feed materials	HCl HClO <sub>4</sub> fusion (Na hydroxide)	sodium citrate citrate + NaOH citrate/NaOH + EDTA, TISAB <sup>1</sup> citrate/HClO <sub>4</sub>	/EDM69/ /EVA70/ /LOO68/ /TUS70a/
urine	HCl none	NaOH/isotonic saline, acetate NaOH/citrate/ acetic acid TISAB <sup>1</sup> TISAB <sup>3</sup> TISAB <sup>4</sup>	/BAR68/ /CER70/ /COL71/ /NEE70/ /SIN69/ /SUN69/ /TUS70/ /TUS72/
water supplies	n/a	TISAB <sup>1</sup> TISAB <sup>2</sup> TISAB <sup>3</sup>	/ERD75/ /FRA68/ /HAR69/

<sup>1)</sup> to approximately 500 ml H<sub>2</sub>O add 57 ml AR grade glacial acetic acid, 58 g AR grade NaCl, 0.3 g sodium citrate; adjust to pH 5.0 to 5.5 using AR 5 M NaOH, cool and dilute to 1 litre.

<sup>2)</sup> as <sup>1)</sup>, except sodium citrate replaced by 1 g EDTA (Merck, Titriplex III).

<sup>3)</sup> as <sup>1)</sup>, except sodium citrate replaced by 1 g CDTA (Merck, Titriplex IV).

<sup>4)</sup> as <sup>1)</sup>, except NaCl replaced by sodium nitrate.

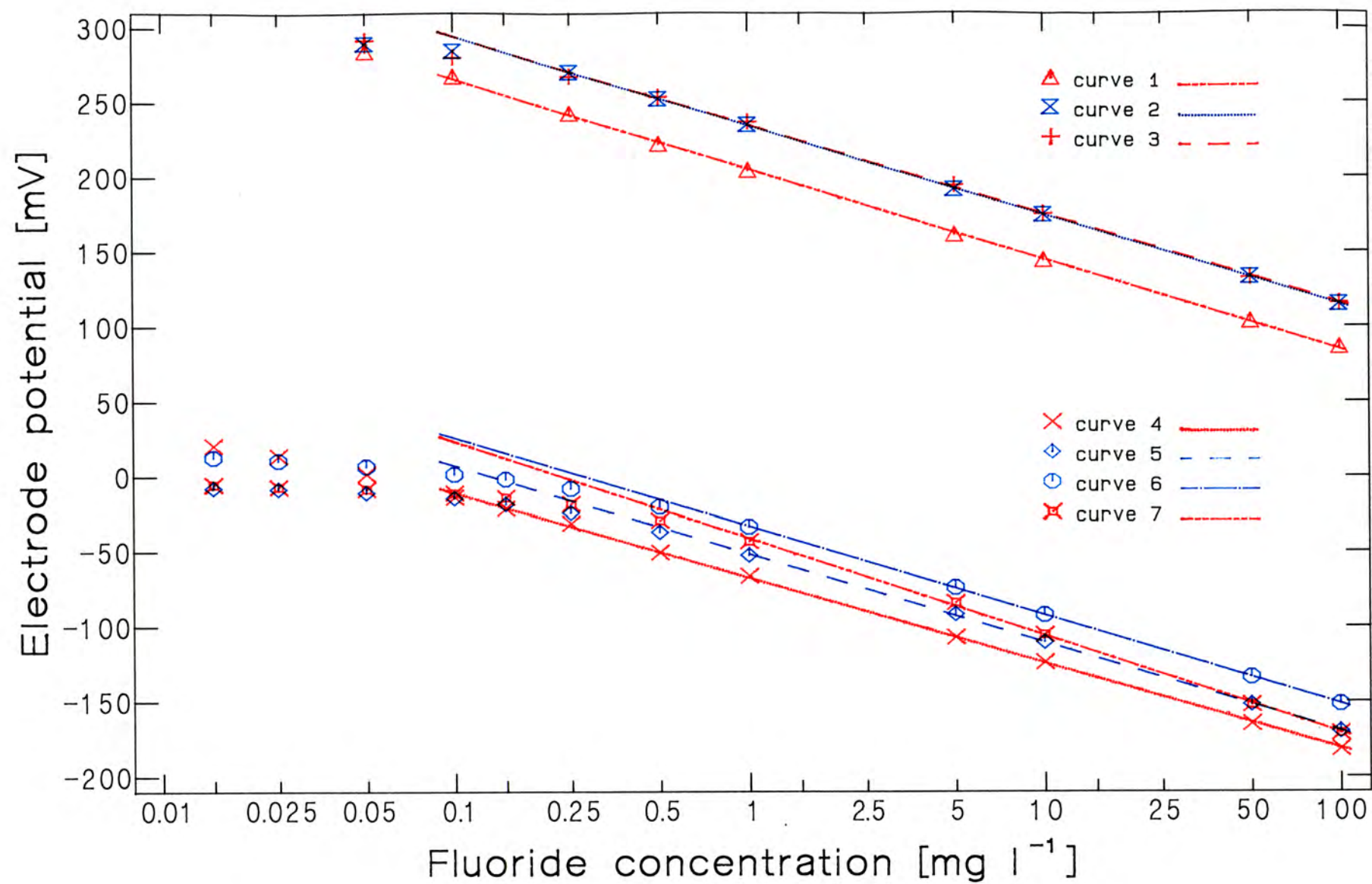


Figure III.2. Influence of ionic strength buffers on standard calibration curves (cf. table III.4).

Table III.4. Calibration line parameters from linear regression analysis (cf. table III.2).

figure III.2	$E_0$	S	$r^2$	data points used for fit
curve 1	204.99	-59.98	0.9996	all points $\geq 0.25 \text{ mg l}^{-1}$
curve 2	234.49	-59.84	1.0000	all points $\geq 0.25 \text{ mg l}^{-1}$
curve 3	234.95	-59.53	0.9991	all points $\geq 0.25 \text{ mg l}^{-1}$
curve 4	-66.15	-57.76	0.9999	all points $\geq 1.0 \text{ mg l}^{-1}$
curve 5	-51.60	-58.98	0.9998	all points $\geq 1.0 \text{ mg l}^{-1}$
curve 6	-33.09	-59.20	0.9999	all points $\geq 1.0 \text{ mg l}^{-1}$
curve 7	-41.10	-64.75	0.9990	all points $\geq 1.0 \text{ mg l}^{-1}$

Reference electrode 1 ( $T=27^\circ\text{C}$ )

curve 1 NaF in water (10 ml)

curve 2 solution from curve 1 after addition of TISAB II (Orion) (10 ml); pH 5.3

curve 3 solution from curve 2 after addition of  $\text{HNO}_3$  (0.5 ml, 70%),  $\text{HClO}_4$  (0.5 ml, 60-62%), and NaOH (1 ml, 15 M); pH 5.3 to 5.8

Reference electrode 2 ( $T=20^\circ\text{C}$ )

curve 4 NaF in water (10 ml)

curve 5 NaF in water (10 ml) after addition of TISAB III (Orion) (1 ml); pH 4.9

curve 6 NaF in water (10 ml) after addition of TISAB II (Orion) (10 ml); pH 5.3

curve 7 citrate buffer (0.5 ml 1 M  $\text{HNO}_3$  (prepared from BDH, Aristar), 0.5 ml 1 M  $\text{HClO}_4$  (prepared from BDH, Aristar), 4 ml buffer (28.9 ml 0.2 M citric acid (May & Baker, Pronalys AR) + 9.4 ml 1 M tri-sodium citrate (BDH, AnalAR), made up to 100 ml with dd water)).

the electrode, e.g. if a  $10 \text{ mg l}^{-1}$  standard is diluted with TISAB, the standard is still designated " $10 \text{ mg l}^{-1}$ ". This nomenclature was followed in the present study for all except the citrate buffer standards, where the listed values equal the actual concentrations. As can be clearly seen from the least squares analyses (table III.4, curves 1-6) the addition of ionic strength buffers hardly affects slope data. However, abscissae ( $E_0$ ) are strongly affected as can be seen by comparison of curves 1 and 2, or curves 4 and 5, or curves 4 and 6. This is partially due to the dilution effect, but mainly due to fixing of the

ionic strength at a high value. Additional contributions of strong acids and high molarity alkaline solutions do not alter the calibration curve further (cf. curve 2 and curve 3).

In all TISAB cases the linearity of the curve is limited to concentrations greater than 0.25 or 1 mg l<sup>-1</sup> (for the two reference electrodes, respectively), owing to dilution and contamination effects. In order to establish the source of the fluoride contamination, blank tests were carried out on all reagents. The dd water yielded a F<sup>-</sup> concentration of less than 0.02 mg l<sup>-1</sup>. Analytical reagent grade acids and NaOH were found to have an inherent fluoride concentration of only 0.15 mg l<sup>-1</sup>. In addition NaOH has been found to be F<sup>-</sup> free /SEK73/. Thus, although Warner /WAR69/ found only 6·10<sup>-7</sup> M (0.01 mg l<sup>-1</sup>) intrinsic fluoride in commercial TISAB (Orion), it would appear that the TISAB solution used in this study was the main contaminator. Since the amount of fluoride in some samples was expected to be near this limit, acids with very low fluoride concentrations (spectroscopic grade) were employed (BDH, Aristar HNO<sub>3</sub>, 69-71%; BDH, Aristar HClO<sub>4</sub>, 72%).

Since the total ionic strength of the adjusted samples and standards varies according to the original solution pH, Orion Research /ORI77/ has discouraged the use of a strong base, such as NaOH, for pH adjustment of acidic solutions. For this reason the effectiveness of a sodium citrate buffer /PER79/ was investigated in the present study. When standardizing the electrodes in these standards, both a calibration slope exceeding the theoretical value and a remarkable shift in the lower limit of detection was observed. Electrode response also became very sluggish and equilibrium readings were obtained only after 15 min, even for standards with very high fluoride concentrations. Another powerful buffer system, based on acetate, was not examined, as acetate ions have been reported to enter the LaF<sub>3</sub> crystal of the membrane electrode /ANF69/. Carboxylate ions are incorporated in the LaF lattice, either in the bulk of the crystal or on its surface, forming complexes of the type [LaF<sub>(3-x)</sub> Ac<sub>x</sub>] /ANF70/. Such an ion exchange will continuously shift the E<sub>0</sub> value and cause sluggish response and deviation from the Nernstian equation. Other chelating ligands, such as lactate, malonate and, as shown in the present study, citrate affected the LaF<sub>3</sub> membrane. It was thus concluded that carboxyl buffers

are unsuitable for all work involving the  $\text{LaF}_3$  electrode /WIL79/.

### 3.7 Conclusions

Contrary to an expected mean fluoride concentration of 2 to 3 mg  $\text{l}^{-1}$  all stone test solutions yielded much lower fluoride values in preliminary investigations using the direct method. In many cases activities determined were near the background concentration. An explanation could be that even with the application of TISABs, the high concentration of  $\text{Ca}^{2+}$ ,  $\text{Mg}^{2+}$  and phosphate in struvite and apatite calculi impedes the direct determination of fluoride in stone solutions. This is substantiated by Singer et al. /SIN68/ who found that up to 20 mM phosphate per litre had no effect on the mV output of the electrode, but that concentrations appreciably greater than 7 to 11 mM Ca per litre 0.3 to 0.4 mM Mg per litre produced measurable errors in the results for fluoride contents. Therefore the high  $\text{Mg}^{2+}$  and  $\text{Ca}^{2+}$  concentrations usually occurring in urinary calculi preclude the application of direct  $\text{F}^-$  determinations. Indeed, no report of any attempt to measure fluoride directly in solutions of digested urinary stones was found in the literature.

As the analysis tends to become more reproducible at higher fluoride ion concentrations /HAL76/, increased sensitivity of the method can only be achieved by reducing the volume in which the stone is dissolved /DUR68/. While in normal operation, measurements can be obtained in 1 - 2 ml solutions, as little as 50  $\mu\text{l}$  samples have been employed /DUR67/. However, too high a concentration can cause calcium phosphate precipitation, which may result in co-precipitation of fluoride.

Besides the problems described above, open tube digestion of calculi can result in fluoride being lost in the form of gaseous HF. It was therefore concluded that too many stumbling-blocks impede the direct measurement of fluoride concentration in digested stone samples for it to be regarded as a feasible method. Instead, separation of the fluoride ion from its mother solution must be accomplished before a

successful determination can be achieved.

#### 4. Diffusion method

Separation from other ions is a necessary first step in the determination of fluoride in most types of samples. This can be accomplished either by steam distillation of HF or diffusion procedures. From aqueous acidic solutions, fluoride can also be selectively extracted by many organic solvents in the form of reaction products of fluoride with Si-organic compounds (e.g. triethylsilanol) /BOC66/. This process is rather slow, but its rate can be increased in solutions of high acidity /BOC67/.

In the diffusion method the sample is acidified with a suitable acid, whereby volatile HF is formed. The gaseous HF is then trapped in an alkaline solution. Very different designs of diffusion vessels have been used during the last 20 years /TUS69/. In the technique of micro-diffusion, the isolation, concentration, and quantitative recovery of fluoride are accomplished using simple inexpensive equipment and a minimum of manual operations: volatile substances are separated by diffusion from one compartment to another in a 'diffusion cell', e.g. a simple disposable plastic petri dish /ROW62/, the orthodox circular Conway unit, or a primitive polystopper /BAE64/. The major advance provided by this method is that fluoride can be accurately determined in samples such as urinary calculi, teeth and bone, which contain large amounts of calcium and phosphate and low levels of fluoride /WHA62/.

##### 4.1 Method development and procedure

###### 4.1.1 Apparatus

In this study tests were conducted with nested polypropylene centrifuge tubes sealed with a nylon plug. However, the nylon desintegrated at elevated temperatures when exposed to the combined attack of nitric and perchloric acids. Subsequently, diffusion cells were manu-



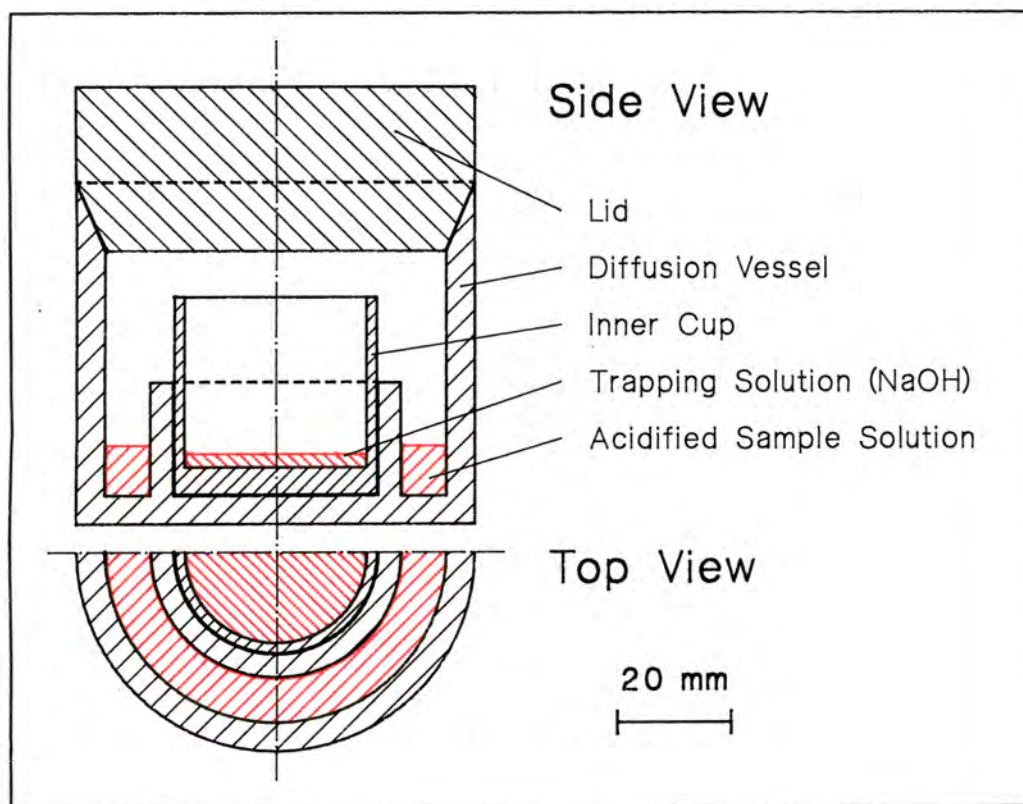


Figure III.3. Diffusion vessel.

factured from polypropylene rods according to the design in figure III.3. According to Conway /CON63/, Berka /BER59/ employed a microdiffusion unit (having a similar design to the one used in the present study) with a special modification for withstanding higher temperatures. The only constraint on the size of the assembly for the present study was imposed by the respective diameters of reference and fluoride electrodes, both of which had to be accommodated in the removable inner container. Except for a faint decolourization, no visible damage to the diffusion vessels was observed, even when samples were digested at temperatures up to 95°C.

#### 4.1.2 Reagents

Acids used were prepared from  $\text{HNO}_3$  (70%) and  $\text{HClO}_4$  (72%) (both BDH, Aristar). Various concentrations were tested and finally 5 M solutions were deemed to yield the best recovery. Acids were impreg-

nated with silicone by shaking 1:1 (v/v) mixtures of 5 M stock solutions with one tenth of their volume of either hexamethyldisiloxane (HMDS, Ega-Chemie) or 1 cSt 200 Fluid (Dow Corning [bulletins 22-069F-01 and 22-507B-01]) for 5 min. The supernatant was discarded and the acid solution was saturated by shaking with the same amount of the relevant Si-organic liquid for a further 5 min. About 50 ml of the mixture was prepared for each experiment.

After checking fluoride contamination in different batches of NaOH pellets and solutions (e.g. BDH, AR grade; Merck, Titrisol) it was concluded that 1 M NaOH solutions prepared from Merck AR grade NaOH contained the least fluoride and these were used for the trapping solutions.

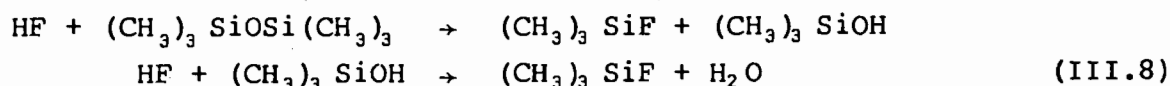
#### 4.1.3 Procedure

As the sample volume in the outer chamber of the diffusion cell is inversely proportional to the absorption rate of fluoride in the trapping solution (NaOH) /CON63/, it was kept as low as possible. Five millilitres of acid mixture was found to be sufficient for digestion of 200 mg sample. Two millilitres of NaOH was found to be adequate to wet the bottom of the inner cup. After pipetting this volume into the inner container, weighed portions of powdered stone fragments were introduced into the outer compartment of the diffusion chamber. HMDS saturated acids were added and the vessel was closed immediately. Steel clamps were used to hold the lids in position. Diffusion was carried out at ca. 75°C for at least 3 to 4 hours but in some cases this was extended to 16 - 24 hours. Solutions were then allowed to cool and pH was adjusted to between 5 and 6 with HNO<sub>3</sub>. Thereafter they were quantitatively transferred to 5 ml volumetric flasks, and diluted to volume with dd water. Solutions were poured back into the inner containers of the diffusion cells, stirred and cell potential was measured with the fluoride electrode as described before. In most cases 0.5 ml of TISAB III (Orion) was added to correct for differences in pH and ionic strength and electrode potential was re-determined. As a third independent procedure, the standard addition method was applied.

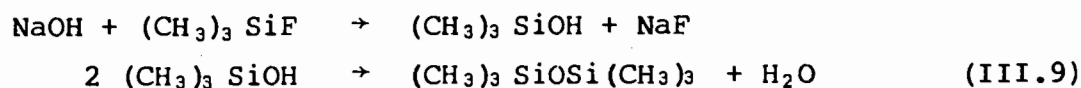
## 4.2 Diffusion parameters

Practical problems associated with the microdiffusion technique include long diffusion times (16 to 24 hours) /BUE63, WEA65/ and the need for an elevated temperature. When perspex vessels are used, a temperature of ca. 60°C is usually considered to be the upper tolerable limit, whereas polypropylene can withstand temperatures up to 120°C and teflon even higher. An increase in temperature considerably shortens the time required for complete diffusion; digestion of samples is also facilitated. Agitation of samples has a pronounced beneficial effect too /SAR75/. Equations, relating various quantities important in calculating a minimal period required for complete diffusion are extremely dependent on the above factors and diffusion cell dimensions. Only for the most simple cases are analytical expressions available /HAN73/.

Petroleum jelly (vaseline) employed as a sealant for the lid of diffusion vessels has been found to dramatically accelerate recovery of fluoride /TAV68/. Based upon this observation as well as the studies of Bock et al. /BOC66, BOC67, BOC73/ it was suggested that methylfluorosilanes rather than hydrogen fluorides were the important gaseous diffusing species under the conditions commonly employed for the diffusion of fluoride /TAV68a/. Viscous silicone fluids, containing mainly the dimethylsilyl group, and HMDS are thus presumed to accelerate the diffusion of fluoride greatly by the formation of hydrophobic fluorosilanes, e.g. trimethylfluorosilane /HAL69, TAV68a/:



In the trapping solution, fluoride is released by hydrolysis of these compounds which in turn is accelerated by reformation of the parent siloxane through condensation of silanol:



Since the reformed HMDS and / or possibly the silanol return to the acid solution and repeat the cycle the whole process becomes catalytic.

No explosive range of concentration ratios exists in the mixture of perchloric acid and HMDS under the conditions indicated /HAL69/, nor were any adverse effects of the silicone present after neutralization of the trapping solution experienced in this study. It should be noted that in those samples with high halogen concentrations, radicals such as chloride will compete with  $F^-$  for the alkali. This could lead to saturation of the trapping solution before all fluoride is collected.

#### 4.3 Recovery, calibration and reproducibility

Recovery tests as a function of time, temperature, and composition were undertaken.

Figure III.4 shows recovery of 0.1 mg fluoride (added as  $100 \text{ mg l}^{-1}$  NaF solution) as a function of diffusion time ( $T=80^\circ\text{C}$ ) for the two different silicone fluids employed. A slightly shorter recovery time is obtained with HMDS, probably due to the immediate availability of more methylfluorosilane groups without the need of prior cracking of the long dimethylsilyl chains. As can be clearly seen, complete diffusion is accomplished in less than 3 hours which is about one tenth of the time needed for the noncatalytic reaction.

Figure III.5 depicts the effect of higher temperatures on the diffusion process. While it is generally accepted that diffusion times are strongly temperature dependent, it can be seen that in the presence of silicone fluids the accelerating effect due to higher temperatures is minimal for total recovery, although initially the %-recovery is greater at elevated temperatures. It was thus arbitrarily decided to conduct all diffusion experiments at  $75^\circ\text{C}$  ( $\pm 3^\circ\text{C}$ ).

Figure III.6 displays calibration graphs. Curve 1 depicts the calibration line obtained by standardizing the electrode assembly in aqueous sodium fluoride standards, according to the procedure described in section 3.3. The 'pure electrode' slope of this curve was subsequently employed in the calculation of fluoride concentrations by the standard addition method, according to equation III.4. Since this curve deviates from linearity at very low fluoride concentrations, a quadra-

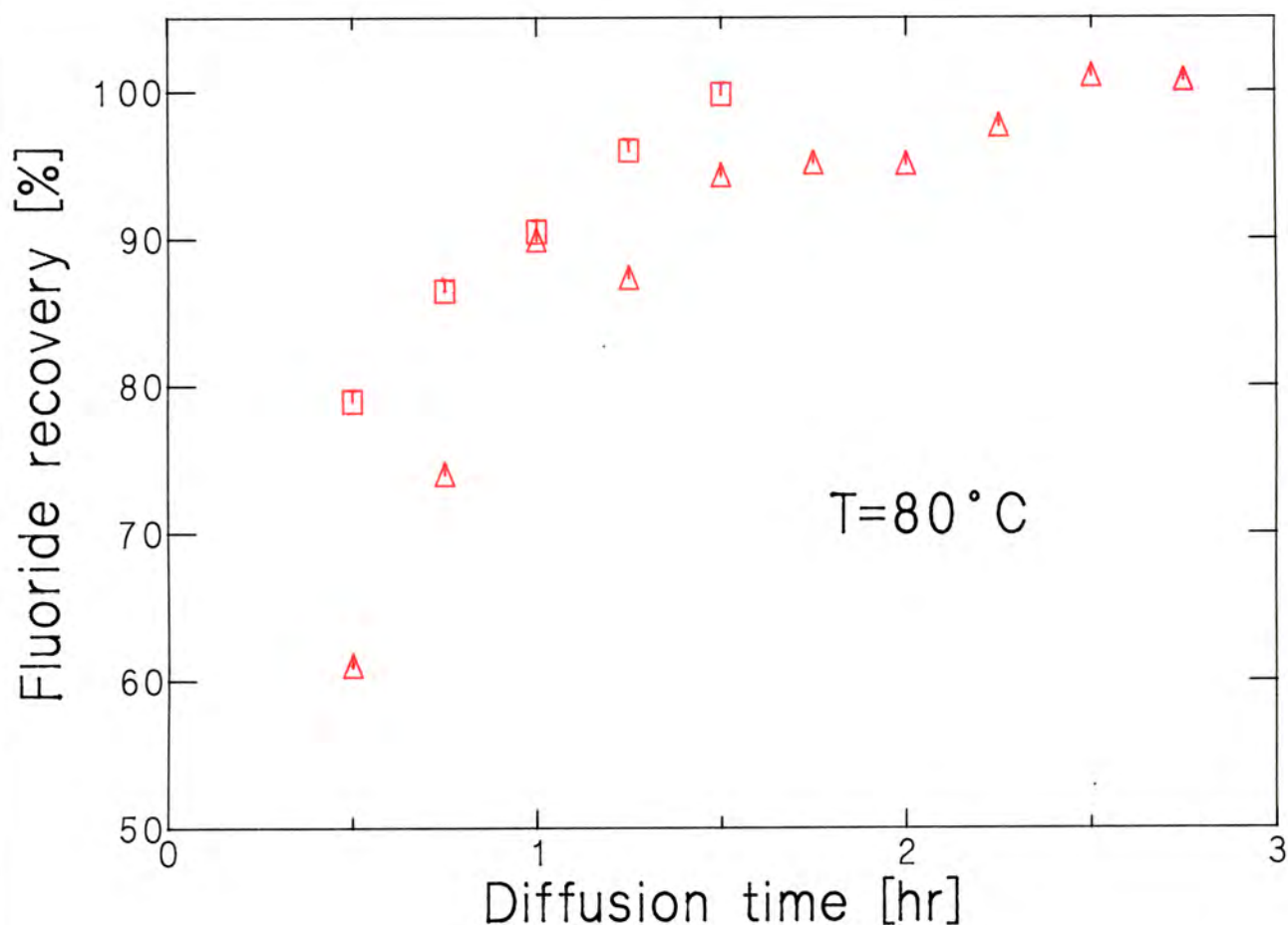


Figure III.4. Recovery of fluoride as a function of diffusion time and silicone fluid employed.

- △ 2 ml NaOH (0.5 M) trapping solution, pH adjusted to 5.5 with  $\text{HNO}_3$ , made up to 10 ml final volume (incl. 0.5 ml TISAB III); digestion with 5 ml  $\text{HNO}_3 + \text{HClO}_4$  (1:1 (v/v), 70%, Aristar), saturated with 1 cSt 200 fluid; addition of 1 ml  $100 \text{ mg l}^{-1}$  aqueous NaF standard (0.1 mg fluoride);
- 2 ml NaOH (0.5 M) trapping solution, pH adjusted to 5.5 with  $\text{HNO}_3$ , made up to 5 ml final volume (incl. 0.5 ml TISAB III); digestion with 4 ml  $\text{HNO}_3 + \text{HClO}_4$  (1:1 (v/v), 70%, Aristar), saturated with HMDS; addition of 1 ml  $100 \text{ mg l}^{-1}$  aqueous NaF standard (0.1 mg fluoride);  
(all points mean of three determinations).

tic expression (table III.5) was fitted to the experimental points /JEN83/, and the slope at the different concentrations was calculated from the derivative. Curve 2 was obtained by subjecting 1 ml of diffe-



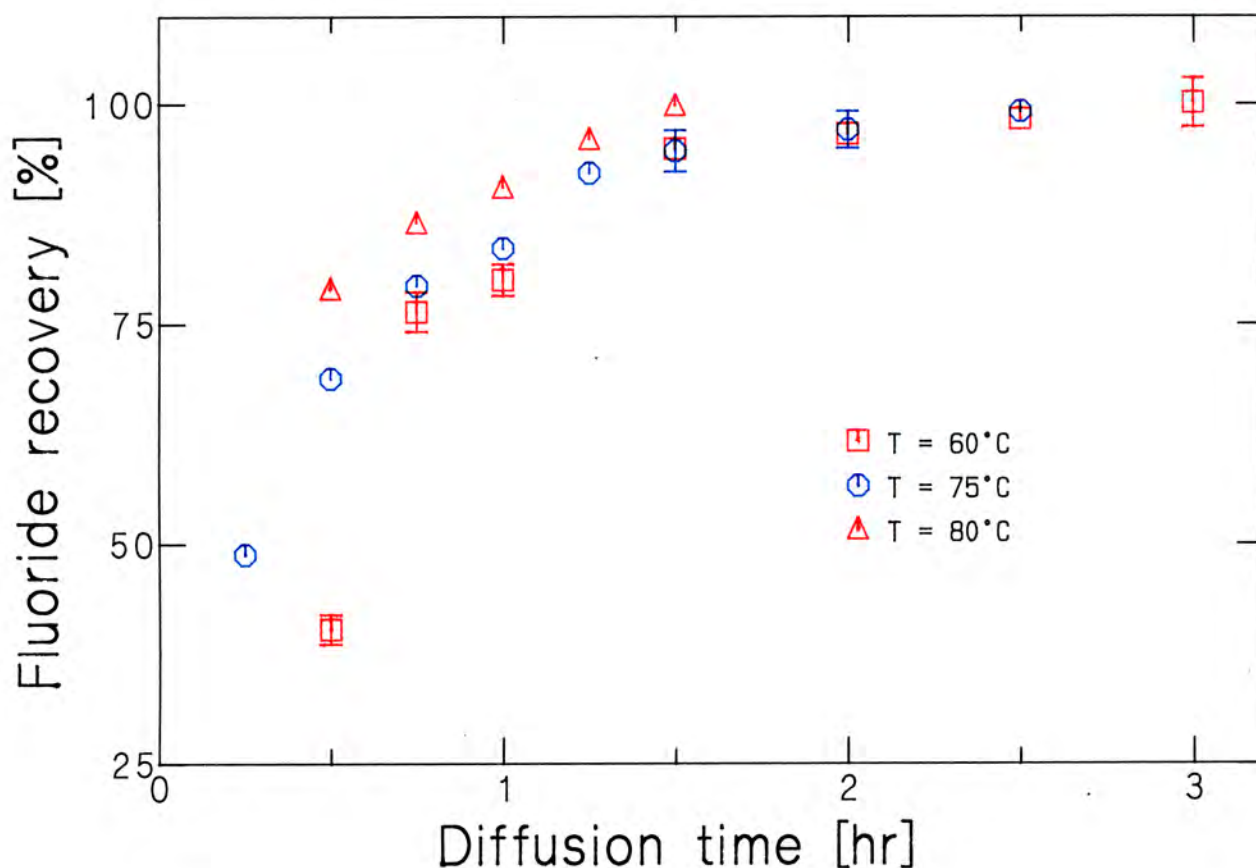


Figure III.5. Recovery of fluoride as a function of diffusion time and temperature.

rent aqueous fluoride standards to the whole diffusion procedure as described in 4.1. Curve 3 represents mV readings obtained after addition of 0.5 ml TISAB III (Orion) to 5 ml of the solutions used for curve 2. In each of the two cases the curve drawn through the experimental points represents a computed third order polynomial, fitted by the least squares method, employing BMDP statistical software /JEN83/. Regression coefficients are given in table III.6. In both cases the contaminating influence of acids and alkaline solutions can be clearly seen. The curves deviate considerably from linearity at lower fluoride concentration values, making an accurate evaluation of unknown samples impossible in this region. A blank concentration value of  $0.27 \text{ mg l}^{-1}$  was derived from these curves. This value was obtained by estimating the electrode potential at which the slopes of curves 2 and 3 tend to zero (approximately 50 mV) and reading the corresponding

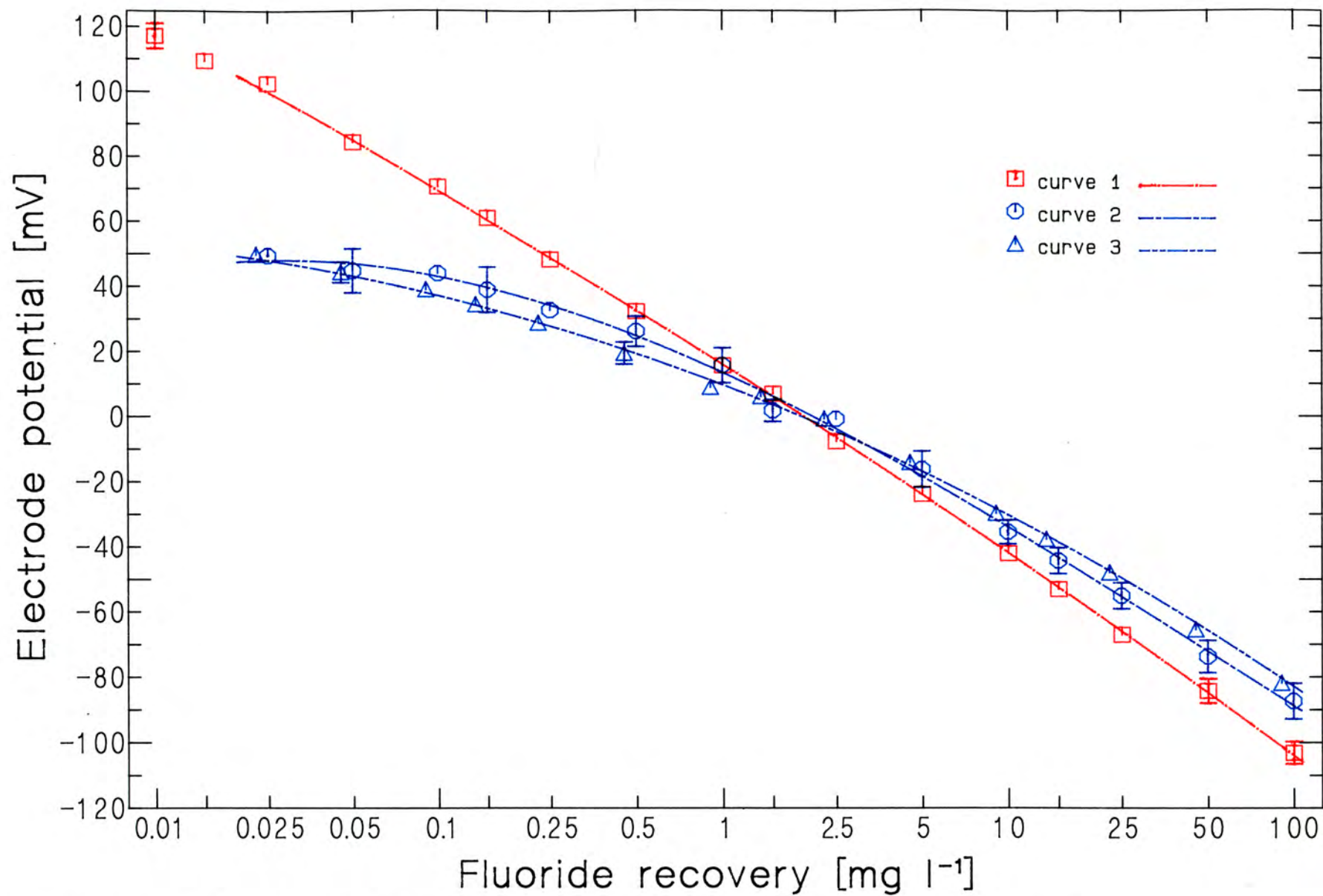


Figure III.6. Calibration of microdiffusion procedure (cf. tables III.5 and III.6).

Table III.5. Regression coefficients for aqueous sodium fluoride standard calibration curve (electrode slope parameters), computed by least squares fit of a second order polynomial in  $\lg(c_F)$  [ $\text{mg l}^{-1}$ ] as independent variable  $x$  and  $E$  [mV] as dependent variable  $y$ :

$$y = a_0 + a_1 x + a_2 x^2 \text{ (figure III.6, curve 1).}$$

$$a_0 = 16.0608$$

$$a_1 = -55.7015$$

$$a_2 = -2.2538$$

Table III.6. Regression coefficients for diffused standard calibration curves (with (figure III.6, curve 3) and without (figure III.6, curve 2) TISAB III addition).

		diffused standards <sup>#</sup>		diffused standards <sup>*</sup>	
		without TISAB	with TISAB	without TISAB	with TISAB
regression coefficients <sup>&amp;</sup>	$a_0$	13.5735	9.7739	0.3885	0.2947
	$a_1$	-40.2272	-33.6749	$-0.2271 \cdot 10^{-1}$	$-0.2735 \cdot 10^{-1}$
	$a_2$	-8.9533	-6.2447	$-0.2034 \cdot 10^{-3}$	$-0.1681 \cdot 10^{-3}$
	$a_3$	1.7462	-0.3203	$-0.1824 \cdot 10^{-5}$	$-0.1021 \cdot 10^{-5}$
residual mean square		5.2600	1.5483	0.0105	0.0014
multiple R-square		0.9980	0.9993	0.9935	0.9991

<sup>&</sup> computed by least squares fit of a third order polynomial in one independent variable to the dependent variable. The form of the regression equation is:  $y = a_0 + a_1 x + a_2 x^2 + a_3 x^3$ .

<sup>#</sup> dependent variable  $y$  is  $E$  [mV], independent variable  $x$  is  $\lg(c_F)$  [ $\text{mg l}^{-1}$ ].

<sup>\*</sup> dependent variable  $y$  is  $\lg(c_F)$  [ $\text{mg l}^{-1}$ ], independent variable  $x$  is  $E$  [mV].



fluoride concentration from curve 1. Only those solution concentrations above ca.  $1 \text{ mg l}^{-1}$  can be determined with the necessary degree of confidence. Although TISAB also contributes to the fluoride blank it is nevertheless highly recommended as additive. As each experimental point is the mean of three values obtained from different samples, the mean single relative standard deviation could be calculated. For the two cases, with and without TISAB III,  $2.24 \text{ mV} \pm 0.85 \text{ mV}$  and  $3.98 \text{ mV} \pm 2.04 \text{ mV}$  were obtained, respectively. Samples with TISAB therefore show a much smaller spread in their mV readings about the mean value, than do samples without TISAB. A mean RSD of  $\pm 2.24 \text{ mV}$  might appear to be rather high, as it constitutes an error of  $0.16 \text{ mg l}^{-1}$  at the  $1 \text{ mg l}^{-1}$  level, but this represents the overall reproducibility of the experimental procedure as a whole for different samples. This compares favourably with reported reproducible potential readings in the same sample of 1 /RAB67, TUS70/ to  $1.5 \text{ mV}$  /EVA70/ at any one fluoride concentration.

Figure III.7 establishes the correlation between fluoride concentration in solution and the expected RSD at any one concentration in the range examined and clearly shows the decline in precision as lower concentration values are approached. Boundary lines were calculated with the TISAB calibration curve regression parameters (table III.6, dependent variable  $\lg(c_F)$ ), assuming a mean RSD of  $\pm 2.24 \text{ mV}$ . The pronounced effect of actual dissolved solids again shows the need for rather large aliquots of stone samples.

Several aspects of this study emphasize the crucial role of standards. There are no readily available fluoride standard samples in the  $\text{ng mg}^{-1}$  concentration range. The best is NBS SRM 1571 (orchard leaves) with  $4 \text{ ng mg}^{-1}$  fluoride, which is not a certified value. Using about  $1 \text{ g}$  aliquots (with  $7 \text{ ml}$  acid mixture) in the diffusion approach, yielded (after correction for the estimated blank of ca.  $0.27 \text{ mg l}^{-1}$ ) a value of  $3.64 \pm 0.23 \text{ ng mg}^{-1}$  as mean of three standard additions. This value compares favourably with the uncertified value of  $4 \text{ ng mg}^{-1}$  and is in good agreement with values reported by other workers ( $3.9 \pm 0.6 \text{ ng mg}^{-1}$ ,  $3.80 \pm 0.32 \text{ ng mg}^{-1}$ ,  $4.3 \text{ ng mg}^{-1}$  /SHR82/).

When digesting calculi containing uric acid, urates, calcium oxa-

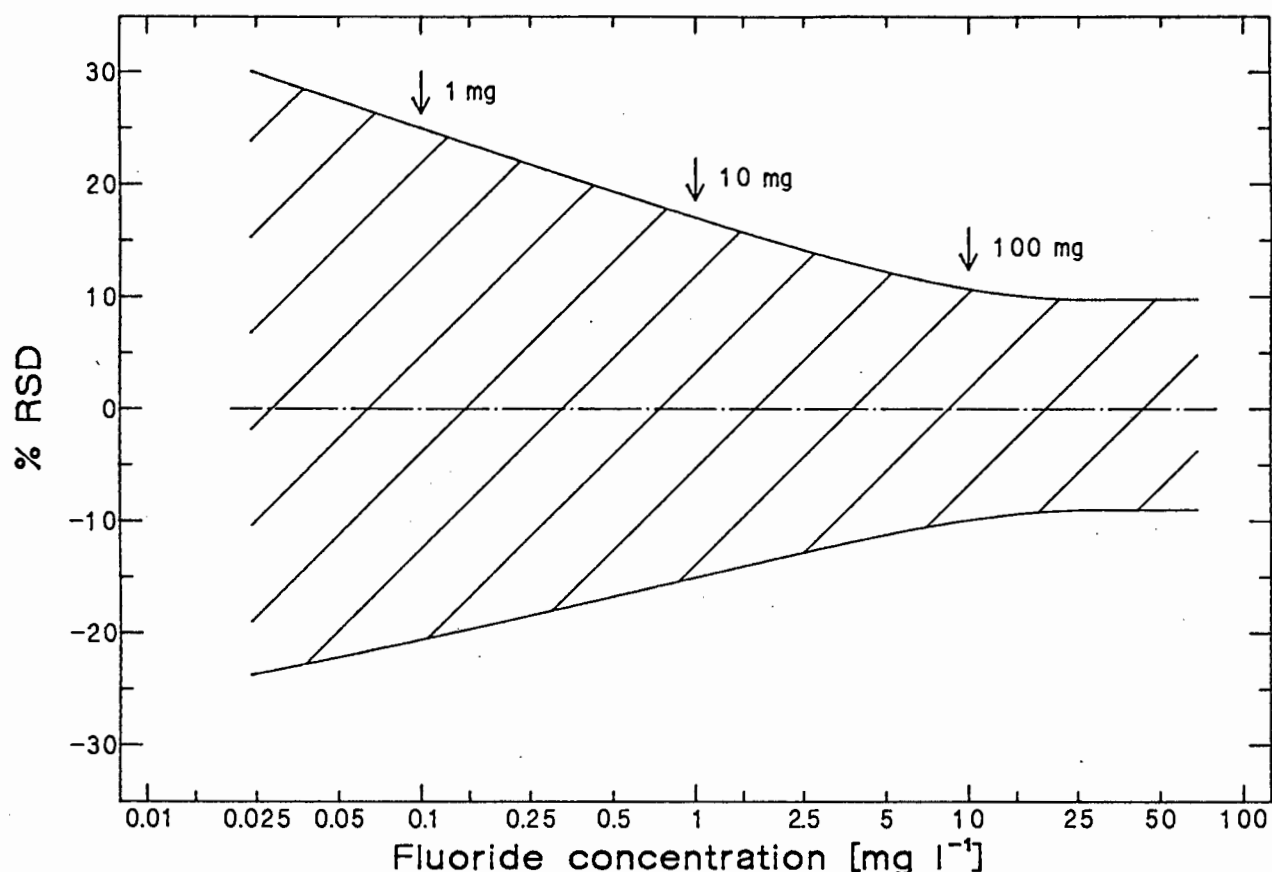


Figure III.7. Expected error as function of solution concentration.

late or carbonate apatite, the evolving carbon dioxide competes with the fluoride for the trapping alkali. Absorbed  $\text{CO}_2$  in the NaOH solution acts like a buffer which hampers adjustment of the solution pH to below 6. When adjusting the pH the gas forms microscopically small bubbles which leave the sample as a fine spray due to action of the rotating magnetic stir bar. To test for possible loss of fluoride in the spray, 70 mg aliquots of uric acid (Merck), ammonium acid urate (BDH), and calcium oxalate monohydrate (BDH) samples were digested and diffused after adding 0.025 mg of fluoride ion to each test solution. Table III.7. shows complete recovery of the fluoride, the somewhat higher values being accounted for by blank and extraneous fluoride contributions. It was therefore concluded that  $\text{CO}_2$  does not interfere with accurate fluoride concentration determination in the procedure described. However, if the absorbing capacity of the trapping solution is exceeded, a situation might arise where some of the fluoride might

remain uncollected. An erroneously low fluoride activity would thus be measured. In addition, high pressure build-up in the diffusion vessel might cause leakage of CO<sub>2</sub> and trimethylfluorosilane /SAR75/, again yielding low fluoride values.

Table III.7. Recovery of fluoride from samples containing carbon dioxide.

	sample	fluoride recovered [μg]	mean value [μg]	
	uric acid	28.3 28.1 27.2	27.9 ± 0.6	
	ammonium acid urate	25.5 25.2	25.4 ± 0.2	
	calcium oxalate monohydrate	28.5 26.5 26.7	27.2 ± 1.1	

To test the reproducibility of the diffusion method, one large stone composed of STR, APA and COM was ground to a homogeneous mixture and 150 mg aliquots were digested and separately diffused. Electrode potentials were determined immediately after pH adjustment as well as after addition of TISAB III. The sample fluoride concentrations were calculated from the relevant calibration curve parameters (table III.6). Three standard additions furnished a third concentration value for each sample all of which are given in table III.8. Mean values obtained from the three different approaches are well within the RSD of the single mean values of each method all of which are in turn always within 4.5% RSD. These results, combined with the results from NBS standard evaluation show that both the precision and the accuracy of the described method more than satisfy the great demands made upon comparable analytical procedures.

Table III.8. Repeat analysis of STR/APA/COM stone.

sample mass [mg]	fluoride concentration [ng mg <sup>-1</sup> ]		
	without TISAB	with TISAB	std. add. mean
152.0	390	412	385
152.5	364	385	358
152.4	353	370	352
152.3	380	405	385
154.7	374	404	383
152.0	358	371	375
153.2	359	380	368
150.7	360	378	372
mean	367 ± 13	388 ± 16	372 ± 13
% RSD	3.54	4.22	3.35

## 5. Results and discussion

Fluoride concentrations determined in 20 urinary calculi from India and 42 urinary calculi from South Africa are presented in tables III.9 and III.10, respectively. In most cases (Indian stones) samples from the nucleus (N) and periphery (P) of the same stone were available and were examined separately. Mean fluoride concentration of all 36 (Indian) determinations was 267 ng mg<sup>-1</sup> with a range from 21 to 1152 ng mg<sup>-1</sup>. This compares with a range from 26 to 9740 ng mg<sup>-1</sup> and a mean value of 1237 ng mg<sup>-1</sup> in the stones of South African origin. These results suggest that mean fluoride concentration in calculi from the Cape Town area is higher than that of their Indian counterparts. However, if these results are grouped and compared according to major stone components, a completely different picture is obtained. Fluoride concentration in 8 stones containing uric acid as major component from India has a mean value of 91 ng mg<sup>-1</sup> (ranging from 27 to 254 ng mg<sup>-1</sup>). This is significantly higher than the mean of 56 ng mg<sup>-1</sup> (range from 26 to 86 ng mg<sup>-1</sup>) in 5 South African stones of similar composition. The same trend occurs in 10 'pure' whewellite stones from India where a mean fluoride concentration of 454 ng mg<sup>-1</sup> (range 22 to 1152 ng mg<sup>-1</sup>)

Table III.9. Fluoride concentration in 20 Indian urinary calculi.

stone# number	components*	sample mass [mg]	fluoride concentration [ng mg <sup>-1</sup> ]&		
			without TISAB	with TISAB	mean
1N	COM	8.2	1269	1035	1152
1P	COM	27.9	648	563	605
2N	UA	17.2	42	55	48
2P	COM	42.5	21	23	22
3N	AAU	17.6	289	274	281
3P	AAU	25.4	237	192	214
4N	COM,AAU	8.1	-	60	60
4P	UA,COM,AAU	16.0	45	48	46
5N	UA,COM	22.3	53	57	55
5P	UA	132.8	36	32	34
6N	AAU	42.6	21	20	21
6P	STR,AAU	75.3	25	31	28
7N	AAU,STR	69.3	385	396	390
7P	AAU	79.5	149	126	138
8N	UA	13.5	253	254	254
8P	STR	84.3	60	50	55
9N	AAU	11.0	176	182	179
9P	UA	74.0	26	28	27
10N	AAU	29.1	81	94	87
10P	UA	61.2	137	127	132
11N	AAU	15.8	-	366	366
11P	UA	77.0	121	147	134
12N	COM,AAU	34.3	532	439	485
12P	COM	31.3	710	641	675
13	COM,COD	25.8	426	444	435
14N	AAU	71.1	187	179	183
14P	AAU	42.8	118	128	123
15	COM	73.7	181	152	166
16	COM	40.3	508	418	463
17N	COM	13.5	713	665	689
17P	COM	53.6	181	173	177
18N	COM	6.6	372	370	371
18P	COM	72.7	380	360	370
19N	AAU	24.6	237	238	238
20N	COM,AAU	5.9	396	381	389
20P	COM	36.9	506	541	523

# P = periphery, N = nucleus;

\* major component is listed first; semi-quantitative determinations were obtained by x-ray powder diffraction (film) technique;

COM = calcium oxalate monohydrate (whewellite);

COD = calcium oxalate dihydrate (weddelite);

UA = uric acid;

AAU = ammonium acid urate;

STR = ammonium magnesium phosphate hexahydrate (struvite);

& calculated according to table III.6.

Table III.10. Fluoride concentration in South African stones.

stone number	composition [wt-%] #							mass [mg]	fluoride concentration [ng mg <sup>-1</sup> ] *			
	AAU	UA	UAD	COM	COO	APA	STR		c <sub>1</sub>	c <sub>2</sub>	c <sub>3</sub>	mean
288		100						143.0	28	24	-	26
279		100						219.2	29	-	24	26
27		90		10				140.2	91	82	-	86
168		85		15				211.3	78	-	75	77
207		75		25				174.1	65	-	64	64
386	95			5				131.6	-	151	153	152
17				100				130.3	251	253	242	249
425				100				156.8	-	172	-	172
488				100				106.7	290	279	306	292
500				100				79.0	228	182	-	205
258				90		10		120.0	211	191	233	212
293				85		15		134.0	-	152	188	170
345			15	85				152.9	-	860	875	867
349				80		20		119.5	-	918	1054	986
351	40			60				124.0	196	179	-	187
481				60		40		122.9	9848	9633	-	9740
389				100				143.4	-	2131	2448	2290
198				85		15		112.8	-	2177	2225	2201
282		15		85				190.3	-	331	352	342
301				55		45		141.8	2395	2688	2744	2609
281					75	25		146.4	5563	5168	5238	5323
319					60	40		169.1	-	3566	3313	3439
358						80	20	191.9	-	2369	2608	2488
322						70	30	158.1	-	781	899	840
400						65	35	141.7	2847	2876	3104	2942
178						60	40	172.1	3571	3371	-	3473
370						60	40	159.6	-	435	392	413
303						45	55	151.0	2515	2711	2523	2583
101						40	60	149.2	311	347	332	330
297						40	60	146.0	971	-	1125	1049
361				10		40	50	152.5	367	388	372	376
379						40	60	155.9	207	211	-	209
99						35	65	156.1	-	1038	1021	1030
320						35	65	115.5	1019	-	1096	1058
135						30	70	148.4	281	294	249	275
339						30	70	173.2	-	417	409	413
172						25	75	149.5	1471	1883	1667	1674
211						25	75	150.7	-	985	949	967
56						20	80	147.9	-	824	791	807
296						20	80	142.4	259	264	245	256
321						15	85	148.1	-	941	938	940
193						5	95	151.3	119	121	132	124

# calculated from elemental (ICP-AES analysis) and phase data (XRD film technique), normalized to 100;

\* c<sub>1</sub> calculated from diffused standards calibration curve parameters (without TISAB);

c<sub>2</sub> calculated from diffused standards calibration curve parameters (with TISAB III);

c<sub>3</sub> mean of three standard additions.

is set against a mean value of  $230 \text{ ng mg}^{-1}$  (range 172 to  $292 \text{ ng mg}^{-1}$ ) in 4 'pure' COM South African stones. No comparison of the large group of 10 'pure' ammonium acid urate calculi in the Indian collection (mean  $183 \text{ ng mg}^{-1} \text{ F}^{-}$ , range 21 to  $366 \text{ ng mg}^{-1}$ ) with an equivalent South African group was possible, as there was only one stone ( $152 \text{ ng mg}^{-1}$  fluoride) having this compound as major component. On the other hand 20 stones from the South African collection have struvite / apatite composition while none of these occur in the Indian group. These stones have a mean concentration of  $1112 \text{ ng mg}^{-1}$  (range 124 -  $3473 \text{ ng mg}^{-1}$ ) and it is this group which results in the South African stones having an overall higher mean concentration.

The high incidence of uric acid and urate stones, as well as the absence of any apatite containing calculi in the Indian collection points to an acidic urine in these patients, as it is well established that uric acid is only poorly soluble in the acidic pH range /GUD09, KOL68/. Undernourishment has been shown to be one of the causes of a higher excretion of uric acid, originating in purine bases from tissue decay, caused by malnutrition /HAM38/. Since detailed patient histories are, however, not available, definite conclusions concerning the high incidence of uric acid in the Indian stones cannot be drawn.

As mentioned above, the Indian stones have higher fluoride content than the South African stones when compared on a group-for-group basis. This could be due to the fact that certain areas in India have an average fluoride concentration of  $16 \text{ mg l}^{-1}$  in the drinking water /JOL80/ which far exceeds the level of 1 -  $2 \text{ mg l}^{-1}$  recommended by the WHO /WHO65/. Prolonged exposure to relatively high fluoride concentrations in Finland was found to play a role in the genesis of urolithiasis: the marked differences in the fluoride content of ground water in the coastal region of southeast Finland ( $1.3$  to  $1.9 \text{ mg l}^{-1}$ ) and in other parts of the country ( $0.06$  to  $0.13 \text{ mg l}^{-1}$ ) is clearly reflected in the higher standard hospital admission rates for urolithiasis in the former /JUJ79/. A further study comparing fluoride concentration in urinary tract calculi from areas with and without drinking water fluoridation /HES78/ established a difference of 41.1% between the two districts, matching that of 40.5% difference between the fluoride concentration in the urines of both groups. In another study /MUE61/,

the formation of considerable amounts of (dental) calculus-like deposits on the upper and lower molars of rats has been reported in the presence of dietary sodium fluoride. This is in accordance with Anasuya's findings /ANA82/ that rats ingesting high fluoride diets exhibited a higher incidence of crystalluria and bladder stones compared with those receiving low fluoride diets. Furthermore, evidence is presented /SUM75/ for a definite increase in the percentage of calcium oxalate stones in a community after it had received a fluoridated water supply. This was confirmed by other investigations /HES78, LJU78, MUE77/.

However, contrary to these observations Zipkin et al. reported only non-significant differences when comparing the fluoride concentration of urinary tract calculi of individuals from a low fluoride area with that from an area where the drinking water contained  $2.6 \text{ mg l}^{-1}$  fluoride /ZIP58/. (See table III.11 for reported values of fluoride concentrations in human stones). Studies of rats fed  $1 \text{ mg l}^{-1}$  and 10 to 500  $\text{mg l}^{-1}$   $\text{F}^{-}$  drinking water also showed that the ingested fluoride did not produce calculi in any of the animals /HER60/. Hering et al. reported that fluoride inhibited artificially induced oxalate stone formation in rats receiving  $10 \text{ mg l}^{-1}$  fluoride in their drinking water /HER85/. It also delayed the initiation of  $\text{CaOx}$  crystallization, but promoted the formation of smaller crystals. Biochemical findings of other researchers /TEO83, TEO84/ further suggest that prolonged ingestion of a high amount of fluoride does not alter plasma and urinary biochemistry to make it congenial for stone formation.

Despite many conflicting reports however, it seems likely that fluoride ingestion may play a significant role in the genesis of urinary calculi. One reason for the differing evidence presented thus far might be the observed mutual effect of other factors on nephrocalcinosis. For example, the apparent protection against calcification afforded by fluoride was found to be influenced by high plasma magnesium levels. This suggests that both elements together may play an inhibitory role /LU076/ (cf. chapter II, section 5.5).



Table III.11. Reported values of fluoride concentration in human stones.

n	fluoride concentration mean [ng mg <sup>-1</sup> ] range		remarks	reference
1	2000		urinary calculus	/DIL54/
10 9	449 624	4 - 1560 0 - 1790	urinary (analyst 1) calculi (analyst 2)	/SPI56/
10	8	2 - 32	biliary calculi	/SPI57/
100	-	0 - 1800	38 renal, 28 ureteral, 34 vesical calculi	/HER58/
4	663	150 - 1100	urinary calculi, 1 g samples	/VOL58/
42 16 17 9	3100 2500 3700 20	20 - 11100	whole study (oven-dry basis) urinary calculi, 0.0 to 0.6 mg l <sup>-1</sup> F <sup>-</sup> in drinking water urinary calculi, 2.6 mg l <sup>-1</sup> F <sup>-</sup> in drinking water biliary calculi, 2.6 mg l <sup>-1</sup> F <sup>-</sup> in drinking water	/ZIP58/
28 11 13	1130 960 200	210 - 10650 270 - 1400 70 - 430	calcium oxalate oxalate / phosphate uric acid kidney stones, prior to drinking water fluoridation (ash basis)	/AUE69/ /AUE71/
200	1400	0 - 3000	calcium containing urinary calculi (total mass basis)	/HOD69/
10 10	48 88		calcium oxalate monohydrate calcium oxalate dihydrate (ash basis)	/HES77/
70 70 20 20 20 20 10 10 10 10 10 10 10	1100 644 808 2005 959 2103 405 457 358 406 345 529 362		1 mg l <sup>-1</sup> F <sup>-</sup> in drinking water 0.25 mg l <sup>-1</sup> F <sup>-</sup> in drinking water COM (0.25 mg l <sup>-1</sup> F <sup>-</sup> ) COM (1 mg l <sup>-1</sup> F <sup>-</sup> ) COD (0.25 mg l <sup>-1</sup> F <sup>-</sup> ) COD (1 mg l <sup>-1</sup> F <sup>-</sup> ) apatite (0.25 mg l <sup>-1</sup> F <sup>-</sup> ) apatite (1 mg l <sup>-1</sup> F <sup>-</sup> ) struvite (0.25 mg l <sup>-1</sup> F <sup>-</sup> ) struvite (1 mg l <sup>-1</sup> F <sup>-</sup> ) uric acid (0.25 mg l <sup>-1</sup> F <sup>-</sup> ) uric acid (1 mg l <sup>-1</sup> F <sup>-</sup> ) cystine	/MUE77/ /HES78/
25 25	22000 6200	8400 - 41500 30 - 9100	endemic fluorotic area (16 mg l <sup>-1</sup> F <sup>-</sup> in drinking water) nonendemic area urinary calculi (ash basis)	/JOL80/

In this study calcium oxalate calculi in both groups (in India and South Africa) had a higher fluoride concentration than uric acid and urate stones. From table III.10 it can be seen that the calculi containing COM as major constituent (but not COD) have lower fluoride content than those stones containing a mixture of both calcium oxalate hydrates (i.e. COM and COD). Furthermore, when the dihydrate is the only  $\text{CaOx}$  phase present, the fluoride concentration is even higher (stones 281 and 319). (The most prevalent additional constituent in those calculi is apatite). Thus, in general, it appears that the fluoride concentration increases with increasing COD content. These observations are not contrary to the findings of Herman /HER56/ who reported a correlation between high calcium and high fluoride concentrations. It is conceivable that with high concentrations of fluoride in urine, calcium fluoride may be precipitated, thereby acting as a potential initiator of crystal formation by aiding heterogeneous nucleation /LAG56/. Calcium oxalate may grow on these crystals, in turn acting as a nucleus for uric acid precipitation /LAG56/. As is evident from table III.11, stones containing calcium oxalate in particular show marked differences in their fluoride content when areas of fluoridated and natural drinking waters are compared /HES78/.

The correlation between high fluoride content and high COD content might be explained by crystal structural considerations. It is well known that weddellite is stabilized by foreign ions in urine, especially magnesium /BER76, HES81/. Due to the special arrangement of the hydrate water molecules, COD offers zeolitic binding sites not only for extra water molecules, but also for extraneous ions which are either embedded in or adsorbed on the surface. Thus fluoride might also be trapped in the COD lattice.

While it is the additive linkage in COD stones which is emphasized, it is the stoichiometric intake of fluorine in the crystal lattice which is of importance in apatite. Apatite is the most abundant of the phosphatic minerals and is contained in almost all calculi where it is commonly present at the surface and at the walls of pores within the stone /TOZ81/. Biological apatites are modified by an exchange of anions and cations, analogous to the process of alteration and regeneration of phosphate minerals. This influences the concentration of many

trace elements that become trapped in apatite, such as fluorine. Examples include fluoroapatite  $[\text{Ca}_{10}(\text{PO}_4)_6(\text{F},\text{OH})_2]$  which is the accessory mineral of igneous rocks; francolite, the carbonate-fluorine bearing variety  $[\text{Ca}_{10}(\text{PO}_4)_{6-x}(\text{CO}_3)_x(\text{F},\text{OH})_2]$ , which comprises the primary marine phosphate in sedimentary rocks; the carbonate-hydroxyapatite, dahllite  $[\text{Ca}_{10}(\text{PO}_4)_{6-x}(\text{CO}_3)_{x+y}(\text{OH},\text{F})_{2-y}]$ , is the mineral matter of bone; hydroxyapatite  $[\text{Ca}_{10}(\text{PO}_4)_6(\text{OH})_2]$  occurs in guano-altered limestone /ALT73/. All normal hard tissues of humans contain apatite, as do many of the pathological calcifications.

Because of similarities between the structures of hydroxyapatite and octacalcium phosphate  $(\text{Ca}_8\text{H}_2(\text{PO}_4)_6 \cdot 5\text{H}_2\text{O})$ , the latter has been proposed as either a suitable substrate which provides seeds for deposition of HAP through an epitaxial mechanism, or as a metastable precursor /BRO64, FRA71/. The effects of fluoride ion on the stability relationships of these calcium phosphates are, however, only poorly understood /BRO73/. It is nevertheless known that fluorine fits readily into the lattice of the apatite molecule and that fluoroapatite is markedly less soluble than hydroxyapatite /AUE69, MUR57/. For the formation of apatite structures under biological conditions, the presence of small quantities of fluoride ions was found to be necessary /NEW61/. This can be explained by the elimination of the relatively unstable salt, OCP, in the presence of fluoride, by converting it to the more stable hydroxyapatite. In in vitro systems, OCP becomes transformed immediately into HAP when in contact with fluoridated solvents /SCH66/. Even mere traces of fluoride ( $10^{-6}$  M - about  $\frac{1}{50}$  of the concentration recommended for drinking water), alters the nature of the precipitate completely /BRO66, NEW60/. Small quantities of fluoroapatite are likely to be formed and they may aid in the deposition of further quantities of apatitic material.

The effect of fluoride ion on the crystal growth of apatite is again complicated. It appears to inhibit the orderly deposition of calcium salt at small concentrations /ROB34/, but enhances growth at greater concentrations /MEY72/. However, it has been shown that during remineralization of partly demineralized tooth enamel, there exists a maximum value of the fluoride concentration gradient above which lesions cannot be successfully repaired /CHR84/. As apatite is one of

the most frequently found major phases in kidney stones and OCP has also been reported as a constituent, the above results suggest that elevated urinary fluoride levels enhance the formation and growth of apatitic concretions. In addition, dissolution of apatite is inhibited by fluoride ions (present in the dissolution medium), the inhibitory effect increasing with the length of time the crystals are exposed to fluoride ions as well as decreasing pH /CHR84a/. The fluoride content of an apatite calculus will therefore vary in relation to the amount of fluorine in the urine, the length of time exposure to fluoride, the percentage of apatite in the calculus and the surface area exposed. It is therefore not surprising that no relation between the calcium to phosphate ratio and fluorine concentration could be established in this or other studies /JOL80, ZIP58/. Likewise, no relation between calcium and fluoride concentration was found in this study while no correlation between sex, age, race and location in the urinary tract on the one hand and fluoride content on the other, has been reported. However, in general, the crystallinity of bone apatite /ZIP62/ and carbonate apatite /HES78/ in urinary stones increases significantly with increasing fluoride content, wherewith a characteristic lattice contraction could be ascertained. The amount of struvite, coprecipitated with apatite in all infection stones, again failed to correlate with fluoride concentration.

The small number of stones investigated in this study prevents complete clarification. However, the results suggest that high intake of fluoride may be of some importance in urinary stone disease. Increased exposure to fluoride evidently changes the physical properties of apatitic calculi, but the exact mechanism of fluoride action in calculogenesis remains unclear.

## Chapter IV

### Crystallization characteristics of synthetic urines in a fast evaporator

#### 1. Introduction

The assumption that stone formation is mainly governed and controlled by crystallization phenomena, and that the organic matrix is only a non-essential concomitant, now receives wide support. According to the crystallization theory, supersaturation of urine is the most fundamental step in the formation of a concretion. Classical thermodynamics predicts that any supersaturated solution must eventually equilibrate by precipitation, a process which will stop only when the solution concerned is just (un)saturated. On the one hand, kinetic factors might alter this precipitation process while on the other hand, metastable solutions might remain supersaturated until nucleation is induced by a seed crystal or other particle. In addition, the mechanisms of nucleation might be modified by the presence of surface-active inhibitors and epitaxially favourable nucleation sites. There are two further important steps in stone formation apart from supersaturation and nucleation. These are crystal growth and aggregation of the formed particles. As with nucleation, crystal growth might also be affected by inhibitors or promoters which may either retard or accelerate the growth of crystallites. Aggregation mechanisms such as polymeric bridging or aggregation by reduction of the zeta potential, will be similarly influenced. The four main crystallization approaches to the investigation of urinary stone formation thus involve examination of (i) the relationship between the concentrations of the precipitating substances in urine and their solubilities, (ii) the role of nucleating substances, (iii) crystal aggregation, and (iv) the role of inhibitors of nucleation, crystal growth and aggregation /FLE77/.

Many different ways have been employed in the past to study the physico-chemical factors governing urolithiasis. Several workers have examined diffusion-limited systems. One realization of this method is

the technique in which component ions are permitted to diffuse into a stagnant urine solution causing encrustations to grow on fibres suspended in the medium /LYO65, SUT69, WEL72/. Chemical supersaturation is reached by the gradual addition of ions. This may be achieved using a simple 'paper wick technique' /VER64/ or more sophisticated gel-systems /BIS75, BIS76, PHA77/. Others have examined the inhibitory effects of certain ions and compounds, again employing static supersaturated systems /MEY75, ROB73, SUT73/. On the other hand, the concept of the urinary tract as a biological analogue of a sequence of continuous crystallizers has enjoyed much support since being first described by Finlayson et al. /FIN72, FIN73/. Many studies have been conducted in such mixed suspension mixed product removal (MSMPR) crystallizers /DRA78, DRA80, ROD81/. The Coulter counter is yet another useful instrument for studying the qualitative and quantitative effect of inhibitors on nucleation and particle growth /DES73, DES78/. Using this instrument, ex-vivo measurements of crystal size distributions permit comparisons between the urines of stone formers and normal controls, or examination of changes in standard synthetic urines after the addition of inhibiting substances /ROB69, RYA81/. Hallson and Rose /HAL78/ employed yet another approach in which human urine samples were subjected to rapid evaporation at 37°C. This process is thought to be analogous to the concentration of urine in the renal tubules, whereby water is removed and a state of supersaturation is maintained.

In the present study a series of crystallization experiments using a standard reference artificial urine (SRAU) were carried out in an attempt to gain insight into some of the physico-chemical factors governing urolithiasis. The precipitates obtained experimentally by evaporation of the SRAU /ROD85/ were compared with those predicted from a 'theoretical solution' by means of an equilibrium speciation computer model /LIN86, LIT84/.

## 2. Experimental conditions

Urine is a buffered solution, containing a great number of ionic and molecular components. Many inorganic, nitrogeneous, nitrogen-free

and high molecular weight organic substances contribute to the chemical composition of urine /LEN81/. The physical properties and concentrations of the normal urinary constituents are obviously highly variable and are largely determined by quantity and type of food consumed as well as the daily voided volume. Since the excretion of many urine constituents is subject to a day / night rhythm, either freshly voided or 24-hour urines are usually compared when assessing physico-chemical data.

Many different recipes have been proposed for artificial solutions simulating urine. These are compared in table IV.1 with a synopsis of human urine as given by successive editions of Documenta Geigy Scientific Tables /DIE62, DIE70, LEN81/ and Achilles et al. /ACH76/. As can be seen, extremely wide variations exist between the synthetic urines employed by different authors, not only in concentration but also in pH and constituent numbers. Furthermore, most of the recipes are restricted to the incorporation of the main inorganic constituents of human urine. That this is not a serious limitation in simulating real urine was shown by Barker et al. /BAR74/. These workers established that their simple 12-component artificial urine inhibited mineralization as effectively as did natural urine. In order to make possible a comparison of results obtained in different laboratories, Burns et al. /BUR80/ suggested the use of a standard reference artificial urine (SRAU) (table IV.2). Although their recipe is not based on the most up-to-date physiological data, it was nevertheless decided to use their recipe in the hope that other researchers would conform by also using the same standard.

One litre stock solutions of SRAU were prepared by dissolving the appropriate amount of inorganic salts (Merck) in the sequence given in table IV.2. 5 M ammonia solution was added dropwise to each litre of solution to adjust the pH to 6.5. Care had to be exercised in this step as too fast an addition resulted in instant turbidity of the SRAU followed by precipitation of calcium and magnesium phosphates. After preparation, urines were refrigerated without delay for short periods (< 4 hours) since slow precipitation takes place /FIN84/. Prior to evaporation, further ingredients were added and / or urinary pH was adjusted to the desired value and the urine was allowed to equilibrate

Table IV.1. Human and artificial urine constituent concentrations [mM l<sup>-1</sup>].

reference constituent	DIE62 <sup>1</sup>	DIE70 <sup>2</sup>		LENB1 <sup>3</sup>	ACH76 <sup>4</sup>	BOY54 <sup>5</sup> ROS75 <sup>6</sup>	LYD65 <sup>7</sup>	ISA69	BAR74 <sup>8</sup> HOW76	GRI76	MIL76 MIL77	GIL77 <sup>9</sup>	DOR78 <sup>8</sup>	GAR78	BUR80	HOD80 <sup>10</sup>	TAW80	ROD81
		men	women															
calcium	5.7	5.7	5.8	4.4	3.8	3.8	-	-	1.9	4.3	9.0	-	0.5	-	5.8	-	5.0	10.0
magnesium	3.9	5.3	4.5	3.9	2.9	3.7	(4.9)	6.7	2.0	3.2	8.1	1.5	2.0	2.5	3.9	3.2	2.3	8.1
potassium	63.7	56.2	47.5	56.2	38.0	38.4	-	92.6	52.0	42.0	111.5	25.3	52.0	8.3	63.7	42.0	7.5	111.5
sodium	182.5	174.4	129.4	179.9	110.0	175.6	172.3	291.2	232.5	118.0	251.4	85.6	224.9	166.5	182.5	126.0	151.2	262.8
ammonia-N	45.4	34.9	26.9	43.9	14.0	22.2	-	65.1	20.0	19.0	59.5	6.8	20.0	-	45.5	23.0	-	59.4
chloride	188.9	181.3	133.5	108.4	-	166.5	154.0	371.5	225.8	-	329.2	106.0	247.0	119.0	208.3	130.0	98.7	349.2
phosphate	32.3	44.5	44.5	47.3	18.0	15.7	-	36.9	16.5	20.5	34.0	7.3	16.5	18.7	32.3	20.0	16.9	36.7
sulphate	20.8	22.2	18.2	29.4	14.5	18.7	18.3	21.7	18.5	16.0	31.6	6.8	18.5	15.6	20.8	19.0	14.1	31.6
citrate	3.2	2.4	2.4	2.1	2.1	4.3	(2.7)	3.1	1.6	2.3	2.7	-	1.6	2.8	3.2	2.3	2.5	2.7
oxalate	0.30	0.34	0.35	0.24	0.14	0.16	-	-	-	0.15	3.0	-	0.50	-	0.30	-	0.25	3.0
uric acid	2.9	3.1	2.5	-	-	3.6	-	-	3.0	-	-	-	-	-	-	2.9	-	-
urea	416.3	338.0	338.0	275.5	-	333.0	416.3	291.4	500.0	416.3	-	249.8	500.0	203.0	-	500.0	-	-
creatinine	17.2	15.7	13.2	10.5	-	7.7	-	-	13.0	9.7	-	8.8	13.0	-	-	11.9	-	-
pH	6.25	5.7	5.8	6.2	5.8	5-6.3	-	5.4	6.5	5.75	5.6	5.8	5.7	5.7	6.5	6.3	-	-
ionic strength	-	-	-	-	-	-	-	0.5	-	-	-	-	0.34	-	-	0.24	-	-

Phosphate values generally include pyrophosphate concentrations;

<sup>1</sup> human urine; concentrations calculated from mean or one-half range 24-hour-urine values, assuming a mean daily volume of 1100 ml;

<sup>2</sup> human urine; calculated as<sup>1</sup>, assuming a mean daily volume of 1015 ml for men and 989 ml for women;

<sup>3</sup> human urine; calculated as<sup>1</sup>, assuming a mean daily volume of 1245 ml;

<sup>4</sup> normal concentrations of 24-hour urine samples (excretion volume 1500 ml);

<sup>5</sup> + 3.9 mM l<sup>-1</sup> hippuric acid;

<sup>6</sup> calcium, phosphate and chloride increased to 9.9, 37.1, and 391.3 mM l<sup>-1</sup>, respectively;

<sup>7</sup> diffusion of calcium and oxalate into basic urine at variable rates;

<sup>8</sup> + 3.0 mM l<sup>-1</sup> hippuric acid;

<sup>9</sup> + dropwise addition of calcium chloride and sodium oxalate;

<sup>10</sup> + pyrophosphate, + chondroitin-4-sulphate, + chondroitin-6-sulphate.



Table IV.2. Components of 1 litre standard reference artificial urine.

component	mass [g]
NaCl	6.1657
$\text{NaH}_2\text{PO}_4 \cdot 2\text{H}_2\text{O}$	5.0390
$\text{Na}_3\text{C}_6\text{H}_5\text{O}_7 \cdot 2\text{H}_2\text{O}$	0.8381
$\text{MgSO}_4 \cdot 7\text{H}_2\text{O}$	0.9489
$\text{Na}_2\text{SO}_4$	2.4075
KCl	4.7489
$\text{CaCl} \cdot 2\text{H}_2\text{O}$	0.6839
$\text{Na}_2\text{C}_2\text{O}_4$	0.0426
$\text{NH}_4\text{Cl}$	1.4764

at 37°C. Aliquots were then transferred to a rotary evaporator (Rota-vapor-R, Büchi Laboratoriums-AG, Flawil, Switzerland) and the vessels were evacuated to ca. 26.7 Pa (~0.2 mm Hg) by means of a mechanical pump equipped with a liquid nitrogen trap. A pressure of ca. 26.7 Pa (~0.2 mm Hg) was maintained by means of an adjustable valve. This effectively permitted control of the evaporation rate and resulted in all water being collected with none diffusing to the cold trap. Using a measuring cylinder adapted to fit the rotary evaporator, it was possible to monitor the volume of evaporated water. Precipitates formed in the experiments were filtered using 0.2 or 0.45  $\mu\text{m}$  PTFE filters (Sartorius SM 11807) preconditioned with methanol. Precipitates were washed with ca. 0.1% (v/v) HCl, distilled water and methanol. After drying, the mass of each precipitate was determined using a 4-figure balance. Semi quantitative x-ray diffraction analysis was performed as described by Rodgers et al. /ROD81c/. For this purpose, as much as possible of the precipitated crystal mass was scraped from the filters and distributed between two glass slides. After grinding the crystals to a fine powder by slow rotation of the glass plates, rubber glue (Dunlop) was added and the powdered sample was rolled to a tiny sphere. This was glued to the tip of a glass fibre and centred in a Debye-Scherrer powder camera of 28.65 mm radius. Diffraction patterns were recorded on DEF-392 film (Kodak) with nickel-filtered Cu  $K_\alpha$  radiation (of wavelength 1.5418 Å). Exposure time was between 2 and 4 hours with x-ray generator settings of 40 kV and 20 mA (Philips model 1008).

In some instances, crystals formed during the evaporation process were deposited on silver filters in an attempt to perform quantitative x-ray diffraction analysis as discussed in chapter I, section 5.5. However, the amount of precipitate formed was so small ( $< 1$  mg), that no definite powder pattern could be recorded. This was particularly the case in the acid pH range. Furthermore, the deposition of COT gave rise to preferred orientation of the crystallites resulting in somewhat doubtful analytical values. Even in the alkaline pH range, where a greater number of crystals formed, true quantitative concentration measurements were not possible. In this pH range a mixture of 3-4 phases (COT, APA, BRU, STR) precipitated, which resulted in severe overlap of peaks in the diffractogram. This in turn prevented accurate quantitative phase determination.

The ICP-AES technique developed in chapter II for stone analysis could also not be applied, since precipitated crystallite mass was below the necessary minimum in all but a few cases. It was also suspected that, despite washing of the precipitate, a large amount of extraneous ions was still present therein, giving rise to inaccurate elemental concentrations. This assumption was confirmed by measurement of the element distribution on the filters with an energy-dispersive x-ray detector attached to a SEM.

Because of these shortcomings it was decided to analyse the precipitated stone-forming solids in a scanning electron microscope (SEM) in addition to XRD. This technique complements the latter by supplying phase information based on the morphology and microchemical composition of the crystals observed. It also permitted comparison of the amount of precipitate from different evaporation experiments. For this purpose, ca.  $1\text{ cm}^2$  sections of the filters were cut out and glued on to aluminium stubs. These were then carbon-coated before being investigated by SEM and element specific electron microprobe techniques.

Specimens were bombarded with a 15 kV, 100  $\mu\text{A}$  electron beam in a Cambridge S 180 SEM. The secondary electron images were recorded on Ilford FP4 roll film with the screen set to 800 lines per frame and 60 second frame period. An energy dispersive x-ray analyzer (KEVEX) was used for the qualitative identification of elements.

A series of 5 experiments was conducted in this study. In the first set of experiments (series 1), the pH of the SRAU was varied from 3.0 to 9.0 in steps of 0.5 pH units. These adjustments were achieved by addition of either 5 M HCl or 5 M  $\text{NH}_4\text{OH}$ . The maximum volumes required in each case constituted negligible changes of 0.7% in the chloride concentration (pH 3) and 3.8% in the ammonia-N concentration (pH 9). 50 ml aliquots of the SRAU were evaporated until 25 ml of distillate had been collected. Precipitates were retrieved by filtration as described earlier. These experiments were repeated in duplicate.

Series 2 did not involve evaporation experiments. SRAU aliquots which had not been previously refrigerated, but which had been thermostatted at 37°C and which were of variable pH, were filtered after ca. 4 days.

In series 3, the composition of the urine was varied to investigate the role of individual constituents in determining the crystallization characteristics. The effect of uric acid (480  $\text{mg l}^{-1}$  /DIE62/), creatinine (1.95  $\text{g l}^{-1}$  /DIE62/) and urea (25  $\text{g l}^{-1}$  /DIE62/) were independently examined. Thereafter, uric acid (480  $\text{mg l}^{-1}$ ) was included as a component in the SRAU and the effect of the other two on this new urine solution was again individually studied. In order to focus attention on calcium oxalate formation in particular, the pH of the solutions was adjusted to 5.5 in most cases. In an attempt to increase the mass of precipitated material, the initial SRAU volume was raised to 150 ml of which 100 ml were evaporated. Evaporation times were thus extended relative to series 1.

In the fourth series of experiments, the influence of potential inhibitors was investigated. Included in the study were magnesium (as  $\text{MgO}$ , 40  $\text{mg l}^{-1}$ ), methylene blue (32  $\text{mg l}^{-1}$ ) and chondroitin sulphate A (20  $\text{mg l}^{-1}$ ). The pH was again left unchanged at 5.5 and two thirds of 150 ml initial volumes were evaporated.

In series 5, the effect of 20, 50 and 100  $\text{mg l}^{-1}$  fluoride concentrations was investigated at pH values 5.5 and 6.5. In these experiments two thirds of 100 ml initial volumes were evaporated at 37°C.

### 3. Results

In series 1, calcium oxalate monohydrate (COM) was formed in the pH range 3 to 5.5, together with the trihydrate (COT), the latter being the major constituent (figure IV.1). At pH values above 5.5, brushite

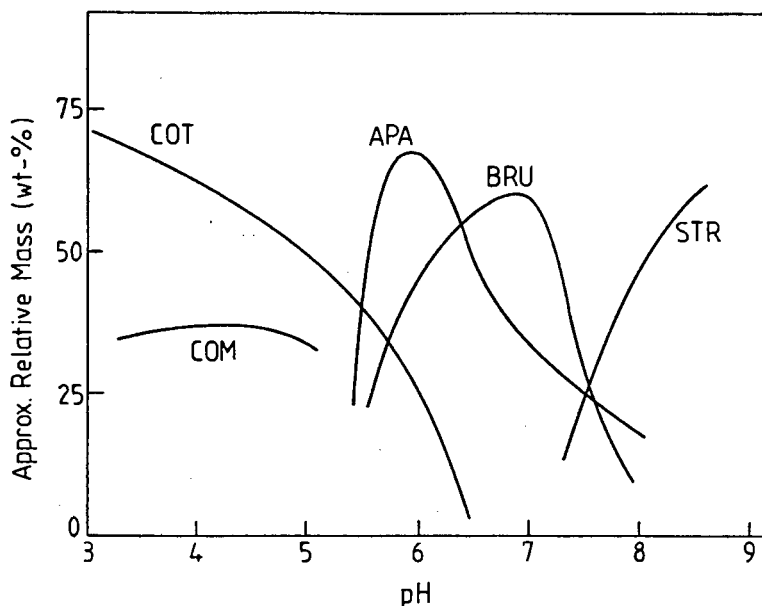
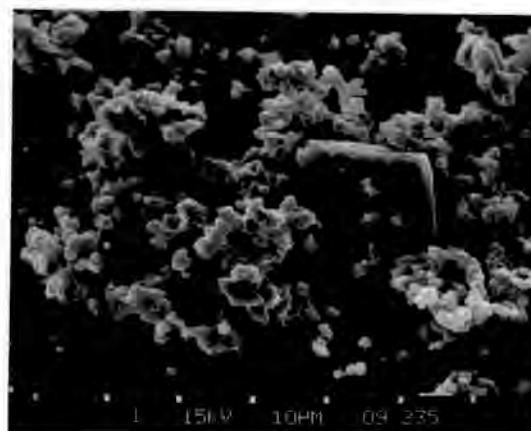
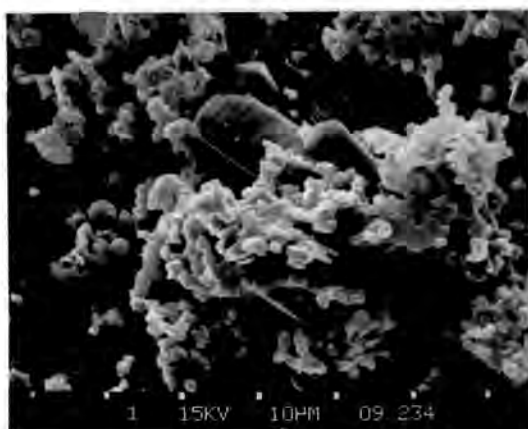


Figure IV.1. Nature and quantity of precipitated solid as function of SRAU solution pH (approximately relative mass [wt-%]).

(BRU) and apatite (APA) were detected as well. COT (but not COM) continued to precipitate with BRU and APA at higher pH levels but finally disappeared at pH values above 6.5. Calcium oxalate dihydrate (COD) was not detected at any pH by XRD. Small amounts were identified by SEM at pH 5.5 (figures IV.2 and IV.3, overleaf). At pH values greater than 7.5, struvite (STR) was identified with BRU and APA. The presence of octacalcium phosphate was suspected at pH values 5.5 and 6. However, due to the co-precipitation of COT, BRU and APA its presence could not be verified from XRD powder diffraction patterns. The total mass of precipitate formed in each experiment of this series was relatively low in the pH range 3 to 6 (< 1 mg) but thereafter increased dramatically, reaching a maximum at pH 8 (~150 mg). The relative mass of COT within



Figures IV.2 and IV.3. Survey pictures showing profuse COM deposits together with a few isolated COD and COT crystals (SRAU, pH 5.5); Mag 1700X.

each precipitate decreased with increasing pH while that of COM remained fairly constant; BRU and APA deposits within the particular mixtures were greatest at pH value 6 and 7, respectively.

In the acidic pH range, COM but not COT was detected in series 2. At pH 6 to 7, whitlockite was detected together with APA at higher pH values. In the alkaline range, STR was found to be present.

When uric acid was added in series 3, uric acid dihydrate (UAD) was the major deposit formed, followed by COD and COT (and probably COM). A considerable amount of UAD also precipitated when the UA-SRAU (pH 6.5) was refrigerated for one day.

When creatinine was included in the SRAU, XRD identified the presence of only COD and COM in the precipitates. SEM studies however revealed small COT deposits ( $\sim 10 \mu\text{m}$ ; figures IV.4 and IV.5, overleaf) interspersed with COD envelope crystals ( $\sim 4 \mu\text{m}$ ) and debris which might possibly be COM.

Evaporation of the SRAU solution to which both UA and creatinine had been added, appeared to inhibit the formation of UAD. COD and COM were the major phases precipitated in this experiment.

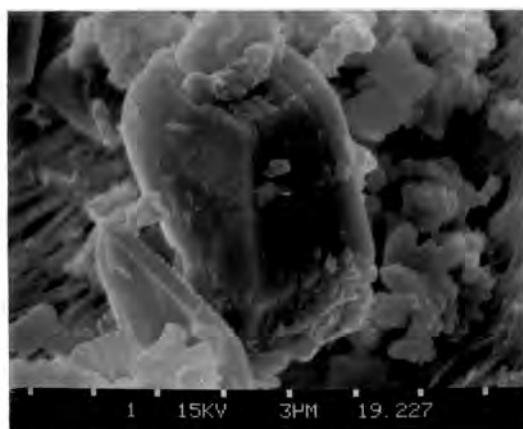


Figure IV.4. Small COT deposit surrounded by 'debris' containing Ca only (possibly COM) (SRAU + creatinine, pH 5.5); Mag 5000X.

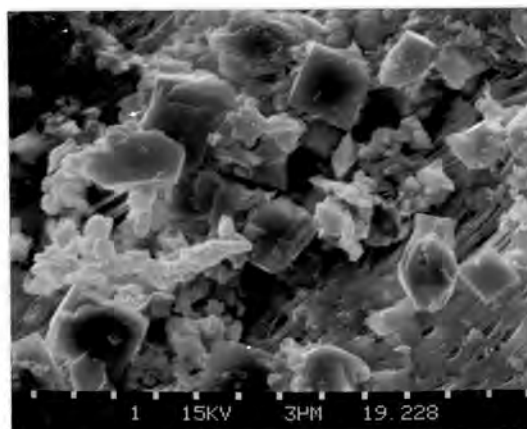


Figure IV.5. Profuse COT deposits surrounded by 'debris' containing Ca only (possibly COM) plus some isolated COD crystals (SRAU + creatinine, pH 5.5); Mag 3200X.

When urea was included as a component of the SRAU, COM and COT, as well as a small amount of COD, were formed. This is clearly shown in figure IV.6 where layered COT deposits are surrounded by small COD crystals and debris of similar appearance to that observed in figures IV.4 and IV.5.

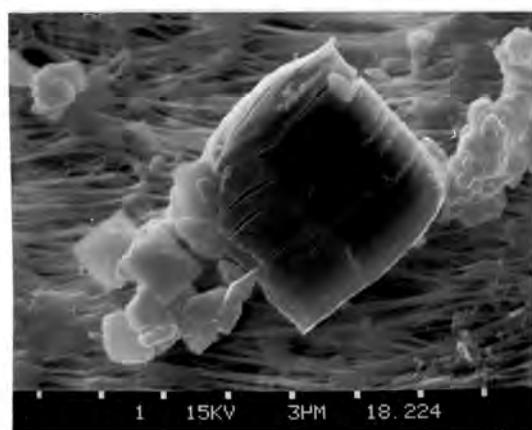


Figure IV.6. Layered COT deposit surrounded by COD (and COM) crystals (SRAU + urea, pH 5.5); Mag 4800X.

The addition of urea to the UA/SRAU solution yielded very little precipitate. This gave a very weak XRD photograph the faint reflections of which suggested the possible presence of COD.

In series 4, the addition of magnesium (as MgO) to the SRAU yielded no visible precipitate. Under the (light) microscope, however, small crystals could be seen and COM and COD (and possibly COT) could be identified with XRD. SEM investigation revealed the presence of only a few small COD crystals ( $\sim 6 \mu\text{m}$ ) distributed over the filter.

With methylene blue, no change in quality nor quantity of precipitate was observed with XRD techniques relative to the MgO experiments. In the electron microscope only one or two isolated COD crystals were observed, which were extremely small ( $< 1 \mu\text{m}$ ).

The addition of chondroitin sulphate A to the SRAU yielded a very fine precipitate of COM only. However in the SEM, isolated COT crystal clusters could be seen (figures IV.7 and IV.8) and only the Ca signal was detected by the energy dispersive x-ray detector. It was therefore concluded that the small spherulites seen in figure IV.8 were probably COM, although very many of the typical COT crystals (figure IV.7) were seen among the smaller debris.

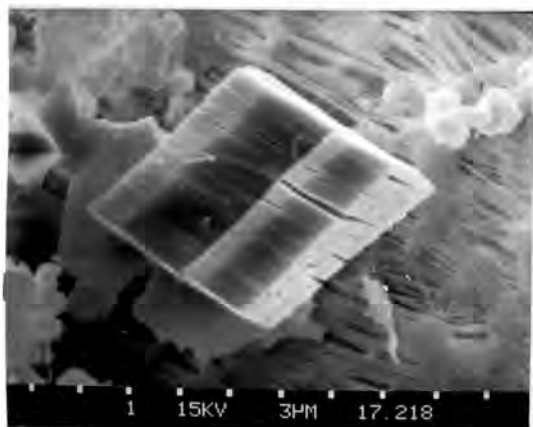


Figure IV.7. Single COT crystal (SRAU + chondroitin sulphate A, pH 5.5); Mag 3900X.

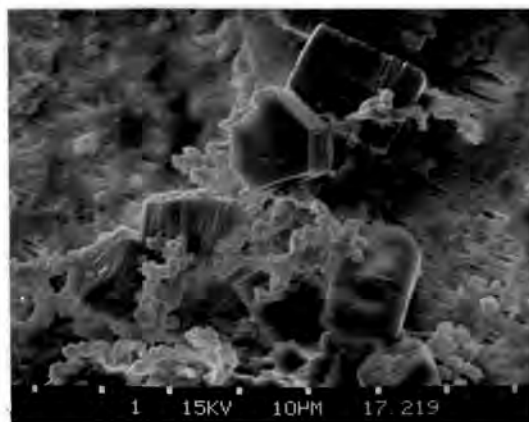
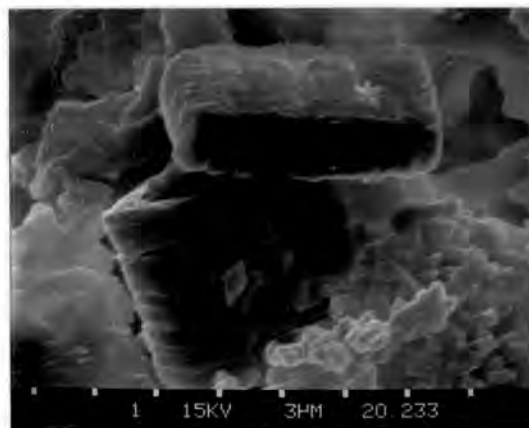
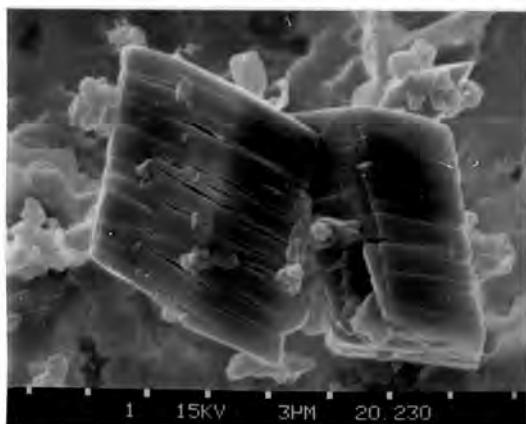


Figure IV.8. Several COT crystals surrounded by non-descript COM deposits (SRAU + chondroitin sulphate A, pH 5.5); Mag 1550X.



In series 5, the experiments conducted at pH 5.5 yielded COT and COM only. SEM studies showed that both crystal types were generally smaller (figures IV.9 and IV.10) than those precipitating from the SRAU (figures IV.2, IV.3 and IV.11).



Figures IV.9 and IV.10. COT crystals (SRAU +  $50 \text{ mg l}^{-1} \text{ F}^-$ , pH 5.5); Mag 4600X.

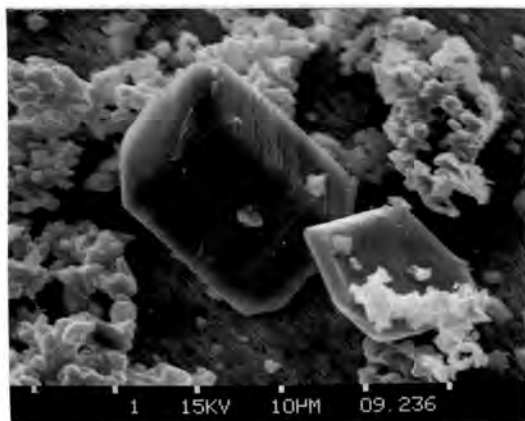
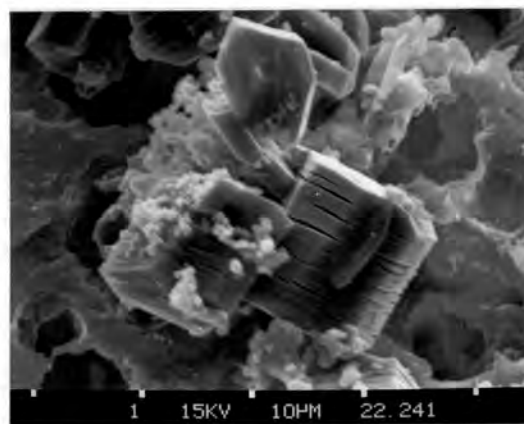
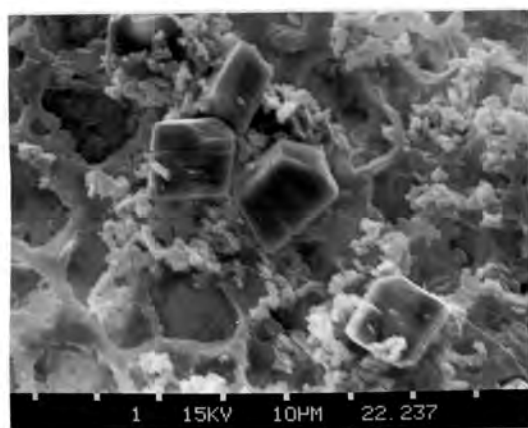


Figure IV.11. Two large COT crystals (SRAU, pH 5.5); Mag 1900X.

At pH 6.5, it was again COT and COM which were precipitated. However, amorphous halos could often be detected on the diffraction photographs. SEM studies revealed that at  $20 \text{ mg l}^{-1} \text{ F}^-$  concentrations COT crystals ( $\sim 14 \mu\text{m}$ ) occurred in small groups. These were generally admixed with a fair amount of COM debris and small deposits containing calcium and phosphorus only (probably apatite; figures IV.12 and IV.13, overleaf). At 50 and  $100 \text{ mg l}^{-1} \text{ F}^-$  concentrations, the amount of



apatite was much greater (figure IV.14) while the size of the COT crystals remained unchanged (figure IV.15).



Figures IV.12 and IV.13. COT crystals admixed with small amounts of COM and APA. Note the clean surface of the COT crystal in figure IV.13 (SRAU + 20 mg l<sup>-1</sup> F<sup>-</sup>, pH 6.5); Mags 1440X and 2500X, respectively.

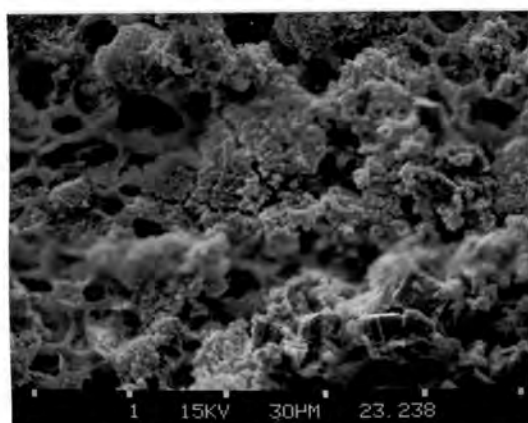


Figure IV.14. Survey picture showing profuse APA deposits (SRAU + 50 mg l<sup>-1</sup> fluoride, pH 6.5); Mag 740X.

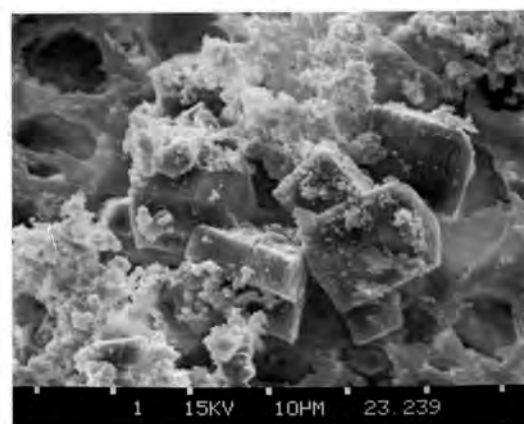


Figure IV.15. COT crystals admixed with APA deposits. Note surfaces of the former (SRAU + 50 mg l<sup>-1</sup> fluoride, pH 6.5); Mag 1770X.

#### 4. Discussion

The formation of COT in the evaporation experiments of the present study is in good agreement with the findings of Lyon et al. /LYO65/ and Gardner /GAR75/ who reported COT to be the initial phase precipitating from solutions supersaturated with respect to  $\text{CaOx}$ . Concomitant formation of COM through nucleation of the latter on the surface of the COT crystals has also been previously reported /SHE84, TOM80/. This was observed in the present study, too, as can be seen, for example, in figures IV.4 and IV.8. The absence of COT in the experiments of series 2 is thought to be due to the fact that initially formed COT readily undergoes transformation to COM /GAR76/. This transformation is completed in about a day if the precipitate is allowed to stand in contact with the mother liquor /SAN33/ and occurs much faster at elevated temperatures /NAN82/. Finlayson /FIN82/ reported a transformation half-time for COT to COM (mediated by dissolution) of ~4.5 hrs at 37°C. The precipitation of COT over almost the entire acid range in series 1 and its absence in series 2 thus again suggests that this species might be a thermodynamically unstable precursor of whewellite /TOM79/.

Although COD is frequently reported as a stone constituent, it could not be detected by XRD in any precipitate in series 1. However, small amounts of tiny COD crystals were observed in the SEM (figures IV.2, IV.3 and IV.16). Other studies have reported precipitation of COD from an artificial urine in a MSMR crystallizer /MIL76/ at much higher calcium and oxalate concentrations than those employed in the present

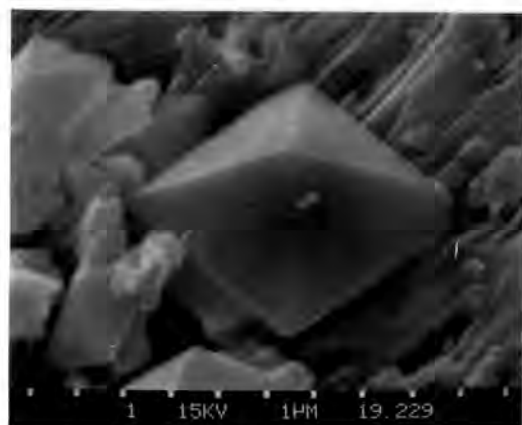


Figure IV.16. Single COD crystal  
(SRAU, pH 5.5);  
Mag 11000X.

study. These observations are in agreement with reports by Gardner et al. /GAR78, GAR78a/ that COT is the important growth phase at low and medium relative supersaturations whereas at high supersaturations the COD form is the principle growth phase.

In the present study, COD was found to be the major phase precipitating when creatinine was included in the SRAU. This might be explained by consideration of the results of Gardner and co-workers who found that various polyelectrolytes retarded the growth of COM whereas compounds of high molecular weight and charge density such as heparin inhibited COT growth /GAR78, GAR78a/. These workers also found that growth of COD was only initially retarded by these compounds. It is perhaps not unreasonable to suggest that creatinine might act in a similar way to heparin.

Urinary trace elements, amongst them magnesium in particular, are known to stabilize COD as discussed in chapter II, section 5.5.2. It is therefore not surprising that COD was formed when MgO was added to the SRAU.

The precipitation of calcium phosphates at pH values greater than 5.5 and magnesium phosphate at pH 7.5 is again in accordance with reports in the literature. For example, Elliot et al. /ELL58/ reported that BRU precipitates in the pH range 5.9-6.6, crystalline APA above 6.6 and STR above 7.2 from a urine saturated with respect to calcium phosphate.

According to Lagergren /LAG56/, brushite is easily precipitated from solutions at pH below 6. Spontaneous precipitation experiments by Pak et al. /PAK71/ showed that when the supernatant fluid was at pH 6.9 or less, the solid phase was BRU. These results are confirmed by those of the present study. Although BRU is often the first phosphate phase which precipitates over almost the entire physiological pH range, it is seldom detected in urinary stones /HER62, MOR67/. The observation that BRU also forms a thin surface layer around some APA / STR calculi /LAG56/ led to the suggestion that BRU may serve as the crystal nidus and precursor of calcium phosphate calculi /PAK71, PAK73/. It is only at high pH values, i.e. above 7.5, that the conversion of BRU to HAP is

so rapid /FRA71/, that little or none of the former is detected.

A similar role to that discussed above for BRU is thought to occur with octacalcium phosphate (OCP), the existence of which could not be definitely established at pH 5.5 and 6 in the present study. There are a number of indications that OCP acts as a precursor to other solid phases, especially hydroxyapatite (HAP). Transformation of OCP to HAP has been observed and both crystal structures have many similarities. It has been suggested that the transition layer between HAP and the aqueous phase consists of half a unit cell of OCP /YOU82/. Both OCP and BRU are known to hydrolyze to more basic calcium phosphates. Despite the fact that both compounds are more soluble than HAP /NAN82/, they nevertheless form under many physiological conditions. This is particularly the case with BRU. It has been suggested that the preferential formation of BRU (and OCP) is a kinetic phenomenon, yet the exact mechanisms allowing their precipitation are not yet known /YOU82/. One reason might be that precipitation from aqueous solutions of hydrated compounds seems to be preferred for various reasons /YOU82/.

The significance of the formation of whitlockite (WHI) in series 2 (pH range 6-7) is unclear. Although WHI is more stable than BRU or OCP, the latter compounds are favoured under most physiological conditions. However, since the conditions of series 2 more closely simulate the achievement of thermodynamic equilibrium than those of series 1, it is conceivable that under these conditions kinetic factors are not predominant and that the thermodynamically more stable phases should form. Tri-calcium phosphate (WHI) has also been suggested as a precursor of HAP formation /FRA71/. It is apparently stabilized by magnesium ions and other small bivalent cations which substitute for calcium in the crystal lattice /ALT73, TRA62/. In such cases, WHI might be even more stable than the microcrystalline HAP usually found in biological concretions. Hence its appearance in series 2.

Apatite, which is the most stable of all calcium phosphates, was found to precipitate over a wide pH range in the experiments of series 1. As early as 1932, Schleede et al. /SCH32/ showed that all calcium phosphates will eventually transform into HAP when water is allowed to flush out excess phosphate radicals from the precursors' lattices. This

early observation might also explain why APA is usually the only calcium phosphate which is co-precipitated with struvite (STR), since the latter captures most of the phosphate, leaving little for the formation of other calcium phosphates. Since APA is often found admixed with calcium oxalate and struvite, thereby suggesting its formation under a variety of conditions, it is not surprising that it occurred over a wide pH range in the present study.

In the urinary tract, struvite crystals form primarily as a result of urease-induced alkalinity in infected urines. The necessity of a high ammonia concentration for the precipitation of STR is clearly demonstrated in the present study where STR formed only at pH values greater than 7.5. Indeed, in a few instances, the pH adjustment of the SRAU with concentrated ammonia solution resulted in immediate precipitation of STR. Localized turbidity was observed even when  $\text{NH}_4\text{OH}$  was added dropwise. This only disappeared after prolonged stirring. The dramatic increase in precipitated mass with increasing pH also suggests that once the formation of STR (and APA) has started, all available ions are incorporated into the respective lattices. In one case, a 200 ml aliquot of SRAU (pH 6.5) was refrigerated for several months. A large STR crystal (0.5 mm) was observed after filtration of this solution (figure IV.17).



Figure IV.17. Large STR crystal (SRAU, pH 6.5).

In the experiments where uric acid (UA) was added to the SRAU (series 3), uric acid dihydrate (UAD) was identified as the major compound precipitated. These evaporations were carried out under condi-

tions which fulfilled the 2 major requirements of uric acid stone formation. In the first instance, the SRAU pH was kept below 6.0 while in the second a high concentration of uric acid ( $480 \text{ mg l}^{-1}$ ) was present. (The solubility of UA in water is only  $65 \text{ mg l}^{-1}$  /GUD09/ but somewhat higher in urine). That the dihydrate and not the anhydrous UA is formed is further confirmation of the hypothesis that hydrated species are 'easier' to precipitate from aqueous solutions (cf. discussion of brushite and octacalcium phosphate in this section). However, UAD is seldom found in calculi where its detection is certainly hampered by its spontaneous dehydration to the thermodynamically more stable anhydrous acid /HES75/. Börner et al. /BOE81/ reported that it is mostly high molecular weight ( $M > 20000$ ) organic substances found in human urine that decrease the incidence of UAD in stones. Since no organic substances (besides UA) were present in the SRAU, the sole precipitation of UAD in series 3 tends to support this idea.

The effect of urea on  $\text{CaOx}$  crystallization is not yet clear. From the general SEM observation in the present study that COT crystals were smaller and occurred only singly when compared with control experiments, it is concluded that urea might show slight solubilizing action. Medes et al. /MED32/ and Miller et al. /MIL58/ reported that the peptizing action of urea might be a factor in increasing the solubility of calcium oxalate in urine, causing a 'supersolubility' of this compound in urine relative to water. Support for this hypothesis was provided by Hartung et al. /HAR76/ who used Coulter counter techniques to show that urea has an inhibitory effect on  $\text{CaOx}$  crystal growth. On the other hand, Finlayson et al. /FIN72/ believe that the effect of urea on divalent ion activity is sufficiently small to justify its omission from first order considerations. Further experiments are therefore needed to clarify the extent to which urea plays a role in  $\text{CaOx}$  formation.

The SEM study of crystals from the SRAU containing methylene blue showed the presence of only few particles. As yet unpublished results by Rodgers et al. of Coulter counter studies have shown that the particle size distribution of solutions containing methylene blue are not different to that of control experiments. It is therefore concluded that methylene blue reduces nucleation rates rather than growth rates.



This confirms observations by Drach et al. /DRA78/ and Miller et al. /MIL76/.

Similar low particle counts and no change in particle size distribution were observed in artificial urines to which chondroitin sulphate A was added (unpublished, Rodgers et al.). Chondroitin sulphates belong to the wide range of mucopolysaccharides (glycosaminoglycans) which are thought to possess some inhibitory activity in urine. In the present study, however, no particular effect on CaOx growth could be established, although total precipitated mass was somewhat lower when compared with control experiments.

The addition of another known inhibitor, MgO, to the SRAU also decreased the amount of precipitate. Crystals were also somewhat smaller than in other precipitates. These results thus confirm a recent study which reported that Mg considerably decreased nucleation and growth rates of COT /LI85/. Magnesium is a well known inhibitor of CaOx precipitation (see chapter II, section 5.5.2). The mechanism by which this is thought to occur is via complexation of oxalate, which lowers the activity of this ion. Oxalate has been shown to be about 16 times more effective in increasing CaOx supersaturation than calcium ions in urine-like solutions /LIN86/. A small decrease in free oxalate thus has a pronounced effect on CaOx precipitation.

The appearance of smaller COT and COD crystals in the SRAU solutions spiked with high concentrations of fluoride relative to the control SRAU suggests a growth retardation process. These crystals were, however, larger than any of those observed in series 4. Therefore, inhibition of growth is weakest in the case of fluoride.

It was generally observed by SEM that the COT crystals in this series were of a superior quality to those observed in the control-SRAU. This can be seen by comparison of figures IV.9 and IV.10 with IV.11. It is interesting to note that high fluoride concentrations have been reported as increasing the crystallinity of bone apatite /ZIP62/ and carbonate apatite /HES78/, as mentioned in chapter III, section 5.

The amorphous halos observed at pH 6.5 and referred to in section

3, may be explained by the detection of APA as revealed in the SEM. It would seem that the amount of APA precipitating in these experiments increases with increasing fluoride concentration. This is well illustrated by comparison of figures IV.13 with IV.15. The former shows the typically 'clean' surfaces observed at  $20 \text{ mg l}^{-1} \text{ F}^{-}$  concentration, while the latter is typical of the surfaces encrusted with APA at higher  $\text{F}^{-}$  concentrations. It is therefore suggested that fluoride favours APA deposition with increasing concentrations (at pH 6.5). This agrees with the observation that the orderly deposition of apatite is enhanced at greater fluoride concentrations /MEY72/, as mentioned in chapter III, section 5.

The identification of APA by XRD in the control-SRAU but the failure of this technique to detect APA at high fluoride concentrations, appears at first glance to be contradictory to the afore-mentioned improved crystallinity of APA in the presence of fluoride /HES78, ZIP62/. However, Christoffersen et al. have demonstrated that there exists a maximum value of fluoride concentration above which partly demineralized tooth enamel cannot be successfully repaired /CHR84/. Since the fluoride concentrations of the present study were exceedingly high, it is suggested that a similar mechanism is operative here.

The results of the series of experiments conducted in the present study suggest that the fast evaporator provides a simple, yet very useful means for studying the crystallization characteristics of urine solutions. By employing a simple inorganic standard reference artificial urine almost all of the important crystalline compounds found in urinary stones were produced by simply varying pH and saturation of the solution. Using XRD and SEM procedures, it is apparent that all three hydrates of calcium oxalate are simultaneously formed to varying extents in the evaporation experiments. It has also been shown that the effect of inhibitors can be conveniently studied with this experimental set-up.

The present experimental approach to the physico-chemical characterization of crystal formation in urines was paralleled by another research group of the University of Cape Town on a theoretical basis



/LIN86, LIT84/. This group has developed an equilibrium speciation computer model which accurately predicts the precipitation of CaOx, BRU and APA under various conditions. For STR, however, experimental results and theoretical predictions do not agree in the acidic pH range. It was therefore possible to compare the results of the present study with the theoretical model on the basis that the precipitates from the evaporated SRAU correspond to the calculated level of precipitation (supersaturation) in the computer model. The programme MINEQL /WES75/ was therefore executed using input concentrations twice as large as those listed in table IV.2. This was necessary to match the theoretical (equilibrium) concentrations with those achieved in the experiment after evaporation of 50% of the initial SRAU volume. The pH was held constant in each computation. Of the 14 potential solids considered in the computer simulations /LIN86/, the model predicted four precipitates, all of which were observed experimentally, viz., COM, BRU, APA and STR. Linder's "intermediate model" takes into account certain kinetic factors and describes a quasi-equilibrium state of the urine /LIN86/. When this model was used, the prediction of experimentally found calcium salts as a function of pH was almost perfect (table IV.3).

Table IV.3. Experimentally observed and predicted precipitations from simulated urine solutions.

pH	intermediate computer model	experiment
4.0	COM	COT COM
5.0	COM BRU	COT COM
5.5	COM BRU STR	COT COM BRU APA
6.0	COM BRU HAP STR	COT BRU APA
6.5	COM BRU HAP STR	COT BRU APA
7.0	BRU HAP STR	BRU APA (STR)
8.0	BRU HAP STR	BRU APA STR

The agreement for STR is not, however, favourable. Kinetic factors, as yet not included in the theoretical model are the possible cause of the discrepancy /LIN86/.

In the SRAU containing UA, the theoretical model predicted the precipitation of COM, BRU, HAP and UA at pH 5.5 /LIN86/. UAD, which had not been included as a species in the model, was experimentally found to be the major solid in the precipitate. COD and COT (and COM?) were also found to be present. Thus, although BRU and HAP were predicted by the model, they were not experimentally detected. In this case, epitaxial considerations might explain the dissimilarity. It is well known, that COD and UA on the one hand and UA and UAD on the other, have many matches of their crystal lattices where the misfit at the atomic level is smaller than 15% /MAN81/. Hence, it is conceivable that COD grows epitaxially on uric acid crystallites at a much faster rate than would be predicted by equilibrium considerations. This process could then be regarded as capturing sufficient calcium to make the SRAU unsaturated with respect to calcium phosphates such as BRU and HAP.

On the whole, the equilibrium speciation model proposed by Linder et al. /LIN86/ yields satisfactory results. However, contrary to their statement /LIN86/, calcium oxalate trihydrate was identified in the precipitates from standard reference artificial urines of pH 7 and lower /ROD85/. Their argument that the COT-to-COM transformation is too rapid for the detection of COT is also not valid. Finlayson /FIN82/ reported a transformation half time of 4.5 hrs for these species in experiments where the COT crystals were allowed to remain in contact with the mother liquor. In air, it is considerably slower and largely dependent on ambient temperature and humidity. In the present study, evaporations never lasted longer than 70 minutes and precipitates were analysed immediately after filtration. Complete transformation of COT to COM is therefore unlikely to have occurred.

Although COT and COM were observed to precipitate in the pH range 3-7 and 3-5.5, respectively, the computer model predicts their precipitation in the pH range 4-5.5 and 4-7, respectively (in equilibrium). This discrepancy might be explained on the basis of simple equilibrium considerations. Since the experimental system is not 'at equilibrium' it is suggested that over a long enough period, the transformation of COT to COM could occur (cf. series 2). In such a case, theoretical predictions and experimental results would agree. This supports the

hypothesis that "the overall process of formation of calcium oxalate [calculi] is the result of competitive kinetic processes such as nucleation, crystal growth, dissolution, and transformation" /NAN82/.

### Concluding comments

In concluding this thesis, there are two aspects to be considered:

- (i) to what extent have the objectives, outlined in the Introduction been achieved, and
- (ii) has the project made contributions to existing knowledge in the field of urolithiasis studies?

The first objective was to review and test existing quantitative x-ray diffraction procedures and, further, to adapt and / or possibly develop new such approaches in the hope of establishing well defined guidelines for other researchers. As a result of the investigations carried out in this study a 'reference intensity ratio' method which had been used only once before in the analysis of calculi, is now fully described. Similarly a micro-analytical procedure, previously used for the determination of quartz in mine dust, has now been successfully adapted and tested for application in urinary stone analysis.

The procedures developed in the present study for the application of ICP-AES in the analysis of calculi are definitive and easily followed and, together with the description of a microwave assisted digestion procedure, will enable investigators to simultaneously determine major and minor elements using the same sample.

The 'covariance biplot' statistical treatment of the ICP data represents an extremely exciting new approach in assessing stone analysis results. Indeed, such an approach might be of some interest to epidemiologists involved in studying stone trends.

The determination of fluoride in urinary calculi has been attempted by several workers in the past with varying degrees of success. Clearly emerging from these studies has been the need for an in-depth assessment of existing techniques and the development of a method that can be universally applied. As with the studies of XRD and ICP-AES, the present research has yielded a procedure which largely satisfies this need. Experimental details for this diffusion technique have been

thoroughly investigated in the present study and have been successfully applied.

The fourth objective was to conduct a series of crystallization experiments in a rotary evaporator in order to assess the value of this approach in acquiring meaningful data. The results of these experiments clearly support the findings of other workers and show that the procedure represents a satisfactory model for studying urinary crystallization phenomena. The present study has established that the role of several physico-chemical factors such as pH, solution composition, constituent concentrations, etc., can be easily studied using such a model. In addition, the important role of inhibitors and promoters of urinary crystallization can be monitored while nucleation, growth and aggregation mechanisms can be studied.

It can thus be stated that the objectives defined for this research project have been achieved. Furthermore it is not unreasonable to suggest that the various results of this study will be of benefit to other scientists involved in the study of urolithiasis.



## References

## 1. Introduction

- /ALK66/ Alken, C.E.  
Gedanken zur Klinik der Nephrolithiasis  
Urologe 5(4), 161, 1966
- /ALK82/ Alken, C.E.  
Urology: guide for diagnosis and therapy  
Thieme, Stuttgart, 1982, pp. 253-276
- /BAC83/ Bach, D.; Hesse, A.; Feuereisen, B.; Vahlensieck, W.; Joost, J.; Lehmann, H.-D.; Wegner, G.  
Optimierung der konservativen Harnstein-Austreibung  
Fortschr. Med. 101(8), 337-342, 1983
- /BAK66/ Baker, G.; Grubb, P.L.  
Unusual vesical calculi of whewellite  
Br. J. Urol. 38, 510-521, 1966
- /BAR74/ Barker, L.M.; Pallante, S.L.; Eisenberg, H.; Joule, J.A.; Becker, G.L.; Howard, J.E.  
Simple synthetic and natural urines have equivalent anticalcifying properties  
Invest. Urol. 12(1), 79-81, 1974
- /BAS74/ Bastian, H.P.; Gebhardt, M.  
The varying composition of the nucleus and peripheral layers of urinary calculi  
Urol. Res. 2, 91-95, 1974
- /BEE64/ Beeler, M.F.; Veith, D.A.; Morriss, R.H.; Biskind, G.R.  
Analysis of urinary calculi - comparison of methods  
Am. J. Clin. Pathol. 41(5), 553-560, 1964
- /BEI55/ Beischer, D.E.  
Analysis of renal calculi by infrared spectroscopy  
J. Urol. 73(4), 653-659, 1955
- /BER68/ Berényi, M.; Liptay, E.; Babics, A.  
Thermoanalytische Untersuchungen von Nierensteinen - II. Kalzium- und magnesiumhaltige Steine  
Z. Urol. 61(4), 209-216, 1968
- /BER73/ Berényi, M.  
New methods of stone analysis  
Urinary Calc. Proc. Int. Symp. 1972, (Publ. 1973), pp. 209-212
- /BER78/ Bertin, E.P.  
Introduction to x-ray spectrometric analysis  
Plenum Press, New York, 1978
- /BLA81/ Blaschke, R.; Leusmann, D.B.; Meyer-Jürgens, U.B.; Tölle, E.  
REM-Analyse von Harnkonkrementen und ihre Bedeutung für die urologische Praxis  
Beitr. elektronenmikroskop. Direktabb. Oberfl. 14, 581-592, 1981

- /BLA82/ Blacklock, N.J.  
Epidemiology of urolithiasis  
in: D.A. Williams, G.D. Chisholm (Eds.); "Scientific foundations of urology, vol. I"; William Heinemann Medical Books, London, 1982, pp. 235-243
- /BOY54/ Boyce, W.H.; Garvey, F.K.; Norfleet, C.M.  
Ion-binding properties of electrophoretically homogeneous mucoproteins of urine in normal subjects and in patients with renal calculus disease  
J. Urol. 72(6), 1019-1031, 1954
- /BOY55/ Boyce, W.H.; Garvey, F.K.; Norfleet, C.M. Jr.  
The metal chelate compounds of urine  
Am. J. Med. 19(1), 87-95, 1955
- /BOY56/ Boyce, W.H.; Garvey, F.K.  
The amount and nature of the organic matrix in urinary calculi: review  
J. Urol. 76(3), 213-227, 1956
- /BOY59/ Boyce, W.H.; King, J.S. Jr.  
Crystal-matrix interrelations in calculi  
J. Urol. 81(3), 351-365, 1959
- /BOY63/ Boyce, W.H.; King, J.S. Jr.  
Present concepts concerning the origin of matrix and stones  
Ann. N. Y. Acad. Sci. 104, 563-578, 1963
- /BRO81/ Brockis, J.G.; Finlayson, B. (Eds.)  
Urinary calculus - International urinary stone conference, Perth, Australia, 1979  
PSG Publishing Comp., Littleton, Mass., USA, 1981
- /BUS68/ Busby, D. E.  
Space clinical medicine - 9. Urinary calculus  
Space Life Sci. 1, 279-299, 1968
- /BUT56/ Butt, A.J.  
Historical survey of etiologic factors in renal lithiasis  
in: A.J. Butt (Ed.); "Etiologic factors in renal lithiasis"; C.C. Thomas, Springfield, Ill., USA, 1956, pp. 3-47
- /CIA58/ Clarke, E.S.  
Renal calculi - A history of the stone  
Hosp. Med. 2(June), 1054-1057, 1968
- /DOS74/ Dosch, W.; Altmann, K.  
Aussagemöglichkeiten und technischer Aufwand verschiedener Methoden der Harnsteinanalyse  
Fortschr. Urol. Nephrol. 4, 1-24, 1974
- /ENG84/ Englehardt, S.L.  
Stosswellen statt Skalpel - Neue Techniken gegen Nierensteine  
Das Beste aus Reader's Digest, German Ed., February 1984, pp. 160-170
- /FIN61/ Finlayson, B.; Vermeulen, C.W.; Stewart, E.J.  
Stone matrix and mucoprotein from urine  
J. Urol. 86(4), 355-363, 1961
- /FIN72/ Finlayson, B.; Meyer, A.S.  
Stone ultrastructure  
in: B. Finlayson, L. Hench, L.H. Smith (Eds.); "Urolithiasis: physical aspects - Proceedings of a Conference of the Medical Sciences"; Natl. Acad. Sci., Washington, 1972, pp. 115-123



- /FIN74/ Finlayson, B.  
Renal lithiasis in review  
Urol. Clin. N. Am. 1(2), 181-212, 1974
- /FIN77/ Finlayson, B.  
Calcium stones: some physical and clinical aspects  
in: D.S. David (Ed.); "Calcium metabolism in renal failure and nephrolithiasis"; J. Wiley & Sons, New York, 1977, pp. 337-383
- /FIN78/ Finlayson, B.  
Physicochemical aspects of urolithiasis  
Kidney Int. 13, 344-360, 1978
- /FLE76/ Fleisch, H.; Robertson, W.G.; Smith, L.H.; Vahlensieck, W. (Eds.)  
Urolithiasis research - Proceedings of the international symposium on urolithiasis research, Davos, Switzerland, 1976  
Plenum Press, New York, 1976
- /FLE78/ Fleisch, H.  
Inhibitors and promoters of stone formation  
Kidney Int. 13, 361-371, 1978
- /GEB/ Gebhardt, M.  
Harnsteine  
Series 'Info-Dienst Harnsäurestoffwechsel', Deutsche Wellcome, Burgwedel, FRG, n.d.
- /GIL76/ Gill, W.B.; Karesh, J.W.  
Demonstration of protective (inhibitory) effects of urinary macromolecules on the crystallization of calcium oxalate  
Urolithiasis Res. Proc. Int. Symp., 3rd, 1976, pp. 277-280
- /GRI73/ Grieve, J.; Zarembski, P.M.  
Infrared spectroscopy in the clinical analysis of renal stones  
Urinary Calc. Proc. Int. Symp. 1972, (Publ. 1973), pp. 231-236
- /GUN68/ Gundlach, G.  
Symposium zur Erforschung der Nierensteine  
Urologe 7(6), 353-354, 1968
- /HAL79/ Hallson, P.C.; Rose, G.A.  
Uromucoids and urinary stone formation  
Lancet 1, 1000-1002, 1979
- /HES72/ Hesse, A.; Schneider, H.-J.; Hienzsch, E.  
Die infrarotspektroskopische Harnsteinanalyse  
Dtsch. Med. Wochenschr. 97(44), 1694-1701, 1972
- /HES77/ Hesse, A.; Dietze, H.-J.; Berg, W.; Hienzsch, E.  
Mass spectrometric trace element analysis of calcium oxalate uroliths  
Eur. Urol. 3, 359-361, 1977
- /HES81/ Hesse, A.; Röhle, G.; Voigt, U.  
Qualitätskontrolle von Harnsteinanalysen - Ergebnisse von zwei Ringversuchen  
Fortschr. Urol. Nephrol. 17, 306-310, 1981
- /HES81a/ Hesse, A.; Hicking, W.; Vahlensieck, W.  
Harnsteinanalyse und ihre diagnostische Bedeutung  
GIT Labor-Med. 4, 19-27, 1981

- /HES81b/ Hesse, A.; Hicking, W.; Bach, D.; Vahlensieck, W.  
Characterisation of urinary crystals and thin polished sections of urinary calculi by means of an optical microscopic and scanning electron microscopic arrangement  
Urol. Int. 36, 281-291, 1981
- /HES82/ Hesse, A.; Bach, D.  
Harnsteine: Pathobiochemie und klinisch-chemische Diagnostik  
Thieme, Stuttgart, 1982, pp. 111-122
- /HES82a/ op. cit., pp. 98-99
- /HES82b/ op. cit., pp. 123-149
- /HES82c/ op. cit., pp. 100-111
- /HES82d/ Hesse, A.; Molt, K.  
Technik der infrarotspektroskopischen Harnsteinanalyse  
J. Clin. Chem. Clin. Biochem. 20, 861-873, 1982
- /HES83/ Hesse, A.; Vahlensieck, W.  
Indizienbeweise durch die Harnsteinstruktur  
Forsch. - Mitteil. Dtsch. Forschungsgem. (2), 6-8, 1983
- /HOD69/ Hodgkinson, A.; Peacock, M.; Nicholson, M.  
Quantitative analysis of calcium-containing urinary calculi  
Invest. Urol. 6(6), 549-561, 1969
- /JEN70/ Jenkins, R.; De Vries, J.L.  
Practical x-ray spectrometry (2nd Ed.)  
MacMillan, London, 1970
- /KEY23/ Keyser, L.D.  
The mechanism of the formation of urinary calculi  
Ann. Surg. 77, 210-222, 1923
- /KLE80/ Kleeman, C.R.; Coburn, J.W.; Brickman, A.S.; Lee, D.B.N.; Narins, R.G.; Ehrlich, R.M.  
Kidney stones  
West J. Med. 132(4), 313-332, 1980
- /KLI74/ Klinger, G.; Hesse, A.  
Infrarotspektroskopische Untersuchungen zur chemischen Struktur und zum Kristallisationsgrad von Zahnhartsubstanzen  
Dtsch. Stomatol. 24(7), 441-447, 1974
- /KOU80/ Koutsoukos, P.G.; Lam-Erwin, C.Y.; Nancollas, G.H.  
Epitaxial considerations in urinary stone formation - I. The urate-oxalate-phosphate system  
Invest. Urol. 18(2), 178-184, 1980
- /KOU81/ Koutsoukos, P.G.; Sheehan, M.E.; Nancollas, G.H.  
Epitaxial considerations in urinary stone formation - II. The oxalate-phosphate system  
Invest. Urol. 18(5), 358-363, 1981
- /LEA77/ Leal, J.J.; Finlayson, B.  
Adsorption of naturally occurring polymers onto calcium oxalate crystal surfaces  
Invest. Urol. 14(4), 278-283, 1977

- /LEU81/ Leusmann, D.B.  
Erste zusammenfassende Ergebnisse der kombinierten Phasen- und Gefügeanalyse von Harnsteinen mittels Röntgenbeugung und Rasterelektronenmikroskopie  
Fortschr. Urol. Nephrol. 17, 275-305, 1981
- /LIP67/ Liptay, G.; Berényi, M.  
Untersuchung von Harnsteinen mit Hilfe eines neuen analytischen Verfahrens  
Z. klin. Chem. klin. Biochem. 5(4), 188-190, 1967
- /LON68/ Lonsdale, K.  
Human stones  
Sci. Am., December 1968, pp. 104-111
- /LON68a/ Lonsdale, K.  
Human stones  
Science (Washington) 159(3820), 1199-1207, 1968
- /LON68b/ Lonsdale, K.  
Epitaxy as a growth factor in urinary calculi and gallstones  
Nature (London) 217, 56-58, 1968
- /MAL77/ Malek, R.S.; Boyce, W.H.  
Observations on the ultrastructure and genesis of urinary calculi  
J. Urol. 117(3), 336-341, 1977
- /MAN80/ Mandel, N.S.; Mandel, G.S.  
Epitaxis between stone-forming crystals at the atomic level  
in: F. Coe, B. Brenner, J. Stein (Eds.); "Nephrolithiasis"; Churchill Livingstone, New York, 1980, pp. 37-58
- /MAU69/ Maurer, C.  
Analysengang zur Beurteilung der quantitativen Zusammensetzung von Harnkonkrementen  
Urologe 8(4), 189-193, 1969
- /MCC73/ McConville, B.E.  
Activation analysis of renal calculi  
Urinary Calc. Proc. Int. Symp. 1972, (Publ. 1973), pp. 275-279
- /MCC80/ McConville, B.E.  
Investigations using autoradiographic analysis of urinary stones  
Br. J. Urol. 52, 243-244, 1980
- /MEY29/ Meyer, J.  
Über die Ausfällung von Sedimenten und die Bildung von Konkrementen in den Harnwegen  
Z. klin. Med. 111, 613-687, 1929
- /MEY71/ Meyer, A.S.; Finlayson, B.; DuBois, L.  
Direct observation of urinary stone ultrastructure  
Br. J. Urol. 43, 154-163, 1971
- /MEY75/ Meyer, J.L.; Bergert, J.H.; Smith, L.H.  
Epitaxial relationships in urolithiasis: the calcium oxalate monohydrate-hydroxyapatite system  
Clin. Sci. Mol. Med. 49(5), 369-374, 1975
- /MEY76/ Meyer, J.L.; Bergert, J.H.; Smith, L.H.  
The epitaxially induced crystal growth of calcium oxalate by crystalline uric acid  
Invest. Urol. 14(2), 115-119, 1976

- /MOD69/ Modlin, M.  
Renal calculus in the Republic of South Africa  
Proc. Renal Stone Res. Symp. 1968, (Publ. 1969), pp. 49-58
- /MOD80/ Modlin, M.  
A history of urinary stone  
S. Afr. Med. J. 58(16), 652-655, 1980
- /MOD81/ Modlin, M.  
Why analyse renal stones?  
S. Afr. Med. J. 59(10), 318-319, 1981
- /MOD81a/ Modlin, M.; Davies, P.J.  
The composition of renal stones analysed by infrared spectroscopy  
S. Afr. Med. J. 59(10), 337-341, 1981
- /MUL62/ Mulvaney, W.P.; Henning, D.C.  
Solvent treatment of urinary calculi: refinements in technique  
J. Urol. 88(2), 145-149, 1962
- /NAN76/ Nancollas, G.H.  
The kinetics of crystal growth and renal stone-formation  
Urolithiasis Res. Proc. Int. Symp., 3rd, 1976, pp. 5-23
- /NAN83/ Nancollas, G.H.  
The mechanism of formation of renal stone crystals  
Proc. Eur. Dial. Transplant. Assoc. 20, 386-397, 1983
- /NOR72/ Nordin, B.E.C.  
Pathogenesis and treatment of calcium stone disease  
Br. J. Urol. 44, 729, 1972
- /OGB81/ Ogbuji, L.U.; Finlayson, B.  
Crystal morphologies in whewellite stones: electron microscopy  
Invest. Urol. 19(3), 182-186, 1981
- /OTT67/ Otto, H.; Ihmann, E.  
IR (Infrarot)-spektrografische Untersuchungen von 700 Harnwegskonkrementen  
Frankf. Z. Pathol. 77, 262-268, 1967
- /PAK75/ Pak, C.Y.C., Ohata, M.; Holt, K.  
Effect of diphosphonate on crystallization of calcium oxalate in vitro  
Kidney Int. 7, 154-160, 1975
- /PAK76/ Pak, C.Y.C.; Hayashi, Y.; Arnold, L.H.  
Heterogeneous nucleation with urate, calcium phosphate and calcium oxalate  
Proc. Soc. Exp. Biol. Med. 153(664), 83-87, 1976
- /PAK76a/ Pak, C.Y.C.  
Disorders of stone formation  
in: B.M. Brenner, F.C. Rector Jr. (Eds.); "The kidney, vol. II"; W.B. Saunders, Philadelphia, Pa., USA, 1976, pp. 1326-1354
- /PAT80/ Paternain, J.L.; Bernshtam, J.; Pinto, B.  
Isolation of a mucoprotein possessing mineral nucleating activity  
Invest. Urol. 18(2), 119-122, 1980
- /PHI58/ Philipsborn, H. von  
Zur Harnsteinbildung aus der Sicht des Mineralogen  
Urol. Int. 7, 28-47, 1958
- /PRI41/ Prien, E.L.  
The use of polarized light in the analysis of calculi and the study of crystals in tissue: a preliminary report on the method employed  
J. Urol. 45(5), 765-769, 1941

- /PRI47/ Prien, E.L.; Frondel, C.  
Studies in urolithiasis - I. The composition of urinary calculi  
J. Urol. 57(6), 949-994, 1947
- /PRI55/ Prien, E.L.  
Studies in urolithiasis - III. Physico-chemical principles in stone formation and prevention  
J. Urol. 73(4), 627-652, 1955
- /PRI74/ Prien, E.L. Sr.  
The analysis of urinary calculi  
Urol. Clin. N. Am. 1(2), 229-240, 1974
- /RAA63/ Raaflaub, J.  
Komplexchemische Grundlagen der Harnsteingenesse  
Helv. Med. Acta 30(6), 724-755, 1963
- /RAN42/ Randall, A.  
Analysis of urinary calculi through the use of the polarizing microscope  
J. Urol. 48(6), 642-649, 1942
- /ROB60/ Robinson, J.W.  
Atomic absorption spectroscopy  
Anal. Chem. 32(8), 17A-29A, 1960
- /ROB76/ Robertson, W.G.; Knowles, F.; Peacock, M.  
Urinary acid mucopolysaccharide inhibitors of calcium oxalate crystallization  
Urolithiasis Res. Proc. Int. Symp., 3rd, 1976, pp. 331-334
- /ROD81/ Rodgers, A.; Spector, M.  
Human stones  
Endeavour 5(3), 119-126, 1981
- /ROD81a/ Rodgers, A.L.; Nassimbeni, L.R.; Mulder, K.J.; Mullins, J.  
Use of a density gradient column in the analysis of urinary calculi  
Invest. Urol. 19(3), 154-156, 1981
- /ROD81b/ Rodgers, A.L.; Mezzabotta, M.; Mulder, K.J.; Nassimbeni, L.R.  
Application of several physical techniques in the total analysis of a canine urinary calculus  
J. S. Afr. Vet. Assoc. 52(2), 139-142, 1981
- /ROD81c/ Rodgers, A.L.  
Analysis of renal calculi by x-ray diffraction and electron microprobe: a comparison of two methods  
Invest. Urol. 19(1), 25-28, 1981
- /ROD82/ Rodgers, A.L.; Nassimbeni, L.R.; Mulder, K.J.  
A multiple technique approach to the analysis of urinary calculi  
Urol. Res. 10(4), 177-184, 1982
- /ROS76/ Rose, G.A.; Woodfine, C.  
The thermogravimetric analysis of renal stones (in clinical practice)  
Br. J. Urol. 48, 403-412, 1976
- /RUT61/ Rutishauser, G.; Heusser, H.; Grütter, O.; Schwander, H.  
Zur chemolytischen Behandlung von Harnwegskonkrementen  
Schweiz. Med. Wochenschr. 91(46), 1362-1366, 1961
- /SAG78/ Sagebiel, W.; Gjavotchanoff, S.  
Harnsteinanalyse heute  
Arztl. Lab. 24, 21-27, 1978

- /SCH67/ Schneider, H.-J.  
Die medikamentöse Therapie der Nephrolithiasis  
Z. ärztl. Fortbild. 61(22), 1113-1118, 1967
- /SCH71/ Schneider, H.-J.; Hesse, A.  
Zur Problematik der Harnsteinanalyse - Teil I  
Zentralbl. Pharm. 110(4), 379-386, 1971
- /SCH71a/ Schneider, H.-J.  
Zur Problematik der Harnsteinanalyse - Teil II  
Zentralbl. Pharm. 110(4), 387-392, 1971
- /SCH73/ Schneider, H.-J.; Berényi, M.; Hesse, A.; Tschamke, J.  
Comparative stone analysis - Quantitative chemical, x-ray diffraction, infrared spectroscopy and thermoanalytical procedures  
Int. Urol. Nephrol. 5(1), 9-17, 1973
- /SCH85/ Schuille, P.O.; Smith, L.H.; Robertson, W.G.; Vahlensieck, W. (Eds.)  
Urolithiasis and related clinical research  
Plenum Press, New York, 1985
- /SMI81/ Smith, L.H.; Robertson, W.G.; Finlayson, B. (Eds.)  
Urolithiasis, clinical and basic research - Proceedings of the fourth international symposium on urolithiasis research, Williamsburg, Virginia, USA, 1980  
Plenum Press, New York, 1981
- /SNA36/ Snapper, I.; Bendien, W.M.; Polak, A.  
Observations on the formation and prevention of calculi  
Br. J. Urol. 8, 337-345, 1936
- /SPE76/ Spector, M.; Garden, N.M.; Rous, S.N.  
Ultrastructural features of human urinary calculi  
Urolithiasis Res. Proc. Int. Symp., 3rd, 1976, pp. 355-359
- /STR66/ Strates, B.S.  
Use of thermal gravimetry in the study of nephroliths  
Experientia 22(9), 574-575, 1966
- /STR69/ Strates, B.; Georgacopoulou, C.  
Derivatographic thermal analysis of renal tract calculi  
Clin. Chem. 15(4), 307-311, 1969
- /SUT71/ Sutor, D.J.  
Crystallographic studies on the formation of renal calculi  
Biochem J. 122, 6P-7P, 1971
- /THO75/ Thomas, W.C. Jr.  
Clinical concepts of renal calculous disease  
J. Urol. 113, 423-432, 1975
- /TOZ81/ Tozuka, K.; Konjiki, T.; Sudo, T.  
Chemical test of phosphates in urinary stones by means of the chromatographic contact print method  
Br. J. Urol. 53, 216-220, 1981
- /TSA61/ Tsay, Y.C.  
Application of infrared spectroscopy to analysis of urinary calculi  
J. Urol. 86(6), 838-854, 1961
- /VAH79/ Vahlensieck, W.  
Epidemiologie  
in: W. Vahlensieck (Ed.); "Urolithiasis 1"; Springer, Berlin, 1979;  
Preprint 'Info-Dienst', Dtsch. Wellcome, pp. 1-8

- /VER51/ Vermeulen, C.W.; Pagins, H.D.; Grove, W.J.; Goetz, R.  
Experimental urolithiasis III - Prevention and dissolution of calculi by alteration of urinary pH  
J. Urol. 66(1), 1-5, 1951
- /VER65/ Vermeulen, C.W.; Lyon, E.S.; Fried, F.A.  
On the nature of the stone-forming process  
J. Urol. 94(2), 176-186, 1965
- /VER65a/ Vermeulen, C.W.; Fried, F.A.  
Observations on dissolution of uric acid calculi  
J. Urol. 94(3), 293-296, 1965
- /VER66/ Vermeulen, C.W.; Ellis, J.E.; Te-Chin, H.  
Experimental observations on the pathogenesis of urinary calculi  
J. Urol. 95(5), 681-690, 1966
- /WEI59/ Weissman, M.; Klein, B.; Berkowitz, J.  
Clinical application of infrared spectroscopy: analysis of renal tract calculi  
Anal. Chem. 31(8), 1334-1338, 1959
- /ZIO77/ Ziolkowski, F.; Perrin, D.D.  
Dissolution of urinary stones by calcium-chelating agents  
Invest. Urol. 15(3), 208-211, 1977

## 2. Chapter I

- /AGA37/ Agafonova, T.N.  
Quantitative mineralogical x-ray analysis  
C. R. (Dokl.) Acad. Sci. URSS 16(7), 367-369, 1937
- /ALB82/ Albinati, A.; Willis, B.T.M.  
The Rietveld method in neutron and x-ray powder diffraction  
J. Appl. Crystallogr. 15(4), 361-374, 1982
- /ALE48/ Alexander, L.; Klug, H.  
Basic aspects of x-ray absorption in quantitative diffraction analysis of powder mixtures  
Anal. Chem. 20(10), 886-889, 1948
- /ALE48a/ Alexander, L.; Klug, H.P.; Kumer, E.  
Statistical factors affecting the intensity of x-rays diffracted by crystalline powders  
J. Appl. Phys. 19(8), 742-753, 1948
- /ALE65/ Alègre, R.  
Généralisation de la méthode d'addition pour l'analyse quantitative par diffraction x  
Bull. Soc. Fr. Minéral. Cristallogr. 88, 569-574, 1965
- /ALE77/ Alexander, L.E.  
Forty years of quantitative diffraction analysis  
Adv. X-Ray Anal. 20, 1-13, 1977
- /ALT77/ Altree-Williams, S.  
Quantitative x-ray diffractometry on milligram samples prepared on silver filters  
Anal. Chem. 49(3), 429-432, 1977

- /ALT77a/ Altree-Williams, S.; Lee, J.; Mezin, N.V.  
Quantitative x-ray diffractometry on respirable dust collected on nucleopore filters  
Ann. Occup. Hyg. 20, 109-126, 1977
- /ALT78/ Altree-Williams, S.  
Calculated x-ray diffraction data and quantitative x-ray diffractometry  
Anal. Chem. 50(9), 1272-1275, 1978
- /ALT81/ Altree-Williams, S.; Byrnes, J.G.; Jordan, B.  
Amorphous surface and quantitative x-ray powder diffractometry  
Analyst (London) 106(1258), 69-75, 1981
- /ARN65/ Arnott, H.J.; Pautard, F.G.E.; Steinfink, H.  
Structure of calcium oxalate monohydrate  
Nature (London), 208(5016), 1197-1198, 1965
- /AZA58/ Azároff, L.V.; Buerger, M.J.  
The powder method in x-ray crystallography  
McGraw-Hill, New York, 1958, pp. 200
- /AZA68/ Azároff, L.V.  
Elements of x-ray crystallography  
McGraw-Hill, New York, 1968, p. 202
- /BAL35/ Bale, W.F.; Fray, W.W.  
A method for analysis of dust samples employing x-ray diffraction  
J. Ind. Hyg. 17, 30-32, 1935
- /BAL43/ Ballard, J.H.; Oshry, H.L.; Shrenk, H.H.  
Sampling, mixing and grinding techniques in the preparation of samples for quantitative analysis by x-ray diffraction and spectrographic methods  
J. Opt. Soc. Am. 33(12), 667-675, 1943
- /BAN36/ Bannister, F.A.; Hey, M.H.  
Report on some crystalline components of the wedell sea deposits  
Discovery Reports 13, 60-75, 1936
- /BAN47/ Bannister, F.A.; Hey, M.H.; Oakley, K.P.  
Identification of a calculus from a hippopotamus  
Nature (London) 160(4066), 470, 1947
- /BAR44/ Barclay, J.A.; Cooke, W.T.; Stacey, M.  
Recognition of renal calculi by chemical methods and x-ray diffraction patterns  
J. Physiol. (London) 103, 24P, 1944/45
- /BAS74/ see Introduction
- /BEE54/ Beevers, C.A.; Raistrick, B.  
Properties of calcium phosphates  
Nature (London) 173(4403), 542-543, 1954
- /BEE58/ Beevers, C.A.  
The crystal structure of dicalcium phosphate dihydrate,  $\text{CaHPO}_4 \cdot 2\text{H}_2\text{O}$   
Acta Crystallogr. 11, 273-277, 1958
- /BEE64/ see Introduction
- /BER70/ Berry, L.G. (Ed.)  
Inorganic index to the powder diffraction file  
JCPDS, Philadelphia, Pa., USA, 1970, pp. 1189-1196



- /BEZ71/ Bezjak, A.; Jelenić, I.  
The application of the doping method in quantitative x-ray diffraction analysis  
Croat. Chem. Acta 43, 193-198, 1971
- /BLA59/ Bland, J.A.; Basinski, S.J.  
Crystal symmetry of struvite (guanite)  
Nature (London) 183, 1385-1387, 1959
- /BLO67/ Bloss, F.D.; Frenzel, G.; Robinson, P.D.  
Reducing preferred orientation in diffractometer samples  
Am. Mineral. 52(7/8), 1243-1247, 1967
- /BOR69/ Borg, I.Y.; Smith, D.K.  
Calculated x-ray powder patterns for silicate minerals  
Mem. - Geol. Soc. Am. 122, 1-896, 1969
- /BRA45/ Brandenberger, E.; Schinz, H.R.  
Über die Natur der Verkalkungen bei Mensch und Tier und das Verhalten der anorganischen Knochensubstanzen im Falle der hauptsächlich menschlichen Knochenkrankheiten  
Helv. Med. Acta 12, Suppl. 16, 1-63, 1945
- /BRA47/ Brandenberger, E.; DeQuervain, F.; Schinz, H.R.  
Röntgenographische und mikroskopisch-kristallographische Untersuchungen an Harnsteinen  
Experientia 3, 106, 1947
- /BRA47a/ Brandenberger, E.; DeQuervain, F.; Schinz, H.R.  
Röntgenographische und mikroskopisch-kristallographische Untersuchungen an Harnsteinen - I.  
Helv. Med. Acta 14(3), 195-211, 1947
- /BRA48/ Brandenberger, E.; Schinz, H.R.  
Zielsetzung und Ergebnisse systematischer Feinstrukturuntersuchungen mittels der Röntgeninterferenzen beim Menschen  
Bull. Schweiz. Akad. Med. Wiss. 3, 262-268, 1947/48
- /BRA49/ Brandenberger, E.; Schinz, H.R.  
Über den Aufbau im Kindesalter gebildeter Harnsteine  
Helv. Chim. Acta 32, 810-812, 1949
- /BRA67/ Bragg, R.H.  
Quantitative analysis by powder diffraction  
in: E.F. Kaelble (Ed.); "Handbook of x-rays"; McGraw-Hill, New York, 1967, Chapter 12
- /BRA67a/ Bradley, A.A.  
The determination of quartz in small samples by an x-ray technique  
J. Sci. Instr. 44(4), 287-288, 1967
- /BRE35/ Brentano, J.C.M.  
The quantitative measurement of the intensity of x-ray reflections from crystalline powders  
Proc. Phys. Soc. (London) 47(5), 932-947, 1935
- /BRI45/ Brindley, G.W.  
The effect of grain or particle size on x-ray reflections from mixed powders and alloys, considered in relation to the quantitative determination of crystalline substances by x-ray methods  
London Edinburgh Dublin Philos. Mag. J. Sci., Ser. 7, 36(256), 347-369, 1945

- /BRI61/ Brindley, G.W.; Kurtosy, S.S.  
Quantitative determination of kaolinite by x-ray diffraction  
Am. Mineral. 46(11/12), 1205-1215, 1961
- /BUM73/ Bumsted, H.E.  
Determination of alpha-quartz in the respirable portion of airborne particulates by x-ray diffraction  
Am. Ind. Hyg. Assoc. J. 34, 150-158, 1973
- /BUN61/ Burn, C.W.  
Chemical crystallography (2nd ed.)  
University Press, Oxford, 1961, p. 223
- /BUR33/ Burgers, W.G.  
Diagnostizierung eines Uretersteines mit Hilfe einer Röntgeninterferenz-aufnahme  
Fortschr. Geb. Röntgenstr. 48, 228, 1933
- /BYE83/ Bye, E.  
Quantitative microanalysis of cristobalite by x-ray powder diffraction  
J. Appl. Crystallogr. 16, 21-23, 1983
- /CAL80/ Calvert, L.D.; Sirianni, A.F.  
A technique for controlling preferred orientation in powder diffraction samples  
J. Appl. Crystallogr. 13(5), 462, 1980
- /CAL83/ Calvert, L.D.; Sirianni, A.F.; Gainsford, G.J.; Hubbard, C.R.  
A comparison of methods for reducing preferred orientation  
Adv. X-Ray Anal. 26, 105-110, 1983
- /CAR53/ Carr, J.A.  
The pathology of urinary calculi: radial striation  
Br. J. Urol. 25(1), 26-32, 1953
- /CAR55/ Carlström, D.  
X-ray crystallographic studies in apatites and calcified structures  
Acta Radiol. Suppl. 121, 1-59, 1955
- /CAR59/ Carlström, D.; Glas, J.E.  
The size and shape of the apatite crystallites in bone as determined from line-broadening measurements in oriented specimens  
Biochim. Biophys. Acta 35, 46-53, 1959
- /CAR69/ Carr, R.J.  
Aetiology of renal calculi: micro-radiographic studies  
Proc. Renal. Stone Res. Symp. 1968, (Publ. 1969), pp. 123-132
- /CAR85/ Carsey, T.P.  
Quantitation of vanadium oxides in airborne dusts by x-ray diffraction  
Anal. Chem. 57(11), 2125-2130, 1985
- /CHU74/ Chung, F.H.  
A new x-ray diffraction method for quantitative multicomponent analysis  
Adv. X-Ray Anal. 17, 106-115, 1974
- /CHU74a/ Chung, F.H.  
Quantitative interpretation of x-ray diffraction patterns of mixtures - I. Matrix-flushing method for quantitative multicomponent analysis  
J. Appl. Crystallogr. 7, 519-525, 1974
- /CHU74b/ Chung, F.H.  
Quantitative interpretation of x-ray diffraction patterns of mixtures - II. Adiabatic principle of x-ray diffraction analysis of mixtures  
J. Appl. Crystallogr. 7, 526-531, 1974

- /CHU75/ Chung, F.H.  
Quantitative interpretation of x-ray diffraction patterns of mixtures -  
III. Simultaneous determination of a set of reference intensities  
J. Appl. Crystallogr. 8(1), 17-19, 1975
- /CIA36/ Clark, G.L.; Reynolds, D.H.  
Quantitative analysis of mine dusts  
Ind. Eng. Chem. Anal. Ed. 8(1), 36-40, 1936
- /CIA73/ Clark, C.; Smith, D.K.; Johnson, G.G. Jr.  
The use of calculated x-ray powder patterns in the interpretation of  
quantitative analysis  
Prog. Anal. Chem. 6, 45-60, 1973
- /CIA74/ Clark, N.H.; Preston, R.J.  
Dilution methods in quantitative x-ray diffraction analysis  
X-Ray Spectrom. 3(1), 21-25, 1974
- /CLI83/ Cline, J.P.; Snyder, R.L.  
The dramatic effect of crystallite size on x-ray intensities  
Adv. X-Ray Anal. 26, 111-117, 1983
- /COC61/ Cocco, G.  
La struttura della whewellite  
Atti Accad. Naz. Lincei Cl. Sci. Fis. Mat. Nat. Rend. 31, 292-298, 1961
- /COC62/ Cocco, G.; Sabelli, C.  
Affinamento della struttura della whewellite con elaboratore elettronico  
Atti Soc. Toscana Sci. Nat. Pisa Mem. Ser. A, 1-12, 1962
- /COP58/ Copeland, L.E.; Bragg, R.H.  
Quantitative x-ray diffraction analysis  
Anal. Chem. 30(2), 196-201, 1958
- /CRA66/ Crable, J.V.; Knott, M.J.  
Quantitative x-ray diffraction analysis of crocidolite and amosite in bulk  
or settled dust samples  
Am. Ind. Hyg. Assoc. J. 27, 449-453, 1966
- /CRO71/ Crosby, M.T.; Hamer, P.S.  
The determination of quartz on personal sampler filters by x-ray  
diffraction  
Ann. Occup. Hyg. 14, 65-70, 1971
- /DAH72/ Dahm, S.; Furseth, R.; Nossun, A.  
The influence of grinding upon the infrared absorption spectrum of adult  
human dentine  
Calcif. Tissue Res. 10, 160-166, 1972
- /DAS75/ Das, P.; Fazil, M.  
A study of mineral composition of urinary calculi by x-ray diffraction  
method  
Indian J. Med. Res. 63(1), 83-92, 1975
- /DAV21/ Davey, W.P.  
A new x-ray diffraction apparatus  
J. Opt. Soc. Am. 5, 479-493, 1921
- /DAV39/ Davey, W.P.  
X-ray diffraction applied to chemical analysis  
J. Appl. Phys. 10, 820-830, 1939
- /DEG80/ Deganello, S.  
The basic and derivative structures of calcium oxalate monohydrate  
Z. Kristallogr. 152, 247-252, 1980

- /DEW59/ DeWolff, P.M.; Taylor, J.M.; Parrish, W.  
Experimental study of effect of crystallite size on x-ray diffractometer intensities  
J. Appl. Phys. 30(1), 63-69, 1959
- /DON73/ Donovan, D.T.; Knauber, J.W.; von der Heiden, F.V.  
Silica analysis of industrial hygiene samples by x-ray diffraction: interim report  
Prog. Anal. Chem. 6, 61-79, 1973
- /DOS74/ see Introduction
- /EDM80/ Edmonds, J.W.  
Generalization of the Frevel ZRD-search-match program for powder diffraction analysis  
J. Appl. Crystallogr. 13(2), 191-192, 1980
- /ELL73/ Elliott, J.C.; Mackie, P.E.; Young, R.A.  
Monoclinic hydroxyapatite  
Science (Washington) 180(4090), 1055-1057, 1973
- /ELL80/ Elliott, J.C.; Bonel, G.; Trambé, J.C.  
Space group and lattice constants of  $\text{Ca}_{10}(\text{PO}_4)_6\text{CO}_3$   
J. Appl. Crystallogr. 13(6), 618-621, 1980
- /ENG55/ Engelhardt, W. von  
Über die Möglichkeit der quantitativen Phasenanalyse von Tonen mit Röntgenstrahlen  
Z. Kristallogr. 106, 430-459, 1955
- /EPP50/ Epprecht, W.; Schinz, H.R.  
Ergebnisse der Feinstrukturuntersuchung von Blasensteinen aus dem Vorderen Orient  
Schweiz. Med. Wochenschr. 80(30), 792-795, 1950
- /FAV39/ Favajee, J.C.L.  
Quantitative röntgenographische Bodenuntersuchungen  
Z. Kristallogr. Kristallgeom. Kristallphys. Kristallchem. 101(3), 259-270, 1939
- /FLO55/ Flörke, O.W.; Saalfeld, H.  
Ein Verfahren zur Herstellung texturfreier Röntgen-Pulverpräparate  
Z. Kristallogr. 106, 460-466, 1955
- /FRA69/ Frazier, P.D.; Coltvét, C.E.  
Adult human enamel - I. Influence of grinding upon x-ray diffraction profile breadth  
Calcif. Tissue Res. 3, 308-317, 1969
- /FRA70/ Frazier, P.D.  
Adult human enamel - II. An electron microscopic study of the effect of grinding  
Calcif Tissue Res. 5, 277-287, 1970
- /FRE76/ Frevel, L.K.; Adams, C.E.; Ruhberg, L.R.  
A fast search-match program for powder diffraction analysis  
J. Appl. Crystallogr. 9(3), 199-204, 1976
- /FRI13/ Friedrich, W.; Knipping, P.; von Laue, M.  
Interferenz-Phänomene mit Röntgenstrahlen  
Ann. Phys. 41, 971-989, 1913
- /FRI45/ Friedman, H.  
Geiger counter spectrometer for industrial research  
Electronics 18(April), 132-137, 1945

- /FR042/ Frondel, C.; Prien, E.L.  
Carbonate apatite and hydroxyl apatite in urinary calculi  
Science (Washington) 95(2469), 431, 1942
- /GAR82/ Garbauskas, M.F.; Goehner, R.P.  
Complete quantitative analysis using both x-ray fluorescence and x-ray diffraction  
Adv. X-Ray Anal. 25, 283-288, 1982
- /GEB76/ Gebhardt, M.; Bastian, H.-P.  
Harnsteingruppierung und Analysengenauigkeit  
Urol. Int. 31, 217-229, 1976
- /GEB79/ Gebhardt, M.  
Harnsteinanalyse mittels Röntgendiffraktion  
in: W. Vahlensieck (Ed.); "Urolithiasis I"; Springer, Berlin, 1979;  
Preprint 'Info-Dienst', Dtsch. Wellcome, pp. 77-121
- /GER70/ Gerasimov, V.N.  
Quantitative analysis of polycomponent systems by diffractometric methods  
(in Russian)  
Appar. Metody Rentgenovskogo Anal. 7, 146-149, 1970
- /GIB65/ Gibbs, R.J.  
Error due to segregation in quantitative clay mineral x-ray diffraction mounting techniques  
Am. Mineral. 50(5/6), 741-751, 1965
- /GIB74/ Gibson, R.I.  
Descriptive human pathological mineralogy  
Am. Mineral. 59, 1177-1182, 1974
- /GLO33/ Glocker, R.  
Über die Grundlagen einer quantitativen Röntgenanalyse der Konzentration von Metallphasen in einer Legierung oder Mischung  
Metallwirtsch. Metallwiss. Metalltechn. 12(42), 599-602, 1933
- /GOE81/ Goebel, H.E.  
The use and accuracy of continuously scanning position-sensitive detector data in x-ray powder diffraction  
Adv. X-Ray Anal. 24, 123-138, 1981
- /GOE82/ Goehner, R.P.  
X-ray diffraction quantitative analysis using intensity ratios and external standards  
Adv. X-Ray Anal. 25, 309-313, 1982
- /GOE83/ Goehner, R.P.; Garbauskas, M.F.  
Computer-aided qualitative x-ray powder diffraction phase analysis  
Adv. X-Ray Anal. 26, 81-86, 1983
- /GOR55/ Gordon, R.L.; Harris, G.W.  
Effect of particle-size on the quantitative determination of quartz by x-ray diffraction  
Nature (London) 175(4469), 1135, 1955
- /GRI78/ Griffith, D.P.  
Struvite stones  
Kidney Int. 13, 372-382, 1978
- /GRU64/ Grünberg, W.  
Vergleichende Untersuchungen zur Bio-Kristallographie - Tierische Harnsteine  
Pathol. Vet. 1, 258-268, 1964

- /HAM29/ Hammarsten, G.  
On calcium oxalate and its solubility in the presence of inorganic salts with special reference to the occurrence of oxaluria  
C. R. Trav. Lab. Carlsberg 17(11), 1-85, 1929
- /HAN38/ Hanawalt, J.D.; Rinn, H.W.; Frevel, L.K.  
Chemical analysis by x-ray diffraction  
Ind. Eng. Chem. Anal. Ed. 10(9), 457-512, 1938
- /HAN74/ Hansen, M.; Dengler, F.  
Ein neuer Präparatträger zur Röntgenbeugungsanalyse von auf Filtern abgeschiedenen Staubproben  
Staub - Reinhalt. Luft 34(7), 264-266, 1974
- /HAY63/ Hayek, E.; Newesely, H.  
Pentacalcium monohydroxyorthophosphate (hydroxylapatite)  
Inorg. Synth. 7, 63-65, 1963
- /HAY81/ Hayakawa, M.; Oka, M.  
XPKFIT: peak separation with arbitrary relations among the component peaks  
J. Appl. Crystallogr. 14(2), 145-148, 1981
- /HAZ74/ Hazarika, E.Z.; Balakrishna Rao, B.N.  
Upper urinary tract calculi: analysed by x-ray diffraction and chemical methods  
Indian J. Med. Res. 62(3), 443-453, 1974
- /HAZ74a/ Hazarika, E.Z.; Balakrishna Rao, B.N.; Kapur, B.M.L.; Misra, R.K.  
Lower urinary tract calculi analysed of x-ray diffraction and chemical methods  
Indian J. Med. Res. 62(6), 893-904, 1974
- /HEC75/ Heck, H.G.  
QXDA - Program for quantitative x-ray diffraction analysis of powder mixtures  
DSM Central Laboratory, Geleen, The Netherlands, 1975
- /HEC75a/ Heck, H.G.; Pijpers, A.P.; Vonk, C.G.  
Semi automatic quantitative analysis of powder mixtures, based on all peaks in the scanned part of the x-ray diagram  
Acta Crystallogr. A31, S199, 1975
- /HEC81/ Heeq, M.  
A fitting method for x-ray diffraction profiles  
J. Appl. Crystallogr. 14(1), 60-61, 1981
- /HED53/ Hedenberg, I.; Engfeldt, B.; Engström, A.  
X-ray absorption and diffraction studies on experimental vesical calculi  
Br. J. Urol. 25(1), 33-37, 1953
- /HEI74/ Heidemanns, G.  
Die röntgenographische Quarzgehaltsbestimmung in dünnen Schichten auf Filtern abgeschiedener Feinstaubproben  
Staub - Reinhalt. Luft 34(7), 260-264, 1974
- /HER62/ Herring, L.C.  
Observations on the analysis of ten thousand urinary calculi  
J. Urol. 88(4), 545-562, 1962

- /HES72/ Hesse, A.; Schneider, H.-J.; Schilling, I.; Schrumpf, G.; Hienzsch, E.  
Infrarotspektroskopische und Röntgenfeinstrukturuntersuchungen an Kalzium-  
Oxalat-Harnsteinen  
Z. Gesamte Inn. Med. Ihre Grenzgeb. 27(13), 560-565, 1972
- /HES81/ see Introduction
- /HES82/ see Introduction
- /HEU76/ Heuvel, H.M.; Huisman, R.; Lind, K.C.J.B.  
Quantitative information from x-ray diffraction of nylon-6 yarns  
J. Polym. Sci. Polym. Phys. Ed. 14, 921-940, 1976
- /HON52/ Honegger, R.  
Das Polyhydrat des Kalzium-Oxalates  
Vierteljahrsschr. Naturforsch. Ges. Zürich Beih. 97(1), 1-44, 1952
- /HOU81/ Houska, C.R.; Smith, T.M.  
Least-squares analyses of x-ray diffraction line shapes with analytic  
functions  
J. Appl. Phys. 52(2), 748-754, 1981
- /HOW83/ Howard, S.A.; Snyder, R.L.  
An evaluation of some profile models and the optimization procedures used  
in profil fitting  
Adv. X-Ray Anal. 26, 73-80, 1983
- /HUA75/ Huang, T.C.; Parrish, W.  
Accurate and rapid reduction of experimental x-ray data  
Appl. Phys. Lett. 27(3), 123-124, 1975
- /HUA78/ Huang, T.C.; Parrish, W.  
Qualitative analysis of complicated mixtures by profile fitting x-ray  
diffractometer patterns  
Adv. X-Ray Anal. 21, 275-288, 1978
- /HUA82/ Huang, T.C.; Parrish, W.  
A new computer algorithm for qualitative x-ray powder diffraction analysis  
Adv. X-Ray Anal. 25, 213-219, 1982
- /HUB75/ Hubbard, C.R.; Swanson, H.E.; Mauer, F.A.  
A silicon powder diffraction standard reference material  
J. Appl. Crystallogr. 8(1), 45-48, 1975
- /HUB76/ Hubbard, C.R.; Evans, E.H.; Smith, D.K.  
The reference intensity ratio,  $I/I_0$ , for computer simulated powder  
patterns  
J. Appl. Crystallogr. 9(2), 169-174, 1976
- /HUB77/ Hubbard, C.R.; Smith, D.K.  
Experimental and calculated standards for quantitative analysis by powder  
diffraction  
Adv. X-Ray Anal. 20, 27-39, 1977
- /HUB80/ Hubbard, C.R.  
Standard reference materials for quantitative analysis and d-spacing  
measurement  
NBS Spec. Publ. (U.S.) 567, 489-502, 1980
- /HUB83/ Hubbard, C.R.; Robbins, C.R.; Snyder, R.L.  
XRD quantitative phase analysis using the NBS\*QUANT82 system  
Adv. X-Ray Anal. 26, 149-156, 1983

- /HUB83a/ Hubbard, C.R.  
Certification of Si powder diffraction standard reference material 640a  
J. Appl. Crystallogr. 16(3), 285-288, 1983
- /HUB83b/ Hubbard, C.R.  
New standard reference materials for x-ray powder diffraction  
Adv. X-Ray Anal. 26, 45-51, 1983
- /HUG44/ Huggins, C.; Bear, R.S.  
The course of prostatic ducts and the anatomy, chemical and x-ray  
diffraction analysis of prostatic calculi  
J. Urol. 51(1), 37-47, 1944
- /HUL17/ Hull, A.W.  
A new method of x-ray crystal analysis  
Phys. Rev. 10(6), 661-696, 1917
- /HUL19/ Hull, A.W.  
A new method of chemical analysis  
J. Am. Chem. Soc. 41(8), 1168-1175, 1919
- /IBA71/ Iball, D.R.  
The application of x-ray crystal analysis to the study of calculi  
IMLT thesis, Dundee, 1971
- /IBE74/ Ibers, J.A.; Hamilton, W.C. (Eds.)  
International tables for x-ray crystallography, vol. IV, revised and  
supplementary tables  
International Union of Crystallography, Kynoch Press, Birmingham, England,  
1974, pp. 61-66
- /JEN40/ Jensen, A.T.  
On concrements from the urinary tract II  
Acta Chir. Scand. 84(3), 207-225, 1940
- /JEN41/ Jensen, A.T.  
On concrements from the urinary tract III  
Acta Chir. Scand. 85(6), 473-486, 1941
- /JEN69/ Jennings, L.D.  
Current status of the I.U.Cr. powder intensity project  
Acta Crystallogr. A25, 217-222, 1969
- /JEN71/ Jenkins, R.; Haas, D.J.; Paolini, F.R.  
A new concept in automated x-ray powder diffractometry  
Norelco Rep. 18(2), 12-27, 1971
- /JEN74/ Jenkins, R.  
Provision, suitability and stability of standards for quantitative powder  
diffractometry  
Adv. X-Ray Anal. 17, 32-43, 1974
- /JEN75/ Jenkins, R.  
Quantitative analysis with the automatic powder diffractometer  
Norelco Rep. 22(1), 7-12, 1975
- /JEN79/ Jenkins, R.; Hubbard, C.R.  
A preliminary report on the design and results of the second round robin  
to evaluate search/match methods for qualitative powder diffractometry  
Adv. X-Ray Anal. 22, 133-142, 1979
- /JEN83/ Jenkins, R.  
Effects of diffractometer alignment and aberrations on peak positions and  
intensities  
Adv. X-Ray Anal. 26, 25-33, 1983



- /JOB82/ Jobst, B.A.; Gübel, H.E.  
IDENT - A versatile microfile-based system for fast interactive XRPD phase analysis  
Adv. X-Ray Anal. 25, 273-282, 1982
- /JOI/ Joint Committee on Powder Diffraction Standards  
Powder diffraction file  
JCPDS, Philadelphia, Pa., USA, n.d.
- /JON62/ Jones, D.W.; Smith, J.A.S.  
The structure of brushite,  $\text{CaHPO}_4 \cdot 2\text{H}_2\text{O}$   
J. Chem. Soc., 1414-1420, 1962
- /JOO83/ Joost, J.; Tessadri, R.  
Combined analysis of kidney stones by x-ray diffraction and electron microprobe  
Eur. Urol. 9(5), 305-311, 1983
- /JUM65/ Jumpertz, E.A.  
Die exakte röntgenographische quantitative Gemenge-Analyse  
Fortschr. Mineral. 42(1), 87-112, 1965
- /KAY64/ Kay, M.I.; Young, R.A.; Posner, A.S.  
Crystal structure of hydroxyapatite  
Nature (London) 204(4963), 1050-1052, 1964
- /KIN74/ King, P.J.; Smith, W.L.  
A computer-controlled x-ray powder diffractometer  
J. Appl. Crystallogr. 7, 603-608, 1974
- /KLU74/ Klug, H.P.; Alexander, L.E.  
X-ray diffraction procedures for polycrystalline and amorphous materials (2nd ed.)  
Wiley-Interscience, New York, 1974, pp. 532
- /KLU74a/ op. cit., pp. 364
- /KOR81/ Korn, S.; Bausch, W.; Bichler, K.-H.  
Wertigkeit quantitativer Harnsteinanalysen - Polarisationsmikroskopie und Röntgendiffraktion  
Therapiewoche 31, 1280-1283, 1981
- /LAG56/ Lagergren, C.  
Biophysical investigations of urinary calculi  
Acta Radiol. Suppl. 133, 1-71, 1956
- /LAG61/ Lagergren, C.  
X-ray crystallography of urinary calculi and its diagnostic value  
Acta Pathol. Microbiol. Scand. Suppl. 144, 55, 1961
- /LEG61/ Legrand, C.; Bertrand, A.  
Remarques sur l'influence du broyage en analyse quantitative par diffraction de rayons x  
Bull. Soc. Fr. Céram. 50, 69-74, 1961
- /LEN57/ Lennox, D.H.  
Monochromatic diffracton-absorption technique for direct quantitative x-ray analysis  
Anal. Chem. 29, 766-770, 1957
- /LER53/ Leroux, J.; Lennox, D.H.; Kay, K.  
Direct quantitative x-ray analysis by diffraction-absorption technique  
Anal. Chem. 25(5), 740-743, 1953

- /LER57/ Leroux, J.  
Direct quantitative x-ray analyses with molybdenum  $K_{\alpha}$  radiation by the diffraction-absorption technique  
Norelco Rep. 4, 107-109, 1957
- /LER60/ Leroux, J.; Mahmud, M.  
Influence of goniometric arrangement and absorption in qualitative and quantitative analysis of powders by x-ray diffractometry  
Appl. Spectrosc. 14(5), 131-134, 1960
- /LER69/ Leroux, J.; Powers, C.A.  
Quantitative röntgenographische Analyse von Quarz in Staubproben auf Silbermembranfiltern  
Staub - Reinhalt. Luft 29(5), 197-200, 1969
- /LER69a/ id.  
Staub - Reinhalt. Luft (English Ed.) 29(5), 26-31, 1969
- /LER69b/ Leroux, J.  
Herstellung dünner Staubschichten zur analytischen Untersuchung mittels Röntgenstrahlenemission und Röntgenbeugung  
Staub - Reinhalt. Luft 29(4), 157-159, 1969
- /LER70/ Leroux, J.; Powers, C.  
Direct x-ray diffraction quantitative analysis of quartz in industrial dust films deposited on silver membrane filters  
Occup. Health Rev. 21(1/2), 26-34, 1970
- /LER70a/ Leroux, J.  
Preparation of thin dust coatings for their analysis by x-ray emission and diffraction  
Occup. Health Rev. 21(1/2), 19-25, 1970
- /LER73/ Leroux, J.; Davey, A.B.C.; Paillard, A.  
Proposed standard methodology for the evaluation of silicosis hazards  
Am. Ind. Hyg. Assoc. J. 34, 409-417, 1973
- /LEU81/ see Introduction
- /LIN79/ Lindqvist, O.; Ljungström, E.  
Profile analysis of diffractometer data  
J. Appl. Crystallogr. 12(1), 134, 1979
- /LON69/ Lonsdale, K.; Sutor, D.J.  
X-ray diffraction studies of urinary calculi  
Proc. Renal. Stone Res. Symp. 1968, (Publ. 1969), pp. 105-112
- /LON72/ Lonsdale, K.; Sutor, D.J.  
Crystallographic studies of urinary and biliary calculi  
Sov. Phys. Crystallogr. Engl. Transl. 16(6), 1060-1068, 1972
- /MAN80/ see Introduction
- /MAR79/ Marquart, R.G.; Katsnelson, I.; Milne, G.W.A.; Heller, S.R.; Johnson, G.G. Jr.; Jenkins, R.  
A search-match system for x-ray powder diffraction data  
J. Appl. Crystallogr. 12(6), 629-634, 1979
- /MAT68/ Matsumura, Y.; Hamada, A.  
Change of surface properties of quartz particles by grinding  
Ind. Health 6, 221-224, 1968

- /MCC49/ McCreery, G.L.  
Improved mount for powdered specimens used on the geiger-counter x-ray spectrometer  
J. Am. Ceram. Soc. 32(4), 141-146, 1949
- /MCC65/ McConnell, D.  
Crystal chemistry of hydroxyapatite - Its relation to bone material  
Arch. Oral. Biol. 10, 421-431, 1965
- /MCC73/ McConnell, D.  
Apatite - Its crystal chemistry, mineralogy, utilization, and geologic and biologic occurrences  
Springer, New York, 1973
- /MCC79/ McCarthy, G.J.; Johnson, G.G. Jr.  
Identification of multiphase unknowns by computer methods: role of chemical information, the quality of x-ray powder data and subfiles  
Adv. X-ray Anal. 22, 109-120, 1979
- /MCC81/ McCarthy, G.J.; Gehringer, R.C.; Smith, D.K.; Injaian, V.M.; Pfoertsch, D.E.; Kabel, R.L.  
Internal standards for quantitative x-ray phase analysis: crystallinity and solid solution  
Adv. X-Ray Anal. 24, 253-264, 1981
- /MOD81/ see Introduction
- /MOR53/ Morozumi, C.; Ritter, H.L.  
Calculated powder patterns from very small crystals: body-centered cubes  
Acta Crystallogr. 6, 588-590, 1953
- /MOR67/ Morriss, R.H.; Beeler, M.F.  
X-ray diffraction analysis of 464 urinary calculi  
Am. J. Clin. Pathol. 48(4), 413-417, 1967
- /MOR77/ Moraweck, B.; De Montgolfier, P.; Renouprez, A.J.  
X-ray line-profile analysis - I. A method for unfolding diffraction profiles  
J. Appl. Crystallogr. 10(3), 184-190, 1977
- /MOS67/ Mossman, M.H.; Freas, D.H.; Bailey, S.W.  
Orienting internal standard method for clay mineral x-ray analysis  
Clays Clay Miner. 27, 441-453, 1967
- /NAI82/ Naidu, S.V.N.; Houska, C.R.  
Profile separation in complex powder patterns  
J. Appl. Crystallogr. 15(2), 190-198, 1982
- /NBSa/ N.N.  
NBS Monograph 25 - Standard x-ray diffraction powder patterns  
U.S. Department of Commerce, National Bureau of Standards, Washington D.C., n.d., Section 8, pp. 154-155
- /NBSb/ op. cit., Section 16, p. 78
- /NBSc/ op. cit., Section 3, p. 41
- /NBSd/ N.N.  
NBS Circular 539 - Standard x-ray diffraction powder patterns  
U.S. Department of Commerce, National Bureau of Standards, Washington D.C., n.d., Volume 9, p. 3
- /NEN73/ Nenadic, C.M.; Crable J.V.  
Application of x-ray diffraction in occupational health studies  
Prog. Anal. Chem. 6, 81-101, 1973

- /NIC75/ Nicol, A.W.  
X-ray diffraction  
in: A.W. Nicol (Ed.); "Physicochemical methods of mineral analysis"; Plenum Press, New York, 1975, pp. 294-320
- /NIC80/ Nichols, M.C.; Johnson, Q.  
The search-match problem  
Adv. X-Ray Anal. 23, 273-278, 1980
- /NIS64/ Niskanen, E.  
Reduction of orientation effects in the quantitative x-ray diffraction analysis of kaolin minerals  
Am. Mineral. 49(5/6), 705-714, 1964
- /OBE68/ Oberg, M.  
Evaluation of quartz in air-borne dust in the 0.5 - 2-micron size range  
Environ. Sci. Technol. 2(10), 795-798, 1968
- /OTN80/ Otnes, B.; Montgomery, O.  
Method and reliability of crystallographic stone analysis  
Invest. Urol. 17(4), 314-319, 1980
- /PAR64/ Parsons, J.  
X-ray diffraction analysis of central asian vesical calculi  
Henry Ford Hosp. Med. Bull. 12, 187-200, 1964
- /PAR65/ Parrish, W.; Hamacher, E.A.; Lowitzsch, K.  
The "Norelco" x-ray diffractometer  
in: W. Parrish (Ed.); "X-ray analysis papers"; Centrex Publishing Comp., Eindhoven, The Netherlands, 1965, pp. 71-81
- /PAR76/ Parrish, W.; Huang, T.C.; Ayers, G.L.  
Profile fitting: a powerful method of computer x-ray instrumentation and analysis  
Trans. Am. Crystallogr. Assoc. 12, 55-73, 1976
- /PAR80/ Parrish, W.; Huang, T.C.  
Accuracy of the profile fitting method for x-ray polycrystalline diffractometry  
NBS Spec. Publ. (U.S.) 567, 95-110, 1980
- /PAR82/ Parrish, W.; Ayers, G.L.; Huang, T.C.  
A versatile microcomputer x-ray search/match system  
Adv. X-Ray Anal. 25, 221-229, 1982
- /PAR83/ Parrish, W.; Huang, T.C.  
Accuracy and precision of intensities in x-ray polycrystalline diffraction  
Adv. X-Ray Anal. 26, 35-44, 1983
- /PEA48/ Pease, R.S.  
The resolution of x-ray doublet diffraction lines into  $\alpha_1, \alpha_2$  components  
J. Sci. Instrum. Phys. Ind. 25(Oct.), 353, 1948
- /PHE39/ Phenister, D.B.; Aronsohn, H.G.; Pepinsky, R.  
Variation in the cholesterol, bile pigment and calcium salts content of gallstones formed in gallbladder and in bile ducts with the degree of associated obstruction  
Ann. Surg. 109(2), 161-186, 1939
- /PHI74/ N.N.  
Instruction manual - Diffractometer kit PW 1349/30  
N.V. Philips' Gloeilampenfabrieken, Eindhoven, The Netherlands, 1974

- /PHI76/ N.N.  
Operating Manual - Automatic x-ray powder diffractometer with PW 1390 - PW 1394  
N.V. Philips' Gloeilampenfabrieken, Eindhoven, The Netherlands, 1976
- /POL69/ Pollack, S.S.; Carlson, G.L.  
A comparison of x-ray diffraction and infrared technics for identifying kidney stones  
Am. J. Clin. Pathol. 52(6), 656-660, 1969
- /POP79/ Popović, S.; Gržeta-Plenković, G.  
The doping method in quantitative x-ray diffraction phase analysis  
J. Appl. Crystallogr. 12(2), 205-208, 1979
- /POP83/ Popović, S.; Gržeta-Plenković, B.; Balić-Žunić, T.  
The doping method in quantitative x-ray diffraction phase analysis - Addendum  
J. Appl. Crystallogr. 16(5), 505-507, 1983
- /POS58/ Posner, A.S.; Perloff, A.; Diorio, A.F.  
Refinement of the hydroxyapatite structure  
Acta Crystallogr. 11(4), 308-309, 1958
- /POS73/ Post, B.  
Laboratory hints for crystallographers  
Norelco. Rep. 20(1), 8-11, 1973
- /PRI47/ see Introduction
- /PRI49/ Prien, E.L.  
Studies in urolithiasis - II. Relationships between pathogenesis, structure and composition of calculi  
J. Urol. 61(5), 821-836, 1949
- /PRI63/ Prien, E.L.  
Crystallographic analysis of urinary calculi  
J. Urol. 89(6), 917-924, 1963
- /PRI74/ see Introduction
- /PYR83/ Pyrros, N.P.; Hubbard, C.R.  
Powder-pattern: A system of programs for processing and interpreting powder diffraction data  
Adv. X-Ray Anal. 26, 63-72, 1983
- /PYR83a/ Pyrros, N.P.; Hubbard, C.R.  
Rational functions as profile models in powder diffraction  
J. Appl. Crystallogr. 16(3), 289-294, 1983
- /QUA70/ Quakernaat, J.  
Direct diffractometric quantitative analysis of synthetic clay mineral mixtures with molybdenite as orientation-indicator  
J. Sediment. Petrol. 40(1), 506-513, 1970
- /RAC48/ Rachinger, W.A.  
A correction for the  $\alpha_1, \alpha_2$  doublet in the measurement of widths of x-ray diffraction lines  
J. Sci. Instrum. Phys. Ind. 25(July), 254-255, 1948
- /RAN31/ Ranganathan, S.  
Researches on "stone" - Part XIII. X-ray diffraction studies on calculi  
Indian J. Med. Res. 19(4), 1153-1161, 1931/32

- /RIC71/ Richesson, M.; Morrison, L.; Cohen, J.B.; Paavola, K.  
An inexpensive computer control for an x-ray diffraction laboratory  
J. Appl. Crystallogr. 4, 524-527, 1971
- /RIN65/ Ringertz, H.  
Optical and crystallographic data of uric acid and its dihydrate  
Acta Crystallogr. 19(2), 286-287, 1965
- /RIN66/ Ringertz, H.  
The molecular and crystal structure of uric acid  
Acta Crystallogr. 20(3), 397-403, 1966
- /ROD82/ see Introduction
- /ROE1895/ Röntgen, W.C.  
Sitzungsber. Med. Phys. Ges. Würzburg 1895 (Publ. 1896), pp. 137
- /ROE68/ Rösch, H.  
Die quantitative röntgenographische Phasenanalyse - Ein Vergleich verschiedener Analysenverfahren  
Neues Jahrb. Mineral. Abh. 108(3), 271-291, 1968
- /ROS82/ Rose, G.L.  
Urinary stones: clinical and laboratory aspects  
MTP Press, Lancaster, England, 1982, pp. 122-133
- /SAA58/ Saalfeld, H.  
Gedanken über die quantitative Röntgenanalyse  
Ber. Dtsch. Keram. Ges. 35, 368, 1958
- /SAU31/ Saupe, E.  
Röntgendiagramme von menschlichen Körpergeweben und Konkrementen  
Fortschr. Geb. Röntgenstr. 44(2), 204-211, 1931
- /SCH38/ Schäfer, K.  
Quantitative Kristallit-Röntgenanalyse  
Z. Kristallogr. Mineral. Petrogr. Abt. A 99(2), 142-152, 1938
- /SCH62/ Schliephake, R.-W.  
Stand der Entwicklung eines Verfahrens zur quantitativen röntgenographischen Quarzbestimmung in Grubenstäuben des Steinkohlenbergbau Vereins - II. Bericht  
Staub 22(9), 364-372, 1962
- /SCH66/ Schroeder, H.E.; Bambauer, H.U.  
Stages of calcium phosphate crystallization during calculus formation  
Arch. Oral Biol. 11, 1-14, 1966
- /SCH70/ Schneider, H.-J.; Hienzsch, E.; Tscharnke, J.  
Die Untersuchung von Harnsteinen mit der Röntgenfeinstrukturanalyse nach Debye-Scherrer  
Urologe 9(4), 171-175, 1970
- /SCH70a/ Schneider, H.-J.; Hienzsch, E.; Tscharnke, J.  
Vorschlag zur Zentralisierung und Standardisierung der Harnsteinanalyse  
Dtsch. Gesundheitswes. 25(41), 1934-1937, 1970
- /SCH74/ Schneider, H.-J.; Hesse, A.; Hienzsch, E.; Tscharnke, J.; Schweder, P.  
Röntgenstrukturuntersuchungen als standardisierte Harnsteinanalyse in der Deutschen Demokratischen Republik  
Z. Urol. 66, 111-119, 1974

- /SCH74a/ Schneider, H.-J.; Tscharnke, J.; Hesse, A.  
Röntgendiffraktionsanalyse  
in: H.-J. Schneider (Ed.); "Technik der Harnsteinanalyse"; Thieme,  
Leipzig, 1974, pp. 74-137
- /SCH83/ Schreiner, W.N.; Jenkins, R.  
Profile fitting for quantitative analysis in x-ray powder diffraction  
Adv. X-Ray Anal. 26, 141-147, 1983
- /SEG72/ Segmüller, A.  
Automated x-ray diffraction laboratory system  
Adv. X-Ray Anal. 15, 114-122, 1972
- /SEI79/ Seifert, K.-F.; Gebhardt, M.A.H.  
Quantitative röntgenographische Harnsteinanalyse mittels Guinier-  
Diffraktometer  
Fortschr. Urol. Nephrol. 14, 275-284, 1979
- /SHI66/ Shirley, R.  
Uric acid dihydrate: crystallography and identification  
Science (Washington) 152(3728), 1512-1513, 1966
- /SHI68/ Shirley, R.  
Anhydrous uric acid: nature and occurrence of a new form in urinary  
calculi  
Science (Washington) 159(3814), 544, 1968
- /SLA72/ Slaughter, M.; Carpenter, D.  
A modular automatic x-ray analysis system  
Adv. X-Ray Anal. 15, 135-147, 1972
- /SMI68/ Smith, D.K.  
Computer simulation of x-ray diffractometer traces  
Norelco Rep. 15(2), 57-65 & 76, 1968
- /SMI79/ Smith, S.T.; Snyder, R.L.; Brownell, W.E.  
Minimization of preferred orientation in powders by spray drying  
Adv. X-Ray Anal. 22, 77-87, 1979
- /SMI79a/ Smith, D.K.; Barrett, C.S.  
Special handling problems in x-ray diffractometry  
Adv. X-Ray Anal. 22, 1-12, 1979
- /SNY81/ Snyder, R.L.; Hubbard, C.R.; Panagiotopoulos, N.C.  
Auto: a real time diffractometer control system  
NBSIR 81-2229, 1981
- /SNY82/ Snyder, R.L.; Hubbard, C.R.; Panagiotopoulos, N.C.  
A second generation automated powder diffractometer control system  
Adv. X-Ray Anal. 25, 245-260, 1982
- /SNY83/ Snyder, R.L.  
Accuracy in angle and intensity measurements in x-ray powder diffraction  
Adv. X-Ray Anal. 26, 1-10, 1983
- /STE65/ Sterling, C.  
Crystal structure analysis of weddellite,  $\text{CaC}_2\text{O}_4 \cdot (2+x)\text{H}_2\text{O}$   
Acta Crystallogr. 18, 917-921, 1965
- /SUO77/ Suortti, P.; Jennings, L.D.  
Accuracy of structure factors from x-ray powder intensity measurements  
Acta Crystallogr. A33(6), 1012-1027, 1977

- /SUT68/ Sutor, D.J.; Scheidt, S.  
Identification standards for human urinary calculus components, using crystallographic methods  
Br. J. Urol. 40(1), 22-28, 1968
- /SUT68a/ Sutor, D.J.  
Difficulties in the identification of components of mixed urinary calculi using the x-ray powder method  
Br. J. Urol. 40, 29-32, 1968
- /SUT69/ Sutor, D.J.; Wooley, S.E.  
Composition of urinary calculi by x-ray diffraction: collected data from various localities - VII  
Br. J. Urol. 41, 397-400, 1969
- /SUT70/ Sutor, D.J.; Wooley, S.E.  
Composition of urinary calculi by x-ray diffraction: collected data from various localities - VIII  
Br. J. Urol. 42, 302-305, 1970
- /SUT71/ Sutor, D.J.; Wooley, S.E.  
Composition of urinary calculi by x-ray diffraction: collected data from various localities - IX-XI  
Br. J. Urol. 43, 268-271, 1971
- /SUT71a/ Sutor, J.D.; Wooley, S.E.; MacKenzie, K.R.; Wilson, R.; Scott, R.; Morgan, H.G.  
Urinary tract calculi - A comparison of chemical and crystallographic analyses  
Br. J. Urol. 43, 149-153, 1971
- /SUT72/ Sutor, D.J.; Wooley, S.E.  
Composition of urinary calculi by x-ray diffraction: collected data from various localities - XII-XIV  
Br. J. Urol. 44, 287-291, 1972
- /SUT74/ Sutor, D.J.; Wooley, S.E.  
Composition of urinary calculi by x-ray diffraction: collected data from various localities - XV-XVII  
Br. J. Urol. 46, 229-232, 1974
- /SZA78/ Szabó, P.  
Optimization of the measuring time in diffraction intensity measurements  
Acta Crystallogr. A34, 551-553, 1978
- /SZA78a/ Szabó, P.; Fuentes-Cobas, L.  
The use of computers in quantitative x-ray diffraction analysis  
Rev. CENIC Cienc. Fis. 9(1), 105-110, 1978
- /SZA80/ Szabó, P.  
Optimization of quantitative x-ray diffraction analysis  
J. Appl. Crystallogr. 13(6), 479-485, 1980
- /SZA82/ Szabó, P.  
Addenda to the optimization of quantitative x-ray diffraction analysis  
J. Appl. Crystallogr. 15(4), 449-451, 1982
- /TAL62/ Talvitie, N.A.; Brewer, L.W.  
Separation and analysis of dust in lung tissue  
Am. Ind. Hyg. Assoc. J. 23, 58-61, 1962
- /TAY44/ Taylor, A.  
The influence of crystal size on the absorption factor as applied to Debye-Scherrer diffraction patterns  
London Edinburgh Dublin Philos. Mag. J. Sci. 35(243), 215-229, 1944



- /TAZ80/ Tazzoli, V.; Domeneghetti, C.  
The crystal structures of whewellite and weddellite: re-examination and comparison  
Am. Mineral. 65(3/4), 327-334, 1980
- /TIA83/ Tian-Hui, L.; Sai-Zhu, Z.; Li-Jun, C.; Xin-Xing, C.  
An improved program for searching and matching powder diffraction patterns  
J. Appl. Crystallogr. 16, 150-154, 1983
- /VAS67/ Vassamillet, L.F.; King, H.W.  
Diffractometer-techniques  
in: E.F. Kaelble (Ed.); "Handbook of x-rays"; McGraw-Hill, New York, 1967, Chapter 9
- /VON77/ Vonk, C.G.; Heck, H.G.; Pijpers, A.P.  
Quantitative x-ray analysis of crystalline components in fertilizers  
New Dev. Phosphate Fert. Technol. Proc. Tech. Conf. ISMA Ltd., 1976, (Publ. 1977), pp. 115-126
- /WAL62/ Walter-Levy, L.; Lanier, J.  
Sur la formation des hydrates de l'oxalate de calcium  
C. R. Hebd. Seances Acad. Sci. 254, 296-298, 1962
- /WAR34/ Warren, B.E.  
Identification of crystalline substances by means of x-rays  
J. Am. Ceram. Soc. 17, 73-77, 1934
- /WAR81/ Warpehoski, M.A.; Buscemi, P.J.; Osborn, D.C.; Finlayson, B.; Goldberg, E.P.  
Distribution of organic matrix in calcium oxalate renal calculi  
Calcif. Tissue Int. 33(3), 211-222, 1981
- /WEI83/ Weiss, Z.; Krajčůvek, J.; Smrček, L.; Fiala, J.;  
A computer x-ray quantitative phase analysis  
J. Appl. Crystallogr. 16(5), 493-497, 1983
- /WIL50/ Wilson, A.J.C.  
Geiger-counter x-ray spectrometer - influence of size and absorption coefficient of specimen on position and shape of powder diffraction maxima  
J. Sci. Instrum. 27(12), 321-325, 1950
- /WIL51/ Wilchinsky, Z.W.  
Effect of crystal, grain and particle size on x-ray power diffracted from powders  
Acta Crystallogr. 4, 1-9, 1951
- /WIL59/ Williams, P.P.  
Direct quantitative diffractometric analysis  
Anal. Chem. 31(11), 1842-1844, 1959
- /WON83/ Wong-Ng, W.; Holomany, M.; McClune, W.F.; Hubbard, C.R.  
The JCPDS data base - present and future  
Adv. X-Ray Anal. 26, 87-88, 1983
- /YOU77/ Young, R.A.; Mackie, P.E.; von Dreele, R.B.  
Application of the pattern-fitting structure-refinement method to x-ray powder diffractometer patterns  
J. Appl. Crystallogr. 10(4), 262-269, 1977
- /YOU82/ Young, R.A.; Wiles, D.B.  
Profile shape functions in Rietveld refinements  
J. Appl. Crystallogr. 15(4), 430-438, 1982

- /ZAV70/ Zav'yalova, L.L.; Ivoilov, A.S.  
Use of addition and dilution methods in x-ray quantitative phase analysis  
(in Russian)  
Appar. Metody Rentgenovskogo Anal. 6, 56-61, 1970
- /ZEV79/ Zevin, L.S.  
Methods of mixing in quantitative x-ray phase analysis  
J. Appl. Crystallogr. 12(6), 582-584, 1979
- /ZWE29/ Zwetsch, A.; Stumpfen, H.  
Über ein Verfahren einer quantitativen Kristallitanalyse durch Röntgen-  
strahlen in besonderer Anwendung auf keramische Fragen  
Ber. Dtsch. Keram. Ges. 10(12), 561-567, 1929

### 3. Chapter II

- /ABD85/ Abdel-Halim, R.E.; Baghlaf, A.O.; Farag, A.-B.B.  
Clinical-chemical study of urinary stones in Saudi Arabia  
Urolithiasis Rel. Clin. Res., Proc. 5th Int. Symp., 1984, (Publ. 1985),  
pp. 715-718
- /ABU75/ Abu-Samra, A.; Morris, J.S.; Koirtyohann, S.R.  
Wet ashing of some biological samples in a microwave oven  
Anal. Chem. 47(8), 1475-1477, 1975
- /ADR73/ Adrian, W.J.  
A comparison of a wet pressure digestion method with other commonly used  
wet and dry-ashing methods  
Analyst (London) 98, 213-216, 1973
- /ANA59/ Analytical Methods Committee, Metallic Impurities in Organic Matter Sub-  
Committee  
Notes on perchloric acid and its handling in analytical work  
Analyst (London) 84, 214-216, 1959
- /AND84/ Anderson, R.A.; Polansky, M.M.; Bryden, N.A.  
Strenuous running - acute effects on chromium, copper, zinc, and selected  
clinical variables in urine and serum of male runners  
Biol. Trace Elem. Res. 6, 327-335, 1984
- /AND84a/ Andrews, J.; Atkinson, G.F.  
Modification of a microwave oven for laboratory use  
J. Chem. Ed. 61(2), 177-178, 1984
- /AZI82/ Aziz, A.; Broekaert, J.A.C.; Leis, F.  
Analysis of microamounts of biological samples by evaporation in a gra-  
phite furnace and inductively coupled plasma atomic emission spectroscopy  
Spectrochim. Acta B37(5), 369-379, 1982
- /BAB47/ Babat, G.I.  
Electrodeless discharges and some allied problems  
J. Inst. Electr. Eng., Pt. 3, 94, 27-37, 1947
- /BAD63/ Badenoch, A.W.  
Some points in the management of uric acid stones  
J. Urol. 90(6), 665-668, 1963
- /BAK66/ see Introduction

- /BAR78/ Barrett, P.; Davidowski, L.J. Jr.; Penaro, K.W.; Copeland, T.R.  
Microwave oven-based wet digestion technique  
Anal. Chem. 50(7), 1021-1023, 1978
- /BAR81/ Barnes, R.M.  
Inductively coupled plasma atomic emission spectroscopy: a review  
TrAC, Trends Anal. Chem. 1(2), 51-55, 1981
- /BAR83/ Barnes, R.M.; Fodor, P.; Inagaki, K.; Fodor, M.  
Determination of trace elements in urine using inductively coupled plasma spectroscopy with a poly(dithiocarbamate) chelating resin  
Spectrochim. Acta B38(1/2), 245-257, 1983
- /BER76/ Berg, W.; Hesse, A.; Schneider, H.-J.  
A contribution to the formation mechanism of calcium oxalate urinary calculi. III. On the role of magnesium in the formation of oxalate calculi  
Urol. Res. 4(4), 161-167, 1976
- /BET78/ Betteridge, D.J.  
Flow injection analysis  
Anal. Chem. 50(9), 832A-846A, 1978
- /BIR63/ Bird, E.D.; Thomas, W.C. Jr.  
The effects of various metals on mineralization in vitro  
Proc. Soc. Exp. Biol. Med. 112(3), 640-643, 1963
- /BLA81/ see Introduction
- /BOC79/ Bock, R.  
A handbook of decomposition methods in analytical chemistry  
International Textbook Company, Glasgow, 1979, pp. 195
- /BOC79a/ op. cit., pp. 211
- /BOC79b/ op. cit., pp. 221
- /BOR69/ Borden, T.A.; Lyon, E.S.  
The effect of magnesium and pH on experimental calcium oxalate stone disease  
Invest. Urol. 6(4), 412-422, 1969
- /BOT85/ Botto, R.I.  
Method for correcting for acid and salt matrix interferences in ICP-AES  
Spectrochim. Acta B40(1/2), 397-412, 1985
- /BOU75/ Boumans, P.W.J.M.; De Boer, F.J.  
Studies of an inductively-coupled high frequency argon plasma for optical emission spectrometry. II. Compromise conditions for simultaneous multi-element analysis  
Spectrochim. Acta B30, 309-334, 1975
- /BOU75a/ Boumans, P.W.J.M.; De Boer, F.J.  
An assessment of the inductively coupled high-frequency plasma for simultaneous multi-element analysis  
Proc. Anal. Div. Chem. Soc. 12(5), 140-152, 1975
- /BOU76/ Boumans, P.W.J.M.  
Einige Überlegungen zur Situation der simultanen Multielementanalyse von Lösungen  
Fresenius' Z. Anal. Chem. 279, 1-16, 1976
- /BOU76a/ Boumans, P.W.J.M.  
Corrections for spectral interferences in optical emission spectrometry with special reference to the rf inductively coupled plasma  
Spectrochim. Acta B31(3), 147-152, 1976

- /BOU76b/ Boumans, P.W.J.M.; van Gool, G.H.; Jansen, J.A.J.  
A computerised programmable monochromator for flexible multi-element analysis with special reference to the inductively coupled plasma  
Analyst (London) 101, 585-587, 1976
- /BOU77/ Boumans, P.W.J.M.; De Boer, F.J.  
An experimental study of a 1 kW 50 MHz rf inductively coupled plasma with pneumatic nebulizer, and a discussion of experimental evidence for a non-thermal mechanism  
Spectrochim. Acta. B32(9/10), 365-395, 1977
- /BOU78/ Boumans, P.W.J.M.  
"Plasma sources" for multielement analysis of solutions: capabilities, limitations, and perspectives  
Mikrochim. Acta 1(3/4), 399-412, 1978
- /BOU78a/ Boumans, P.W.J.M.; Bastings, L.C.; De Boer F.J.; van Kollenburg, L.W.J.  
ICP-atomic emission spectrometry as a tool for flexible single-element analysis of non-routine samples  
Fresenius' Z. Anal. Chem. 291, 10-19, 1978
- /BOU80/ Boumans, P.W.J.M.  
Line coincidence tables for inductively coupled plasma atomic emission spectrometry (vol. 1 and 2)  
Pergamon Press, Oxford, 1980
- /BOY78/ Boyer, K.W.; Tanner, J.T.; Gajan, R.J.  
Multielement analytical techniques of the FDA  
Am. Lab. (Fairfield, Conn.) 10, 51-65, 1978
- /BRO39/ Brown, H.  
Micromethods for the quantitative analysis of urinary calculi  
J. Lab. Clin. Med. 24, 976-981, 1939
- /BRO83/ Browner, R.F.  
Sample introduction for inductively coupled plasmas and flames  
TrAC, Trends Anal. Chem. (Pers. Ed.) 2(5), 121-124, 1983
- /BUR55/ Burton, H.; Praill, P.F.G.  
Perchloric acid and some organic perchlorates  
Analyst (London) 80, 4-15, 1955
- /BUS68/ see Introduction
- /CAR80/ Carni, J.J.; James, W.D.; Koirttyohann, S.R.; Morris, E.R.  
Stable tracer iron-58 technique for iron utilization studies  
Anal. Chem. 52(1), 216-218, 1980
- /CHR69/ Christian, C.D.  
Medicine, trace elements and atomic absorption spectroscopy  
Anal. Chem. 41, 24A-30A, 1969
- /CHU80/ Church, S.E.  
Trace element determinations in geological reference materials - an evaluation of the ICP-AES method for geochemistry applications  
Dev. At. Plasma Spectrochem. Analysis, Proc. Int. Winter Conf. 1980, (Publ. 1981), pp. 410-434
- /COO77/ Cooley, T.N.; Martin, D.F.; Quinzel, R.H.  
Fume scrubber for a modified microwave oven for wet ashing biological samples  
J. Environ. Sci. Health A12(1-2), 15-19, 1977

- /DAH78/ Dahlquist, R.L.; Knoll, J.W.  
Inductively coupled plasma-atomic emission spectrometry: analysis of biological materials and soils for major, trace, and ultra-trace elements  
Appl. Spectros. 32(1), 1-30, 1978
- /DEB83/ De Boer, J.L.M.; Maessen, F.J.M.J.  
A comparative examination of sample treatment procedures for ICAP-AES analysis of biological tissue  
Spectrochim. Acta B38(5/6), 739-746, 1983
- /DEL74/ Dell, H.-D.; Fiedler, J.  
Bestimmung organisch gebundenen Fluors in biologischem Material  
Fresenius' Z. Anal. Chem. 270(4), 278-282, 1974
- /DEN80/ Denton, J.E.; Potter, G.D.; Santolucito, J.A.  
A comparison of skull and femur lead levels in adult rats  
Environ. Res. 23(2), 264-269, 1980
- /DES73/ Desmars, J.F.; Tawashi, R.  
Dissolution and growth of calcium oxalate monohydrate. I. Effect of magnesium and pH  
Biochim. Biophys. Acta 313, 256-267, 1973
- /DES80/ Dessy, R.E.; Starling, M.K.  
Fourth generation languages for laboratory applications  
Am. Lab. (Fairfield, Conn.) 12(2), 21-22 & 24-28 & 30 & 32, 1980
- /DEV83/ De Villiers, D.B.  
A century of spectroscopy in South Africa  
Spectrochim. Acta B38(5/6), 881-884, 1983
- /DIX85/ Dixon, W.J. (Chief Ed.)  
BMDP statistical software, 1985 Manual  
University of California Press, Berkely, 1985, pp. 80-85
- /DIX85a/ op. cit., pp. 133-141
- /DON77/ Donev, I.; Mashkarov, S.; Maritchkova, L.; Gotsev, G.  
Quantitative investigation of some trace elements in renal stones by neutron activation analysis  
J. Radioanal. Chem. 37, 441-449, 1977
- /DRA80/ Drašković, R.J.; Jaćimović, L.; Drašković, R.S.  
Some application of activation analysis in medicine  
Trace Elem. Anal. Chem. Med. Biol., Proc. Int. Workshop, 1st, 1980; pp. 173-180
- /DUN73/ Dunckley, J.V.  
Estimation of gold in urine by atomic absorption spectroscopy  
Clin. Chem. 19(9), 1081-1082, 1973
- /ELL67/ Elliot, J.S.; Eusebio, E.  
Calcium oxalate solubility: the effect of trace metals  
Invest. Urol. 4(5), 428-430, 1967
- /EJS67/ Eusebio, E.; Elliot, J.S.  
Effect of trace metals on the crystallization of calcium oxalate  
Invest. Urol. 4(5), 431-435, 1967
- /FAS74/ Fassel, V.A.; Kniseley, R.N.  
Inductively coupled plasma-optical emission spectroscopy  
Anal. Chem. 46(13), 1110A-1120A, 1974

- /FAS74a/ Fassel V.A.; Kniseley, R.N.  
Inductively coupled plasma  
Anal. Chem. 46(13), 1155A-1164A, 1974
- /FAS78/ Fassel, V.A.  
Quantitative elemental analyses by plasma emission spectroscopy  
Science 202(4364), 183-191, 1978
- /FEI80/ Feinendegen, L.E.; Kasperek, K.  
Medical aspects of trace element research  
Trace Elem. Anal. Chem. Med. Biol., Proc. Int. Workshop, 1st, 1980, pp. 1-37
- /FEL74/ Feldman, C.  
Perchloric acid procedure for wet-ashing organics for the determination of mercury (and other metals)  
Anal. Chem. 46(11), 1606-1609, 1974
- /FEL84/ Fell, G.S.  
Accuracy of trace element analysis in biological samples  
TrAC, Trends Anal. Chem. 3(7), IX-X, 1984
- /FIS25/ Fiske, C.H.; Subbarow, Y.  
The colorimetric determination of phosphorous  
J. Biol. Chem. 66(2), 375-400, 1925
- /FLE65/ Fleisch, H.; Bisaz, S.; Russell, R.  
The activating effect of lead on the precipitation of calcium phosphate  
Proc. Soc. Exp. Biol. Med. 118, 882-884, 1965
- /FLO85/ Floyd, M.A.; Halorna, A.A.; Morrow, R.W., Farrar, R.B.  
Rapid multi-element analysis of water samples by sequential ICP-AES  
Int. Lab. 15(4), 24-36, 1985
- /FOG58/ Fogg, D.N.; Wilkinson, N.T.  
The colorimetric determination of phosphorous  
Analyst (London) 83(988), 406-414, 1958
- /FRY77/ Fry, R.C.; Denton, M.B.  
High solids sample introduction for flame atomic absorption analysis  
Anal. Chem. 49(9), 1413-1417, 1977
- /FRY80/ Fry, R.C.; Northway, S.J.; Brown, R.M.; Hughes, S.K.  
Atomic fluorine spectra in the argon inductively coupled plasma  
Anal. Chem. 52(11), 1716-1722, 1980
- /GAB71/ Gabriel, K.R.  
The biplot graphical display of matrices with application to principal component analysis  
Biometrika 58, 458-467, 1971
- /GER34/ Gerlach, W.  
Zur Chemie der Konkreme  
Verh. Dtsch. Ges. Pathol. 27, 277-282, 1934
- /GLA80/ Gladney, A.S.  
Elemental concentrations in NBS biological and environmental standard reference materials  
Anal. Chim. Acta. 118, 385-396, 1980
- /GOM42/ Gomori, G.  
A modification of the colorimetric phosphorus determination for use with the photoelectric colorimeter  
J. Lab. Clin. Med. 27, 955-960, 1942

- /GOR70/ Gorsuch, T.T.  
The destruction of organic matter  
Pergamon Press, Oxford, 1970
- /GOU52/ Gourley, D.R.H.  
Failure of phosphorus-32 to exchange with organic phosphorus compounds  
Nature (London) 169(4292), 192-193, 1952
- /GRE64/ Greenfield, S.; Jones, I.L.; Berry, C.T.  
High pressure plasmas as spectroscopic emission sources  
Analyst (London) 89, 713-720, 1964
- /GRE75/ Greenfield, S.; Jones, I.L.; McGeachin, H.M.; Smith, P.B.  
Automatic multi-sample simultaneous multi-element analysis with a h. f.  
plasma torch and direct reading spectrometer  
Anal. Chim. Acta, 74, 225-245, 1975
- /GRE75a/ Greenfield, S.; McGeachin, McD.; Smith, P.B.  
Plasma emission sources in analytical spectroscopy - I  
Talanta 22, 1-15, 1975
- /GRE75b/ Greenfield, S.; McGeachin, McD.; Smith, P.B.  
Plasma emission sources in analytical spectroscopy - II  
Talanta 22, 553-562, 1975
- /GRE76/ Greenfield, S.; McGeachin, H. McD., Smith, P.B.  
Plasma emission sources in analytical spectroscopy - III  
Talanta 23, 1-14, 1976
- /GRE81/ Greenfield, S.  
FIA weds ICP - A marriage of convenience  
Ind. Res. Dev. 23, 140-145, 1981
- /GRE82/ Greenacre, M.J.; Underhill, L.G.  
Scaling a data matrix in a low dimensional Euclidean space  
in: D.M. Hawkins (Ed.), "Topics in applied multivariate analysis",  
Cambridge University Press, Cambridge, 1982, pp. 183-268
- /GRE84/ Greenacre, M.J.  
Theory and applications of correspondence analysis  
Academic Press, London, 1984, Appendix A
- /GRU64/ see Chapter I
- /GUN68/ see Introduction
- /HAM29/ see Chapter I
- /HAM31/ Hammarsten, G.  
The solubility of uric acid and the primary urates in water and salt  
solutions at 37°, with special reference to the formation of sediment in  
the urinary passages  
C. R. Trav. Lab. Carlsberg 19(7), 1-66, 1931
- /HAM37/ Hammarsten, G.  
Eine experimentelle Studie über Calciumoxalat als Steinbildner in den  
Harnwegen. Speziell mit Rücksicht auf die Bedeutung des Magnesiums  
Acta. Univ. Lund. Sec. 2, 32(12), 1-155, 1937
- /HAR49/ Harris, E.M.  
Perchloric acid fires  
Chem. Eng. (N.Y.) 56, 116-117, 1949

- /HAR73/ Harwood, J.E.; Hattingh, W.H.J.  
Colorimetric methods of analysis of phosphorus at low concentrations in water  
in: E.J. Griffith, A. Beeton, J.M. Spencer, D.T. Mitchell (Eds.); "Environmental phosphorus handbook"; J. Wiley, New York, 1973, Chapter 14, pp. 289-301
- /HAR85/ Hardman, D.; Verbek, A.A.  
Some observations on internal standardization in sequential ICP-AES  
S. Afr. J. Chem. 38(3), 145-148, 1985
- /HES74/ Hese, J.A.; Wilson, R.C.  
Use of a microwave oven in in-process control  
Anal. Chem. 46(8), 1160, 1974
- /HES76/ Hesse, A.; Berg, W.; Schneider, H.-J.; Hienzs, E.  
A contribution to the formation mechanism of calcium oxalate urinary calculi - I  
Urol. Res. 4, 125-128, 1976
- /HES76a/ Hesse, A.; Berg, W.; Schneider, H.-J.; Hienzs, E.  
A contribution to the formation mechanism of calcium oxalate urinary calculi - II  
Urol. Res. 4, 157-160, 1976
- /HES77/ see Introduction
- /HES78/ Hesse, A.; Schneider, H.-J.; Berg, W.  
Die Bedeutung von Spurenelementen in der Harnsteingenes  
Zentralbl. Pharm. 117(7), 753-756, 1978
- /HOD69/ Hodgkinson, A.; Peacock, M.; Nicholson, M.  
Quantitative analysis of calcium-containing urinary calculi  
Proc. Renal. Stone Res. Symp. 1968, (Publ. 1969), pp. 113-122
- /HOL53/ Holt, P.F.; Tarnoky, A.L.  
The analysis of calculi using microchemical methods  
J. Clin. Pathol. 6(2), 114-117, 1953
- /HOO64/ Hooft, C.; van Acker, K.; Valcke, R.  
Zink en Niersteenvorming  
Mem. Acad. R. Med. Belg. 26, 357-372, 1964
- /HUM76/ Human, H.G.C.; Scott, R.H.; Oakes, A.R.; West, C.D.  
The use of a spark as a sampling-nebulising device for solid samples in atomic-absorption, atomic-fluorescence and inductively coupled plasma emission spectrometry  
Analyst (London) 101, 265-271, 1967
- /JAN81/ Janghorbani, M.; Ting, B.T.G.; Istfan, N.W.; Young, V.R.  
Measurement of  $^{68}\text{Zn}$  and  $^{70}\text{Zn}$  in human-blood in reference to the study of zinc metabolism  
Am. J. Clin. Nutr. 34(4), 581-591, 1981
- /KAH82/ Kahn, H.L.  
AA or ICP? Each technique has its own advantages  
Ind. Res. Dev. 24(2), 156-160, 1982
- /KAH82a/ Kahn, H.L.  
AA or ICP? Which technique is best for you?  
Ind. Res. Dev. 24(3), 150-153, 1982
- /KIN67/ King, J.S. Jr.  
Etiologic factors involved in urolithiasis: A review of recent research  
J. Urol. 97(4), 583-591, 1967



- /KIN68/ King, J.S.; O'Connor, F.J. Jr.; Smith, M.J.V.; Crouse, L.  
The urinary calcium/magnesium ratio in calcigerous stone formers  
Invest. Urol. 6(1), 60-65, 1968
- /KIN71/ King, J.S. Jr.  
Currents in renal stone research  
Clin. Chem. 17(10), 971-982, 1971
- /KIR60/ Kirsten, W.J.; Carlsson, M.E.  
Investigation of the determination of phosphorus in organic compounds  
Microchem. J. 4(1), 3-31, 1960
- /KIR82/ Kirkbright, G.F.; Walton, S.J.  
Optical emission spectrometry with an inductively coupled radiofrequency argon plasma source and direct sample introduction from a graphite rod  
Analyst (London) 107, 267-281, 1982
- /KLU81/ Kluckner, P.D.; Brown, D.F.  
Analysis of teeth by plasma emission spectrometry  
Dev. At. Plasma Spectrochem. Anal., Proc. Int. Winter Conf. 1980, (Publ. 1981), pp. 713-717
- /KNA84/ Knapp, G.  
Decomposition methods in elemental trace analysis  
TRAC, Trends Anal. Chem. 38(7), 182-185, 1984
- /KNI73/ Kniseley, R.N.; Fassel, V.A.; Butler, C.C.  
Application of inductively coupled plasma excitation sources to the determination of trace metals in microliter volumes of biological fluids  
Clin. Chem. 10(8), 807-812, 1973
- /KOH80/ Koh, T.-S.  
Microwave drying of biological tissues for trace element determination  
Anal. Chem. 52(12), 1978-1979, 1980
- /KOI75/ Koirtjohann, S.R.; Lichte, F.R.  
The effect of acid concentration on the emission intensity from the inductively coupled plasma  
Abstr. Pap. - Int. Conf. At. Spectrosc., 5th, 1975, Paper B26
- /KOI81/ Koirtjohann, S.R.; Glass, E.D.; Lichte, F.E.  
Some observations on perchloric acid interferences in furnace atomic absorption  
Appl. Spectrosc. 35(1), 22-26, 1981
- /KOL68/ Kollwitz, A.-A.  
Technik und Bedeutung der Harnsteinanalyse  
Dtsch. Med. J. 19(1), 22-28, 1968
- /KOV85/ Kovalev, M.M.  
Qualitative spectral analysis of drinking water and urinary calculi  
Klin. Med. (Moscow) 33(11), 54-56, 1955
- /KRA79/ Krasowska, J.A.; Copeland, T.R.  
Matrix interferences in furnace atomic absorption spectrometry  
Anal. Chem. 51(11), 1843-1849, 1979
- /LAG56/ see Chapter I
- /LAR75/ Larson, G.F.; Fassel, V.A.; Scott, R.H.; Kniseley, R.N.  
Inductively coupled plasma-optical emission analytical spectrometry. A study of some interelement effects  
Anal. Chem. 47(2), 238-243, 1975

- /LEE83/ Lee, J.  
Calcium matrix effects in multi-element analysis of animal bone by ICP-AES  
Anal. Chim. Acta 152, 141-147, 1983
- /LEE83a/ Lee, J.  
Multi-element analysis of animal tissue by inductively coupled plasma  
emission spectrometry  
ICP Inf. Newsl. 8(10), 553-561, 1983
- /LEI81/ Leighty, D.A.; Chase, D.S.; Klein, V.F.  
ICP atomic emission spectroscopy - Training seminar notes  
Instrumentation Laboratory Inc.; Analytical Instrument Division; July  
1981, IL P/N 120915
- /LEN81/ Lentner, C. (Ed.)  
Geigy scientific tables; 8th ed.; Vol. 1; Units of measurement, body  
fluids, composition of the body, nutrition  
Ciba-Geigy Ltd., Basle, Switzerland, 1981, pp. 53-107
- /LEO56/ Leonard, R.H.; Butt, A.J.  
Analysis of urinary calculi using flame photometry for calcium deter-  
minations  
in: A.J. Butt (Ed.); "Etiologic factors in renal lithiasis"; C.C. Thomas,  
Springfield, Ill., USA, 1956, Chapter 18, pp. 359-371
- /LEV78/ Levinson, A.A.; Nosal, M.; Davidman, M.; Prien, E.L. Sr.; Prien, E.L. Jr.;  
Stevenson, R.G.  
Trace elements in kidney stones from three areas in the United States  
Invest. Urol. 15(4), 270-274, 1978
- /LIC80/ Lichte, F.E.; Hopper, S.; Osborn, T.W.  
Determination of silicon and aluminium in biological materials by induc-  
tively coupled plasma emission spectrometry  
Anal. Chem. 52(1), 120-124, 1980
- /LON80/ Lonnerdal, B.; Clegg, M.; Keen, C.L.; Hurley, L.S.  
Effects of wet ashing techniques on the determination of trace element  
concentrations in biological samples  
Trace Elem. Anal. Chem. Med. Biol., Proc. Int. Workshop, 1st, 1980, pp.  
619-628
- /LYO65/ Lyon, E.S.; Vermeulen, C.W.  
Crystallization concepts and calculogenesis: observations on artificial  
oxalate concretions  
Invest. Urol. 3(3), 390-320, 1965
- /MAH83/ Mahanti, H.S.; Barnes, R.M.  
Determination of major, minor and trace elements in bone by ICP emission  
spectrometry  
Anal. Chim. Acta 151, 409-417, 1983
- /MAT40/ Mathé, C.P.; Archanbeault, R.C.  
Spectrographic analysis of urinary calculi (Preliminary Report)  
Pac. Coast Med. 7(1), 13-19, 1940
- /MAT40a/ Mathé, C.P.; Archanbeault, R.C.  
Spectrographic analysis of urinary calculi  
Urol. Cutaneous Rev. 44(3), 161-164, 1940
- /MCQ79/ McQuaker, N.R.; Brown, D.F.; Kluckner, P.D.  
Digestion of environmental materials for analysis by inductively coupled  
plasma-atomic emission spectrometry  
Anal. Chem. 51(7), 1082-1084, 1979

- /MEL71/ Melnick, I.; Landes, R.R.; Hoffmann, A.A.; Burch, J.F.  
Magnesium therapy for recurring calcium oxalate urinary calculi  
J. Urol. 105(1), 119-122, 1971
- /MER82/ Mermet, J.M.; Hubert, J.  
Analysis of biological materials using plasma atomic emission spectroscopy  
Prog. Anal. At. Spectrosc. 5(1), 1-33, 1982
- /MEY72/ Meyer, J.L.; Nancollas, G.H.  
Effect of stannous and fluoride ions on the rate of crystal growth of hydroxyapatite  
J. Dent. Res. 51(5), 1443-1450, 1972
- /MEY77/ Meyer, J.L.; Angino, E.F.  
The role of trace metals in calcium urolithiasis  
Invest. Urol. 14(5), 347-350, 1977
- /MEY82/ Meyer, J.L.; Thomas, W.C. Jr.  
Trace metal-citric acid complexes as inhibitors of calcification and crystal growth - I. Effects of Fe(III), Cr(III) and Al(III) complexes on calcium phosphate crystal growth  
J. Urol. 128, 1372-1375, 1982
- /MEY82a/ Meyer, J.L.; Thomas, W.C. Jr.  
Trace metal citric-acid complexes as inhibitors of calcification and crystal growth - II. Effects of Fe(III), Cr(III) and Al(III) on calcium oxalate crystal growth  
J. Urol. 128, 1376-1378, 1982
- /MIL79/ Miller, J.M.  
The inhibition of the formation of struvite crystals on latex catheters by silver ion  
Invest. Urol. 17(1), 60, 1979
- /MIN82/ Minoia, C.; Pozzoli, L.; Angeleri, S.; Tempini, G.; Candura, F.  
Determination of silicon in urine by inductively coupled plasma emission spectroscopy  
At. Spectrosc. 3(3), 70-72, 1982
- /MOD69/ Modlin, M.  
Urinary sodium and renal stone  
Proc. Renal Stone Res. Symp., 1968, (Publ. 1969), pp. 209-220
- /MON72/ Monar, I.  
Analysenautomat zur simultanen Mikrobestimmung von C, H und N  
Mikrochim. Acta (6), 784-806, 1972
- /MOO64/ Moore, C.A.; Bunce, G.E.  
Reduction of frequency of renal calculus formation by oral magnesium administration - A preliminary report  
Invest. Urol. 2(1), 7-13, 1964
- /MOO82/ Moore, G.L.  
Some candle ...!  
ChemSA 8(7), 80-81, 1982
- /MOO85/ Moore, C.B.; Canepa, J.A.  
Geological and inorganic materials  
Anal. Chem. 57(5), 88R-94R, 1985
- /MOR80/ Morris, J.S.; Anderson, H.  
The analysis of selenium in botanical samples via INAA using  $^{77m}\text{Se}$   
Trans. Am. Nucl. Soc. 34, 174-175, June 1980

- /MUR56/ Murphy, J.; Riley, J.P.  
The storage of sea-water samples for the determination of dissolved inorganic phosphate  
Anal. Chim. Acta 14, 318-319, 1956
- /MUS72/ Muse, L.A.  
Safe handling of the perchloric acid in the laboratory  
J. Chem. Ed. 49(9), A463-A466, 1972
- /NAD84/ Nadkarni, R.A.  
Applications of microwave oven sample dissolution in analysis  
Anal. Chem. 56(12), 2233-2237, 1984
- /NAG63/ Nagy, Z.; Szabó, E.; Kelenhegyi, M.  
Spektralanalytische Untersuchungen von Nierensteinen auf metallische Spurenelemente  
Z. Urol. 56(4), 185-190, 1963
- /NAN74/ Nancollas, G.H.; Wefel, J.S.  
Effect of stannous fluoride, sodium fluoride and stannous chloride on crystallization of dicalcium phosphate dihydrate at constant pH  
J. Cryst. Growth 23(3), 169-176, 1974
- /NEU53/ Neuman, W.F.; Neuman M.W.  
The nature of the mineral phase of bone  
Chem. Rev. 53(1), 1-45, 1953
- /NEU62/ Neuman, W.F.; Toribara, T.Y.; Mulryan, B.J.  
Synthetic hydroxyapatite crystals - I. Sodium and potassium fixation  
Arch. Biochem. Biophys. 98(3), 384-390, 1962
- /NEW61/ Newesely, H.  
Changes in crystal types of low solubility calcium phosphates in the presence of accompanying ions  
Arch. Oral Biol., Special Suppl. 6, 174-180, 1961
- /NIC80/ Nichols, J.A.; Woodriff, R.  
Coprecipitation of heavy metals directly in graphite crucibles for furnace atomic absorption spectrometry  
J. Assoc. Off. Anal. Chem. 63(3), 500-505, 1980
- /NIX74/ Nixon, D.E.; Fassel, V.A.; Kniseley, R.N.  
Inductively coupled plasma-optical emission analytical spectroscopy - Tantalum filament vaporization of microliter samples  
Anal. Chem. 46(2), 210-213, 1974
- /NOR80/ Northway, S.J.; Brown, R.M.; Fry, R.C.  
Atomic nitrogen spectra in the argon inductively coupled plasma  
Appl. Spectrosc. 34(3), 338-348, 1980
- /NOR80a/ Northway, S.J.; Fry, R.C.  
Atomic oxygen spectra in the argon inductively couple plasma (ICP)  
Appl. Spectrosc. 34(3), 332-338, 1980
- /NYG84/ Nygaard, D.  
Inductively coupled plasma methods manual  
Allied Analytical Systems, Andover, Ma., USA, 1984
- /NYG84a/ Nygaard, D.D.; Chase, D.S.; Leighty, D.A.  
Vacuum monochromator with ICP lets analysts find hidden elements  
Res. Dev. 26(2), 172-175, 1984
- /NYG85/ Nygaard, D.D.; Schleicher, R.G.; Leighty, D.A.  
Determination of halides by ICP emission spectrometry  
Am. Lab. (Fairfield, Conn.) 17(6), 59-61, 1985

- /OGB81/ see Introduction
- /OHT53/ Ohta, N.  
Inorganic constituents of biological materials - I  
J. Chem. Soc. Jpn. Pure Chem. Sect. 74, 506-510, 1953
- /OHT55/ Ohta, N.  
Inorganic constituents in biological materials - IV. Iron and manganese of human stones, blood and organs  
J. Chem. Soc. Jpn. Pure Chem. Sect. 76, 590-593, 1955
- /OHT55a/ Ohta, N.  
Sodium and potassium contents of human stones  
J. Chem. Soc. Jpn. Pure Chem. Sect. 76, 1235-1237, 1955
- /OHT57/ Ohta, N.  
Inorganic constituents in biological materials - VIII. Copper, zinc, and iron contents of gallstones  
J. Chem. Soc. Jpn. Pure Chem. Sect. 78, 7-13, 1957
- /OHT57a/ Ohta, N.  
Inorganic constituents in biological material - IX. Copper, zinc, and iron contents of urinary and pancreatic calculi  
J. Chem. Soc. Jpn. Pure Chem. Sect. 78, 13-16, 1957
- /OHT57b/ Ohta, N.  
Studies on inorganic constituents in biological materials - On the inorganic constituents in human stones  
Bull. Chem. Soc. Jpn. 30(8), 833-841, 1957
- /OLS84/ Olsen, S.D.; Böhmer, R.G.  
The inductively coupled plasma as spectroscopic source  
Analytika (Johannesburg), June, 7-13, 1984
- /OLS85/ Olsen, S.D.; Rama, D.B.K.; Böhmer, R.G.  
Biomedical and nutritional applications of inductively coupled plasma  
ChemSA 11(6), 144-148, 1985
- /PAK67/ Pak, C.Y.C.; Bartter, F.C.  
Ionic interaction with bone mineral - II. The control of  $\text{Ca}^{2+}$  and  $\text{PO}_4^{2-}$  exchange by univalent cation  $\text{Ca}^{2+}$  substitution at the hydroxyapatite crystal surface  
Biochim. Biophys. Acta 141, 410-420, 1967
- /PAT80/ Patel, P.N.  
Magnesium calcium hydroxylapatite solid solutions  
J. Inorg. Nucl. Chem. 42(8), 1129-1132, 1980
- /PEI82/ Peisach, M.; Jacobson, L.; Boule, G.J.; Gihwala, D.; Underhill, L.G.  
Multivariate analysis of trace elements determined in archaeological materials and its use for characterization  
J. Radioanal. Chem. 69(1-2), 349-364, 1982
- /PHI53/ Philipsborn, H. von  
Zur mineralogischen Untersuchung der Harnsteine  
Fortschr. Mineral. 31, 62-69, 1953
- /PHI58/ see Introduction
- /POU85/ Pougnet, M.A.B.; Orren, M.J.; Haraldsen, L.  
Determination of beryllium and lithium in coal ash by inductively coupled plasma atomic emission spectroscopy  
Int. J. Env. Anal. Chem. 21, 213-228, 1985

- /POU86/ Pougnet, M.A.B.; Wandt, M.A.E.  
Microwave digestion procedure for ICP-AES analysis of biological samples  
ChemSA 12(1), 16-18, 1986
- /POU86a/ Pougnet, M.A.B.; Orren, M.J.  
The determination of boron by inductively coupled plasma atomic emission spectroscopy  
Int. J. Env. Anal. Chem. (in press)
- /REE61/ Reed, T.B.  
Induction-coupled plasma torch  
J. Appl. Phys. 32(5), 821-824, 1961
- /REE61a/ Reed, T.B.  
Growth of refractory crystals using the induction plasma torch  
J. Appl. Phys. 32(12), 2534-2535, 1961
- /REE62/ Reed, T.B.  
Plasma torches  
Int. Sci. Technol., June, 42-48, 1962
- /ROD82/ see Introduction
- /ROD84/ Rodgers, A.L.; Scaillet, S.; Wandt, M.A.E.  
Procedure for the characterization of apatite in urinary calculi  
Urinary Stone, Proc. 2nd Int. Urinary Stone Conf. 1983, (Publ. 1984), pp. 331-338
- /RUS80/ Rushton, H.G.; Spector, M.; Rodgers, A.L.; Magura, C.E.  
Crystal deposition in the renal tubules of hyperoxaluric and hypomagnesemic rats  
Scanning Electron Micros. III, 387-398, 1980
- /RUS81/ Rushton, H.G.; Spector, M.; Rodgers, A.L.; Hughson, M.; Magura, C.E.  
Developmental aspects of calcium oxalate tubular deposits and calculi induced in rat kidneys  
Invest. Urol. 19(1), 52-57, 1981
- /SAL79/ Salin, E.D.; Horlick, G.  
Direct sample insertion device for inductively coupled plasma emission spectroscopy  
Anal. Chem. 51(13), 2284-2286, 1979
- /SCH60/ Schumacher, J.C.  
Perchlorates - Their properties, manufacture and uses  
ACS Monogr. 146, 1-257, 1960
- /SCH66/ see Chapter I
- /SCH68/ Schneider, H.-J.  
Die anorganischen Bestandteile der Nierensteine und deren Einfluss auf die Steinart  
Urologe 7(6), 347-352, 1968
- /SCH69/ Schneider, H.-J.  
Die Gesetzmäßigkeiten des Aufbaues anorganischer Nierensteine  
Urologe 8(4), 180-184, 1969
- /SCH70/ Schneider, H.-J.; Straube, G.; Anke, M.  
Zink in Harnsteinen  
Z. Urol. 63(12), 895-900, 1970
- /SCH71/ Schneider, H.-J.; Hesse, A.  
Spurenelemente in Harnsteinen: Lithium  
Z. Urol. 64(10), 759-761, 1971

- /SCH82/ Schramel, P.; Xu-Li-Giang  
Investigation of interelement effects in trace element analysis in biological and environmental samples by ICP spectrometry  
ICP Inf. Newsl. 7(9), 429-440, 1982
- /SCH83/ Schramel, P.  
Consideration of inductively coupled plasma spectroscopy for trace element analysis in the bio-medical and environmental fields  
Spectrochim. Acta 38(1/2), 199-206, 1983
- /SCH85/ Schwille, P.O.; Hamper, A.; Sigel, A.  
Urinary and serum sulfate in idiopathic recurrent calcium urolithiasis  
Urolithiasis Rel. Clin. Res., Proc. 5th Int. Symp. 1984, (Publ. 1985), pp. 339-342
- /SC074/ Scott, R.H.; Fassel, V.A.; Kniseley, R.N.; Nixon, D.E.  
Inductively coupled plasma-optical emission analytical spectrometry  
Anal. Chem. 46(1), 75-80, 1974
- /SC082/ Scott, R.; Cunningham, C.; McLelland, A.; Fell, G.S.; Fitzgerald-Finch, O.P.; McKellar, N.  
The importance of cadmium as a factor in calcified upper urinary tract stone disease - a prospective 7-year study  
Br. J. Urol. 54(6), 584-589, 1982
- /SHE02/ Sherman, H.C.  
The determination of sulphur and phosphorus in organic materials  
J. Am. Chem. Soc. 24, 1100-1109, 1902
- /SIM68/ Simpson, D.R.  
Substitutions in apatite - I. Potassium-bearing apatite  
Am. Mineral. 53(3/4), 432-444, 1968
- /SK080/ Skoog, D.A.; West, D.M.  
Principles of instrumental analysis, 2nd ed.  
Saunders College, Philadelphia, 1980, pp. 336-351
- /SMI57/ Smith, G.F.  
Wet oxidation of organic matter employing perchloric acid at graded oxidation potentials and controlled temperatures  
Anal. Chim. Acta 17, 175-158, 1957
- /SMI65/ Smith, G.F.  
The wet chemical oxidation of organic compositions employing perchloric acid  
G.F. Smith Chemical Co., Columbus, Oh., USA, 1965, pp. 1-105
- /SMI83/ Smith, S.B. Jr.; Schleicher, R.G.; Dennison, A.G.; McLean, G.A.  
Consideration on the design of a sample introduction and plasma generation system for ICP spectrometry  
Spectrochim. Acta 38(1/2), 157-163, 1983
- /SOB49/ Sobel, A.E.; Nobel, S.; Hanok, A.  
The reversible inactivation of calcification in vitro  
Proc. Soc. Exp. Biol. Med. 72(367), 68-72, 1949
- /SPI76/ Spillman, R.W.; Malmstadt, H.V.  
Computer-controlled programmable monochromator system with automated wavelength calibration background correction  
Anal. Chem. 48(2), 303-311, 1976
- /STR78/ Strandberg, M.; Östling, G.  
A microwave heating device for a discrete automatic analysis system  
Chem. Instrum. 8(3), 205-214, 1978

- /STU85/ Sturgeon, R.F.; Willie, S.N.; Berman, S.S.  
Preconcentration of selenium and antimony from seawater for determination by graphite furnace atomic absorption spectrometry  
Anal. Chem. 57(1), 6-9, 1985
- /SUB82/ Subramanian, K.S.; Meranger, J.C.  
Simultaneous determination of 20 elements in some human kidney and liver autopsy samples by inductively-coupled plasma atomic emission spectrometry  
Sci. Total Environ. 24, 147-157, 1982
- /SUT69/ Sutor, D.J.  
Growth studies of calcium oxalate in the presence of various ions and compounds  
Br. J. Urol. 41, 171-178, 1969
- /SUT70/ Sutor, D.J.; Wooley, S.E.  
Growth studies of calcium oxalate in the presence of various compounds and ions - Part II  
Br. J. Urol. 42, 296-301, 1970
- /THO81/ Thompson, M.; Goulter, J.E.; Sieper, F.  
Laser ablation for the introduction of solid samples into an inductively coupled plasma for atomic emission spectrometry  
Analyst (London) 106(1258), 32-39, 1981
- /THO82/ Thomas, W.C. Jr.  
Trace metal-citric acid complexes as inhibitors of calcification and crystal formation  
Proc. Soc. Exp. Biol. Med. 170(3), 321-327, 1982
- /TOZ81/ see Introduction
- /TRA64/ Trautz, O.R.; Zapanta-LeGeros, R.; LeGeros, J.P.  
Effect of magnesium on various calcium phosphates - II  
J. Dent. Res. 43(5), 751, 1964
- /TYS81/ Tyson, J.F.; Idris, A.B.  
Flow injection sample introduction for atomic-absorption spectrometry: Applications of a simplified model for dispersion  
Analyst (London) 106, 1125-1129, 1981
- /UND85/ Underhill, L.G.  
SVDD: A computer programme for graphical displays using singular value decomposition  
Technical Reports, Department of Mathematical Statistics, University of Cape Town, 1985
- /WAL79/ Walsh, G.E.; Ainsworth, K.A.; Rigby, R.  
Resistance of red mangrove (*Rhizophora mangle* L.) seedlings to lead, cadmium, and mercury  
Biotropica 11(1), 22-27, 1979
- /WAN84/ Wandt, M.A.E.; Pougnet, M.A.B.; Rodgers, A.L.  
Determination of calcium, magnesium and phosphorus in human stones by inductively coupled plasma atomic-emission spectroscopy  
Analyst (London) 109, 1071-1074, 1984
- /WAN85/ Wandt, M.A.E.; Pougnet, M.A.B.; Rodgers, A.L.  
Analysis of urinary calculi by inductively coupled plasma atomic emission spectroscopy : new insight into stone structure  
Urolithiasis Related Clin. Res., Proc. 5th Int. Symp., 1984, (Publ. 1985), pp. 699-702
- /WAN86/ to be published



- /WEN65/ Wendt, R.H.; Fassel, V.A.  
Induction-coupled plasma spectrometric excitation source  
Anal. Chem. 37(7), 920-922, 1965
- /WEN66/ Wendt, R.H.; Fassel, V.A.  
Atomic absorption spectroscopy with induction-coupled plasmas  
Anal. Chem. 38(2), 337-338, 1966
- /WES70/ Westbury, E.J.; Omenogor, P.  
A quantitative approach to the analysis of renal calculi  
J. Med. Lab. Technol. 27, 462-474, 1970
- /WIN77/ Winge, R.K.; Fassel, V.A.; Kniseley, R.N.; DeKalb, E.; Haas, W.J. Jr.  
Determination of trace elements in soft, hard, and saline waters by the inductively coupled plasma, multi-element atomic emission spectroscopy (ICP-MAES) technique  
Spectrochim. Acta B32(9/10), 327-345, 1977
- /WUN81/ Wunderlich, W.  
Aspects of the influence of magnesium ions on the formation of calcium oxalate  
Urol. Res. 9(4), 157-161, 1981
- /YAN85/ Yang, J.Y.; Yang, M.H.; Lin, S.M.  
Study of the effect of decomposition methods on the accurate determination of zinc in biological samples by electrophoresis  
Anal. Chem. 57(2), 472-474, 1985
- /ZAP73/ Zapanta-LeGeros, R.; Morales, P.  
Renal stone crystals grown in gel systems - A preliminary report  
Invest. Urol. 11(1), 12-16, 1973

#### 4. Chapter III

- /ALT73/ Altschuler, Z.S.  
The weathering of phosphate deposits - geochemical and environmental aspects  
in: E.J. Griffith, A. Beeton, J.M. Spencer, D.T. Mitchell (Eds.); "Environmental phosphorus handbook"; J. Wiley, New York, 1973, pp. 33-96
- /ANA82/ Anasuya, A.  
Role of fluoride in formation of urinary calculi: studies in rats  
J. Nutr. 112(9), 1787-1795, 1982
- /ANF69/ Anfält, T.; Jagner, D.  
Effect of acetate buffer on the potentiometric titration of fluoride with lanthanum using a lanthanum fluoride membrane electrode  
Anal. Chim. Acta 47, 483-494, 1969
- /ANF70/ Anfält, T.; Jagner, D.  
Effect of carboxylic acid buffers on the potentiometric titration of fluoride with lanthanide nitrates using a lanthanum fluoride membrane electrode  
Anal. Chim. Acta 50, 23-30, 1970
- /ARM33/ Armstrong, W.D.  
Modification of the Willard-Winter method for fluorine determination  
J. Am. Chem. Soc. 55, 1741-1742, 1933

- /AUE62/ Auermann, E.  
Untersuchungen über die Fluorausscheidung im Urin  
Dtsch. Gesundheitswes. 17(40), 1735-1741, 1962
- /AUE69/ Auermann, E.; Kühn, H.  
Untersuchungen über den Fluorgehalt von Harnsteinen  
Dtsch. Gesundheitswes. 24, 565-569, 1969
- /AUE71/ Auermann, E.; Kühn, H.  
Fluoride content of kidney stones  
Fluoride 4(3), 150-151, 1971
- /BAE64/ Bäumler, J.  
Mikrofluorbestimmung in biologischem Material  
Chimia 18, 218-219, 1964
- /BAE64a/ Bäumler, J.; Glinz, E.  
Bestimmung von Fluoridionen im Mikrogrammbereich  
Mitt. Geb. Lebensmittelunters. Hyg. 55, 250-264, 1964
- /BAI76/ Bailey, P.L.  
Analysis with ion-selective electrodes  
Heyden, London, 1976, p. 43
- /BAR68/ Barnes, F.W.; Runcie, J.  
Potentiometric method for the determination of inorganic fluoride in biological material  
J. Clin. Pathol. 21, 668-670, 1968
- /BAU68/ Baumann, E.W.  
Trace fluoride determination with specific ion electrode  
Anal. Chim. Acta 42, 127-132, 1968
- /BAU71/ Baumann, E.W.  
Sensitivity of the fluoride-selective electrode below the micromolar range  
Anal. Chim. Acta 54, 189-197, 1971
- /BEL58/ Belcher, R.; Leonard, M.A.; West, T.S.  
The preparation and analytical properties of NN-di(carboxymethyl)ammonio-methyl derivatives of some hydroxyanthraquinones  
J. Chem. Soc., June, 2390-2393, 1958
- /BER59/ Berka  
Pravcovni lekarstvi 1, 1959  
(cited by /CON63/)
- /BER76/ Berg, W.; Schnapp, J.-D.; Schneider, H.-J.; Hesse, A.; Hienzsch, E.  
Crystaloptical and spectroscopical findings with calcium oxalate crystals in the urine sediment. A contribution to the genesis of oxalate stones  
Eur. Urol. 2, 92-97, 1976
- /BEY63/ Beyermann, K.  
Abtrennung und elektrochemische Bestimmung von Nanogrammmengen von Fluorid  
Fresenius' Z. Anal. Chem. 194, 1-19, 1963
- /BIX84/ Bixler, J.W.; Solomon, L.S.  
Restoration of unresponsive fluoride ion selective electrodes  
Anal. Chem. 56(14), 3004-3005, 1984
- /BOC66/ Bock, R.; Semmler, H.-J.; Behrends, K.  
Eine Verteilungsreaktion des Fluorid-Ions  
Naturwissenschaften 53(12), 305, 1966

- /BOC67/ Bock, R.; Semmler, H.-J.  
Separation and determination of fluoride ion with the aid of organic silicon compounds  
Fresenius' Z. Anal. Chem. 230(3), 161-184, 1967
- /BOC68/ Bock, R.; Strecker, S.  
Direkte elektrometrische Bestimmung des Fluorid-Ions  
Fresenius' Z. Anal. Chem. 235, 322-334, 1968
- /BOC73/ Bock, R.; Strecker, S.  
Abtrennung und gas-chromatographische Bestimmung von Fluoridspuren  
Fresenius' Z. Anal. Chem. 266, 110-116, 1973
- /BOY85/ Boyer, K.W.; Horwitz, W.; Albert, R.  
Interlaboratory variability in trace element analysis  
Anal. Chem. 57(2), 454-459, 1985
- /BRA80/ Brätter, P.; Behne, D.; Gawlik, D.; Gessner, H.; Höfer, T.; Rösick, U.  
On the bone trace element content during pregnancy and lactation  
Trace Elem. Anal. Chem. Med. Biol., Proc. Int. Workshop, 1st, 1980, pp. 47-56
- /BRO64/ Brown, W.E.; Nylen, M.U.  
Role of octacalcium phosphate in formation of hard tissues  
J. Dent. Res. 43(5), 751-752, 1964
- /BRO66/ Brown, W.E.  
Crystal growth of bone mineral  
Clin. Orthop. Relat. Res. 44, 205-220, 1966
- /BRO73/ Brown, W.E.  
Solubilities of phosphates and other sparingly soluble compounds  
in: E.J. Griffith, A. Beeton, J.M. Spencer, D.T. Mitchell (Eds.);  
"Environmental phosphorus handbook"; J. Wiley, New York, 1973, pp. 203-239
- /BRU68/ Brudevold, F.; McCann, H.G.; Grøn, P.  
An enamel biopsy method for determination of fluoride in human teeth  
Arch. Oral Biol. 13, 877-885, 1968
- /BUE63/ Büttner, W.; Schülke, S.; Soyka, S.  
Eine einfache Bestimmung kleiner Mengen von Fluor (5-30 µg) in Knochen und Zahnhartgeweben durch Diffusion  
Dtsch. Zahnärztl. Z. 18(1), 24-28, 1963
- /CER70/ Cernik, A.A.; Cooke, J.A.; Hall, R.J.  
Specific ion electrode in the determination of urinary fluoride  
Nature (London) 227, 1260-1261, 1970
- /CHR84/ Christoffersen, J.; Christoffersen, M.R.; Arends, J.  
A simple model for the effect of fluoride ions on remineralization of partly demineralized tooth enamel  
J. Cryst. Growth 67(1), 102-106, 1984
- /CHR84a/ Christoffersen, M.R.; Christoffersen, J.; Arends, J.  
Kinetics of dissolution of calcium hydroxyapatite - VII. The effect of fluoride ions  
J. Cryst. Growth 67(1), 107-114, 1984
- /COL71/ Collombel, C.; Bureau, J.; Cotte, J.  
Dosages des fluorures dans les eaux et les urines au moyen d'une electrode specifique  
Ann. Pharm. Fr. 29(11), 541-552, 1971

- /CON63/ Conway, E.J.  
Microdiffusion analysis and volumetric error  
Chemical Publishing Co., New York, 1963
- /CZA85/ Czaban, J.D.  
Electrochemical sensors in clinical chemistry: yesterday, today, tomorrow  
Anal. Chem. 57(2), 345A-356A, 1985
- /DIE80/ Dieumegard, D.; Maurel, B.; Amsel, G.  
Microanalysis of fluorine by nuclear reactions - I.  $^{19}\text{F}(\text{p}, \alpha_0)^{16}\text{O}$  and  $^{19}\text{F}(\text{p}, \alpha\gamma)^{16}\text{O}$  reactions  
Nucl. Instrum. Methods 168, 93-103, 1980
- /DIL54/ Dillon, C.  
Fluorine content of a renal calculus  
Dental Prac. 4, 181, 1954
- /DUR67/ Durst, A.; Taylor, J.K.  
Modification of the fluoride activity electrode for microchemical analysis  
Anal. Chem. 39(12), 1483-1485, 1967
- /DUR68/ Durst, R.A.  
Fluoride microanalysis by linear null-point potentiometry  
Anal. Chem. 40(6), 931-935, 1968
- /EDI85/ N.N. (Editor's page)  
Fluoridation: a new report on effectiveness and safety  
Int. Lab. 15(2), 4, 1985
- /EDM69/ Edmond, C.R.  
Direct determination of fluoride in phosphate rock samples using the specific ion electrode  
Anal. Chem. 41(10), 1327-1328, 1969
- /ERD75/ Erdmann, D.E.  
Automated ion-selective electrode method for determining fluoride in natural waters  
Environ. Sci. Technol. 9, 252-253, 1975
- /EVA70/ Evans, L.; Hoyle, R.D.; Macaskill, J.B.  
An accurate and rapid method of analysis for fluorine in phosphate rocks  
N. Z. J. Sci. 13(1), 143-148, 1970
- /FEI80/ see Chapter II
- /FRA66/ Frant, M.S.; Ross, J.W. Jr.  
Electrode for sensing fluoride ion activity in solution  
Science 154(3756), 1553-1555, 1966
- /FRA68/ Frant, M.S.; Ross, J.W. Jr.  
Use of a total ionic strength adjustment buffer for electrode determination of fluoride in water supplies  
Anal. Chem. 40(7), 1169-1171, 1968
- /FRA71/ Francis, M.D.; Webb, N.C.  
Hydroxyapatite formation from a hydrated calcium monohydrogen phosphate precursor  
Calcif. Tissue Res. 6, 335-342, 1971
- /FRY80/ see Chapter II
- /GRO69/ Grøn, P.; Yao, K.; Spinelli, M.  
A study of inorganic constituents in dental plaque  
J. Dent. Res., Suppl. 48(5), 799-805, 1969

- /GUD09/ Gudzent, F.  
Physikalisch-chemische und chemische Untersuchungen über das Verhalten der Harnsäure in Lösungen  
Hoppe-Seyler's Z. Physiol. Chem. 60, 25-37, 1909
- /HAL60/ Hall, R.J.  
The determination of microgram amounts of fluorine by diffusion  
Analyst (London) 85(1013), 560-563, 1960
- /HAL69/ Hall, R.J.  
The diffusion of fluoride with hexamethyldisiloxane  
Talanta 16(1), 129-133, 1969
- /HAL76/ Hallsworth, A.S.; Weatherell, J.A.; Deutsch, D.  
Determination of subnanogram amounts of fluoride with the fluoride electrode  
Anal. Chem. 48(12), 1660-1664, 1976
- /HAM38/ Hammarsten, G.  
Harnsäuresteine und Harn-pH  
C. R. Trav. Lab. Carlsberg Ser. Chim. 22, 193-198, 1938
- /HAN73/ Hanocq, M.  
Étude de la microdiffusion de l'ion fluorure sous forme de fluorure d'hydrogène  
Mikrochim. Acta, 729-743, 1973
- /HAN84/ Hanson, A.L.; Kraner, H.W.; Shroy, R.E.; Jones, K.W.  
Measurement of the fluorine content of three NBS standard reference materials by use of the  $^{19}\text{F}(p,p')^{19}\text{F}$  reaction  
Nucl. Instrum. Methods Phys. Res. B4, 401-403, 1984
- /HAR69/ Harwood, J.E.  
The use of an ion-selective electrode for routine fluoride analyses on water samples  
Water Res. 3, 273-280, 1969
- /HER56/ Herman, J.R.  
Fluorine in urinary tract calculi  
Proc. Soc. Exp. Biol. Med. 91, 189-191, 1956
- /HER58/ Herman, J.R.; Mason, B.; Light, I.  
Fluorine in urinary tract calculi  
J. Urol. 80(4), 263-268, 1958
- /HER60/ Herman, J.R.; Papadakis, L.  
The relationship of sodium fluoride to nephrolithiasis in rats  
J. Urol. 83(6), 799-800, 1960
- /HER85/ Hering, F.; Briellmann, T.; Seiler, H.; Rutishauser, G.  
Role of fluoride in formation of calcium oxalate stones  
Urolithiasis Related Clin. Res., Proc. 5th Int. Symp. 1984, (Publ. 1985), pp. 383-386
- /HES77/ see Introduction
- /HES78/ Hesse, A.; Müller, R.; Schneider, H.J.; Taubert, F.  
Analytische Untersuchungen zur Bedeutung des Fluorgehaltes von Harnsteinen  
Urologe A 17(4), 207-210, 1978
- /HES81/ see Introduction
- /HOD69/ see Chapter II

- /JEN83/ Jennrich, R.; Mündle, P.  
Polynomial regression, P5R  
in: W.J. Dixon (Ed.); "BMDP statistical software, 1983"; University of  
California Press, Berkeley, 1983, pp. 283-288
- /JOL80/ Jolly, S.S.; Sharma, O.P.; Garg, G.; Sharma, R.  
Kidney changes and kidney stones in endemic fluorosis  
Fluoride 13, 10-16, 1980
- /JON76/ Jones, K.W.; Gorodetzky, P.; Jacobson, J.S.  
Determination of fluorine in vegetation by proton activation analysis  
Int. J. Environ. Anal. Chem. 4, 225-231, 1976
- /JUE80/ Jueneman, F.B.  
Fluoridation: the great dilemma  
Res. Dev. 22(3), 17, 1980
- /JUE84/ Jueneman, F.B.  
Fluoride: a factor in aging  
Res. Dev. 26(2), 17, 1984
- /JUJ79/ Juuti, M.; Heinonen, O.P.  
Incidence of urolithiasis leading to hospitalization in Finland  
Acta Med. Scand. 206, 397-403, 1979
- /KOL68/ see Chapter II
- /LAG56/ see Chapter I
- /LEA63/ Leach, S.A.; Griffiths, M.  
A simple method for the determination of submicrogram amounts of fluoride  
Arch. Oral Biol. 8, 781-782, 1963
- /LIG69/ Light, T.S.; Mannion, R.F.  
Microdetermination of fluorine in organic compounds by potentiometric  
titration using a fluoride electrode  
Anal. Chem. 41(1), 107-111, 1969
- /LIN67/ Lingane, J.J.  
A study of the lanthanum fluoride membrane electrode for end point detec-  
tion in titrations of fluoride with thorium, lanthanum, and calcium  
Anal. Chem. 39(8), 881-887, 1967
- /LIN68/ Lingane, J.J.  
Further study of the lanthanum fluoride membrane electrode for potentio-  
metric determination and titration of fluoride  
Anal. Chem. 40(6), 935-939, 1968
- /LJU78/ Ljunghall, S.  
Regional variations in the incidence of urinary stones  
Br. Med. J. 1(6110), 439, 1978
- /LOO68/ Van Loon, J.C.  
The rapid determination of fluoride in mineral fluorides using a specific  
ion electrode  
Anal. Lett. 1(6), 393-398, 1968
- /LUJ76/ Luoma, H.; Nuuja, T.; Collan, Y.; Nurmikoski, P.  
The effect of magnesium and fluoride on nephrocalcinosis and aortic calci-  
fication in rats given high sucrose diets with added phosphates  
Calcif. Tissue Res. 20, 291-302, 1976
- /MCC62/ McConnell, D.  
Dating of fossil bones by the fluorine method  
Science 136(3512), 241-244, 1962

- /MCC68/ McCann, H.G.  
Determination of fluoride in mineralized tissues using the fluoride ion electrode  
Arch. Oral. Biol. 13, 475-477, 1968
- /MER80/ Mertz, W.  
Trace elements in nutrition  
Trace Elem. Anal. Chem. Med. Biol., Proc. Int. Workshop, 1st, 1980, pp. 727-744
- /MEY72/ see Chapter II
- /MUE61/ Mühlemann, H.R.; König, K.G.; Marthaler, T.M.  
The cariostatic effect of sodium fluoride when combined with phosphates in animal experimentation  
Helv. Odontol. Acta 5, 4-9, 1961
- /MUE77/ Müller, R.C.  
Analytische Untersuchungen zur Bedeutung des Spurenelementes Fluor bei der Harnsteinbildung  
Dissertation, Friedrich-Schiller-Universität, Jena, 1977
- /MUR57/ Murray, M.M.  
Nutritional requirements and food fortification. Physiological aspects of fluorine  
Chem. Ind. (London), January, 5-6, 1957
- /NEE70/ Neefus, J.D.; Cholak, J.; Saltzman, B.E.  
The determination of fluoride in urine using a fluoride-specific ion electrode  
Am. Ind. Hyg. Assoc. J. 31, 96-99, 1970
- /NEW60/ Newesely, H.  
Darstellung von "Oktacalciumphosphat" (Tetracalciumhydrogentrisphosphat) durch homogene Kristallisation  
Monatsh. Chem. 91(6), 1020-1023, 1960
- /NEW61/ Newesely, H.  
Changes in crystal types of low solubility calcium phosphates in the presence of accompanying ions  
Arch. Oral. Biol. Special Suppl. 6, 174-180, 1961
- /NEW85/ N.N.  
How fluoride might damage your health  
New Sci. 1445, 20, 1985 (28 February)
- /ORI77/ Orion Research  
Instruction manual fluoride electrodes model 94-09, model 96-09  
Orion Research Inc., Cambridge, Ma., USA, 1977, pp. 27
- /ORI78/ Orion Research  
Analytical methods guide, 9th edition  
Orion Research Inc., Cambridge, Ma., USA, 1978, pp. 4
- /ORI79/ Orion Research  
Instruction manual model 901 microprocessor ionalyzer  
Orion Research Inc., Cambridge, Ma., USA, 1979
- /PER79/ Perrin, D.D.; Dempsey, B.  
Buffers for pH and metal ion control  
Chapman & Hall, London, 1979, pp. 47 and pp. 132
- /RAB45/ Rabinowitch, I.M.  
Acute fluoride poisoning  
Can. Med. Assoc. J. 52, 345-349, 1945

- /RAB67/ Raby, B.A.; Sunderland, W.E.  
Direct determination of fluoride in tungsten using the fluoride ion activity electrode  
Anal. Chem. 39(11), 1304-1305, 1967
- /ROB34/ Robison, R.; Rosenheim, A.H.  
Calcification of hypertrophic cartilage in vitro  
Biochem J. 28(1), 684-698, 1934
- /ROW62/ Rowley, R.J. Farrah, G.H.  
Diffusion method for the determination of urinary fluoride  
Am. Ind. Hyg. Assoc. J. 23, 314-318, 1962
- /SAR75/ Sara, R.; Wänninen, E.  
Separation and determination of fluoride by diffusion with hexamethyldisiloxane and use of a fluoride-sensitive electrode  
Talanta 22(12), 1033-1036, 1975
- /SCH66/ see Chapter I
- /SEK73/ Sekerka, I.; Lechner, J.F.  
Automated determination of fluoride ion in the parts per milliard range  
Talanta 20, 1167-1172, 1973
- /SHR78/ Shroy, R.E.; Kraner, H.W.; Jones, K.W.; Jacobson, J.S.; Heller, L.I.  
Determination of fluorine in food samples by the  $^{19}\text{F}(p,p')^{19}\text{F}$  reaction  
Nucl. Instrum. Methods 149, 313-316, 1978
- /SHR82/ Shroy, R.E.; Kraner, H.W.; Jones, K.W.; Jacobson, J.S.; Heller, L.I.  
Proton activation analysis for the measurement of fluorine in food samples  
Anal. Chem. 54(3), 407-413, 1982
- /SIN54/ Singer, L.; Armstrong, W.D.  
Determination of fluoride - procedure based upon diffusion of hydrogen fluoride  
Anal. Chem. 26(5), 904-906, 1954
- /SIN68/ Singer, L.; Armstrong, W.D.  
Determination of fluoride in bone with fluoride electrode  
Anal. Chem. 40(3), 613-614, 1968
- /SIN69/ Singer, L.; Armstrong, W.D.; Vogel, J.J.  
Determination of fluoride content of urine by electrode potential measurement  
J. Lab. Clin. Chem. 74(2), 354-358, 1969
- /SPI56/ Spira, L.  
Urinary calculi and fluorine  
Exp. Med. Surg. 14(1), 72-88, 1956
- /SPI57/ Spira, L.  
Cholelithiasis and fluorine  
S. Afr. Med. J. 31(25), 621-624, 1957
- /SRI68/ Srinivasan, K.; Rechnitz, G.A.  
Activity measurements with a fluoride-selective membrane electrode  
Anal. Chem. 40(3), 509-512, 1968
- /STA12/ Starck, G.; Thorin, E.  
Die quantitative Bestimmung des Fluors als Kalziumfluorid  
Z. Anal. Chem. 51, 14-18, 1912



- /STE59/ Stegemann, H.; Jung, G.F.  
Abtrennung von Fluorwasserstoff durch Diffusion und Mikroanalyse von Fluorid  
Hoppe Seyler's Z. Physiol. Chem. 315, 222-227, 1959
- /SUM75/ Summers, J.L.; Keitzer, W.A.  
Effect of water fluoridation on urinary tract calculi  
Ohio State Med. J. 71, 25-27, 1975
- /SUN69/ Sun, M.W.  
Fluoride ion activity electrode for determination of urinary fluoride  
Am. Ind. Hyg. Assoc. J. 30, 133-136, 1969
- /TAV68/ Taves, D.R.  
Effect of silicone grease on diffusion of fluoride  
Anal. Chem. 40(1), 204-206, 1968
- /TAV68a/ Taves, D.R.  
Separation of fluoride by rapid diffusion using hexamethyldisiloxane  
Talanta 15(9), 969-974, 1968
- /TEO83/ Teotia, M.; Teotia, S.P.S.; Singh, D.P.; Singh, C.V.  
Chronic ingestion of natural fluoride and endemic bladder stone disease  
Ind. Pediatrics 20, 637-642, 1983
- /TEO84/ Teotia, M.; Teotia, S.P.S.; Singh, D.P.; Singh, C.V.  
Chronic ingestion of natural fluoride and endemic bladder stone disease  
Urinary Stone, Proc. Int. Urinary Stone Conf., 2nd, 1983, (Publ. 1984), pp. 24-29
- /TOZ81/ see Introduction
- /TUS69/ Tušl, J.  
A study of the influence of silicone grease on spectrophotometric methods for the determination of fluoride  
Anal. Chem. 41(2), 352-355, 1969
- /TUS70/ Tušl, J.  
Direct determination of fluoride in human urine using fluoride electrode  
Clin. Chim. Acta 27, 216-218, 1970
- /TUS70a/ Tušl, J.  
Direct determination of fluoride in phosphate materials in mineral feeds with the fluoride ion activity electrode  
J. Assoc. Off. Anal. Chem. 53(2), 267-269, 1970
- /TUS72/ Tušl, J.  
Fluoride ion activity electrode as a suitable means for exact direct determination of urinary fluoride  
Anal. Chem. 44(9), 1693-1694, 1972
- /VOG78/ Vogel, A.; Bassett, J.; Denney, R.C.; Jefferey, G.H.; Mendham, J. (Eds.)  
Textbook of quantitative inorganic analysis (4th ed.), Longman, London, 1978, pp. 569
- /VOL36/ Volkmann, J.  
Versuche mit Fluormatriumbehandlung bei Knochenbrüchen, verzögerter Knochenbruchheilung und Ähnlichem  
Bruns' Beitr. Klin. Chir. 164, 487-491, 1936
- /VOL58/ Volkmann, J.  
Fluorgehalt in Harnsteinen  
Z. Urol. 51(6), 341-348, 1958

- /WAR69/ Warner, T.B.  
Lanthanum fluoride electrode response in water and in sodium chloride  
Anal. Chem. 41(3), 527-529, 1969
- /WEA65/ Weatherell, J.A.; Hargreaves, J.A.  
The micro-sampling of enamel in thin layers by means of strong acids  
Arch. Oral Biol. 10, 139-142, 1965
- /WEA82/ Weast, R.C.; Astle, M.J. (Eds.)  
CRC handbook of chemistry and physics (63rd edition), 1982-1983  
CRC Press Inc., Boca Raton, Florida, USA, 1982, pp. B16
- /WHA62/ Wharton, H.W.  
Isolation and determination of microgram amounts of fluoride in materials containing calcium and orthophosphate  
Anal. Chem. 34(10), 1296-1298, 1962
- /WHO58/ World Health Organization (WHO)  
Comité d'experts de la fluoration de l'eau  
Rapport technique no 146, 1958
- /WHO65/ World Health Organization (WHO)  
Normes internationales pour l'eau de boisson  
Genève, 1965
- /WHO69/ World Health Organization (WHO)  
Fluoration et hygiène dentaire  
Résolution WHA 22-30 du 23 juillet 1969
- /WIL33/ Willard, H.H.; Winter, O.B.  
Volumetric method for determination of fluorine  
Ind. Eng. Chem., Anal. Ed. 5(1), 7-10, 1933
- /WIL79/ Williams, J.W.  
Handbook of anion determination  
Butterworths, London, 1979, pp. 335-373
- /WIN79/ Windsor, D.L.; Denton, M.B.  
Elemental analysis of gas chromatographic effluents with an inductively coupled plasma  
J. Chromatogr. Sci. 17(9), 492-496, 1979
- /ZIP58/ Zipkin, I.; Lee, W.A.; Leone, N.C.  
Fluoride content of urinary and biliary tract calculi  
Proc. Soc. Exp. Biol. Med. 97, 650-653, 1958
- /ZIP62/ Zipkin, I.; Posner, A.S.; Eanes, E.D.  
Effect of fluoride on the x-ray diffraction pattern of the apatite of human bone  
Biochim. Biophys. Acta 59, 255-258

## 5. Chapter IV

- /ACH76/ Achilles, W.; Cumme, G.A.; Scheffel, M.  
Investigation of complex-chemical equilibria in urinary systems with respect to calcium oxalate formation  
Urolithiasis Res Proc. Int. Symp., 3rd, 1976, pp. 229-232
- /ALT73/ see Chapter III

- /BAR74/ see Introduction
- /BIS75/ Bisailon, S.; Tawashi, R.  
Growth of calcium oxalate in gel systems  
J. Pharm. Sci. 64(3), 458-460, 1975
- /BIS76/ Bisailon, S.; Tawashi, R.  
Retardation of dissolution and growth of calcium oxalate monohydrate  
J. Pharm. Sci. 65(2), 222-225, 1976
- /BOE81/ Börner, R.H.; Schneider, H.-J.; Berg, W.  
Stabilizing factor for uric acid dihydrate - a contribution to uric acid stone formation  
Urolithiasis Clin. Basic Res., Proc. Int. Symp., 4th, 1980, (Publ. 1981), pp. 465-468
- /BOY54/ Boyce, W.H.; Garvey, F.K.; Norfleet, C.M.  
The turbidity of urine in the normal and in patients with urinary calculi  
Exp. Med. Surg. 12(4), 450-459, 1954
- /BUR80/ Burns, J.R.; Finlayson, B.  
A proposal for a standard reference artificial urine in in vitro urolithiasis experiments  
Invest. Urol. 18(2), 167-169, 1980
- /CHR84/ see Chapter III
- /DES73/ see Chapter II
- /DES78/ Desjardins, A.; Tawashi, R.  
Growth retardation of calcium oxalate by sodium copper chlorophyllin  
Eur. Urol. 4, 294-297, 1978
- /DIE62/ Diem, K. (Ed.)  
Documenta Geigy - Scientific tables (6th ed.)  
J.R. Geigy S.A., Basle, Switzerland, 1962, pp. 527-537
- /DIE70/ Diem, K.; Lentner, C. (Eds.)  
Documenta Geigy - Scientific tables (7th ed.)  
Ciba-Geigy Ltd., Basle, Switzerland, 1970, pp. 661-678
- /DOR78/ Doremus, R.H.; Teich, S.; Silvis, P.X.  
Crystallization of calcium oxalate from synthetic urine  
Invest. Urol. 15(6), 469-472, 1978
- /DRA78/ Drach, G.W.; Randolph, A.D.; Miller, J.D.  
Inhibition of calcium oxalate dihydrate crystallization by chemical modifiers: I. Pyrophosphate and methylene blue  
J. Urol. 119, 99-103, 1978
- /DRA80/ Drach, G.W.; Thorson, S.; Randolph, A.  
Effects of urinary organic macromolecules on crystallization of calcium oxalate: enhancement of nucleation  
J. Urol. 123, 519-523, 1980
- /ELL58/ Elliot, J.S.; Quaide, W.L.; Sharp, R.F.; Lewis, L.  
Mineralogical studies of urine: The relationship of apatite, brushite and struvite to urinary pH  
J. Urol. 80(4), 269-271, 1958
- /FIN72/ Finlayson, B.  
The concept of a continuous crystallizer  
Invest. Urol. 9(4), 258-263, 1972

- /FIN73/ Finlayson, B.; DuBois, L.  
Kinetics of calcium oxalate deposition in vitro  
Invest. Urol. 10(6), 429-433, 1973
- /FIN82/ Finlayson, B.  
Pathologic mineralization, nucleation, growth and retention  
in: G.H. Nancollas (Ed.); "Biological mineralization and demineralization,  
Dahlem Konferenzen"; Springer, Berlin, 1982, pp. 271-285
- /FIN84/ Finlayson, B.  
private communication
- /FLE77/ Fleisch, H.; Russell, R.G.G.  
Experimental and clinical studies with pyrophosphate and diphosphonates  
in: D.S. David (Ed.); "Calcium metabolism in renal failure and  
nephrolithiasis"; Wiley, New York, 1977, Chapter 9, pp. 293-336
- /FRA71/ see Chapter III
- /GAR75/ Gardner, G.L.  
Nucleation and crystal growth of calcium oxalate trihydrate  
J. Cryst. Growth 30, 158-168, 1975
- /GAR76/ Gardner, G.L.  
Kinetics of the dehydration of calcium oxalate trihydrate crystals in  
aqueous solution  
J. Colloid Interface Sci. 54(2), 298-310, 1976
- /GAR78/ Gardner, G.L.; Doremus, R.H.  
Crystal growth inhibitors in human urine  
Invest. Urol. 15(6), 478-485, 1978
- /GAR78a/ Gardner, G.L.  
Effect of pyrophosphate and phosphonate anions on the crystal growth  
kinetics of calcium oxalate hydrates  
J. Phys. Chem. 82(8), 864-870, 1978
- /GIL77/ Gill, W.B.; Karesh, J.W.; Garsin, L.; Roma, M.J.  
Inhibitory effects of urinary macromolecules on the crystallization of  
calcium oxalate  
Invest. Urol. 15(2), 95-99, 1977
- /GRI76/ Griffith, D.P.; Musher, D.M.; Itin, C.  
Urease - The primary cause of infection-induced urinary stones  
Invest. Urol. 13(5), 346-350, 1976
- /GUD09/ see Chapter III
- /HAL78/ Hallson, P.C.; Rose, G.A.  
A new urinary test for stone "activity"  
Br. J. Urol. 50, 442-448, 1978
- /HER62/ see Chapter I
- /HES75/ Hesse, A.; Schneider, H.-J.; Berg, W.; Hienzsich, E.  
Uric acid dihydrate as urinary calculus component  
Invest. Urol. 12(5), 405-409, 1975
- /HES78/ see Chapter III
- /HOD80/ Hodgkinson, A.  
Solubility of calcium oxalate in human urine, simulated urine, and water  
Invest. Urol. 18(2), 123-126, 1980

- /HOW76/ Howard, J.E.  
Studies on urinary stone formation: a saga of clinical investigation  
Johns Hopkins Med. J. 139, 239-252, 1976
- /ISA69/ Isaacson, L.C.  
Urinary composition in calcific nephrolithiasis  
Invest. Urol. 6(4), 356-363, 1969
- /LAG56/ see Chapter I
- /LEN81/ see Chapter II
- /LI85/ Li, M.K.; Blacklock, N.J.; Garside, J.  
Effects of magnesium on calcium oxalate crystallization  
J. Urol. 133(1), 123-125, 1985
- /LIN86/ Linder, P.W.; Little, J.C.  
Prediction by computer-modelling of the precipitation of stone-forming solids from urine  
Inorg. Chim. Acta 123(3), 1986 (in press)
- /LIT84/ Little, J.  
Chemical modelling of urine  
M. Sc. Thesis, Dept. of Physical Chemistry, University of Cape Town, 1984
- /LYO65/ see Chapter II
- /MAN81/ Mandel, N.S.; Mandel, G.S.  
Epitaxis between stone-forming crystals at the atomic level  
Urolithiasis Clin. Basic Res., Proc. Int. Symp., 4th, 1980, (Publ. 1981), pp. 469-480
- /MEY72/ see Chapter II
- /MEY75/ Meyer, J.L.; Smith, L.H.  
Growth of calcium oxalate crystals I  
Invest. Urol. 13(1), 31-35, 1975
- /MIL76/ Miller, J.D.; Randolph, A.D.; Drach, G.W.  
Some observations of calcium oxalate crystallization in urine-like mother liquors  
in: B. Finlayson, W.C. Thomas Jr. (Eds.); "Colloquium on Renal Lithiasis"; University Press of Florida, Gainesville, 1976, pp. 33-40
- /MIL77/ Miller, J.D.; Randolph, A.D.; Drach, G.W.  
Observations upon calcium oxalate crystallization kinetics in simulated urine  
J. Urol. 117, 342-345, 1977
- /MOR67/ see Chapter I
- /NAN82/ Nancollas, G.H.  
Phase transformation during precipitation of calcium salts  
in: G.H. Nancollas (Ed.); "Biological mineralization and demineralization, Dahlem Konferenzen"; Springer, Berlin, 1982, pp. 79-99
- /PAK71/ Pak, C.Y.C.; Eanes, E.D.; Ruskin, B.  
Spontaneous precipitation of brushite in urine: evidence that brushite is the nidus of renal stones originating as calcium phosphate  
Proc. Nat. Acad. Sci. USA 68(7), 1456-1460, 1971
- /PAK73/ Pak, C.Y.C.; Chu, S.  
A simple technique for the determination of urinary state of saturation with respect to brushite  
Invest. Urol. 11(3), 211-215, 1973

- /PHA77/ Phaneuf-Mimeault, F.; Tawashi, R.  
Scanning electron microscopic study of calcium oxalate concretions grown in gel system and calcium oxalate stones  
Eur. Urol. 3, 171-175, 1977
- /ROB69/ Robertson, W.G.  
A method for measuring calcium crystalluria  
Clin. Chim. Acta 26, 105-110, 1969
- /ROB73/ Robertson, W.G.; Peacock, M.; Nordin, B.E.C.  
Inhibitors of the growth and aggregation of calcium oxalate crystals  
Clin. Chim. Acta 43, 31-37, 1973
- /ROD81/ Rodgers, A.L.; Garside, J.  
The nucleation and growth kinetics of calcium oxalate in the presence of some synthetic urine constituents  
Invest. Urol. 18(6), 484-488, 1981
- /ROD81c/ see Introduction
- /ROD85/ Rodgers, A.L.; Wandt, M.  
Crystallization characteristics of synthetic urine in a fast evaporator  
Urolithiasis Related Clin. Res., Proc 5th Int. Symp., 1984, (Publ. 1985), pp. 765-768
- /ROS75/ Rose, M.B.  
Renal stone formation: The inhibitory effect of urine on calcium oxalate precipitation  
Invest. Urol. 12(6), 428-433, 1975
- /RYA81/ Ryall, R.L.; Bagley, C.J.; Marshall, V.R.  
Independent assessment of the growth and aggregation of calcium oxalate crystals using the Coulter counter  
Invest. Urol. 18(5), 401-405, 1981
- /SAN33/ Sandell, E.B.; Kolthoff, I.M.  
Studies in coprecipitation III  
J. Phys. Chem. 37(2), 153-170, 1933
- /SCH32/ Schleede, A.; Schmidt, W.; Kindt, H.  
Zur Kenntnis der Calciumphosphate und Apatite  
Z. Elektrochem. 33(8a), 633-641, 1932
- /SHE84/ Sheehan, M.E.; Nancollas, G.H.  
The kinetics of crystallization of calcium oxalate trihydrate  
J. Urol. 132(1), 158-163, 1984
- /SUT69/ see Chapter II
- /SUT73/ Sutor, D.J.  
Experiments on the nucleation and growth of calcium oxalate in normal and stone formers' urine  
Urinary Calc. Proc. Int. Symp. 1972, (Publ. 1973), pp. 313-317
- /TAW80/ Tawashi, R.; Cousineau, M.  
Growth retardation of weddellite (calcium oxalate dihydrate) by sodium copper chlorophyllin  
Invest. Urol. 18(2), 86-89, 1980
- /TOM79/ Tomažić, B.B.; Nancollas, G.H.  
A study of the phase transformation of calcium oxalate trihydrate-monohydrate  
Invest. Urol. 16(5), 329-335, 1979

- /TOM80/ Tomazić, B.; Nancollas, G.H.  
Crystal growth of calcium oxalate hydrates: A comparative kinetics study  
J. Colloid Interface Sci. 75(1), 149-160, 1980
- /TRA62/ Trautz, O.R.; Zapanta, R.R.  
Effect of magnesium on various calcium phosphates  
J. Dent. Res. 41(5), 28, 1962
- /VER64/ Vermeulen, C.W.; Lyon, E.S.; Gill, W.B.  
Artificial urinary concretions  
Invest. Urol. 1(4), 370-386, 1964
- /WEL72/ Welshman, S.G.; McGeown, M.G.  
A quantitative investigation of the effects on the growth of calcium oxalate crystals on potential inhibitors  
Br. J. Urol. 44, 677-680, 1972
- /WES75/ Westall, J.C.; Zachary, J.L.; Morel, F.M.M.  
MINEQL - A computer program for the calculation of chemical equilibrium composition of aqueous systems  
Tech. Note 18, Water Quality Lab., MIT, Cambridge, Mass., USA, 1975
- /YOU82/ Young, R.A.; Brown, W.E.  
Structures of biological minerals  
in: G.H. Nancollas (Ed.); "Biological mineralization and demineralization, Dahlem Konferenzen"; Springer, Berlin, 1982, pp. 101-141
- /ZIP62/ see Chapter III





## CURRICULUM VITAE

Michael A.E. Wandt

Born 14 May 1955 in Stuttgart (FRG)

- Secondary School - Schickhardt-Gymnasium in Stuttgart (FRG), 1966 - 1974; 'Abitur' on 31 May 1974.
- Academic Training - Full time student in the Department of Physics, Albert-Ludwigs-University, Freiburg/Brsg. (FRG), 1974 - 1976, and Eberhard-Karls-University, Tübingen (FRG), 1976 - 1981; Graduating with degree 'Diplom-Physiker' (M.Sc) in June 1981; Thesis: "Automatically Compensating Torque Magnetometer for the Measurement of Magnetic Properties of Spin Glasses in the Temperature Range from 1.8 to 300 K".
- Summer School "Electronspectroscopic Methods in the Analysis of the Solid State and Surfaces" (1980) and Summer School "Physics of Polymers" (1981) at the Kernforschungsanlage Jülich (FRG).
  - Since January 1982 registered in the Department of Physical Chemistry, University of Cape Town (RSA) for degree Ph.D (Science).
  - In 1982 training in Electron Microscopy and X-Ray Analysis, Electron Microscope Unit, University of Cape Town (RSA).
  - Course on Theory and Practice of X-Ray Fluorescence Spectrometry, Department of Geochemistry, University of Cape Town (1983).
- Experience - Scientific Assistant, Institute of Crystallography, University of Tübingen (FRG), September 1978 - March 1981.
- Graduate Assistant, Department of Mechanical Engineering, University of Cape Town (RSA), August 1981 - December 1981.
  - Part-time Assistant Lecturer (1982) and Part-time Teaching Assistant (1st half of 1984), Department of Physical Chemistry, University of Cape Town (RSA).
  - Since July 1984 Researcher, Ion-solid Interaction Division, Van de Graaff Group, National Accelerator Centre, Council for Scientific and Industrial Research, Faure, (RSA).